Atlas of Echocardiography in Pediatrics and Congenital Heart Diseases

Maryam Moradian
Azin Alizadehasl
Editors

Springer

Atlas of Echocardiography in Pediatrics and Congenital Heart Diseases

Maryam Moradian • Azin Alizadehasl
Editors

Atlas of Echocardiography in Pediatrics and Congenital Heart Diseases

Springer

Editors
Maryam Moradian
Pediatric Cardiology, Rajaie Cardiovascular Medical & Research Center
Iran University of Medical Sciences
Tehran
Iran

Azin Alizadehasl
Department of Cardio-Oncology and Research Center, Rajaie Cardiovascular Medical & Research Center
Iran University of Medical Sciences
Tehran
Iran

ISBN 978-3-662-62340-4 ISBN 978-3-662-62341-1 (eBook)
https://doi.org/10.1007/978-3-662-62341-1

This Springer imprint is published by the registered company Springer-Verlag GmbH, DE part of Springer Nature.
The registered company address is: Heidelberger Platz 3, 14197 Berlin, Germany

Foreword

The *Atlas of Echocardiography in Pediatric and Congenital Heart Disease* represents an exciting and important new contribution to the field of pediatric/congenital cardiology. Written by veteran and acclaimed pediatric and adult cardiologists, Drs. Maryam Moradian and Azin Alizadehasl, this atlas is far from comprehensive—in fact, it is far more valuable than that. With a distinctly clinical approach, and based on the authors' extensive experience in the field of pediatric and congenital echocardiography, the text examines the pertinent echocardiographic findings encountered in the most common forms of pediatric and congenital heart disease. With beautifully illustrative smartly selected figures throughout the atlas, the authors choose to focus on echocardiographic areas of particular clinical interest—with special attention to areas that are most important and perhaps most challenging to evaluate correctly. What are the most important fetal echocardiographic clues to the diagnosis of tetralogy of fallot? What are the key echocardiographic findings to prognosticate in children with Ebstein's anomaly of the tricuspid valve? How does transesophageal and/or 3D echocardiography contribute to the evaluation of patients with mitral valve pathology? Rather than attempt an exhaustive review of the field, the authors provide an insightful series of clinically important hints and clues on how/why to evaluate the most common forms of heart disease in the fetus, child, and young adult. The result is a clinically invaluable tool for all of those who perform/interpret pediatric/congenital echocardiography—written in a refreshingly conversational and easy-to-read style, but covering a wide range of vitally important concepts of the most common forms of congenital/pediatric heart disease. This innovative and practical new atlas is certain dramatically to improve the real world, clinical practice of pediatric/congenital echocardiography, from the fetus to the adult.

Mark S. Sklansky
Professor and Chief, Pediatric Cardiology
Co-Director, Pediatric/Congenital Heart Program
Medical Director, UCLA Children's Heart Center
Director, UCLA Fetal Cardiology Program
UCLA Mattel Children's Hospital
David Geffen School of Medicine at UCLA,
Los Angeles, CA, USA

Preface

Nowadays, figure-based books are receiving more attention. All the chapters of this book deal with a specific diagnosis of cardiovascular disease using educative and attractive echocardiographic figures of pediatric cardiology. Almost all of the figures are not simply a single good illustration, but rather they are a sequence of images prepared and gathered from our patients with the problem being demonstrated showing the necessary features for the diagnosis and its severity.

The target group of this book is both those who are new to the field of pediatric cardiology and those who are skilled in different areas of this field. This is not intended to be a textbook, but it is a practical figure-based guide to all medical students, cardiology residents, fellows in different aspects of pediatric cardiology such as echocardiography, interventional cardiology, and cardiac surgeons. Of course, this atlas can be helpful for adult echocardiography fellows and also adult congenital heart disease fellows.

All of the images of different chapters used in this book were collected by our colleagues/authors whom we owe a great debt. As the adult population with congenital heart disease is increasing rapidly, in this Atlas we used both options of displaying the apical and subcostal views, regarding cardiac apex, to be more useful for both pediatric and adult cardiologists.

Our thanks go to all our families who understand the importance of the time spent for preparing and writing this book.

Special appreciation and thanks to **Springer company**, Grant Weston, and Anand Shanmugam for their editorial assistance in the preparation of the content of the book.

Tehran, Iran — Maryam Moradian
Tehran, Iran — Azin Alizadehasl

Contents

Contributors

Azin Alizadehasl, MD, FACC, FASE Department of Cardio-Oncology and Research Center, Rajaie Cardiovascular, Medical & Research Center, Iran University of Medical Sciences, Tehran, Iran

Shamsi Ghaffari, MD Pediatric Cardiology, Cardiovascular Research Center, Tabriz University of Medical Sciences, Tabriz, Iran

Majid Maleki, MD Cardiovascular Intervention Research Center, Rajaie Cardiovascular, Medical & Research Center, Iran University of Medical Sciences, Tehran, Iran

Maryam Moradian, MD Pediatric Cardiology, Rajaie Cardiovascular, Medical & Research Center, Iran University of Medical Sciences, Tehran, Iran

Feridoun Noohi, MD Cardiovascular Intervention Research Center, Rajaie Cardiovascular, Medical & Research Center, Iran University of Medical Sciences, Tehran, Iran

Atrial Septal Defect (ASD)

1

Maryam Moradian and Azin Alizadehasl

Abstract

To evaluate an ASD by echocardiography it is important to evaluate its location, size, enlargement of right side chambers, associated anomalies, and not to confuse it with normal variants like prominent Eustachian valve. As atrial septum is a posterior structure if its visualization is not straight forward contrast study and transesophageal echocardiography (TEE) would be helpful.

Atrial Septal Defect (ASD)

1. Evaluate the enlargement of right atrium (RA) and right ventricle (RV) (hallmarks of atrial level shunt) and dilation of pulmonary artery
2. Evaluate the ASD in different views especially subcostal views (coronal and sagittal views) (Fig. 1.1)
3. Dose the edge of the defect produce any T-artifact? (Defect edges are more echogenic producing the so-called T-artifact)
4. Where is the location of the defect in the septum? Secundum ASD, primum ASD, sinus venousus (Fig. 1.2), unroofed coronary sinus defect (Fig. 1.3a, b)
5. Do not confuse the Eustachian valve with the rim of ASD (Fig. 1.4a). Also check for prominent chiary net (Fig. 1.4b).
6. Evaluate paradoxical septal motion both by two dimensional (2D) and M mode echocardiography in parasternal views, also in parasternal long axis view evaluate mitral valve prolapse (MVP), and by angling the transducer toward the left shoulder evaluate pulmonary valve leaflets for doming and stenosis

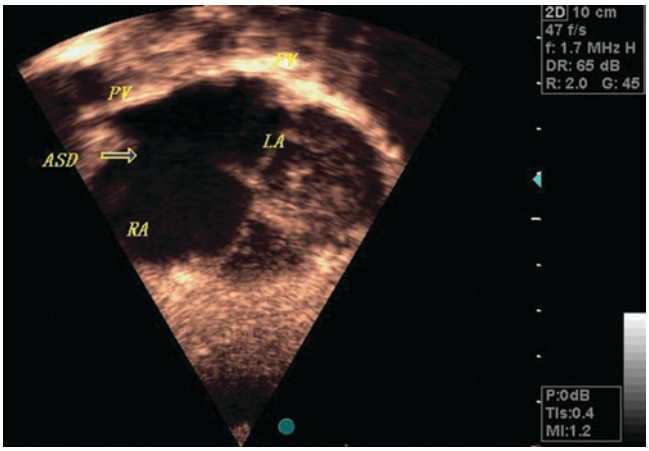

Fig. 1.1 Subcostal view showing large ASD secundum (arrow). *ASD* atrial septal defect, *PV* pulmonary vein, *LA* left atrium, *RA* right atrium

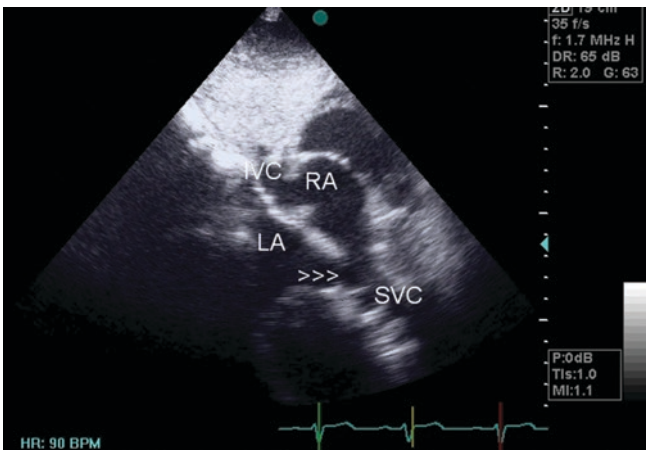

Fig. 1.2 Subcostal sagittal view showing sinus venosus defect (arrow heads). *IVC* inferior vena cava, *SVC* superior vena cava, *LA* left atrium, *RA* right atrium

M. Moradian
Pediatric Cardiology, Rajaie Cardiovascular, Medical & Research Center, Iran University of Medical Sciences, Tehran, Iran

A. Alizadehasl (✉)
Department of Cardio-Oncology and Research Center, Rajaie Cardiovascular, Medical & Research Center, Iran University of Medical Sciences, Tehran, Iran

M. Moradian, A. Alizadehasl (eds.), *Atlas of Echocardiography in Pediatrics and Congenital Heart Diseases*,
https://doi.org/10.1007/978-3-662-62341-1_1

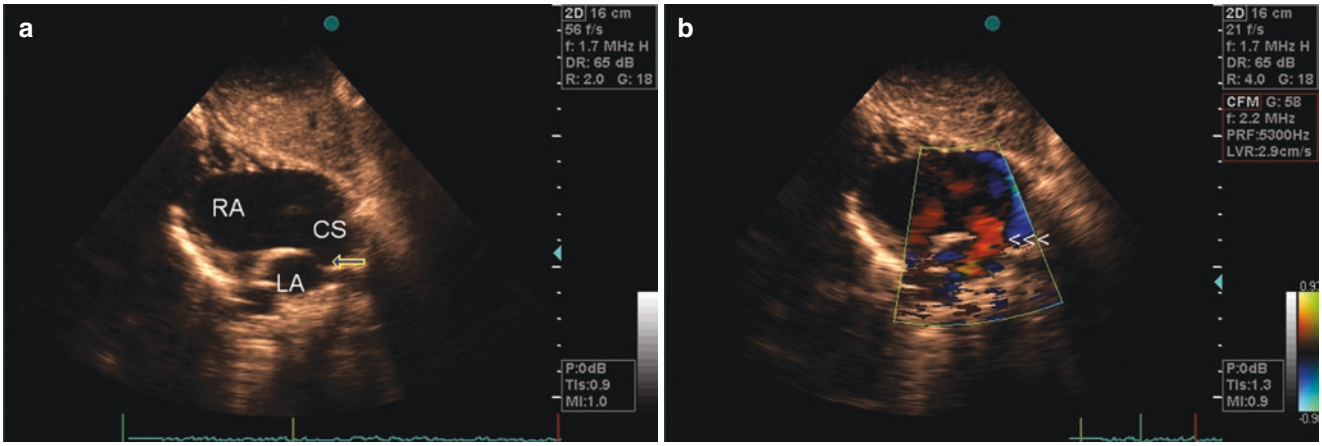

Fig. 1.3 (**a**, **b**) Subcostal coronal view with posterior angulation showing unroofed coronary sinus defect with left to right shunt from LA to dilated coronary sinus (arrow heads). *LA* left atrium, *RA* right atrium *CS* coronary sinus

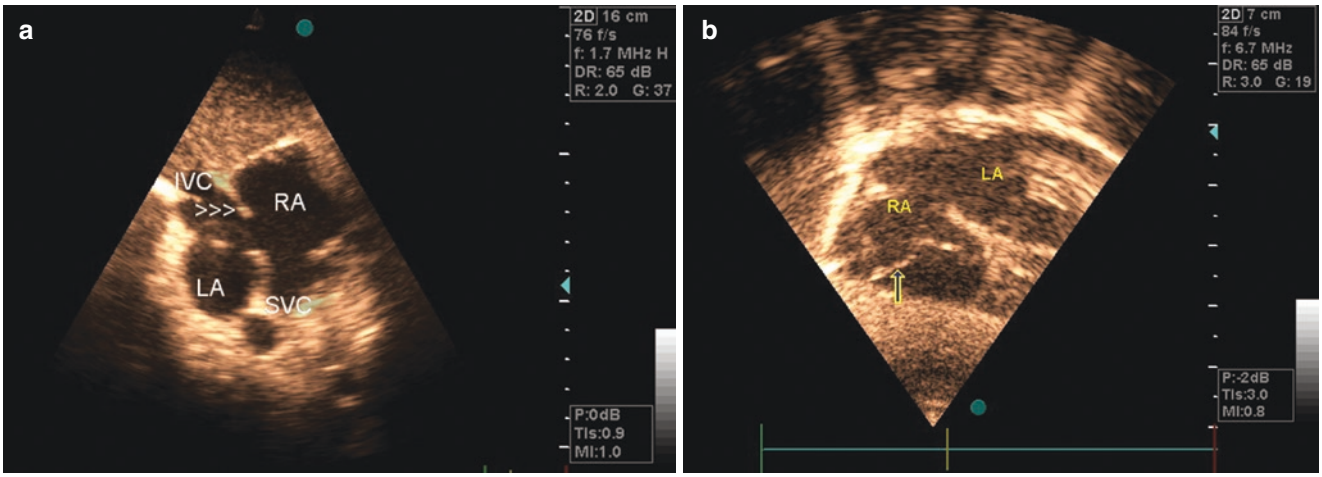

Fig. 1.4 (**a**) Transthoracic echocardiography (TTE) subcostal sagittal image, arrow heads point to prominent Eustachian valve. (**b**) Transthoracic echocardiography subcostal coronal image, arrow indicates prominent chiary net. *LA* left atrium, *RA* right atrium

7. Crab view (suprasternal short axis view) is very useful for demonstrating the pulmonary veins connection to left atrium (LA)
8. Use color Doppler and Doppler profile to evaluate the atrial level shunt direction, tricuspid regurgitation and its pressure gradient for estimation of right ventricular systolic pressure, also evaluate the presence of any pulmonary valve stenosis and/or pulmonary hypertension
9. Contrast study and transesophageal echocardiography (TEE) are useful to evaluate more details (Fig. 1.5a, b)
10. During fetal life if the foramen ovale (FO) size is more than 28–33% of the interatrial septal length size, one may consider an ASD after birth (Fig. 1.6)
11. ASD can also be evaluated using three dimensional (3D) echocardiography (Fig. 1.7)

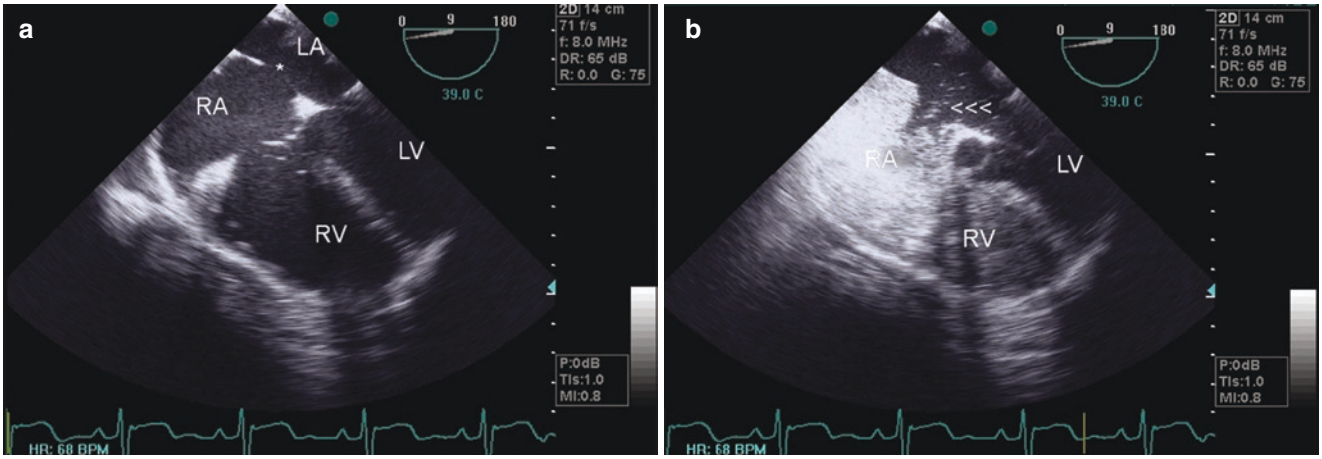

Fig. 1.5 (**a**, **b**) TEE four chamber view. ASD secundum is shown by asterisk, the same patient after contrast injection arrow heads are pointed to negative washout of contrast bubbles by left to right shunt

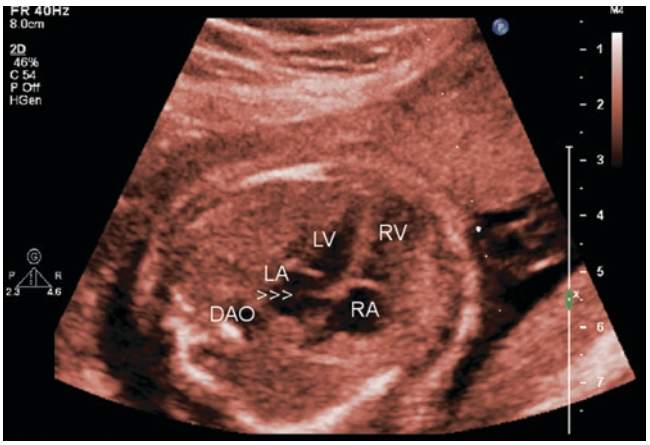

Fig. 1.6 In this four chamber view of fetal heart arrow heads point to flap of foramen ovale

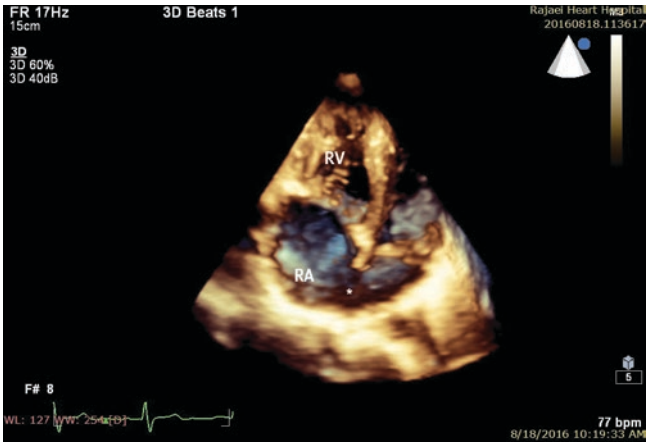

Fig. 1.7 In This 3D apical four chamber view ASD secundum is shown by asterisk. RA and RV are enlarged

Suggested Reading

Anon. The four-chamber view (Chapter 7). In: Chiappa EM, Cook AC, Botta G, Silverman NH, editors. Echocardiographic anatomy in the fetus. Italia: Springer-Verlag; 2008, 2nd printing 2009. p. 71–88.

Anon. Atrial, ventricular, and atrioventricular septal defects (Chapter 18). In: Abuhamad A, Chaoui R, editors. A practical guide to fetal echocardiography: normal and abnormal hearts. 3rd ed: Wolters Kluwer; 2016. p. 253–80.

Bertrand PB, Levine RA, et al. Fact or artifact in two-dimensional echocardiography: avoiding misdiagnosis and missed diagnosis. J Am Soc Echocardiogr. 2016;29(5):381–91.

Bezold LI. Atrial abnormalities and atrial septal defects. In: Wong PC, Miller-Hance WC, editors. Transesophageal echocardiography for congenital heart disease. London: Springer-Verlag; 2014. p. 171–93.

Cabalka AK. Abnormalities of atria and atrial septation (chapter 6). In: Eidem BW, O'leary PW, Cetta F, editors. Echocardiography in pediatric and adult congenital heart disease. 2nd ed: Wolters Kluwer; 2015. p. 111–30.

Hahn, et al. Guidelines for performing a comprehensive transesophageal echocardiographic examination: recommendations from the American Society of Echocardiography and the Society of Cardiovascular Anesthesiologists. J Am Soc Echocardiogr. 2013;26:921–64.

Lopez, et al. Recommendations for quantification methods during the performance of a pediatric echocardiogram: a report from the pediatric measurements writing group of the American Society of Echocardiography Pediatric and Congenital Heart Disease Council. J Am Soc Echocardiogr. 2010;23:465–95.

Martin, et al. Atrial septal defects—clinical manifestations, echo assessment, and intervention. Clin Med Insights: Cardiol. 2014;8(s1):93–8. https://doi.org/10.4137/CMC.s15715.

Sachdeva R. Atrial septal defects (Chapter 28). In: Allen HD, Shaddy RE, Penny DJ, Feltes TF, Cetta F, editors. Moss and Adams' heart disease in infants, children, and adolescents including the fetus and young adults. 9th ed: Wolters Kluwer; 2016. p. 739–56.

Snider R, Serwer GA, Ritter SB, editors. Echocardiography in pediatric heart disease. 2nd ed. St. Louis, MO: Mosby-Year Book, Inc.; 1997. p. 235–96.

Stamm ER. Atrial septal defects. In: Drose JA, editor. Fetal echocardiography. 2nd ed: Saunders Elsevier; 2010. p. 91–104.

Atrioventricular Septal Defect (AVSD)

2

Maryam Moradian and Azin Alizadehasl

Abstract

Evaluate the diagnostic echocardiography features of atrioventricular septal defects (AVSDs) including the same insertion of atrioventricular valves, presence of an ASD primum, "goose neck" deformity, counterclockwise rotation of left ventricular papillary muscles, and cleft of left atrioventricular valve. Assess if it is suitable for biventricular repair.

Atrioventricular Septal Defect (AVSD)

1. Evalute these important anatomic findings shared by all types of AVSDs (partial, transitional, intermediate, and complete).
   (a) Same insertion of atrioventricular valve in apical four chamber view. In all forms of AVSD left and right component of atrioventricular valve (AV valve) insert at the same level (Fig. 2.1).
   (b) Presence of a primum type of atrial septal defect ASD primum (ASD primum).
   (c) Elongation of left ventricular out flow tract (LVOT) in long axis views (parasternal and subcostal) so called "goose neck" deformity (Fig. 2.2).
   (d) Counterclockwise rotation of LV papillary muscles. Evaluate this in parasternal short axis view at 3 and 7 o'clock position in comparison with normal subject that papillary muscles are located at 4 and 8

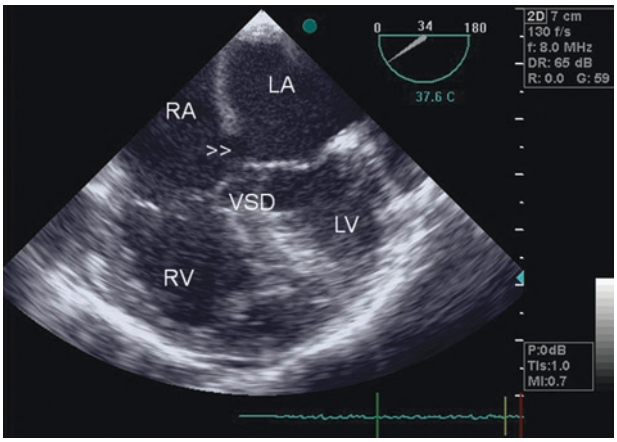

Fig. 2.1 In this TEE four chamber view of transitional AVSD, arrow heads point to ASD primum. Both AV valves insert at same level. Ventricular level shunt through VSD is minimal due to" tricuspid pouch" formation. *LA* left atrium, *RA* right atrium, *LV* left ventricle, *RV* right ventricle, *VSD* ventricular septal defect

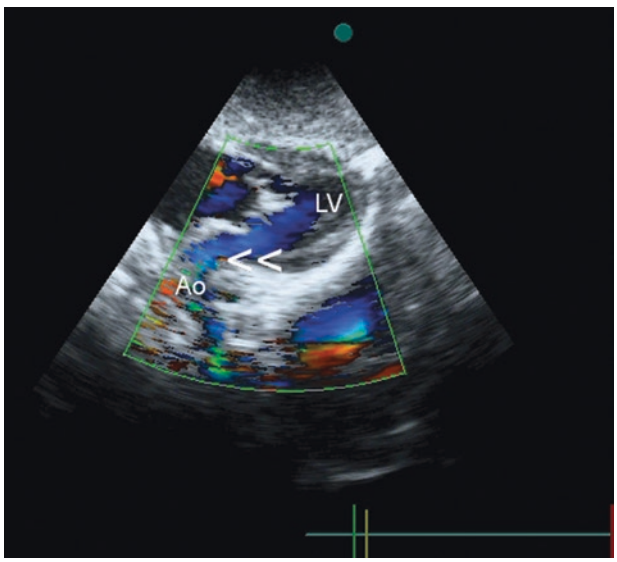

Fig. 2.2 In this subcostal view using color Doppler arrow heads point to "goose neck deformity "in this patient with an AVSD

M. Moradian (✉)
Pediatric Cardiology, Rajaie Cardiovascular, Medical & Research Center, Iran University of Medical Sciences, Tehran, Iran

A. Alizadehasl
Department of Cardio-Oncology and Research Center, Rajaie Cardiovascular, Medical & Research Center, Iran University of Medical Sciences, Tehran, Iran

M. Moradian, A. Alizadehasl (eds.), *Atlas of Echocardiography in Pediatrics and Congenital Heart Diseases*,
https://doi.org/10.1007/978-3-662-62341-1_2

o'clock position. Also evaluate the number of MV papillary muscles.

(e) Cleft of left AV valve in AVSD is directed toward the mid-portion of ventricular septum. (In parasternal and subcostal short-axis views).

2. Evaluate ASD primum in **Partial AVSD** especially in diastolic frames in apical four chamber view, systolic frames may underestimate the real size of ASD primum. Also evaluate the cleft of anterior mitral valve (MV) leaflet in parasternal short axis view at MV leaflets level using color flow Doppler will help you to evaluate the direction of the mitral regurgitation jet. Remember that, with time, this regurgitation may cause leaflet thickening and resembling as mitral valve prolapse (MVP).
3. In **Transitional AVSD** evaluate the small VSD beside ASD primum and mitral valve cleft. The shunt via these inlet VSDs are small due to obliteration of VSD by chordal septal attachments (Fig. 2.1).
4. Assess **Intermediate AVSD** and **complete AVSD** from the apical and subcostal four-chamber views and especially subcostal enface view to evaluate whether a tongue of tissue connects the superior and inferior bridging leaflets to form two distinct orifices in intermediate type.
5. Also pay attention to any aberrant left atrioventricular valve chordal insertion and or displacement of a papillary muscle into left ventricular out flow tract (LVOT). Presence of "goose neck "deformity along with these findings provides substrate for LVOT obstruction especially in partial AVSD (Fig. 2.3).
6. Appreciate other abnormalities of mitral valve (MV), especially double- orifice and parachute mitral valve
7. Evaluate if the ventricles are balanced in subcostal sagittal plane, enface view. Remember that the right ventricular (RV) dominancy may be associated with coarctation of aorta (COA) and arch abnormalities and left ventricular (LV) dominancy may be associated with pulmonary stenosis and atresia. Estimate the atrioventricular valve index (AVVI) or left AV valve area/right AV valve area in subcostal en face view. The amount of less than 0.67% suggests uni-ventricular surgical approach (Fig. 2.4a). Also you may consider the modified AVVI the ratio of left AV valve area/total AV valve area. AVVI between 0.4 and 0.6 is consid-

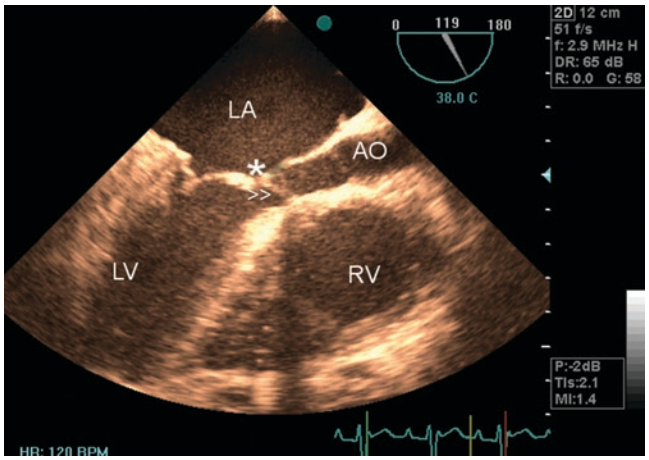

Fig. 2.3 In this trans esophageal long axis view at midesophageal level, cleft of anterior mitral leaflet (AML) is shown by asterisk, arrow heads point to abnormal chordal attachments causing subaortic narrowing and stenosis

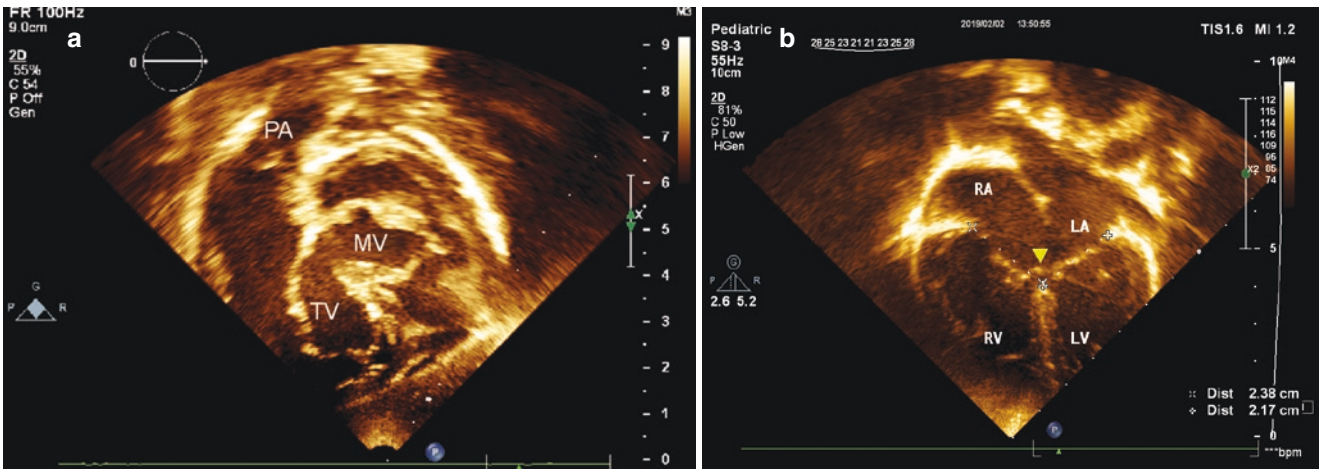

Fig. 2.4 (**a**) Subcostal sagittal plane, enface view can be used to assess "balanced" versus "unbalanced "ventricles. In this patient, atrioventricular inlet is shared equally by both ventricles which was confirmed by mitral valve (MV) area and tricuspid (TV) area planimetry. (**b**) Apical four chamber view showing RV: LV inflow angle in systole. The yellow arrow head points to junction of the two lines at the crest of the ventricular septum (RV: LV angle)

ered balanced AVSD, an AVVI <0.4 is considered right ventricular dominant, and AVVI >0.6 is considered left ventricular dominant.

8. You may also use RV: LV inflow angle in systole. The angle between two lines that pass from each lateral hinge point of left and right AV valves and cross at crest of the ventricular septum at four chamber view. In cases of angle ≤114 ° consider single ventricular approach (Fig. 2.4b).
9. If there is any doubt about real hypoplasia of LV use "potential volume" method by assuming normal septal configuration in parasternal short axis view.
10. Visualize the anatomy of common AV valve in complete AVSDs in en face view and classify it into Rastelli Type A, B, or C:

    Type A → superior bridging leaflet is evenly divided between the two ventricular inlets and attached to crest of ventricular septum with multiple chordal attachments (Fig. 2.5).

    Type B → superior bridging leaflet is partially divided into two components, but not attached to crest of septum. Chordal attachment is from superior leaflet to a papillary muscle in RV septal surface.

    Type C → the bridging leaflet is completely undivided, unattached and free floating with chordal attachments to papillary muscle on RV free wall
11. Three dimension echocardiography (3D) will help to evaluate the AV valve morphology and regurgitation (Fig. 2.6a, b).
12. During fetal life AVSD can easily be detected in four chamber view (Figs. 2.7 and 2.8)
13. Measuring the atrioventricular length ratio during fetal life is increased in AVSD comparing to normal fetuses. The normal value for atrial septal length to ventricular septal length ratio is 0.47 but in fetuses suffering from AVSD this ratio is 0.77

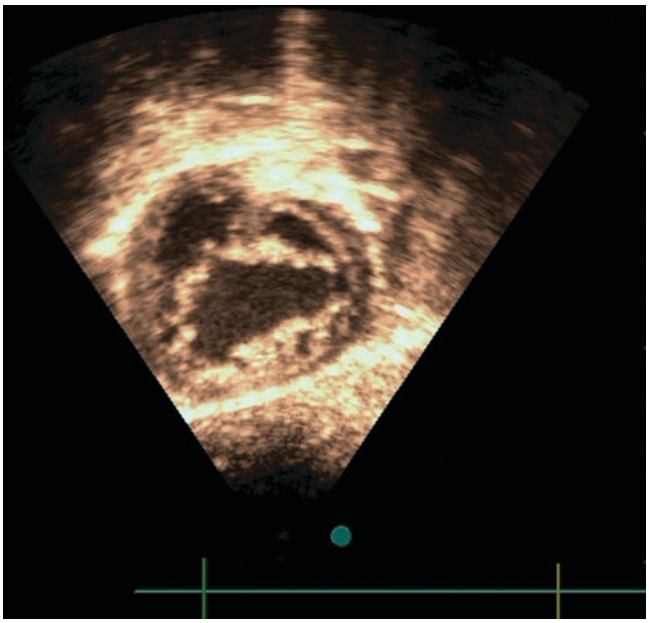

Fig. 2.5 TTE: subcostal coronal view, diastolic enface view of a complete AVSD case (Rastelli type A)

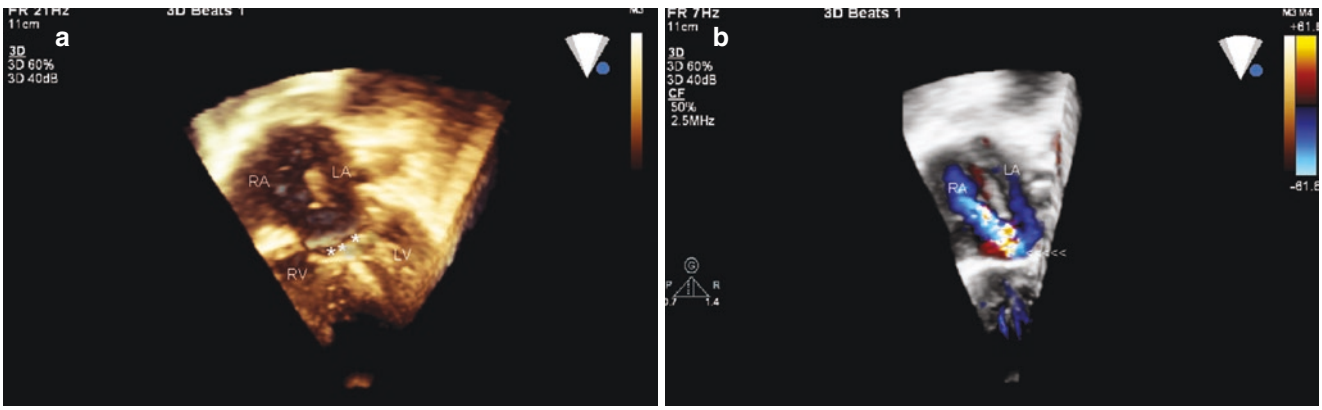

Fig. 2.6 (**a**, **b**) In this 3D TTE, common AV valve is shown by asterisks, and the regurgitation jets are seen using CFM in the same patient. Both ASD primum and secundum exist in this patient

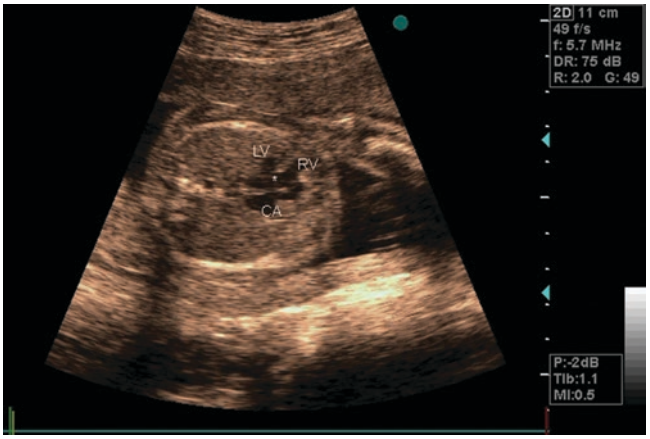

Fig. 2.7 Fetal echocardiogram in four chamber view of a complete AVSD, inlet VSD is demonstrated by asterisk. *CA* common atrium, *RV* right ventricle, *LV* left ventricle

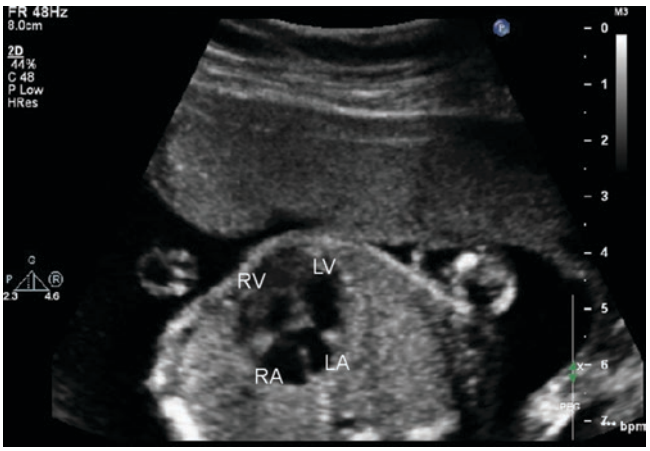

Fig. 2.8 Fetal echocardiography in four chamber view showing AVSD. *RV* right ventricle, *LV*. left ventricle, *RA* right atrium, *LA* left atrium

Suggested Reading

Arunamata A, Balasubramanian S, Mainwaring R, et al. Right-dominant unbalanced atrioventricular septal defect: echocardiography in surgical decision making. J Am Soc Echocardiogr. 2017;30(3):216–26.

Cheng HL, Huang CH, Tsai HE, et al. Intraoperative assessment of partial atrioventricular septal defect with a cleft mitral valve by real-time three-dimensional transesophageal echocardiography. Anesthesia Analgesia. 2012;114(4):731–4.

Cohen MS, Jacobs M, Weinberg PM, et al. Morphometric analysis of unbalanced common atrioventricular canal using two-dimensional echocardiography. JACC. 1996;28(4):1017–23.

Cohen MS, Jegatheeswaran A, Baffa JM, et al. Echocardiographic features defining right dominant unbalanced atrioventricular septal defect A Multi-institutional Congenital Heart Surgeons' Society study. Circ Cardiovasc Imaging. 2013;6:508–13.

Jegatheeswaran A, Pizarro C, Caldarone CA, et al. Echocardiographic definition and surgical decision-making in unbalanced atrioventricular septal defect: a Congenital Heart Surgeons' Society multiinstitutional study. Circulation. 2010;122(Suppl. 1:S209–15.

Kim HK, Kim WH, Hwang SW, et al. Predictive value of intraoperative transesophageal echocardiography in complete atrioventricular septal defect. Ann Thorac Surg. 2005;80:56–9.

Machlitt A, Heling KS, Chaoui R. Increased cardiac atrial-to-ventricular length ratio in the fetal four-chamber view: a new marker for atrioventricular septal defects. Ultrasound Obstet Gynecol. 2004;24:618–22.

Overman DM, Baffa JM, Cohen MS, et al. Unbalanced atrioventricular septal defect: definition and decision making. World J Pediatr Congenital Heart Surg. 2010;1:91–6.

Phoon CL, Silverman NH, et al. Conditions with right ventricular pressure and volume overload, and a small left ventricle: [a]hypoplastic left ventricle or simply a squashed ventricle? JACC. 1997;30(6):1547–53.

Rouerson DA, Muhiudeen IA, Silverman NH, et al. Intraoperative transesophageal echocardiography of atrioventricular septal defect. JACC. 1991;18(2):537–45.

Ventricular Septal Defect (VSD)

3

Maryam Moradian and Azin Alizadehasl

Abstract

Try to evaluate different locations of VSDs by using different echo windows. Assess the nearby structures, especially aortic valve for prolaptic cusp which its ignorance may lead to serious consequences though VSD itself may seem a simple disease. Use color flow mapping to find tiny VSDs.

Ventricular Septal Defect (VSD)

1. Explain where the VSD is located: Centeral or Perimembranous, Inlet, Muscular, or Outlet. Use different echocardiography views.
2. Explain if there is any malalignment of septum.
3. Describe the extension of the defect to adjacent cardiac structures
4. Describe if the **perimembranous** or **Centeral** VSD:
   (a) Extends toward the tricuspid valve (perimembranous inlet) or the aortic valve (perimembranous outlet) (Fig. 3.1a, b)
   (b) Is associated with anterior or posterior malalignment of outlet septum (like VSDs in tetralogy of Fallot or VSDs in interrupted aortic arch respectively) (Fig. 3.1c)
   (c) Dose it cause some distortion of tricuspid valve septal leaflet (ventricular septal aneurysm) and/or tricuspid regurgitation (Fig. 3.2)
5. Also evaluate if blood traverses through the aneurysmal tissue, cross the tricuspid valve into right atrium versus the" Gerbode defect" in which the left ventricular (LV) to right atrium (RA) shunt is due to deficiency of the membranous ventricular septum between LV and RA (Fig. 3.3)

   In "Gerbode defect" direction of the high velocity jet is atypical and if pulmonary artery pressure is not increased, the pulmonary valve regurgitant velocity in diastole would be normal, indicating that the high velocity jet is not due to increased RV pressure
6. Evaluate the prolapse of right or non- coronary cusp of aortic valve in parasternal long and short axis views
7. Do not miss to report any sub aortic ridge, ring, or fibromuscular narrowing with or without subaortic obstruction (Fig. 3.4)
8. **Outlet** VSDs, also known as type 1, subpulmonic, and supracristal are best evaluated in parasternal long and short axis views (Fig. 3.5). Describe if the VSD is associated with prolapse of right coronary cusp of aortic valve and distortion of the valve (Fig. 3.6)
9. Discribe if the **inlet** VSD is associated with some degree of AV valve straddling and overriding of AV valve (Fig. 3.7)
10. Describe the location of **muscular** VSD as being anterior, mid- muscular, posterior, or apical. Take several imaging planes to be able to determine its precise location. Don't miss multiple VSDs (Swiss cheese type) Using color Doppler will help you to find even tiny VSDs (Fig. 3.8)
11. As VSDs are not always circular, try to measure them at least at two orthogonal views. Compare its size with the aortic annulus diameter. VSD is considered small if its diameter is ≤1/3 of the aortic annulus diameter, medium if its diameter is 1/3 to 2/3 aortic annulus diameter and is large if its diameter is more than 2/3 aortic annulus diameter.

M. Moradian (✉)
Pediatric Cardiology, Rajaie Cardiovascular, Medical & Research Center, Iran University of Medical Sciences, Tehran, Iran

A. Alizadehasl
Department of Cardio-Oncology and Research Center, Rajaie Cardiovascular, Medical & Research Center, Iran University of Medical Sciences, Tehran, Iran

M. Moradian, A. Alizadehasl (eds.), *Atlas of Echocardiography in Pediatrics and Congenital Heart Diseases*,
https://doi.org/10.1007/978-3-662-62341-1_3

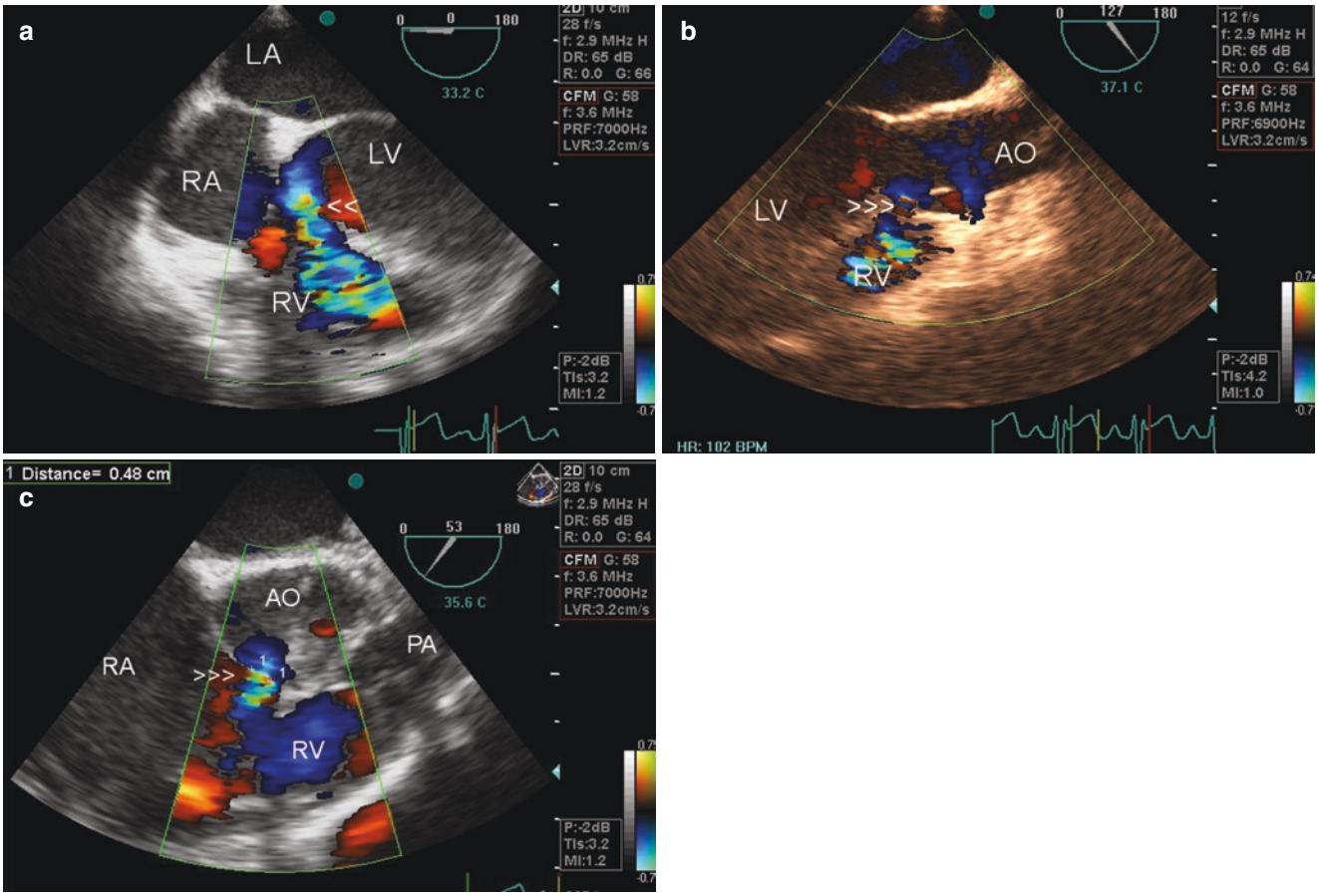

Fig. 3.1 (**a**–**c**) Transesophageal echocardiography (TEE) of different VSDs. (**a**) TEE mid esophageal four chamber view with mild ante flexing and using color flow Doppler shows left to right shunt through the perimembranous defect adjacent to the tricuspid valve (arrow heads). (**b**) TEE mid esophageal aortic valve long axis view arrow heads points to left to right flow via perimembranous VSD which extends to aortic valve. (**c**) TEE mid esophageal aortic valve short axis view using color Doppler indicate left to right shunt through perimembranous VSD with mild anterior malalignment of outlet septum (arrow heads)

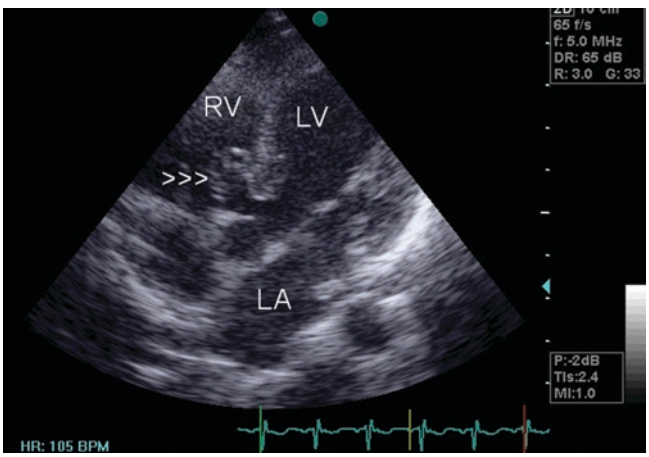

Fig. 3.2 Transthoracic echocardiography (TTE): Apical five chamber view showing ventricular septal aneurysm (arrow heads)

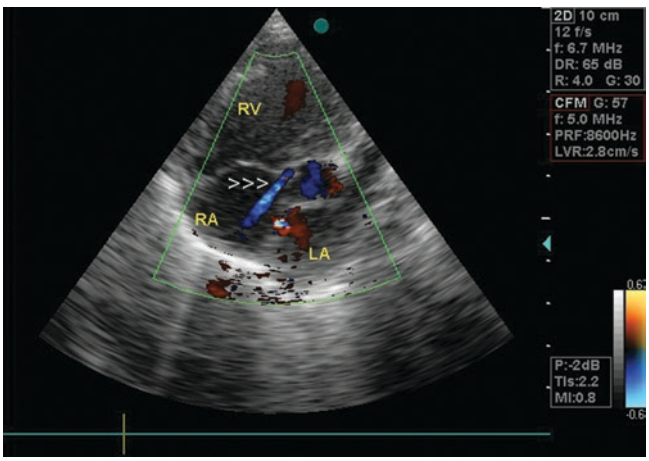

Fig. 3.3 TTE: In this apical five chamber view using color Doppler mapping, arrow heads point to LV to RA shunt (Gerbode defect)

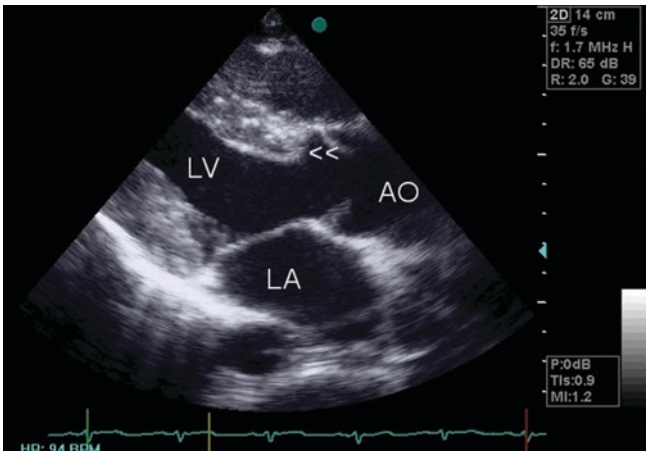

Fig. 3.4 TTE: In this parasternal long axis view subaortic ridge is shown by arrow heads, there is no subaortic obstruction

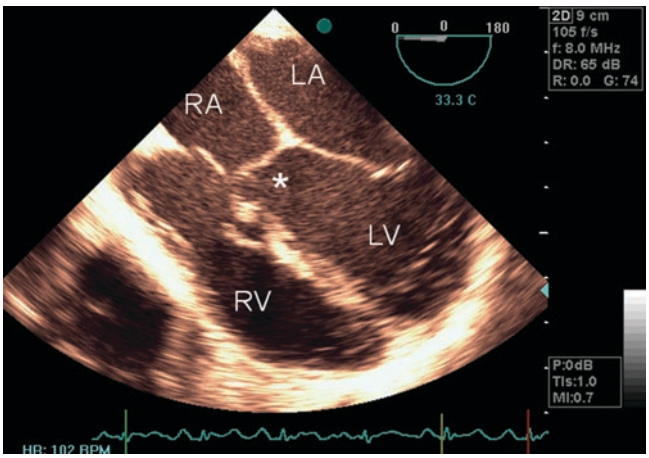

Fig. 3.7 TEE An inlet VSD with straddling and overriding of right AV valve (tricuspid valve) is shown by asterisk in this mid esophageal four chamber view

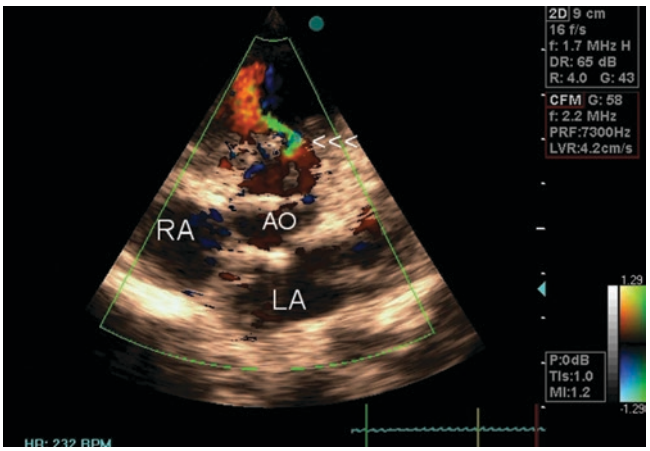

Fig. 3.5 In this TTE, parasternal short axis view arrow heads point to color Doppler flow of outlet VSD at 1 o'clock

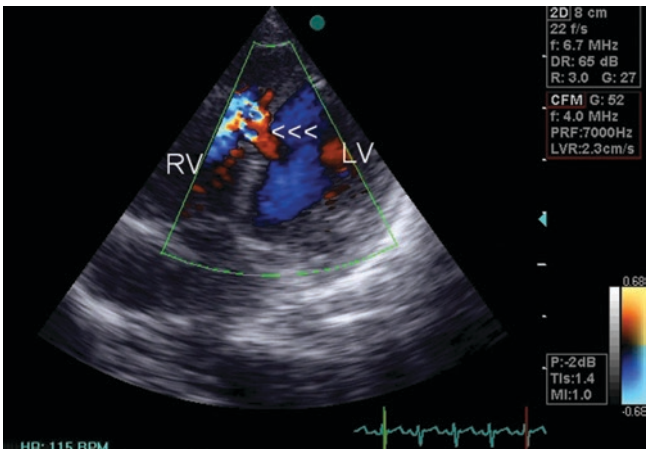

Fig. 3.8 An off axis TTE in four chamber view using color Doppler, arrow heads point to left to right shunt through midmuscular VSD

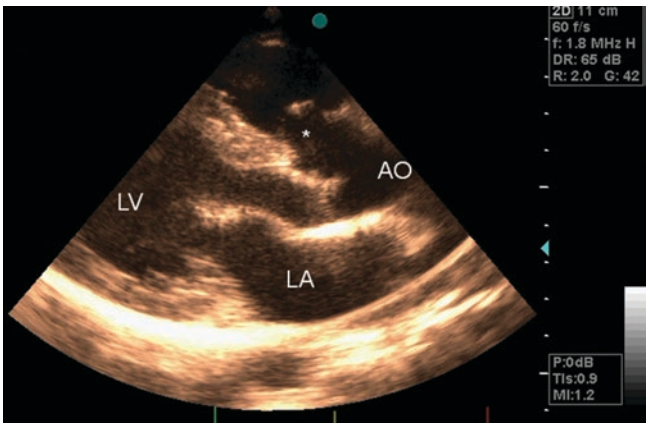

Fig. 3.6 TTE: prolapse of right coronary cusp of aortic valve into VSD is shown by asterisk in this parasternal long axis view of outlet VSD

12. Use Doppler and estimate the pressure gradient across the VSD
13. Detecting VSD during fetal life is challenging because, the pressure gradient between LV and RV is null, making the low velocity bidirectional flow of a fetal VSD detectable only with appropriate color set up. The best approach for detecting perimembranous VSD, would be subcostal five chamber view. When it is approached parallel (apical four chamber view) the "T sign" may be helpful to distinguish a real VSD from pseudo VSD (Fig. 3.9). The "in-plane" view, which can be is acquired by turning the transducer perpendicular from a long-axis view of the LV is useful to confirm VSD presence (Fig. 3.10).

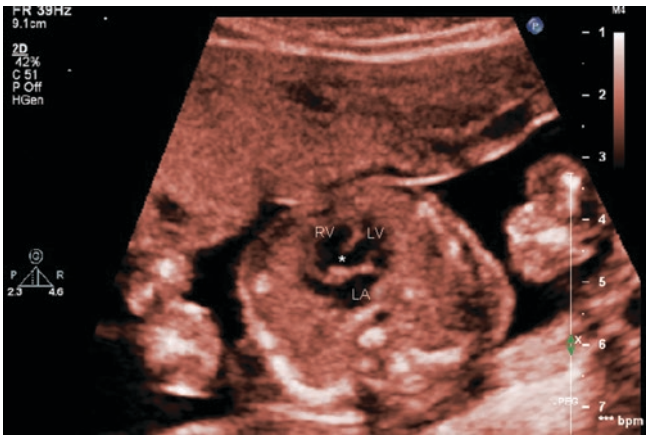

Fig. 3.9 Fetal echocardiogram four chamber view showing a large inlet VSD (asterisk)

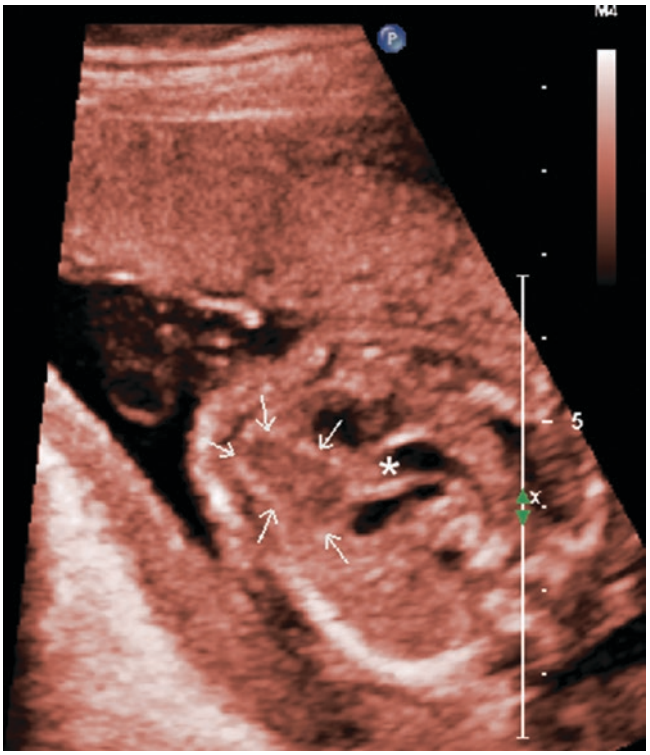

Fig. 3.10 In-plane view of the interventricular septum (a surface view of the septum) (arrows). Asterisk indicates the aorta

Suggested Reading

Anon. Defects in cardiac septation (Chapter 6). In: Snider R, Serwer GA , Ritter SB, editors. Echocardiography in pediatric heart disease, 2nd ed. Mosby-Year Book Inc., 1997, pp. 235-296

Anon. The four-chamber view (Chapter 7). In: Chiappa EM, Cook AC, Botta G, Silverman NH, editors. Echocardiographic anatomy in the fetus. Italia: Springer-Verlag; 2008. p. 59–75. 2nd printing 2009.

Anon. Atrial, ventricular , and atrioventricular septal defects (Chapter 18). In: Abuhamad A, Chaoui R, editors. A practical guide to fetal echocardiography: normal and abnormal hearts. 3rd ed: Wolters Kluwer; 2016. p. 253–80.

Cohen MS, Lopez L. Ventricular septal defects (Chapter 30). In: Allen HD, Shaddy RE, Penny DJ, Feltes TF, Cetta F, editors. Moss and Adams' Heart disease in infants, children, and adolescents including the fetus and young adults. 9th ed: Wolters Kluwer; 2016. p. 783–802.

Gelehrter S, Ensing G. Ventricular septal defects (Chapter 11). In: idem BW, O'leary PW, Cetta F, editors. Echocardiography in pediatric and adult congenital heart disease. 2nd ed: Wolters Kluwer; 2015. p. 198–219.

Kung GC, Wong PC. Ventricular septal defects. In: Wong PC, Miller-Hance WC, editors. Transesophageal echocardiography for congenital heart disease. London: Springer-Verlag; 2014. p. 241–52.

Paladini D, Russo MG, Vassallo M, Tartaglione A. The 'in-plane' view of the inter-ventricular septum. A new approach to the characterization of ventricular septal defects in the fetus. Prenat Diagn. 2003;23:1052–5.

Saker E, Bahri GN, Montalbano MJ, et al. Gerbode defect: a comprehensive review of its history, anatomy, embryology, pathophysiology, diagnosis, and treatment. J Saudi Heart Assoc. 2017;29:283–92.

Patent Ductus Arteriosus (PDA)

4

Azin Alizadehasl and Maryam Moradian

Abstract

Use suprasternal, high parasternal, and parasternal short axis views for direct visualization of PDA, and evaluation of blood flow through it. Pay attention to echocardiographic features of significant left to right shunt, left chambers enlargement.

Patent Ductus Arteriosus (PDA)

1. Assess the presence of patent ductus arteriosus (PDA) in suprasternal long axis, parasternal short axis, and high left parasternal short axis (ductal) views (Fig. 4.1).
2. Evaluate the indirect signs of left to right shunt by two dimensional echocardiography (2D) in four chamber view, left atrial and left ventricular enlargement.
3. Historically M mode echocardiography was used and the left atrium –to aortic ratio (LA/AO ratio) more than 1.15 was considered as a sign of significant left to right shunt
4. Though the normal course of PDA is oblique, in cases of right ventricular out flow tract obstruction (RVOTO), PDA will have vertical orientation and in cases of hypoplastic left heart syndrome (HLHS) and interrupted aortic arch (IAA) it would be large.
5. Use color Doppler to evaluate the flow direction and to align the spectral Doppler beam.
6. Asses the systolic and diastolic pressure gradient between aorta and pulmonary artery (PA) using continuous wave Doppler (CW-Doppler). When pulmonary artery pressure is normal and PDA is restrictive, continuous flow above the base line peaks in late systole (Fig. 4.2).
7. In cases of right to left shunt through PDA like pulmonary artery hypertension, interrupted aortic arch, and HLHS, the spectral Doppler, which shows a continuous flow below the base line, peaks in early systole.
8. Remember that, just after birth, in a normal neonate the PDA shunt would be bidirectional for a while and after some hours it changes to continuous left to right shunt before complete closure (Fig. 4.3).
9. PDA can be evaluated in TEE by locating the probe in the upper esophageal aortic arch short axis position (Fig. 4.4).
10. During fetal life, the ductus arteriosus connects the pulmonary artery and the descending aorta taking part to form the so called, ductal arch (Fig. 4.5).

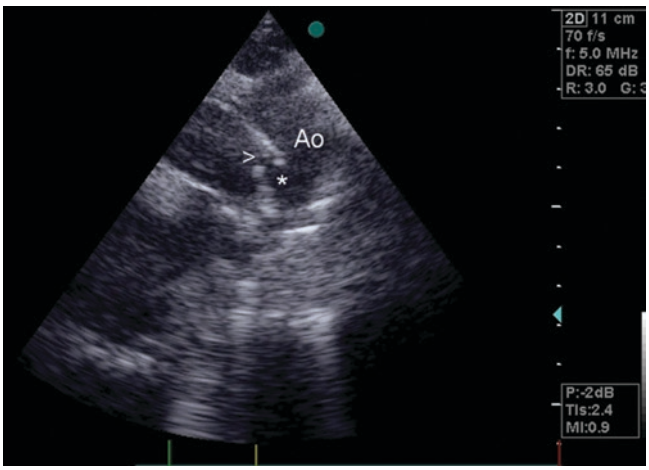

Fig. 4.1 In this suprasternal long axis view asterisk indicate the aortic end and arrow head points to pulmonic end of PDA

A. Alizadehasl (✉)
Department of Cardio-Oncology and Research Center, Rajaie Cardiovascular, Medical & Research Center, Iran University of Medical Sciences, Tehran, Iran

M. Moradian
Pediatric Cardiology, Rajaie Cardiovascular, Medical & Research Center, Iran University of Medical Sciences, Tehran, Iran

M. Moradian, A. Alizadehasl (eds.), *Atlas of Echocardiography in Pediatrics and Congenital Heart Diseases*,
https://doi.org/10.1007/978-3-662-62341-1_4

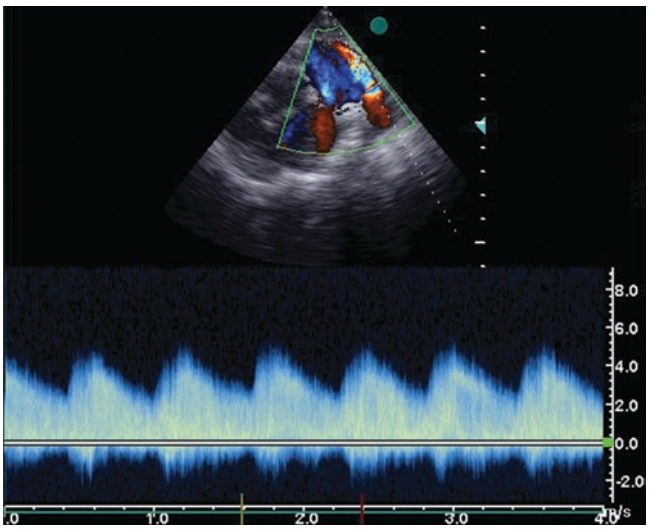

Fig. 4.2 In this oblique left high parasternal view (ductal view) using color Doppler in an infant with normal pulmonary artery pressure, a high velocity turbulent flow can be seen from descending aorta toward pulmonary artery via PDA (upper part of picture) and its Doppler interrogation (lower part of picture) shows continuous left to right shunt above the base line

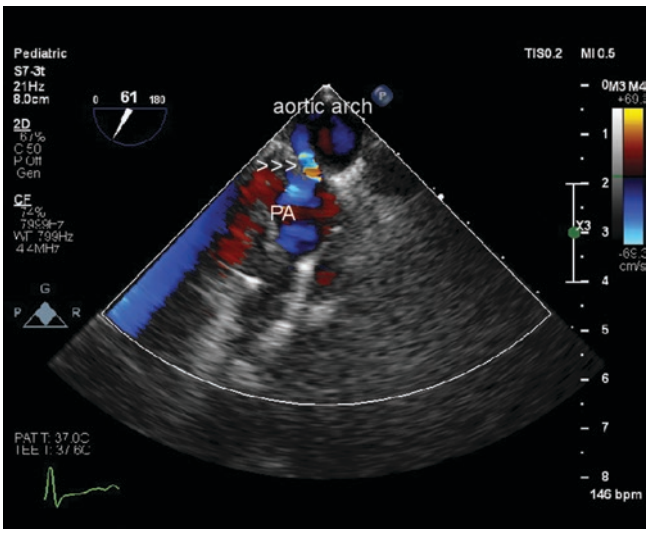

Fig. 4.4 Transesophageal echocardiography (TEE) using color flow Doppler showing turbulent flow (arrow heads) from aorta to pulmonary artery (PA) in upper esophageal aortic arch short axis view

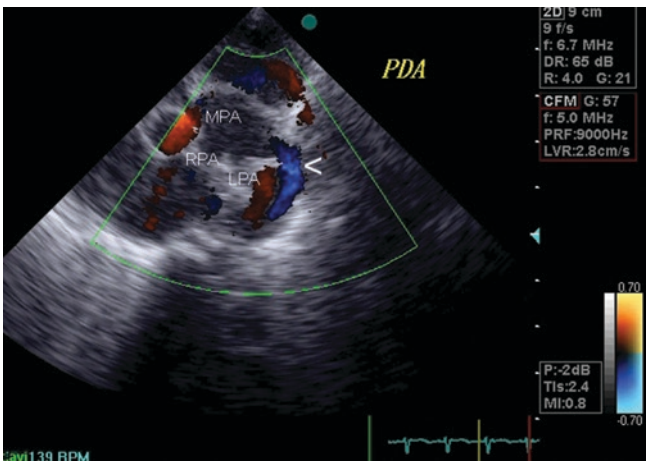

Fig. 4.3 In this ductal view using color Doppler, arrow head points to PDA. The shunt flows from PA to descending aorta due to pulmonary artery hypertension, so it is blue

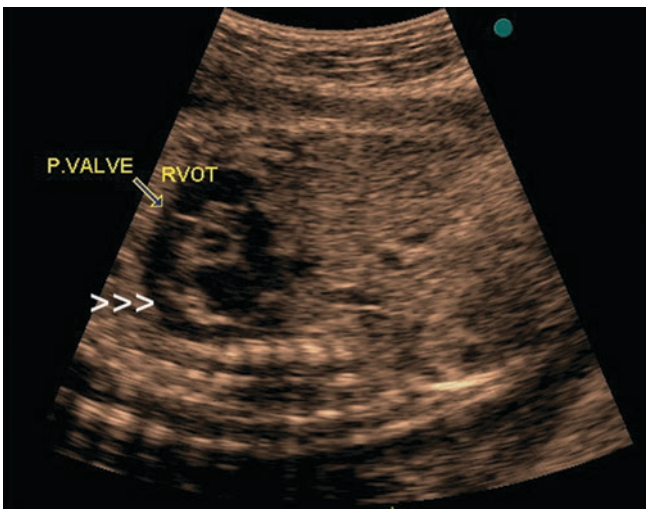

Fig. 4.5 Fetal echocardiography, parasagittal view of ductal arch. Arrow heads indicate the ductus arteriosus. *P. valve* pulmonary valve

Suggested Reading

Anon. Abnormal vascular connections and structures (Chapter 11). In: Snider R, Serwer GA, Ritter SB, editors. Echocardiography in pediatric heart disease, 2nd ed. Mosby-Year Book, Inc. 1997, pp. 235-296

Arlettaz R. Echocardiographic evaluation of patent ductus arteriosus in preterm infant. Front Pediatr. 2017;5:147. https://doi.org/10.3389/fped.2017.00147.

Gournay V. The ductus arteriosus: physiology, regulation, and functional and congenital anomalies. Arch Cardiovasc Dis. 2011;104:578–85.

Miller-Hance WC. Great artery and other vascular abnormalities (Chapter 13). In: Wong PC, Miller-Hance WC, editors. Transesophageal echocardiography for congenital heart disease. London: Springer-Verlag; 2014. p. 341–69.

Sachdeva R. Patent ductus arteriosus and aortopulmonary window (Chapter 19). In: Eidem BW, O'leary PW, Cetta F, editors. Echocardiography in pediatric and adult congenital heart disease. 2nd ed: Wolters Kluwer; 2015. p. 364–73.

Su B, Watanabe T, Shimizu M, Yanagisawa M. Echocardiographic assessment of patent ductus arteriosus shunt flow pattern in premature infant. Arch Dis Childhood. 1997;77:F36–40.

Su BH, Peng CT, Tsai CH. Echocardiographic flow pattern of patent ductus arteriosus: a guide to indomethacin treatment in premature infants. Arch Dis Child Fetal Neonatal Ed. 1999;81:F197–200.

Taggart NW, Qureshi MY. Patent ductus arteriosus and aortopulmonary window (Chapter 31). In: Allen HD, Shaddy RE, Penny DJ, Feltes TF, Cetta F, editors. Moss and Adams' Heart disease in infants, children, and adolescents including the fetus and young adults. 9th ed: Wolters Kluwer; 2016. p. 803–21.

Wu TW, Azhibekov T, Seri I. Transitional hemodynamics in preterm neonates: clinical relevance. Pediatr Neonatal. 2016;57:7–18.

Zhang XY, Cao TS, lJ Y, et al. Value of the echocardiographic suprasternal view for diagnosis of patent arteriosus subtypes. J Ultrasound Med. 2012;31:1421–7.

Aortopulmonary Window Defect (AP Window)

5

Maryam Moradian

Abstract

Use parasternal short axis, subcostal, and suprasternal views for direct visualization of AP window. Commonly the left to right shunt causes left atrial and ventricular enlargement and pulmonary artery dilation.

Aortopulmonary Window Defect (AP Window)

1. Always remember that the important anatomic finding of aortopulmonary widow is the location of the defect, between ascending aorta and the pulmonary artery above aortic and pulmonary valves.
2. The best echocardiographic views for evaluation of AP window are parasternal short axis, subcostal, and suprasternal (Fig. 5.1). So evaluate the size and type of the defect (Type I, II, III, or intermediate) in these views as follow:
   (a) **Type I**, the most common type, the defect is midway between the semilunar valves and pulmonary bifurcation, so it is proximal
   (b) **Type II** or distal defect, the communication is between posterior wall of ascending aorta at the junction of right pulmonary artery (RPA) and main pulmonary artery (MPA).
   (c) **Type III**, or total defect the entire length of pulmonary trunk from semilunar valve to bifurcation and proximal of RPA is absent.
   (d) **Intermediate type** which is recommended by the Society of Thoracic Surgeons the defect is small and central with a circumferential rim of tissue (Fig. 5.2)
3. The effects of left to right shunt can be seen as Left atrial enlargement (LAE), left ventricular enlargement (LVE)

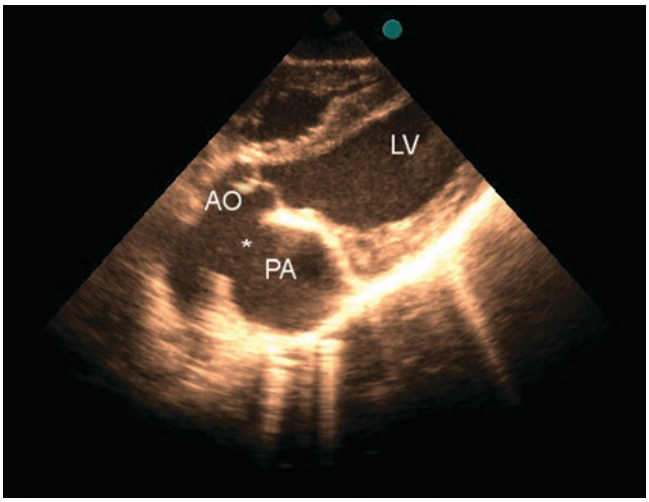

Fig. 5.1 In this subcostal coronal view the asterisk indicate the large window between aorta and dilated MPA. *LV* left ventricle, *AO* aorta, *PA* dilated main pulmonary artery

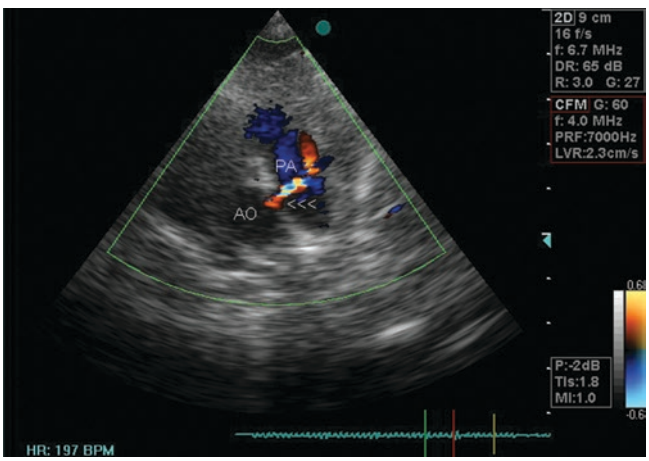

Fig. 5.2 Parasternal short axis view using color Doppler. The arrow heads points to intermediate type AP window *AO* aorta, *PA* pulmonary artery

M. Moradian (✉)
Pediatric Cardiology, Rajaie Cardiovascular, Medical & Research Center, Iran University of Medical Sciences, Tehran, Iran

M. Moradian, A. Alizadehasl (eds.), *Atlas of Echocardiography in Pediatrics and Congenital Heart Diseases*,
https://doi.org/10.1007/978-3-662-62341-1_5

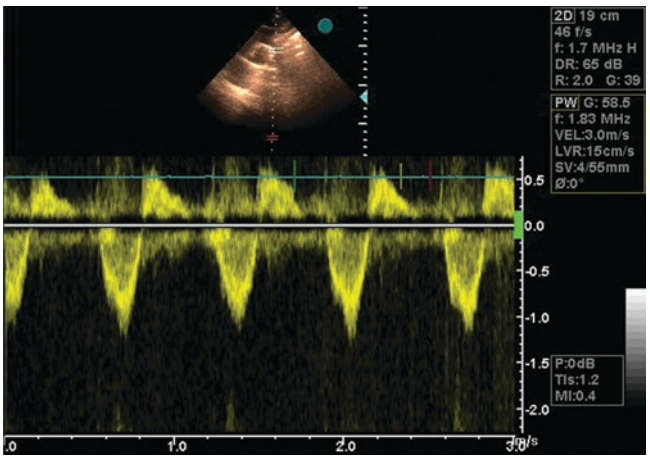

Fig. 5.3 Suprasternal long axis view showing retrograde diastolic flow above the baseline by using PW Doppler and putting the sample volume in proximal descending aorta, the so called diastolic runoff

and, pulmonary artery dilation in four chamber and parasternal short axis views.

4. Use pulsed wave (PW) Doppler interrogation in descending aorta and evaluate the retrograde diastolic flow in proximal descending aorta (Fig. 5.3).
5. Also use PW Doppler interrogation to evaluate the continuous antegrade flow in pulmonary artery distal to AP window, caused by large left to right shunt from aorta to pulmonary artery in cases of normal pulmonary artery pressure.
6. It is particularly important not to forget to evaluate for other associated cardiac anomalies especially interrupted aortic arch.
7. In Transesophageal echocardiography use high eshophageal ascending aorta short axis view to see any defect between pulmonary artery and ascending aorta.
8. Three vessel view in fetal echocardiography would be helpful to show aortopulmonary window defect as a connection between two great arteries.

Suggested Reading

Backer CL, Mavroudis C. Surgical management of aortopulmonary window: a 40-year experience. Eur J Cardiothorac Surg. 2002;21(5):773–9.

El Haouati R, Boukaidi Y, Zouizra Z. Boumzebra aortopulmonary window associated with an ascending aorta aneurysm in an adult. J Teh Univ Heart Ctr. 2015;10(3):156–8.

Kadohira I, Miyakoshi K, Yoshimura Y. Prenatal images of the aortopulmonary window with an interrupted. Aortic Arch Pediatric Cardiol. 2013;34(5):1288–9.

Pillekamp F, Hannes T, Koch D, Brockmeier K, Sreeram N. Transcatheter closure of symptomatic aortopulmonary window in an infant. Images Paediatr Cardiol. 2008;10(2):11–7.

Sachdeva R. (Chapter 19). In: Idem B W, O'leary PW, Cetta F, editors. Echocardiography in pediatric and adult congenital heart disease .2nd ed. Wolters Kluwer, 2015. p 364–73

Taggart NW, Qureshi MY. Patent ductus arteriosus and aortopulmonary window (Chapter 31). In: Allen HD, Shaddy RE, Penny DJ, Feltes TF, Cetta F, editors. Moss and Adams' Heart disease in infants, children, and adolescents including the fetus and young adults. 9th ed: Wolters Kluwer; 2016. p. 803–20.

Tirado AM, De Soto JS, Montero JG, et al. Aortopulmonary window: clinical assessment and surgical results. Rev Esp Cardiol. 2002;55(3):266–70.

Valsangiacomo ER, Smallhorn JF. Prenatal diagnosis of aortopulmonary window by fetal echocardiography. Circulation. 2002;105:e192.

Anomalous Left Coronary Artery from the Pulmonary Artery (ALCAPA)

6

Maryam Moradian

Abstract

Left ventricular endocardial fibrotic changes and mitral regurgitation in an infant are important clues and one have to rule out the abnormal origin of left coronary artery from pulmonary artery in different echocardiography windows especially parasternal short axis view.

Anomalous Left Coronary Artery from the Pulmonary Artery (ALCAPA)

1. Evaluate the size and origin of coronary arteries in parasternal short axis view. Rotate the transducer clockwise and counter clockwise to see the origin of left main coronary artery (LMCA) and right coronary artery (RCA), respectively. Pay attention to any abnormal dilation of RCA, sometimes by using higher frequency you will get better penetration and better resolution to find the origination of left coronary artery (LCA) from main pulmonary artery (MPA) (Fig. 6.1).
2. Use color Doppler to evaluate the left to right shunt from coronary artery to pulmonary artery (PA) which is prominently diastolic, don't forget to reduce the Nyquist limit to 20–40 cm/s. Also evaluate collateral vessels with abnormal diastolic flow and tortuous course in the ventricular septum and left ventricular free wall (Figs. 6.2 and 6.3)
3. Evaluate the size and function of both ventricles. Any regional wall motion abnormality (RWMA), and endocardial fibrotic changes in left ventricle (LV) should be mentioned. In some patients development of collaterals preserve LV function.

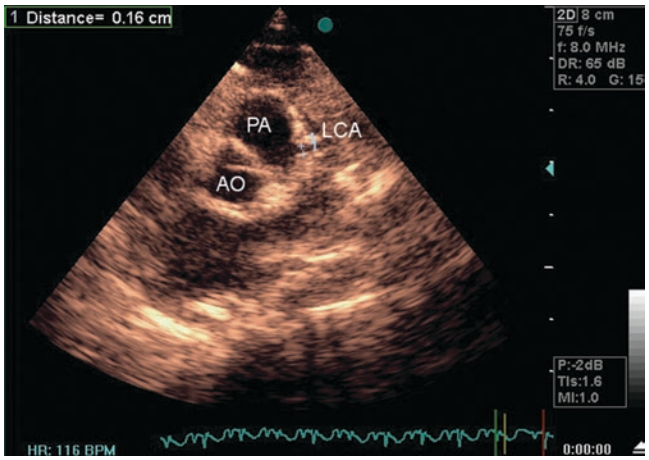

Fig. 6.1 In this parasternal short axis view the abnormal origin of left coronary artery (LCA) from pulmonary artery (PA) can be seen

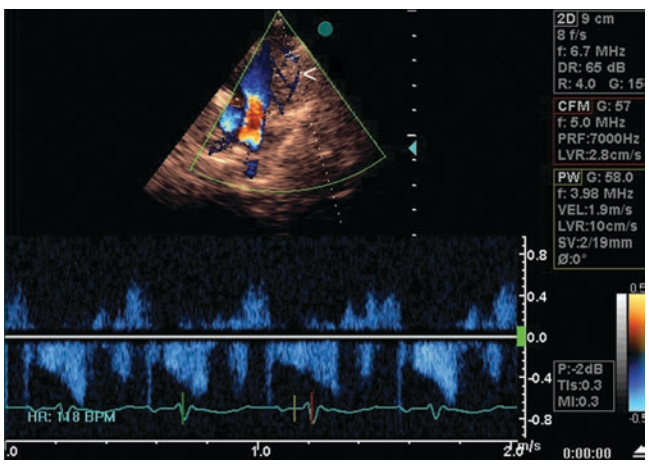

Fig. 6.2 Mainly diastolic flow of coronary collateral vessels in this case of ALCAPA is shown by PW Doppler profile. Arrow head points to a collateral vessels

M. Moradian (✉)
Pediatric Cardiology, Rajaie Cardiovascular, Medical & Research Center, Iran University of Medical Sciences, Tehran, Iran

M. Moradian, A. Alizadehasl (eds.), *Atlas of Echocardiography in Pediatrics and Congenital Heart Diseases*,
https://doi.org/10.1007/978-3-662-62341-1_6

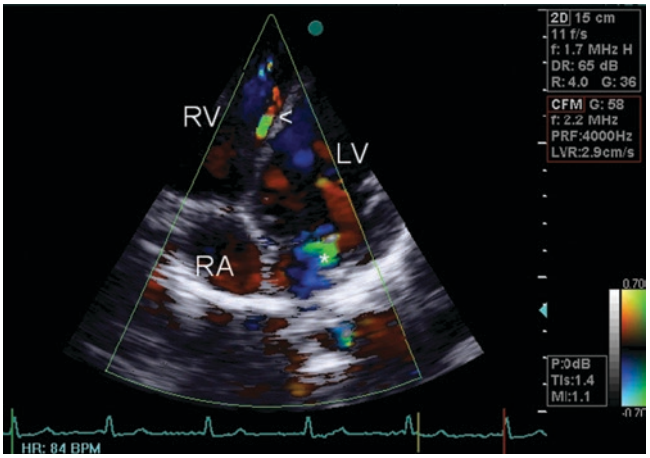

Fig. 6.3 In this color Doppler interrogation of septum at four chamber view, coronary collateral flow is indicated by arrow head, and mitral regurgitation is shown by asterisk

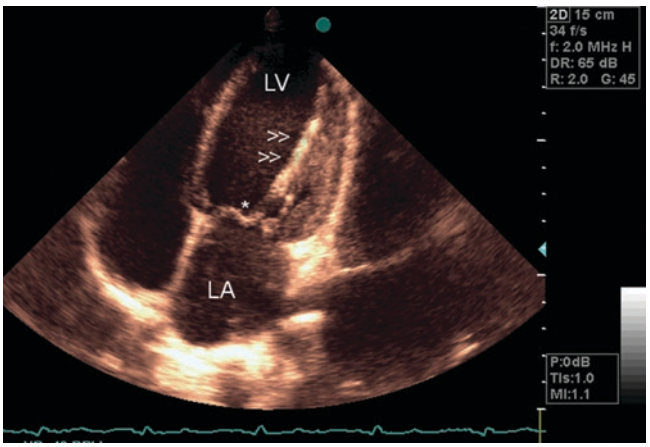

Fig. 6.4 Fibrotic changes of chorda and papillary muscle of mitral valve (MV) are indicated by arrow heads and the asterisk shows mitral valve prolapse (MVP). Also left atrial (LA) and ventricular (LV) enlargement can be appreciated in this apical four chamber view

4. Chronic ischemia will cause fibrotic changes on mitral valve (MV), chorda, and papillary muscles which can lead to the development of mitral valve prolapse and regurgitation (Fig. 6.4)
5. Remembere that, ALCAPA may be associated with tetralogy of Fallot or other congenital heart diseases (Fig. 6.5)
6. In transesophageal echocardiography mid- esophageal aortic valve short axis view is helpful to evaluate the origin of LCA
7. ALCAPA is well tolerated during fetal life and has no harmful effect because both pressures and oxygen saturations are similar in the aorta and pulmonary artery and LMCA and RCA receive forward flow from the great arteries

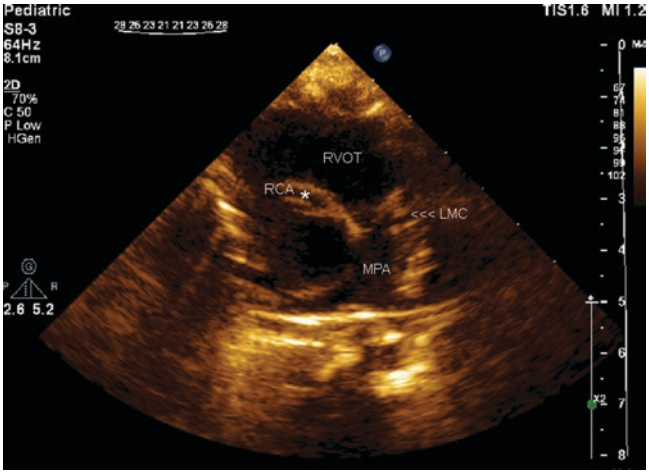

Fig. 6.5 Parasternal short axis view of a child who suffered from Tetralogy of Fallot and severe LV dysfunction due to ALCAPA. Arrow heads point to pulmonary origin of LMC asterisk indicate the normal origin of RCA from aorta. *RVOT* right ventricular out flow tract, *MPA* main pulmonary artery, *LMC* left main coronary artery, *RCA* right coronary artery

Suggested Reading

Frommelt PC. Congenital coronary artery anomalies (Chapter 14). In: Wong PC, Miller-Hance WC, editors. Transesophageal echocardiography for congenital heart disease. London: Springer-Verlag; 2014. p. 371–82.

Frommelt MA, Frommelt PC. Vascular anomalies (Chapter 26). In: Idem BW, O'leary PW, Cetta F, editors. Echocardiography in pediatric and adult congenital heart disease. 2nd ed: Wolters Kluwer; 2015. p. 364–73.

Hallmark K. Anomalous Left Coronary Artery from the Pulmonary Artery (ALCAPA). JDMS. 2005;21:142–7.

Lim DS, Matherne GP. Congenital anomalies of the coronary vessels and the aortic root. In: Allen HD, Shaddy RE, Penny DJ, Feltes TF, Cetta F, editors. Moss and Adams' Heart disease in infants, children, and adolescents including the fetus and young adults. 9th ed: Wolters Kluwer; 2016. p. 821–33.

Oncel G, Once D. Anomalous origin of the left coronary artery from the pulmonary artery: diagnosis with CT angiography. J Clin Imaging Sci. 2013;3:4.

Varghese MJ, Kothari SS. The caveats in the diagnosis of anomalous origin of left coronary artery from pulmonary artery (ALCAPA). Images Paediatr Cardiol. 2010;12(3):3–8.

Haiyan Yang, Jinqing Li, Xiaojuan Ji. Diagnosis of anomalous origin of the left coronary artery from the pulmonary artery with echocardiography and digital subtraction angiography

Coronary Artery Fistula (CAF) or Coronary Cameral Fistula

7

Maryam Moradian

Abstract

Dilatation of the origin of one coronary artery while the other is normal size along with dilation of left cardiac chambers should rise the suspicion of presence of large coronary artery fistula. Following the course of fistula by color Doppler interrogation help to find the receiving chamber which would be dilated as well.

Coronary Artery Fistula (CAF) or Coronary Cameral Fistula

1. If the origin of coronary arteries are normal, but one of them, especially right coronary artery (RCA) is dilated and tortuous, don't forget to check for coronary artery fistula (CAF) or coronary-cameral fistula. Remember that most coronary artery fistulas originate from right coronary artery (Figs. 7.1 and 7.2)
2. By using color Doppler, track the course and drainage site which most probably would be one of the right chambers including right ventricle (RV), right atrium (RA), coronary sinus (CS), pulmonary artery, and pulmonary vascular bed (Fig. 7.3).
3. Use different windows to follow the CAF course. Try to evaluate the flow which is prominently diastolic by Doppler interrogation (Fig. 7.4a–c)
4. If the shunt is not significant; the size of the receiving chamber will be normal but in cases of significant shunt both left chambers and the receiving chamber are enlarged and there would be diastolic aortic runoff, while interrogating aortic arch by color flow Doppler.
5. As even small sized coronary fistulae may grow up over time, follow up imaging is reasonable.

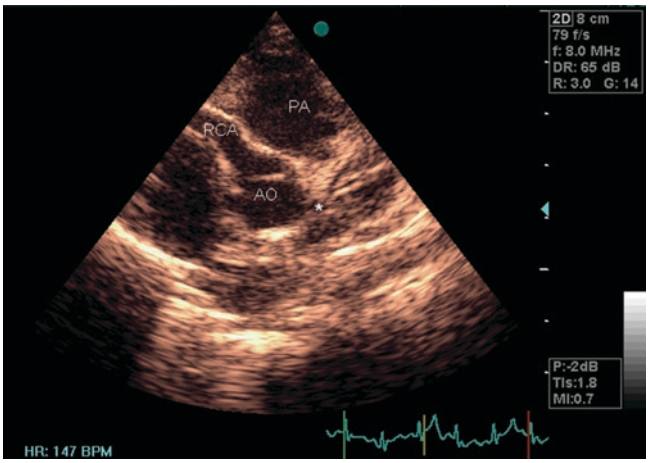

Fig. 7.1 Parasternal short axis view showing severely dilated right coronary artery (RCA) asterisk indicate the left coronary artery (LCA). Compare the size of RCA and LCA. RCA is massively dilated and LCA has normal size. *PA* pulmonary artery, *AO* aorta, *RCA* right coronary artery

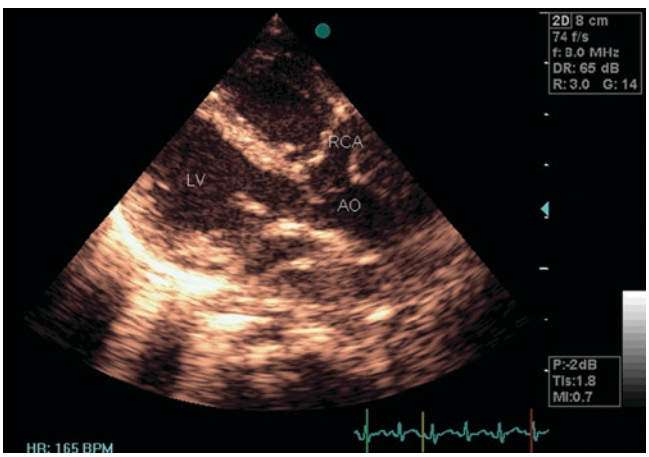

Fig. 7.2 Parasternal long axis view of the same patient as above. *LV* left ventricle

M. Moradian (✉)
Pediatric Cardiology, Rajaie Cardiovascular, Medical & Research Center, Iran University of Medical Sciences, Tehran, Iran

M. Moradian, A. Alizadehasl (eds.), *Atlas of Echocardiography in Pediatrics and Congenital Heart Diseases*,
https://doi.org/10.1007/978-3-662-62341-1_7

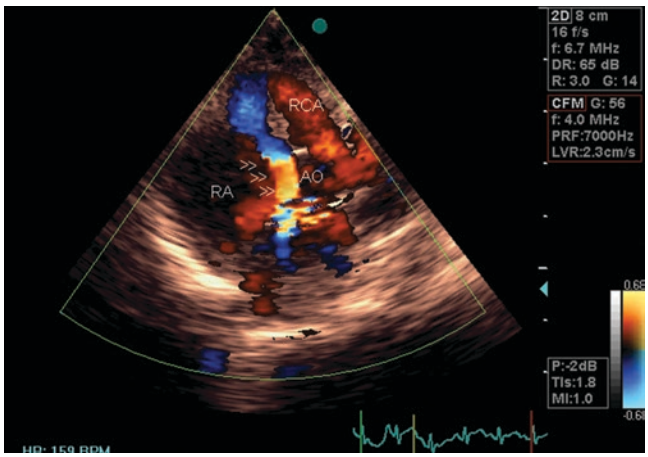

Fig. 7.3 Fistula course of the above patient is tracked by using color Doppler. Dilated and tortuous RCA fistula empties into left atrium (arrow heads show the course of fistula toward LA)

Fig. 7.5 Transesophageal echocardiography (TEE) in mid esophageal aortic valve short axis view showing normal size both coronary arteries. *LA* left atrium, *RA* right atrium, *AO* aorta, *LCA* left coronary artery, *RCA* right coronary artery

Fig. 7.4 (**a**–**c**) Transethoracic echocardiography showing dilation of left coronary artery (LCA) and left anterior descending artery (LAD) in two dimensional echocardiography (**a**). Color Doppler interrogation (**b**) is used to track the course of fistula and pulse Doppler profile confirm its prominently diastolic flow (**c**)

6. Evaluate the coronary artery size and origin in transesophageal echocardiography (TEE) and use mid esophageal aortic valve short axis view (Fig. 7.5) to evaluate the origin of both right and left coronary arteries
7. Visualization of normal size coronary artery in fetal echocardiography is difficult but dilation of coronary vessels make them visible in cases of large CAF.

Suggested Reading

Anon. Abnormal vascular connections and structures (Chapter 11). In: Snider R, Serwer GA, Ritter SB, editors. Echocardiography in pediatric heart disease. 2nd ed: Mosby-Year Book, Inc.; 1997. p. 235–96.

Chae U, Lee MY, Kim H, et al. Prenatal diagnosis of isolated coronary arteriovenous fistula. Obstet Gynecol Sci. 2018;61(1):161–4.

Chen BH, Lin CC, Weng HW, et al. Echocardiographic diagnosis of incidentally found left coronary artery to pulmonary artery fistula in an 11-year-old girl. Acta Cardiol Sin. 2016;32:359362.

Frommelt PC. Congenital coronary artery anomalies (Chapter 14). In: Wong PC, Miller-Hance WC, editors. Transesophageal echocardiography for congenital heart disease. London: Springer-Verlag; 2014. p. 371–82.

Frommelt MA, Frommelt PC. Vascular anomalies (Chapter 26). In: Idem BW , O'leary PW, Cetta F, editors . Echocardiography in pediatric and adult congenital heart disease. 2nd ed. Wolters Kluwer, 2015, pp. 470-485

Jung C, Jorns C, Huhta J. Doppler findings in a rare coronary artery fistula. Cardiovasc Ultrasound. 2007;5:10.

Lim DS, Matherne GP. Congenital anomalies of the coronary vessels and the aortic root (Chapter 32). In: Allen HD, Shaddy RE, Penny DJ, Feltes TF, Cetta F, editors. Moss and Adams' heart disease in infants, children, and adolescents Including the fetus and young adults. 9th ed: Wolters Kluwer; 2016. p. 821–33.

Nagiub M, Mahadin D, Gowda S, Aggarwal S. Prenatal diagnosis of coronary artery fistula: a case report and review of literature. Am J Perinatol Rep. 2014;4:e83–6.

Song G, Zhang J, Ren W, et al. Pediatric coronary artery fistula: echocardiographic case reports and literature review of treatment strategy. Springer Plus. 2016;5:1583.

Xie M, Li L, Cheng TO, et al. Coronary artery fistula: comparison of diagnostic accuracy by echocardiography versus coronary arteriography and surgery in 63 patients studied between 2002 and 2012 in a single medical center in China. Int J Cardiol. 2014;176(2):470–7.

Aortic-Left Ventricular Defect (Tunnel)

8

Maryam Moradian

Abstract

Severe aortic regurgitation during infancy should rise the suspicion of aortic-left ventricular tunnel. Adding Color flow Doppler on two dimensional echocardiography will show non-valvular aortic regurgitation through aortic -left ventricular tunnel. Differentiating from rupture of Valsalva sinus is also challenging.

Aortic-Left Ventricular Defect (Tunnel)

1. Significant aortic regurgitation especially in an infant should raise the suspicion of aortic-left ventricular tunnel, which in fact is a non valvular aortic regurgitation
2. Evaluate this extra cardiac tubular structure in different echocardiography views including parasternal long and short axis, and subcostal views (Fig. 8.1)
3. These tunnels are commonly short and direct.
4. Most commonly these tunnels opening in aorta lie above the right coronary sinus of Valsalva and terminate in the left ventricle.
5. Use color Doppler and continuous Doppler profile to confirm that aortic regurgitation is not through the aortic valve. Also Doppler study will show diastolic flow from aorta to the left ventricle, and systolic flow from left ventricle to aorta (Figs. 8.2 and 8.3).
6. Don't forget to evaluate the size of entry and exit of the tunnel as well as size and function of left ventricle. Occurrence of Heart failure depends on the cross-sectional area of tunnel and the amount of non-valvular aortic regurgitation through the tunnel.
7. Pay attention to any aortic dilation (aortopathy), deformation and sagging of right coronary cusp which is

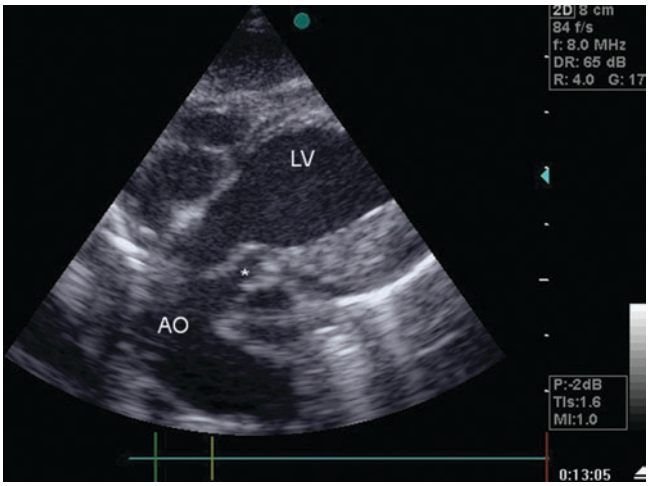

Fig. 8.1 Subcostal coronal view, the asterisk indicate an aortic-left ventricular tunnel. *LV* left ventricle, *AO* aorta

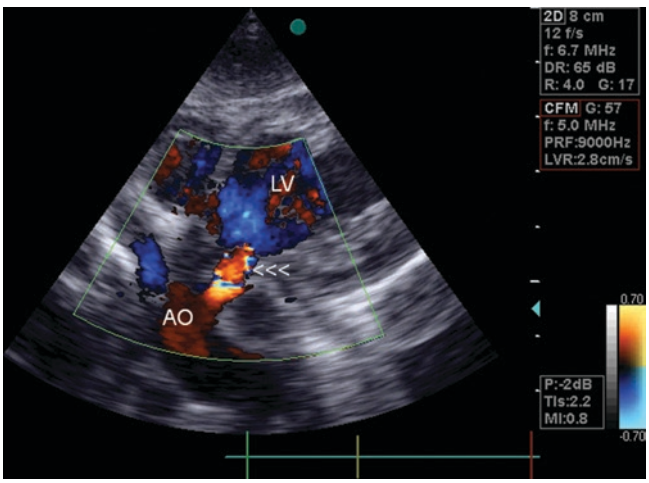

Fig. 8.2 Color flow Doppler in same patient as above, this diastolic frame shows non-valvular aortic regurgitation through aortic-left ventricular tunnel (arrow heads)

M. Moradian (✉)
Pediatric Cardiology, Rajaie Cardiovascular, Medical & Research Center, Iran University of Medical Sciences, Tehran, Iran

M. Moradian, A. Alizadehasl (eds.), *Atlas of Echocardiography in Pediatrics and Congenital Heart Diseases*,
https://doi.org/10.1007/978-3-662-62341-1_8

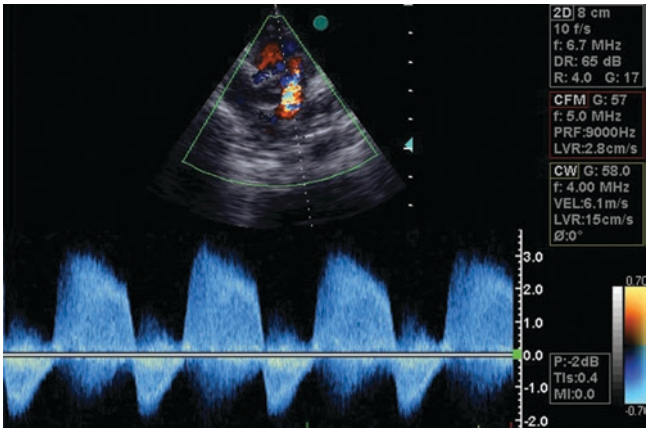

Fig. 8.3 Doppler interrogation via Aortic-left ventricular tunnel of the same patient as above showing to and fro passage of blood through tunnel (diastolic flow from aorta to the left ventricle, and systolic flow from left ventricle to aorta)

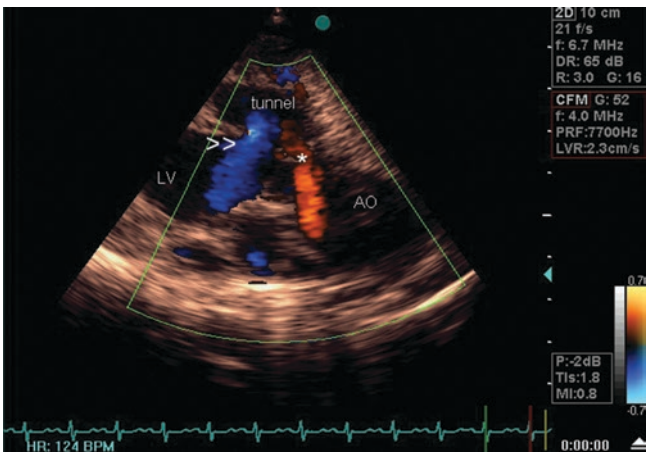

Fig. 8.4 Parasternal long axis view using color Doppler, showing the entry (asterisk) and the exit (arrow heads) of a large aneurysmal AO-LV tunnel. There is no regurgitation through aortic valve but severe non-valvular aortic regurgitation leads to left ventricular enlargement. Aorta is also dilated in this case

common in this anomaly. Also aortic cusps may be thickened and there may be associated bicuspid aortic valve or aortic stenosis

8. Sometimes these tunnels are large and aneurysmal (Fig. 8.4).
9. Differentiate this anomaly from fistula of coronary artery to left ventricular by the finding of normal size right and left main coronary arteries
10. This anomaly may be mistaken with VSD in two dimensional echo, but color flow mapping confirms that there is no communication between left and right ventricles
11. To differentiate this anomaly from ruptured sinus of Valsalva aneurysm show that aortic end of tunnel is above the coronary ostium and Valsalva sinus is not dilated. In ruptured sinus of Valsalva the defect is located under coronary ostium. Also as most of the sinus of Valsalva aneurysms are located in the right aortic sinus and rupture to right side chambers (right ventricle and right atrium) they produce continuous flow profile in Doppler study (Fig. 8.5)
12. On fetal echocardiography presence of aortic root dilation and blood flow around aortic valve and within the tunnel as well as reduced left ventricular function should rise the suspicion of this diagnosis

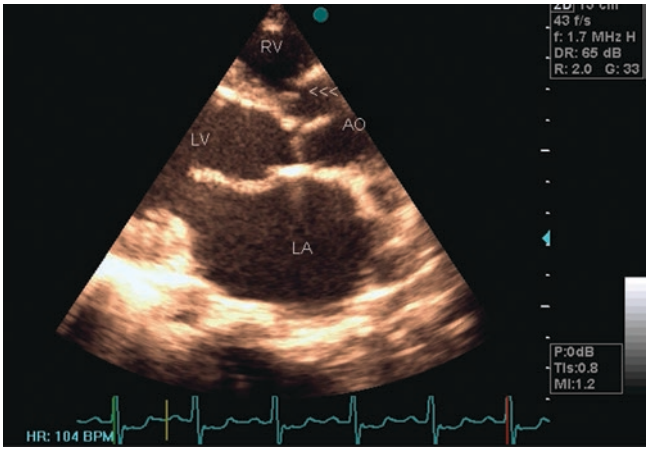

Fig. 8.5 Transthoracic parasternal long axis view of a patient with ruptured Valsalva sinus to right ventricle. Arrow heads point to defect between right sinus of Valsalva and right ventricle. Pay attention to enlarged Left ventricle and left atrium due to significant left to right shunt. *LV* left ventricle, *LA* left atrium, *AO* aorta, *RV* right ventricle

Suggested Reading

Anon. Abnormalities of ventricular outflow (Chapter 10). In: Snider R, Serwer GA, Ritter SB, editors. Echocardiography in pediatric heart disease. 2nd ed: Mosby-Year Book, Inc.; 1997. p. 408–51.

Caliani JA, Gouvêa FR, Simões LC, Dorigo AH, et al. Surgical treatment of aortic-left ventricular fistula. Rev Bras Cir Cardiovasc. 2004;19(2):183–5.

Kathare P, Subramanyam RG, Dash TK, Muthuswamy KS, et al. Diagnosis and management of aorto-left ventricular tunnel. Ann Pediatr Cardiol. 2015;8(2):103–7.

Lim DS, Matherne GP. Congenital anomalies of the coronary vessels and the aortic root (Chapter 32). In: Allen HD, Shaddy RE, Penny DJ, Feltes TF, Cetta F, editors. Moss and Adams' Heart disease in infants, children, and adolescents Including the fetus and young adults. 9th ed: Wolters Kluwer; 2016. p. 821–33.

Martins JD, Sherwood MC, John E, Mayer JE, Keane JF. Aortico–left ventricular tunnel: 35-year experience. J Am College Cardiol. 2004;44(2):446–50.

McKay R. Aorto-ventricular tunnel. Orphanet J Rare Dis. 2007;2:41.

Moradian M. Diagnostic errors in echocardiography: review of five interesting pediatric cases. J Teh Univ Heart Ctr. 2012;7(1):33–6.

Saritas T, Erol N, Erdem A, Karaci K, Celebi A. Management of aortico-left ventricular tunnel. J Cardiovasc Dis Res. 1(4):206–9.

Cranial Arteriovenous Malformation (Cranial AV Malformation)

9

Maryam Moradian

Abstract

One severe type of cranial AV malformation, vein of Galen aneurysm, causes sign and symptoms soon after birth which are confused with congenital heart defects. Even echocardiography may be tricky and misinterpreted as persistence pulmonary hypertension of newborn syndrome (PPHNS) but diastolic reversal flow (diastolic runoff) in descending aorta and dilated brachiocephalic arteries help the diagnosis.

Cranial Arteriovenous Malformation (Cranial AV Malformation)

1. In a newborn presenting with cyanosis and heart failure be careful not to miss vein of Galen aneurysm. Systemic arteriovenous malformations (AVM) especially large cranial AV malformation or vein of Galen aneurysm may present with cardiac symptoms soon after birth.
2. Simultanous dilation of right cardiac chambers, ascending aorta, carotid arteries, and superior vena cava (SVC) in two dimensional echocardiography should rise the suspicion of cranial AV malformation (Figs. 9.1 and 9.2).
3. Use color Doppler interrogation to evaluate the direction of shunt via patant ductus arteriosus (PDA) (Fig. 9.3a, b) and patent foramen ovale (PFO) (Fig. 9.4a, b). During neonatal period, elevated pulmonary vascular resistance and decrease in the total systemic vascular resistance caused by the presence of a large AV malformation promotes right-to-left ductal shunting and also large venous return to the right atrium from the AV malformation leads to right-to-left shunt via foramen ovale. These findings

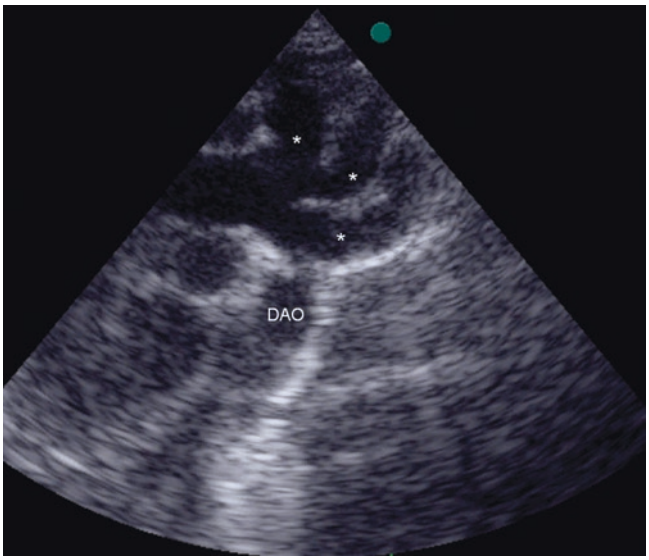

Fig. 9.1 Suprasternal long axis view showing dilated ascending aorta and brachiocephalic arteries (asterisks)

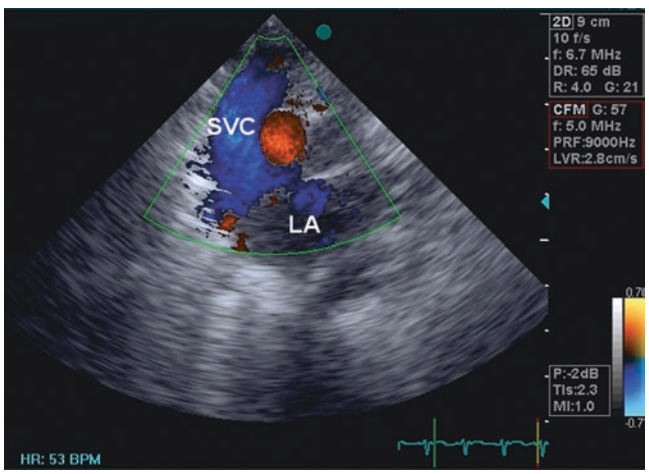

Fig. 9.2 Transthoracic suprasternal short axis view in a new born suffering from cranial AV malformation. Superior vena cava (SVC) is dilated

M. Moradian (✉)
Pediatric Cardiology, Rajaie Cardiovascular, Medical & Research Center, Iran University of Medical Sciences, Tehran, Iran

M. Moradian, A. Alizadehasl (eds.), *Atlas of Echocardiography in Pediatrics and Congenital Heart Diseases*,
https://doi.org/10.1007/978-3-662-62341-1_9

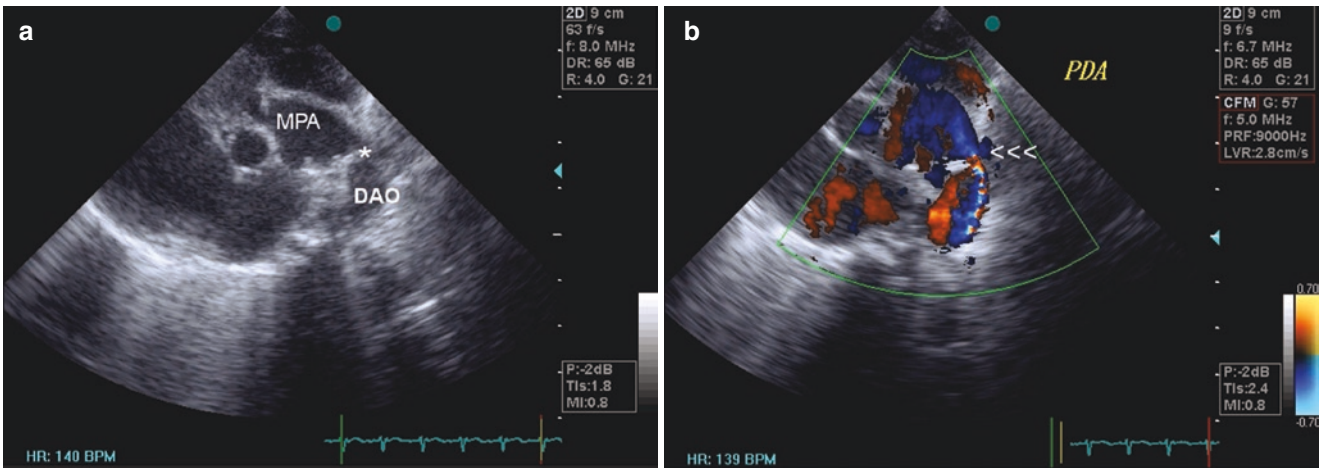

Fig. 9.3 (**a**, **b**) Ductal view of a neonate suffering from large aneurysm of vein of Galen in figure (**a**) asterisk indicate the PDA connecting dilated main pulmonary artery to descending aorta and in figure (**b**) right to left shunt via PDA is demonstrated. *MPA* main pulmonary artery, *DAO* descending aorta

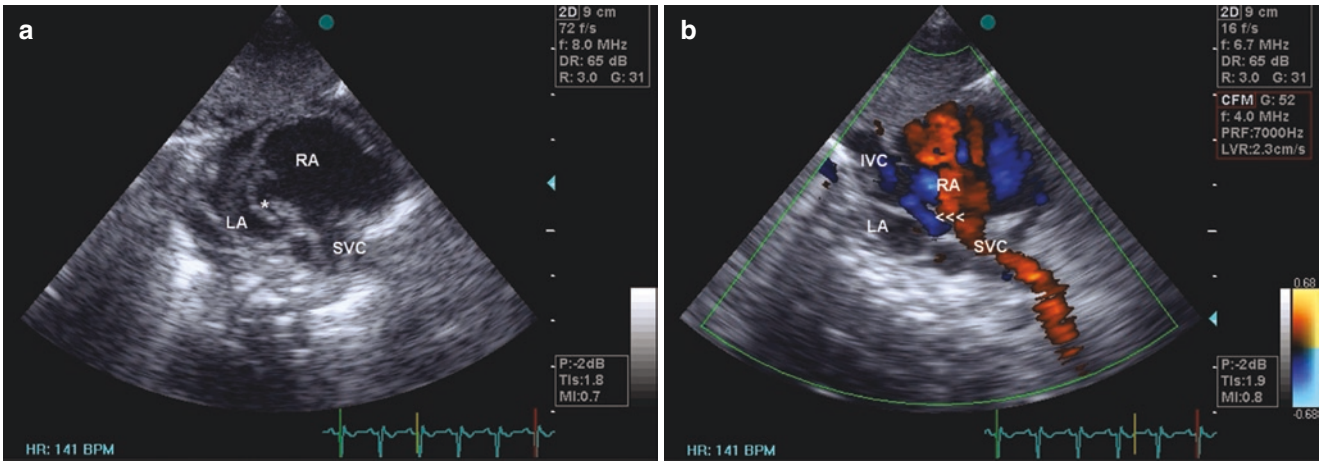

Fig. 9.4 (**a**, **b**) Subcostal short axis view of a neonate suffering from cranial AV malformation. Right atrium is dilated and asterisk indicate patent foramen ovale (PFO) (**a**) and right to left shunt via PFO is indicated by arrow heads in (**b**)

may be misinterpreted as persistence pulmonary hypertension of newborn syndrome (PPHNS)

4. Spectral Doppler interrogation of PDA, will confirm continuous flow below the base line, peaks in early systole indicating pulmonary hypertension (Fig. 9.5)
5. Color and spectral Doppler will also help to evaluate retrograde diastolic flow in descending aorta into cerebral arteries or aortic diastolic runoff (Figs. 9.6 and 9.7). Remember that aortopulmonary window, severe aortic valve regurgitation, coronary artery fistulas, and systemic-to-pulmonary fistulas should be ruled out.
6. Aneurysm of the vein of Galen can be diagnosed by antenatal ultrasonography and may lead to cardiomegaly, nonimmune hydrops, and hydrocephalus.

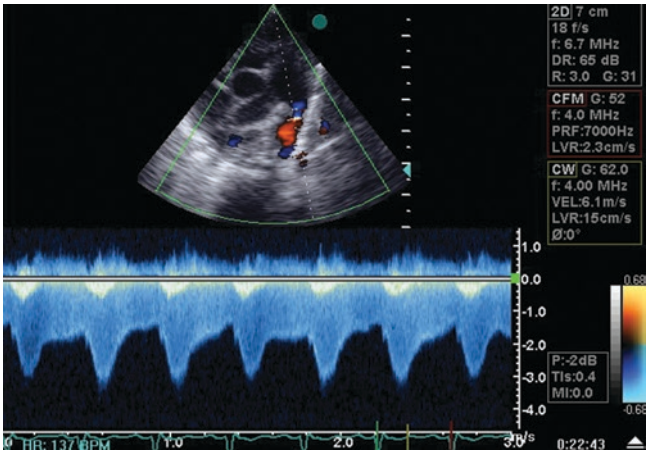

Fig. 9.5 Right to left shunt through PDA in a newborn suffering from cranial AV malformation and pulmonary artery hypertension, the spectral Doppler shows a continuous flow below the base line, which peaks in early systole Compare this figure with Fig. 4.2

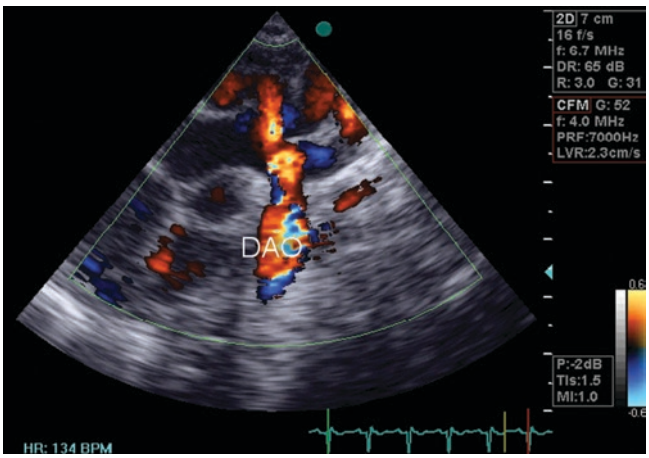

Fig. 9.6 Diastolic retrograde flow via descending aorta (DAO) is seen (red flow) using color Doppler interrogation

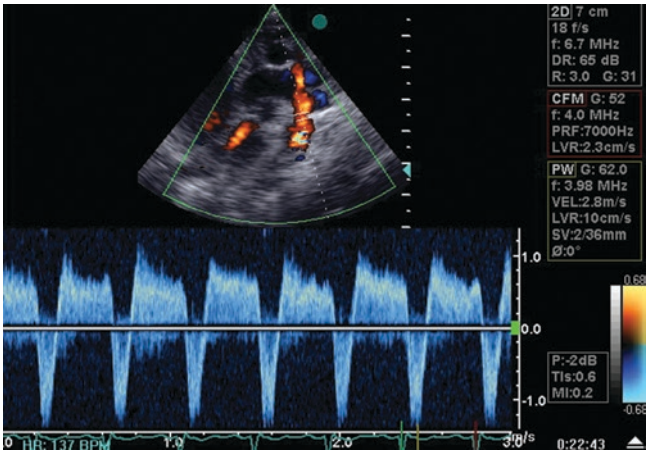

Fig. 9.7 Spectral Doppler interrogation of descending aorta showing retrograde diastolic flow (above the baseline)

Suggested Reading

Frawley GP, Dargaville PA, et al. Clinical course and medical management of neonates with severe cardiac failure related to vein of Galen malformation. Arch Dis Child Fetal Neonatal Ed. 2002;87:F144–9.

Grifka RG, Preminger TJ. Vascular anomalies. In: Allen HD, Driscoll DJ, Shaddy RE, Feltes TF, editors. Moss and Adams' heart disease in infants, children, and adolescents including the fetus and young adult. 7th ed. Philadelphia/Baltimore/New York/London/Buenos Aires/Hong Kong/Sydney/Tokyo: Wolters Kluwer Health|Lippincott Williams & Wilkins; 2008. p. 715–28.

Hoang S, Choudhri O, et al. Vein of galen malformation. Neurosurg Focus. 2009;27

Karadeniz L, Coban A, et al. Vein of Galen aneurysmal malformation: prenatal diagnosis and early endovascular management. J Chinese Med Assoc. 2011;74:134e137.

Madhuban A, Van den Heuvel F, et al. Vein of Galen aneurysmal malformation in neonates resenting with congestive heart failure. Child Neurol Open. 2016;3:1–4.

Moradian M. Diagnostic errors in echocardiography: review of five interesting pediatric cases. J Teh Univ Heart Ctr. 2012;7(1):33–6.

Moradian M, et al. Aortic runoff as a sign of intracranial arteriovenous malformation: report of two cases. Iran J Pediatr. 2013;23:229–32.

Snider AR, Serwer GA, Ritter SB. Abnormal vascular connections and structures. In: Echocardiography in pediatric heart disease. 2nd ed: Mosby; 1997. p. 452–96.

Malposition of Septum Primum

10

Maryam Moradian

Abstract

Septum primum malposition is responsible for different degrees of abnormal drainage of pulmonary veins. It is usually accompanied by heterotaxy and polysplenia. Abnormal deviation of septum primum toward the anatomic left atrium in echocardiography should rise the suspicion of this diagnosis.

Malposition of Septum Primum

1. IF in four chamber view septum primum is displaced toward the anatomic left atrium (LA) and results in the drainage of some or all the pulmonary veins into the morphologic right atrium (RA) malposition of septum primum should be considered
2. Pay attention that pulmonary veins are normally connected to posterior wall of morphologic LA (Fig. 10.1)
3. Remember that septum primum may not reach the posterior wall of LA so there will be an intera atrial communication that is a "septum primum mal position defect "not ASD or PFO. Sometimes septum primum has multiple small fenestrations.
4. Don't forget that this anomaly is more common in heterotaxy, polysplenia, and hypoplastic left heart syndrome patients

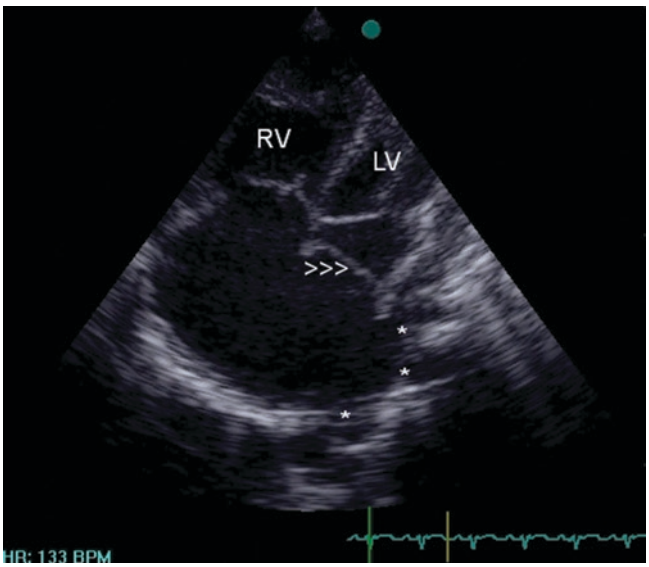

Fig. 10.1 Apical four chamber view showing leftward malposition of septum primum (arrow heads). Asterisks indicate normal connection of pulmonary veins to posterior wall of LA

Suggested Reading

Brown DW , Geva T. Anomalies of pulmonary veins (Chapter 35). In: Allen HD, Shaddy RE, Penny DJ, Feltes TF, Cetta F editors. Moss and Adams' heart disease in infants, children, and adolescents including the fetus and young adults. 9th ed. Wolters Kluwer 2016, pp. 881-910

Cuttone F, Hadeed K, Lacour-Gayet F, Lucron H, Hascoet S, Acar P, et al. Isolated severe leftward displacement of the septum primum: anatomic and 3D echocardiographic findings and surgical repair. Interact CardioVasc Thorac Surg. 2017;24:772–7.

Gajjar T, Desai N. Septum primum malposition defect: a rare congenital anomaly. Türk Göğüs Kalp Damar Cerrahi si Dergi si. 2013;21(1):245–9.

Park MV, et al. Leftward displacement of septum primum in hypoplastic left heart syndrome. Pediatr Cardiol. 2013;34(4):942–7.

M. Moradian (✉)
Pediatric Cardiology, Rajaie Cardiovascular, Medical & Research Center, Iran University of Medical Sciences, Tehran, Iran

M. Moradian, A. Alizadehasl (eds.), *Atlas of Echocardiography in Pediatrics and Congenital Heart Diseases*,
https://doi.org/10.1007/978-3-662-62341-1_10

11 Anomalies of the Pulmonary Venous Connections [Total (TAPVC) & Partial (PAPVC)]

Maryam Moradian and Shamsi Ghaffari

Abstract

Evaluation of all echocardiographic views are helpful in diagnosis of anomalies of pulmonary veins connection. In four chamber view enlargement of right heart chambers should raise the suspicion. Both Total and partial anomalous pulmonary venous drainage have different anatomic variants. During echocardiography individual pulmonary veins should be evaluated both by two dimensional (2D) and color and pulsed Doppler modalities.

Anomalies of the Pulmonary Venous Connections [Total (TAPVC) & Partial (PAPVC)]

1. All echocardiographic views, including subcostal, parasternal, apical, and suprasternal will help you to identify pulmonary veins connection to left atrium (LA). Evaluate right upper pulmonary vein (RUPV) in subcostal sagittal view (or subcostal short axis view) as it enters LA while traveling between superior vena cava and right pulmonary artery. Right lower pulmonary vein (RLPV) can be demonstrated in subcostal coronal view (or subcostal four chamber view). In parasternal long axis and short axis views left and right pulmonary veins can be demonstrated. In apical four chamber view both right lower and left lower pulmonary veins can be seen (Fig. 11.1). In suprasternal short axis or crab view all four pulmonary veins can be identified (Fig. 11.2)

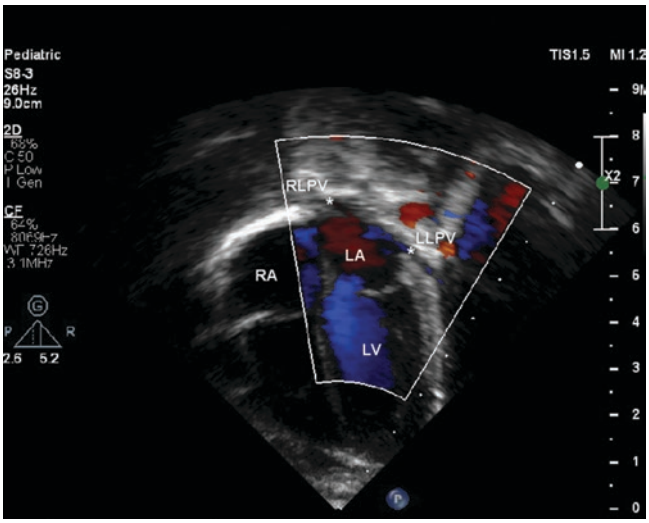

Fig. 11.1 Transthoracic four chamber view showing normal connection of right (RLPV) and left lower pulmonary veins (LLPV) to left atrium (LA)

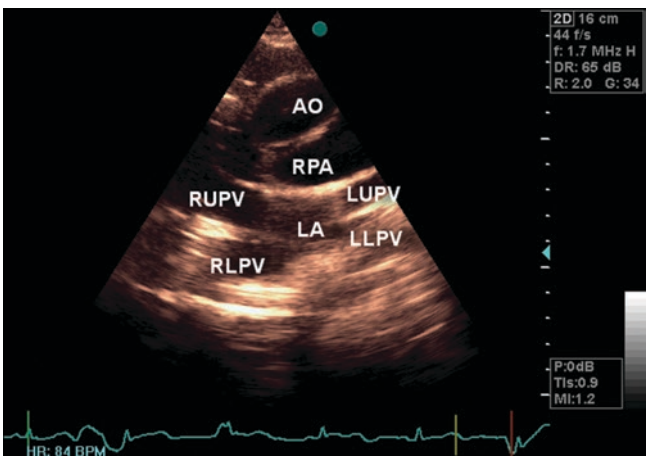

Fig. 11.2 Suprasternal short axis view (crab view), all four pulmonary veins are seen draining to left atrium (LA). *AO* aorta, *RPA* right pulmonary artery, *LUPV* left upper pulmonary vein, *LLPV* left lower pulmonary vein, *RUPV* right upper pulmonary vein, *RLPV* right lower pulmonary vein

M. Moradian (✉)
Pediatric Cardiology, Rajaie Cardiovascular, Medical & Research Center, Iran University of Medical Sciences, Tehran, Iran

S. Ghaffari
Pediatric Cardiology, Cardiovascular Research Center, Tabriz University of Medical Sciences, Tabriz, Iran

M. Moradian, A. Alizadehasl (eds.), *Atlas of Echocardiography in Pediatrics and Congenital Heart Diseases*,
https://doi.org/10.1007/978-3-662-62341-1_11

2. Transesophageal echocardiography (TEE) is also helpful. Evaluate drainage and connection of pulmonary veins by TEE in 55° for right, and 110° for left pulmonary veins. When imaging venous flow with color flow Doppler, reduce the Nyquist limit to correspond to the lower venous flow velocities (Fig. 11.3).
3. Appreciate pulmonary venous flow by pulsed wave (PW) Doppler. Venous flow is low velocity, 40–50 cm/s, and triphasic, consisting of a systolic S wave, early diastolic D wave, and an A wave during atrial systole. As in all Doppler analysis, interrogation should be performed as parallel to the direction of flow as possible (Fig. 11.4).
4. Small left atrium (LA) concomitant with right atrial and ventricular enlargement in a neonate should rise the suspicion of total anomalous pulmonary venous connection (TAPVC)
5. You may use the most common type of classification and according to the sites where the abnormal connections occur explain if it is supracardiac (the most common), cardiac, infracardiac, or mixed type (the least common). Also evaluate obstruction and stenosis of pulmonary veins.
6. Find the pulmonary venous confluence(PVC)with high frequency transducers using far field focusing, and follow the pulmonary veins by color flow Doppler and pulsed wave Doppler (Fig. 11.5).
7. In any type of TAPVC, follow the vertical vein (VV), using color Doppler and evaluate for any stenosis if flow is aliased (Fig. 11.6).
8. In cardiac type TAPVC, pulmonary veins most commonly connect to coronary sinus (CS), which in subcostal coronal view resembles as tail of the whale (Fig. 11.7).

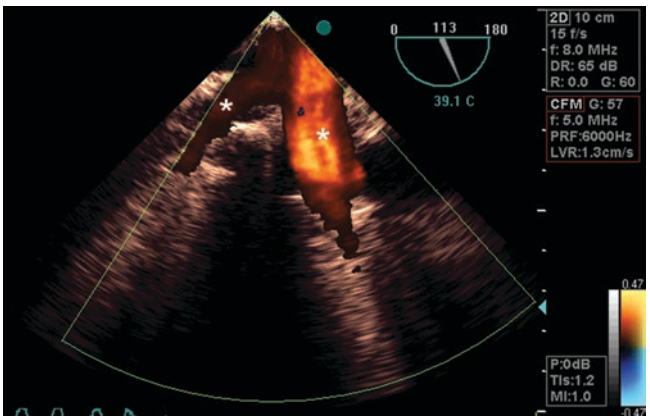

Fig. 11.3 Transesophageal echocardiography (TEE) at midesophageal level demonstrating left pulmonary veins (asterisks) entering left atrium

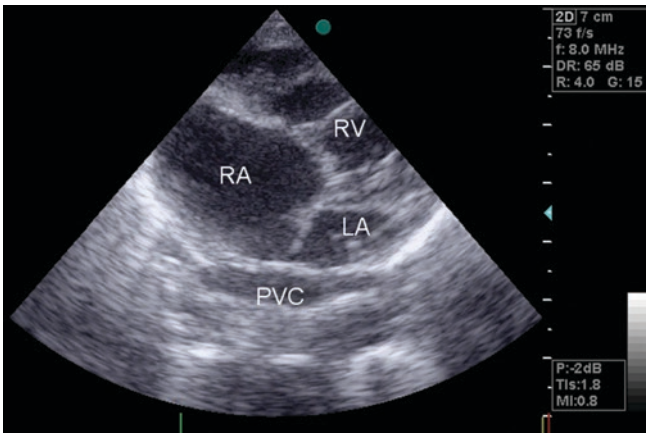

Fig. 11.5 Four chamber view showing enlargement of right atrium (RA) and right ventricular enlargement (RV), small left atrium (LA), and pulmonary venous confluence (PVC) on top of LA, the so called "hat appearance"

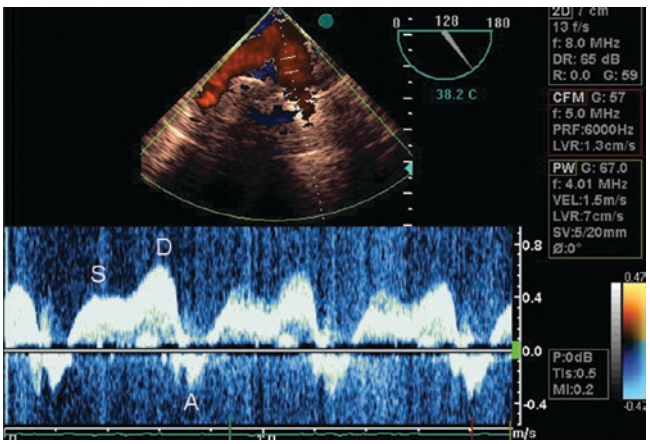

Fig. 11.4 Transesophageal echocardiography (TEE) at mid esophageal level showing two left pulmonary veins using color Doppler (upper image) and PW Doppler to evaluate triphasic venous flow S, D, and A (lower image)

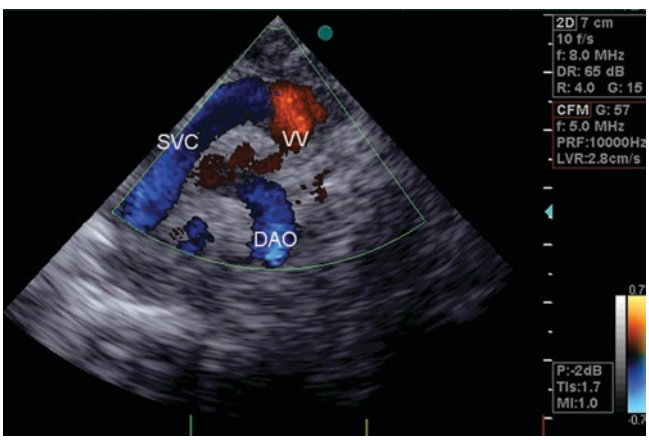

Fig. 11.6 Suprasternal long axis image using color Doppler to show left sided vertical vein (VV) connecting to innominate vein. Superior vena cava (SVC) is dilated in this case of supracardiac TAPVC

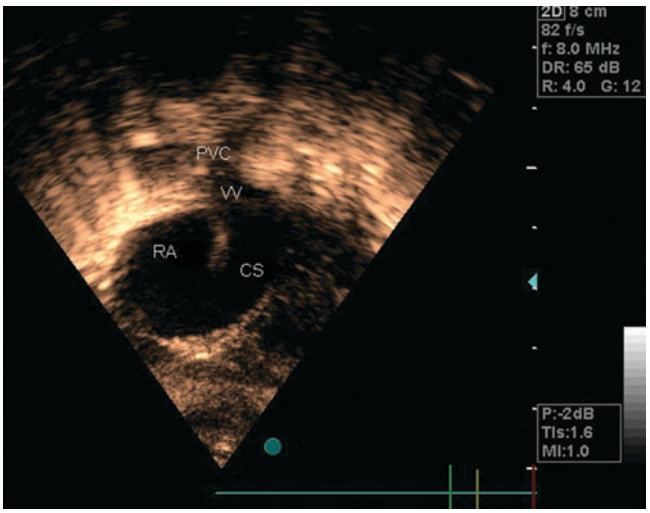

Fig. 11.7 Subcostal coronal view showing the so called" whale tail "appearance, abnormal pulmonary veins drain to pulmonary venous confluence (PVC) that connects to vertical vein (VV) and coronary sinus (CS). Coronary sinus (CS) is enlarged

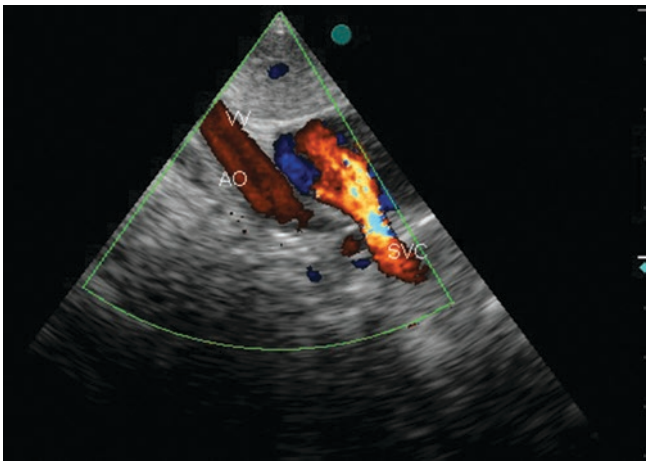

Fig. 11.8 Color Doppler examination in sagittal subcostal view in infracardiac TAPVC showing VV in longitudinal section, anterior to descending aorta (AO) that direct the flow away from the heart

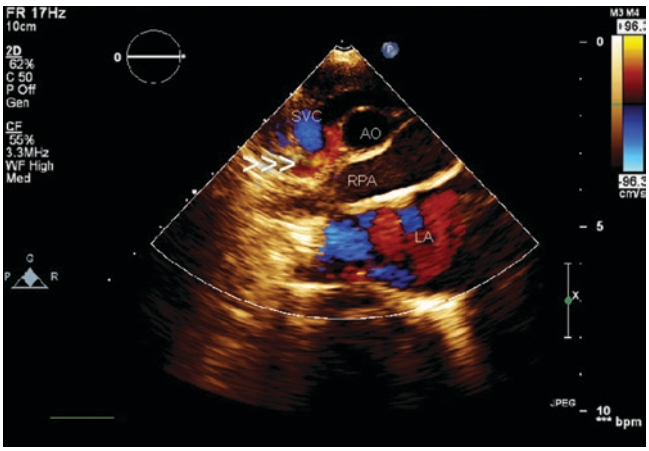

Fig. 11.9 Suprasternal coronal view using color Doppler, showing abnormal connection of a right pulmonary vein to SVC (arrow heads). *SVC* superior vena cava, *AO* aorta, *RPA* right pulmonary artery, *LA* and left atrium

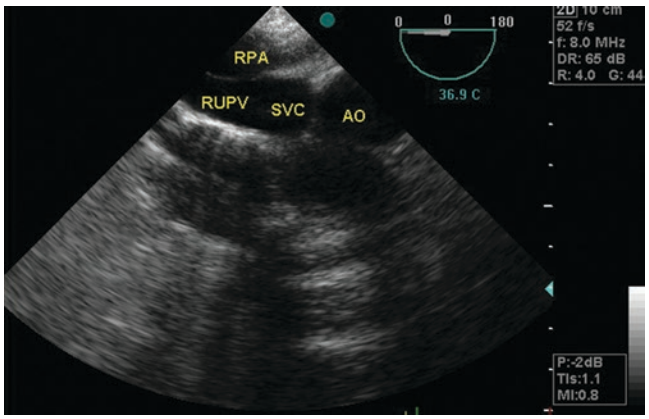

Fig. 11.10 TEE at mid esophageal level, ascending aorta short axis view, showing the entrance of RUPV to SVC in a child suffering from PAPVC. Pay attention to "tear drop appearance" of SVC instead of round shape

9. In infracardiac type TAPVC follow the pulmonary venous confluence (PVC)behind the left atrium(LA), and vertical vein (VV) which penetrates the diaphragm as it goes away from the heart into portal system or inferior vena cava (IVC). Also check by color Doppler any turbulence in these structure for any obstruction (Fig. 11.8).
10. Remember that in mixed type TAPVC, which is the least common, a combination of other forms would be seen.
11. Evaluate the right to left shunt via atrial septal defect (ASD) or patent foramen ovale (PFO) in these patients
12. In partial anomalous pulmonary venous connection (PAPVC) at least one pulmonary vein connects normally to LA. The most common form of PAPVC, excluding PAPVC with sinus venosus defect (Fig. 11.9), is the connection of a left pulmonary vein to left innominate vein via a vertical vein. Evaluate this anomaly in high parasternal view.
13. The abnormal connection of right upper pulmonary vein (RUPV) to superior vana cava (SVC) can be evaluated by transesophageal echocardiography (TEE) as well (Fig. 11.10).
14. Turbulent flow in color Doppler and lack of typical phasic variation in pulsed wave Doppler interrogation of pulmonary veins and/or vertical vein are in favor of stenosis in these veins (Fig. 11.11).
15. In fetal echocardiography the RLPV and LLPV can be imaged in four chamber view and color and pulsed Doppler should be used to confirm the normal flow pattern within them (Figs. 11.12 and 11.13). The possibility

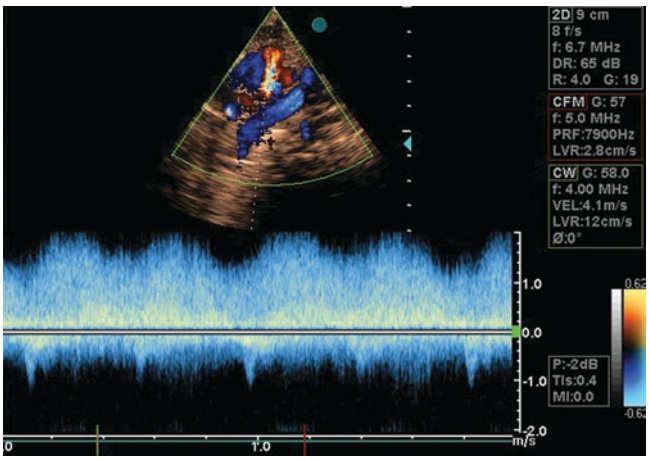

Fig. 11.11 The phasic pattern of venous flow is blunted in this patient suffering from supracardiac TAPVC with stenosis in vertical vein

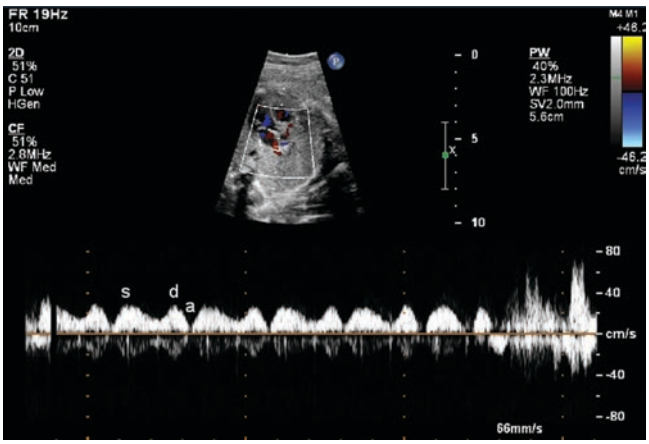

Fig. 11.13 Showing normal pulmonary venous triphasic flow in a fetus with normal pulmonary venous return to LA. The "s," "d," and "a" waves corresponding to ventricular systole, early ventricular diastole, and atrial contraction

Fig. 11.12 Fetal echocardiography, four chamber view showing normal return of RLPV (arrow heads) and LLPV (asterisk) to left atrium (LA)

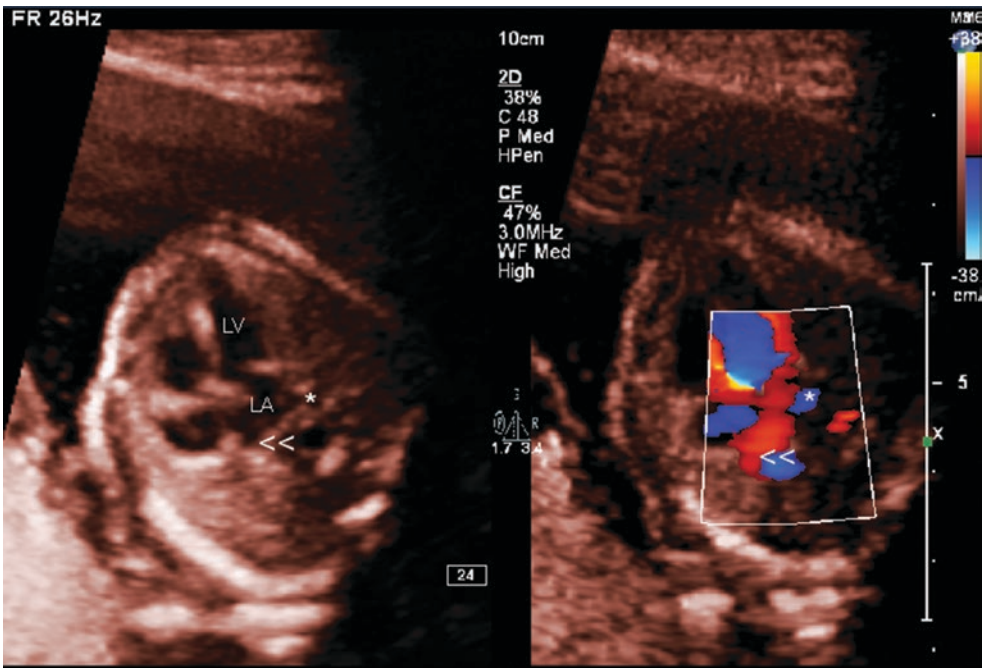

of abnormality in pulmonary venous return raises if there is no connection between pulmonary veins and left atrium, and right heart chambers are enlarged. By precise evaluation you may even find the PVC behind LA and a forth vessel in three vessel tracheal view in supracardiac type TAPVC.

Suggested Reading

Anon. Abnormal vascular connections and structures (Chapter 11). In: Snider R, Serwer GA, Ritter SB, editors. Echocardiography in pediatric heart disease. 2nd ed: Mosby-Year Book Inc.; 1997. p. 452–96.

Anon. Anomalies of systemic and pulmonary venous connections (Chapter 31). In: Abuhamad A, Chaoui R, editors. A practical guide

to fetal echocardiography: normal and abnormal hearts. 3rd ed: Wolters Kluwer; 2016. p. 505–36.

Brown DW, Geva T. Anomalies of the pulmonary veins (Chapter 35). In: Allen HD, Shaddy RE, Penny DJ, Feltes TF, Cetta F, editors. Moss and Adams' heart disease in infants, children, and adolescents including the fetus and young adults. 9th ed: Wolters Kluwer; 2016. p. 881–910.

Cetta F, Ammash N. Anomalies of the pulmonary and systemic venous connections (Chapter 5). In: Eidem BW, O'leary PW, Cetta F, editors. Echocardiography in pediatric and adult congenital heart disease. 2nd ed: Wolters Kluwer; 2015. p. 91–110.

Ganesan, et al. Prenatal findings in total anomalous pulmonary venous return a diagnostic road map starts with obstetric screening views. J Ultrasound Med. 2014;33:1193–207.

Huang X, Huang Y, et al. Individual pulmonary vein imaging by transthoracic echocardiography: an inadequate traditional interpretation. Eur J Echocardiogr. 2008;9:655–60.

Kao CC, Chiang CH, et al. Total anomalous pulmonary venous connection: from embryology to a prenatal ultrasound diagnostic update. J Med Ultrasound. 2017;25(3):130–7.

Tacy TA. Systemic and pulmonary venous anomalies. In: Wong PC, Miller-Hance WC, editors. Transesophageal echocardiography for congenital heart disease. London: Springer-Verlag; 2014. p. 145–70.

Cortriatriatum Sinister

12

Maryam Moradian

Abstract

A membrane within left atrium divides it into two chambers a proximal chamber receiving pulmonary veins flow and a distal chamber which includes the left atrial appendage and is in contact with the atrioventricular valve. Due to obstruction in pulmonary venous flow, this anomaly may cause pulmonary venous hypertension. It is important to differentiate this anomaly from supravalvar mitral ring and echocardiography has crucial role in this regard.

Cortriatriatum Sinister

1. A linear membrane within the left atrial (LA) cavity specially in apical four chamber view should rise the suspicion of this diagnosis. Evaluate if the left atrial appendage (LAA) can be seen between the membrane and the mitral valve. This membrane separates the pulmonary venous confluence (PVC) from the low-pressure distal chamber, which includes the left atrial appendage and is in contact with the atrioventricular valve. The membrane has windsock motion during diastole toward mitral valve (Fig. 12.1).
2. Pulmonary venous confluence (PVC) joins to LA through narrow opening(s). Color Doppler interrogation will reveal continuous, turbulent flow across membrane, and RV enlargement may ensues due to pulmonary venous hypertension (Fig. 12.2).
3. Cortriatriatum should be differentiated from supravalvar mitral ring which is also a membrane within the left atrial cavity causing pulmonary venous obstruction. Supravalvar

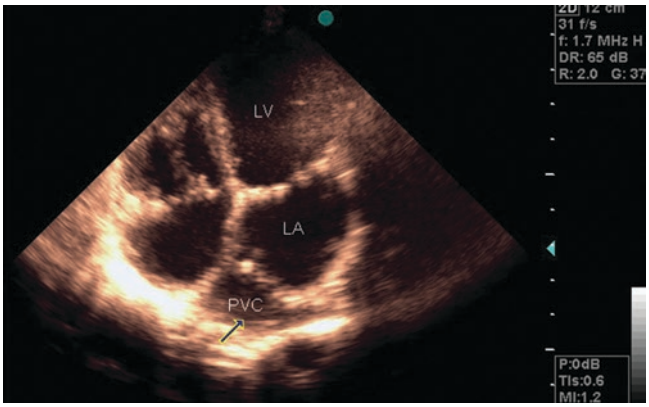

Fig. 12.1 Apical four chamber view showing classic form of cor triatriatum sinister. *PVC* pulmonary venous confluence, *LA* left atrium, *LV* left ventricle

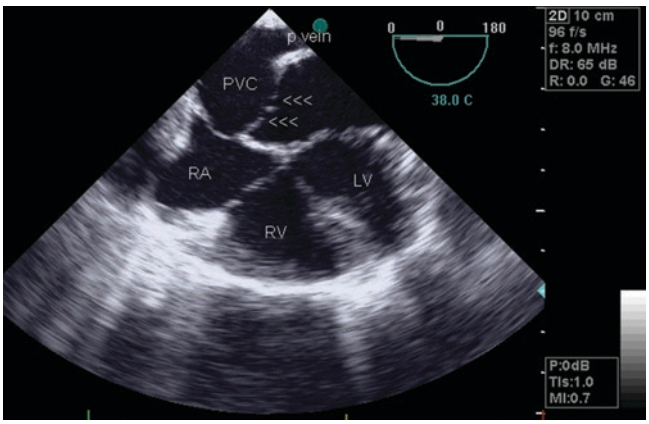

Fig. 12.2 Transesophageal echocardiography at mid esophageal level, four chamber view of a patient with cor triatriatum, arrow heads indicate the linear membrane and fenestrations. *PVC* pulmonary venous confluence, *LV* left ventricle, *RA* right atrium, *RV* right ventricle

M. Moradian (✉)
Pediatric Cardiology, Rajaie Cardiovascular, Medical & Research Center, Iran University of Medical Sciences, Tehran, Iran

M. Moradian, A. Alizadehasl (eds.), *Atlas of Echocardiography in Pediatrics and Congenital Heart Diseases*,
https://doi.org/10.1007/978-3-662-62341-1_12

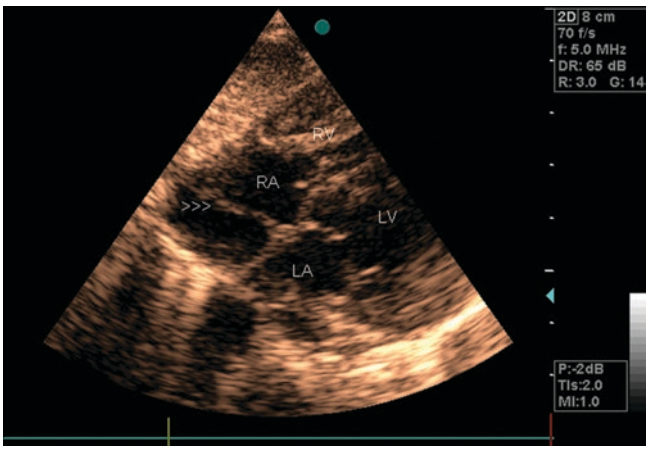

Fig. 12.3 The Eustachian valve is generally small but it can become large and make the appearance of cor triatriatum dexter. In this subcostal view arrow heads indicate an enlarged and fenestrated Chiari net. *LV* left ventricle, *RA* right atrium, *RV* right ventricle

mitral ring is relatively immobile and adheres to the base of mitral leaflets at its atrial surface. Left atrial appendage (LAA) and foramen ovale are proximal to supravalvar mitral ring

4. Carfully check for any atrial septal defect (ASD) and patent foramen ovale (PFO) and use color Doppler to see the interatrial shunt(s) direction.
5. Appreciate pulmonary venous return to the PVC using 2D, color flow mapping, and Doppler modalities.
6. Remember that the so called cor triatriatum dexter is usually a persistence of a large right valve of sinus venosus that produces double-chambered right atrium (Fig. 12.3).
7. In fetal echocardiography discrepancy between ventricular size and a membrane dividing LA into two cavity should raise the suspicion of this anomaly
8. These membranes are not always stenotic so the patient may be asymptomatic and the diagnosis is made incidentally in adulthood.

Suggested Reading

Anon. Abnormalities of ventricular inflow (Chapter 9). In: Snider R, Serwer GA, Ritter SB, editors. Echocardiography in pediatric heart disease. 2nd ed: Mosby-Year Book Inc.; 1997. p. 385–407.

Brown DW, Geva T. Anomalies of the pulmonary veins (Chapter 35). In: Allen HD, Shaddy RE, Penny DJ, Feltes TF, Cetta F, editors. Moss and Adams' heart disease in infants, children, and adolescents including the fetus and young adults. 9th ed: Wolters Kluwer; 2016. p. 881–910.

Cabalka AK. Abnormalities in atria and atrial septation (Chapter 6). In: Eidem BW , O'leary PW, Cetta F, editors. Echocardiography in pediatric and adult congenital heart disease, 2nd ed. Wolters Kluwer 2015, pp. 111–130

Hamdan R, et al. Cor Triatriatum Sinister diagnosed in adult life with three dimensional transesophageal echocardiography. BMC Cardiovasc Disord. 2010;10:54.

Nassar PN, Hamdan R. Cor Triatriatum sinistrum: classification and imaging modalities. Eur J Cardiovasc Med. 2011;1(3):84–7.

Yang PK, et al. Cor triatriatum sinister presenting in the fetus: beware of association with total anomalous pulmonary venous connection. Ultrasound Obstet Gynecol. 2015;45:622–4.

Scimitar Syndrome

13

Maryam Moradian

Abstract

Combination of Dextroposition of heart, hypoplasia of right pulmonary artery, blunted right border of left atrium in crab view due to anomalous connection of right pulmonary vein(s) to inferior vena cava is called Scimitar syndrome. Subcostal echocardiographic views are extremely useful to find abnormal venous connection in this anomaly.

Scimitar Syndrome

1. Dextroposition of the heart should raise the suspicion for Scimitar syndrome especially if right pulmonary artery (RPA) is hypoplastic and smaller than left pulmonary artery (LPA).
2. Check the right border of left atrium (LA) in crab view, in scimitar it is blunted (Fig. 13.1)
3. In subcostal view check any abnormal flow of scimitar vein into inferior vena cava (IVC), use color flow mapping and Doppler interrogation to evaluate triphasic pulmonary vein pattern (Fig. 13.2a, b)
4. Follow the descending abdominal aorta in subcostal view to find any aberrant artery providing blood supply to the affected lobe of the right lung originated from the abdominal aorta.
5. Check for any associated congenital cardiovascular anomalies.

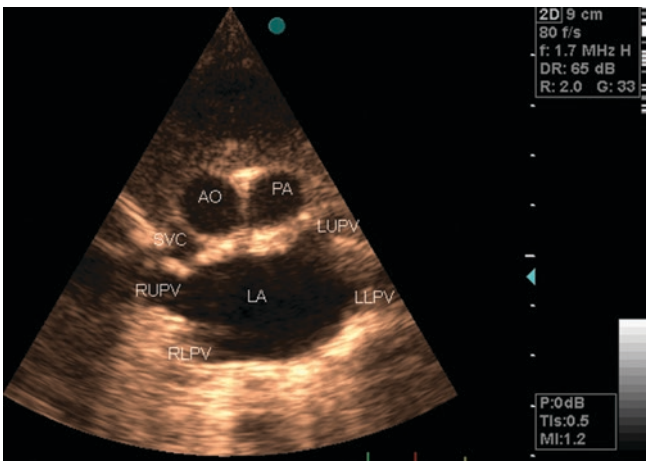

Fig. 13.1 Suprasternal short axis view or "crab view" of a normal infant. In Scimitar syndrome right left atrium (LA) border would be blunted due to abnormal return of right pulmonary vein (or veins) to Scimitar vein and inferior vena cava (IVC). *LA* left atrium, *AO* aorta, *PA* pulmonary artery, *LUPV* left upper pulmonary vein, *LLPV* left lower pulmonary vein, *RUPV* right upper pulmonary vein, *RLPV* right lower pulmonary vein, *SVC* superior vana cava

6. During fetal life, right lung hypoplasia or pulmonary sequestration along with cardiac dextroposition may be signs of Scimitar syndrome. Color flow mapping and pulse Doppler study will help to find the feeding artery arising from the aorta (Fig. 13.3).
7. In transesophageal echocardiography (TEE) find any abnormal vessel (Scimitar vein) entering inferior vena cava (IVC) in lower esophageal IVC long axis view (Fig. 13.4).

M. Moradian (✉)
Pediatric Cardiology, Rajaie Cardiovascular, Medical & Research Center, Iran University of Medical Sciences, Tehran, Iran

M. Moradian, A. Alizadehasl (eds.), *Atlas of Echocardiography in Pediatrics and Congenital Heart Diseases*,
https://doi.org/10.1007/978-3-662-62341-1_13

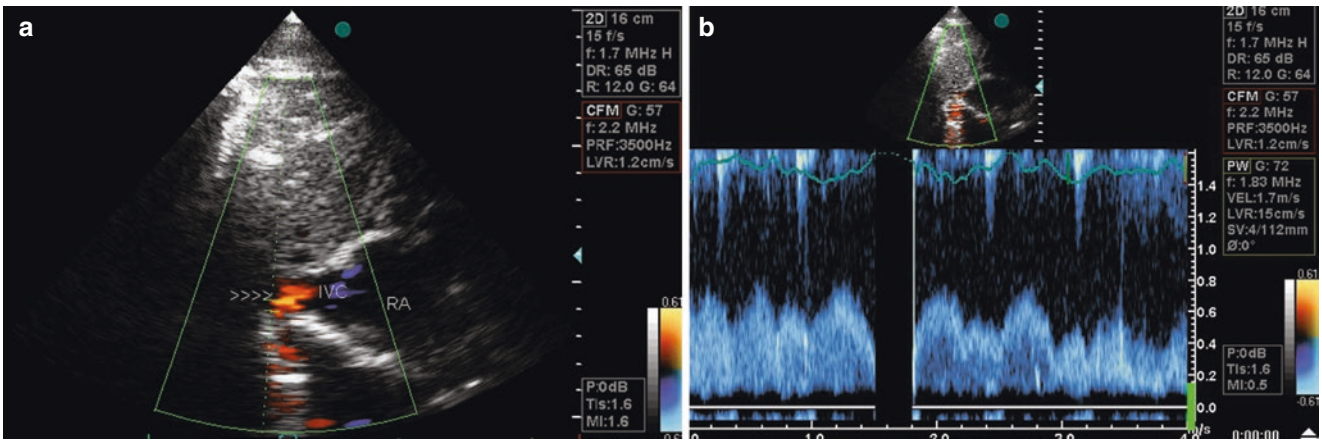

Fig. 13.2 (**a**, **b**) Subcostal view, arrow heads indicate the entrance of Scimitar vein into right atrium (RA) just above the inferior vena cava (IVC). Doppler profile of Scimitar vein can be seen in picture (**b**)

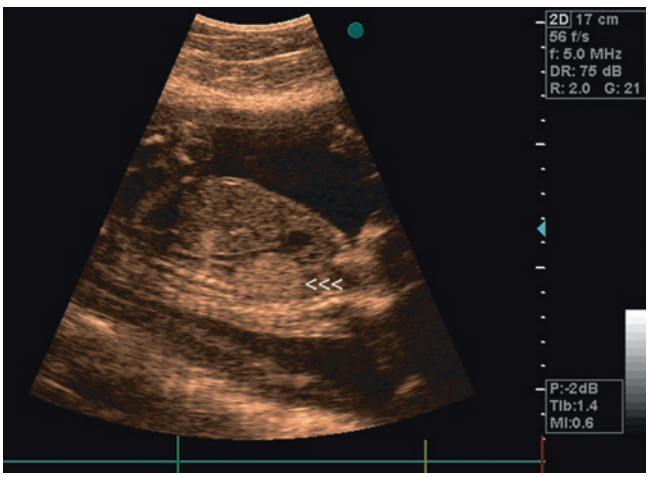

Fig. 13.3 Fetal echocardiography, sagittal view showing echogenic mass of pulmonary sequestration (arrow heads)

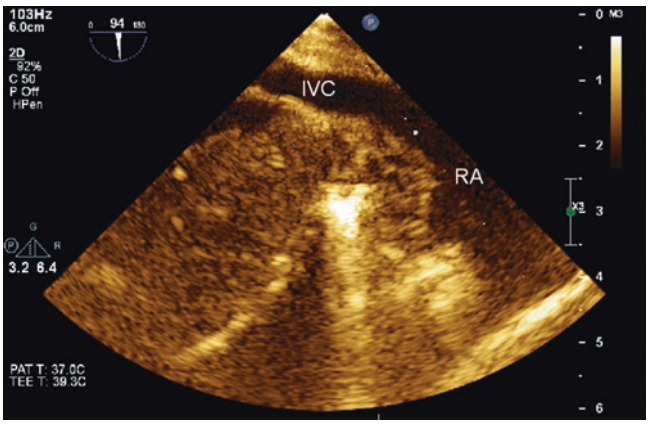

Fig. 13.4 TEE at Lower esophageal level showing long axis view of inferior vena cava (IVC) normally entering right atrium. Any abnormal connection of pulmonary veins to IVC can be evaluated in this view

Suggested Reading

Anon. Abnormal vascular connection and structures (Chapter 11). In: Snider R, Serwer GA, Ritter SB, editors. Echocardiography in pediatric heart disease. 2nd ed. Inc.: Mosby-Year Book; 1997. p. 452–96.

Anon. Anomalies of systemic and pulmonary venous connections (Chapter 31). In: Abuhamad A, Chaoui R, editors. A practical guide to fetal echocardiography: normal and abnormal hearts, 3rd ed. Wolters Kluwer, 2016, pp. 505-536

Brink J, et al. Surgery for scimitar syndrome: the Melbourne experience interactive. Cardiovasc Thorac Surg. 2015;20:31–4.

Brown DW, Geva T. Anomalies of the pulmonary veins (Chapter 35). In: Allen HD, Shaddy RE, Penny DJ, Feltes TF, Cetta F, editors. Moss and Adams' heart disease in infants, children, and adolescents including the fetus and young adults. 9th ed: Wolters Kluwer; 2016. p. 881–910.

Cetta F, Ammash NM. Anomalies of the pulmonary and systemic venous Connections (Chapter 5). In: Eidem BW , O'leary PW, Cetta F, editors. Echocardiography in pediatric and adult congenital heart disease, 2nd ed. Wolters Kluwer, 2015, pp. 91–110

Tacy TA. Systemic and pulmonary venous anomalies. In: Wong PC, Miller-Hance WC, editors. Transesophageal echocardiography for congenital heart disease. London: Springer-Verlag; 2014. p. 145–70.

Vida VL, et al. Natural history and clinical outcome of "uncorrected" scimitar syndrome patients: a Multicenter Study of the Italian Society of Pediatric Cardiology. Rev Esp Cardiol. 2013;66:556–60.

Wang CC, et al. Scimitar syndrome: incidence, treatment, and prognosis. Eur J Pediatr. 2008;167(2):155–60.

Persistent Left Superior Vena Cava (LSVC)

14

Azin Alizadehasl and Maryam Moradian

Abstract

Dilation of coronary sinus on echocardiography is considered the first clue to diagnosis of persistent left superior vena cava. Although rare, it is the most common anomaly of systemic veins and may have clinical consequences especially when is associated with other congenital heart disease.

Persistent Left Superior Vena Cava (LSVC)

1. Dilated coronary sinus (CS) should raise the suspicion of persistent left superior vena cava (LSVC). Other etiologies of dilated CS should be kept in mind including anomalous pulmonary venous return to the coronary sinus, elevated right atrial pressure, and coronary arteriovenous fistula to coronary sinus. Dilated CS can be imaged from the parasternal, apical, and subcostal windows (Figs. 14.1, 14.2, and 14.3).
2. This anomaly is rare, 0.3–0.5% of the general population. In most cases, the LSVC drains into the right atrium via coronary sinus and is almost clinically insignificant though may cause conduction abnormalities and arrhythmia, most commonly atrial fibrillation.
3. Evaluate accompanying structural heart disease. Its prevalence has been reported to as high as 5–10% in association with congenital heart disease including heterotaxy syndromes, conotruncal anomalies, tetralogy of Fallot, atrioventricular septal defects, and mitral atresia. In these situations persistent LSVC may cause difficulties during catheterization and cardiac surgery.
4. It is especially important if LSVC drains into LA due to partially or completely unroofed coronary sinus which leads to mixing of LSVC blood with pulmonary venous blood in the LA. LSVC can be imaged from the suprasternal and high left parasternal windows.

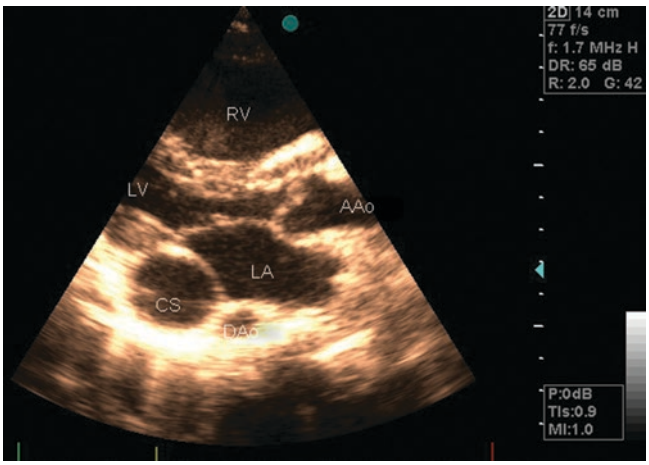

Fig. 14.1 Parasternal long axis view showing severely enlarged coronary sinus (CS), right ventricle (RV) is also enlarged and inter ventricular septum is deviated toward left. *LV* left ventricle, *AAO* ascending aorta, *LA* left atrium, *DAO* descending aorta

A. Alizadehasl
Department of Cardio-Oncology and Research Center, Rajaie Cardiovascular, Medical & Research Center, Iran University of Medical Sciences, Tehran, Iran

M. Moradian (✉)
Pediatric Cardiology, Rajaie Cardiovascular, Medical & Research Center, Iran University of Medical Sciences, Tehran, Iran

M. Moradian, A. Alizadehasl (eds.), *Atlas of Echocardiography in Pediatrics and Congenital Heart Diseases*,
https://doi.org/10.1007/978-3-662-62341-1_14

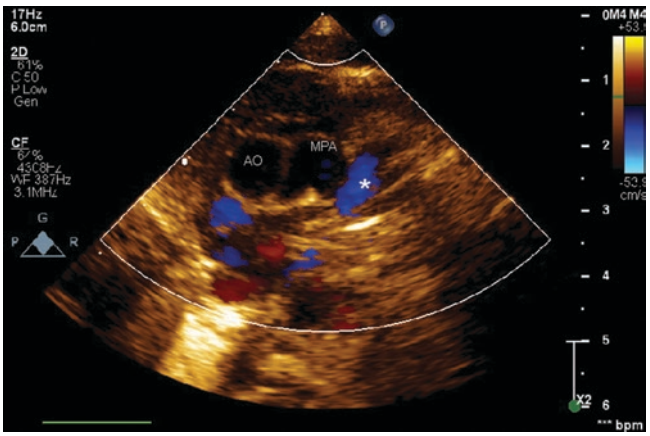

Fig. 14.2 Parasternal short axis view using color flow mapping. Main pulmonary artery and its branches can be seen in this view. Asterisk indicate left superior vena cava (LSVC) anterior to left pulmonary artery. *AO* aorta, *MPA* main pulmonary artery

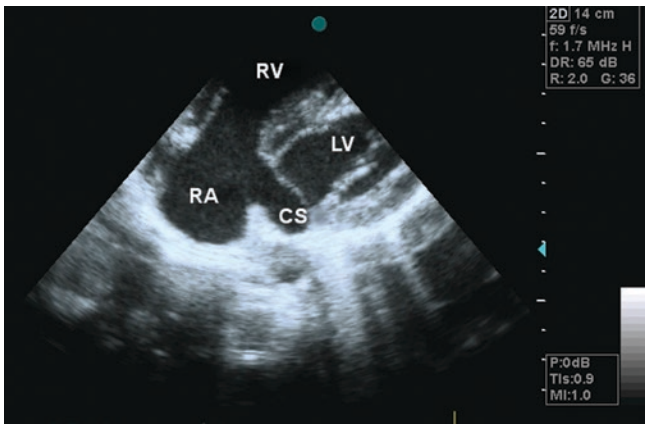

Fig. 14.3 Apical four chamber view with posterior projection showing dilated coronary sinus (CS) in atrioventricular groove. *RA* right atrium, *RV* right ventricle, *LV* left ventricle

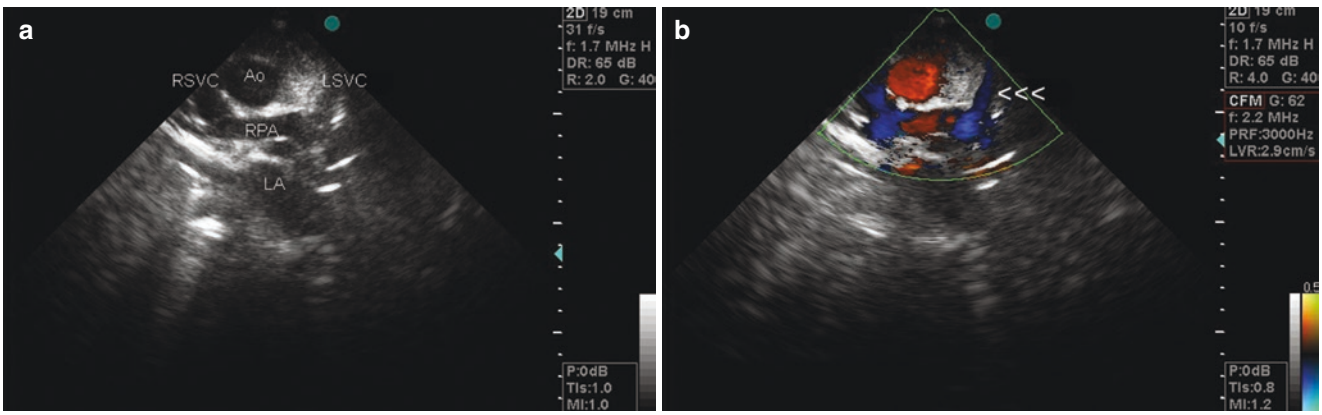

Fig. 14.4 (**a**, **b**) Suprasternal short axis views showing right superior vena cava(RSVC) and left superior vena cava(LSVC) by 2D and color flow mapping (arrow heads in figure **b** points to LSVC). *AO* aoric arch, *RPA* right pulmonary artery, *LA* left atrium

5. Meanwhile evaluate the presence of right SVC, and bridging vein (left brachiocephalic vein) in suprasternal views. Use color flow mapping (CFM) and Doppler profile to evaluate the triphasic venous flow pattern and the direction of blood toward CS in LSVC. Also you may use contrast echocardiography and confirm the diagnosis by injecting the agitated saline into a left-sided brachial vein and follow the bubbles in coronary sinus (CS) (Fig. 14.4a, b).
6. In transesophageal echocardiography (TEE) CS can be evaluated in midesophageal four chamber and two chamber views (Fig. 14.5)
7. Finding a dilated CS during fetal echocardiography should raise the suspicion of persistent LSVC and/or TAPVC (Figs. 14.6 and 14.7).

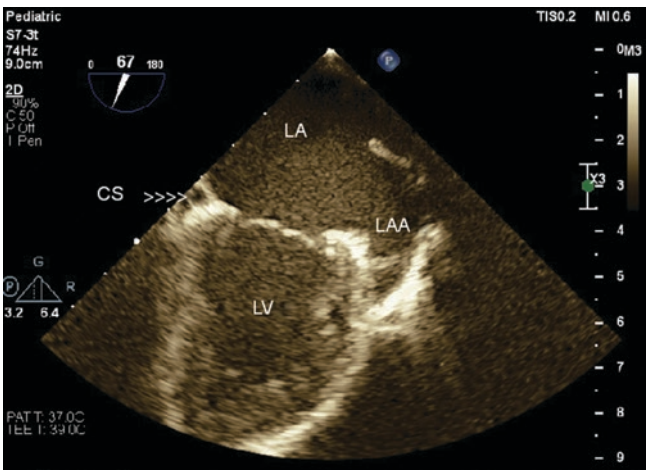

Fig. 14.5 TEE, mid esophageal two chamber view, arrow heads point to normal size coronary sinus (CS). *LA* left atrium, *LAA* left atrial auricle, *LV* left ventricle

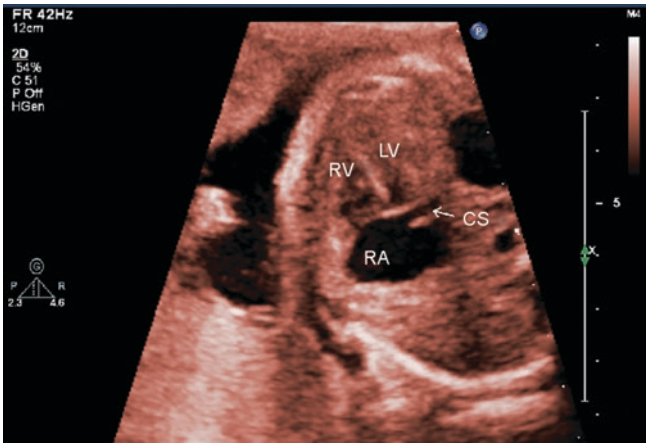

Fig. 14.6 Fetal echocardiography showing normal size coronary sinus (CS) in apical four chamber view. *RA* right atrium, *RV* right ventricle, *LV* left ventricle

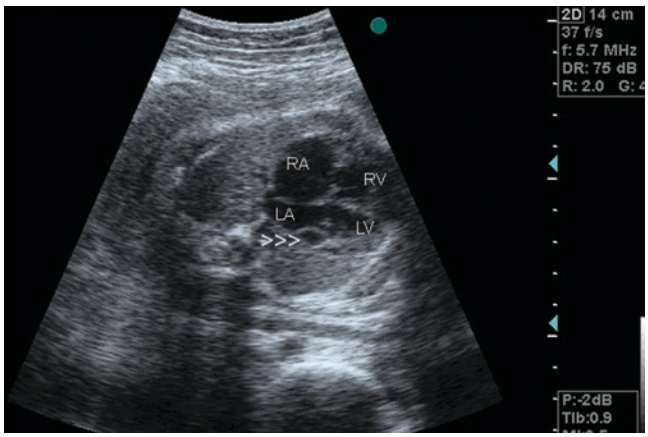

Fig. 14.7 Subcostal four chamber view of a fetus showing dilated CS (arrow heads) as well as RA, and RV enlargement. *RA* right atrium, *RV* right ventricle, *LV* left ventricle

Suggested Reading

Bolognesi M. Dilated coronary sinus due to persistent left superior vena cava in a healthy athlete: case report with brief review. J Integr Cardiol. 2015;1(5):115–7.

Fernando RJ, Johnson SD. Inability to Utilize retrograde cardioplegia due to a persistent left superior vena cava. Case Rep Anesthesiol. 2017;2017:4671856. 3 pages

Geva T. Abnormal systemic venous connections (Chapter 36). In: Allen HD, Shaddy RE, Penny DJ, Feltes TF, Cetta F, editors. Moss and Adams' Heart disease in infants, children, and adolescents including the fetus and young adults. 9th ed: Wolters Kluwer; 2016. p. 911–34.

Irwin RB, Greaves M, Schmitt M. Left superior vena cava: revisited. Eur Heart J Cardiovasc Imaging. 2012;13:284–91.

Moradian M, Mortezaeian H, Baghaei R, Ghadrdoost B. Left atrial drainage of the right superior vena cava: a case report. J Teh Univ Heart Ctr. 2018;13(2):84–7.

Rawal G, Kumar R, Yadav S, Verma D. Persistent left superior vena cava: a rare case with clinical significance. J Clin Diagn Res. 2016;10(5):OD17–8.

Tacy TA. Systemic and pulmonary venous anomalies. In: Wong PC, Miller-Hance WC, editors. Transesophageal echocardiography for congenital heart disease. London: Springer-Verlag; 2014. p. 145–70.

Interrupted Inferior Vena Cava

15

Azin Alizadehasl and Maryam Moradian

Abstract

Echocardiographic subcostal windows are very helpful to evaluate the junction of inferior vena cava (IVC) to right atrium (RA). Absence of intra hepatic segment of IVC, interruption of IVC, should be suspected when IVC-RA junction cannot be seen, especially in association with heterotaxy syndrome.

Interrupted Inferior Vena Cava

1. Evaluate the cross sectional view of Inferior Vena Cava (IVC) in subcostal area, the normal IVC is located anterior and to the right of spine. In this view descending abdominal aorta is seen in the left of spine (Fig. 15.1).
2. By rotating the transducer slightly counter clockwise from this view, follow the connection of inferior vena cava (IVC) to right atrium in subcostal sagittal view (Figs. 15.2 and 15.3).
3. In cases of azygos continuation of the interrupted IVC, an enlarged azygos vein can be seen near the midline, posterior to aorta and when followed cranially its connection with SVC can be demonstrated using color Doppler (Fig. 15.4a, b).
4. Appreciate the so called "seagull sign "in fetal echocardiography, and screen the normal connection of IVC and SVC to RA and compare their sizes (Fig. 15.5).

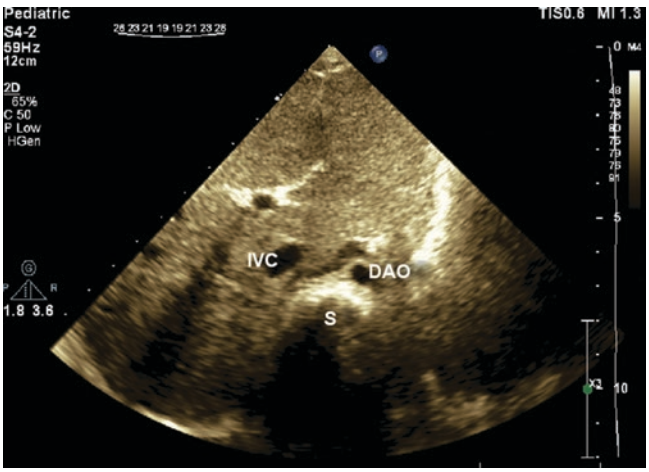

Fig. 15.1 Transthoracic echocardiography, subcostal cross sectional view of Inferior Vena Cava (IVC) and descending abdominal aorta(DAO)and their relation to spine (S)

5. In cases of interrupted IVC with azygos continuation in fetus, azygos vein is dilated and is seen near the abdominal aorta in axial plan of upper abdomen, the so called "double vessel sign" (Fig. 15.6a, b).
6. Don't forget to evaluate for other associated anomalies especially heterotaxy and left isomerism in which interrupted IVC is common.

A. Alizadehasl
Department of Cardio-Oncology and Research Center, Rajaie Cardiovascular, Medical & Research Center, Iran University of Medical Sciences, Tehran, Iran

M. Moradian (✉)
Pediatric Cardiology, Rajaie Cardiovascular, Medical & Research Center, Iran University of Medical Sciences, Tehran, Iran

M. Moradian, A. Alizadehasl (eds.), *Atlas of Echocardiography in Pediatrics and Congenital Heart Diseases*,
https://doi.org/10.1007/978-3-662-62341-1_15

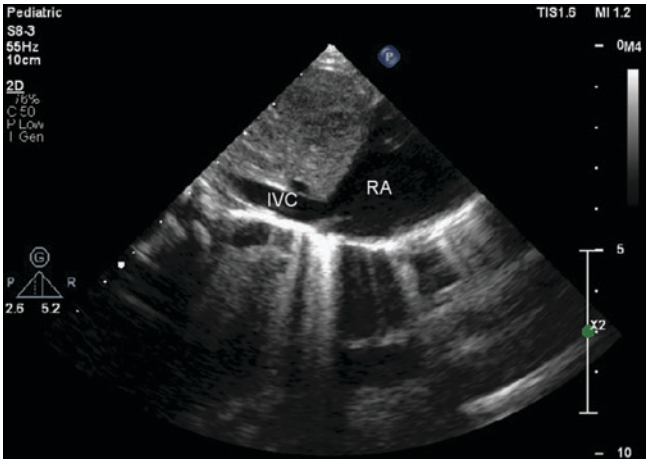

Fig. 15.2 Connection of inferior vena cave and right atrium is seen in this subcostal view. *IVC* inferior vena cava, *RA* right atrium

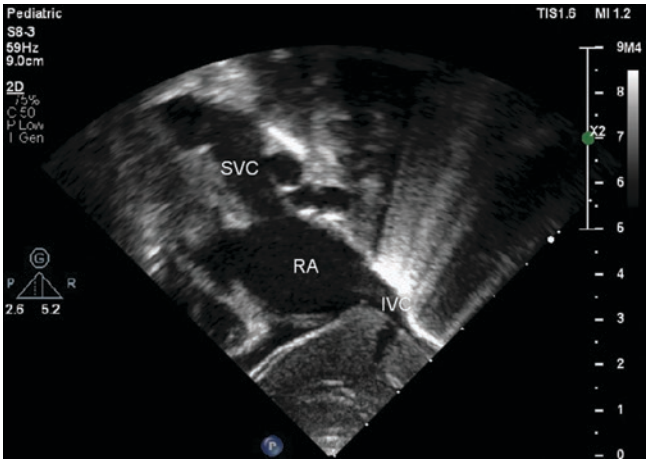

Fig. 15.3 Subcostal sagittal view showing normal connection of inferior and superior vena cava to right atrium. In this case superior vena cava is dilated due to supracardiac total anoumalous pulmonary venous connection (TAPVC). *IVC* inferior vena cava, *SVC* superior vena cava, *RA* right atrium

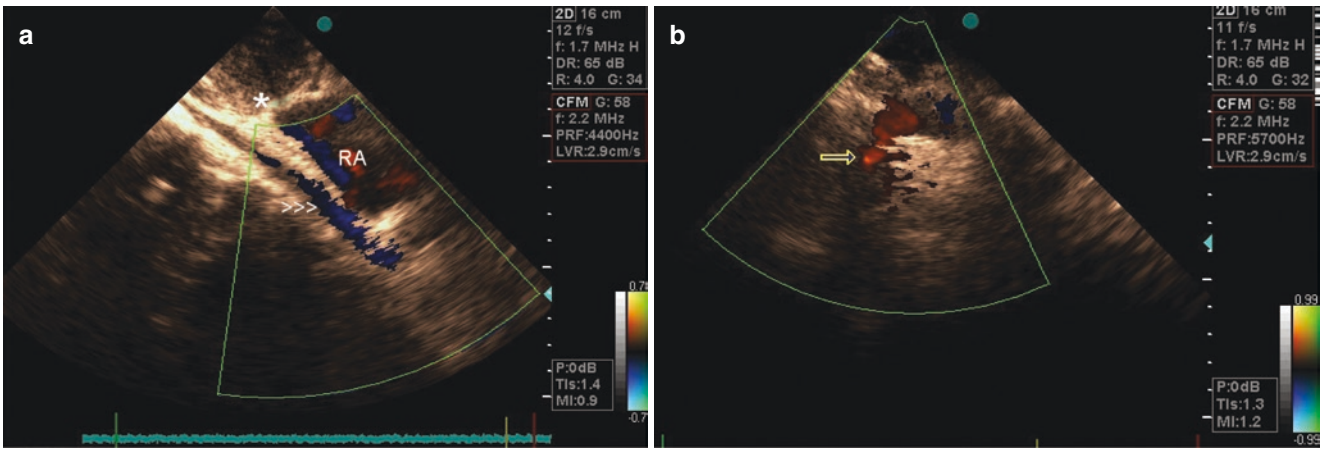

Fig. 15.4 (**a**, **b**) Arrow heads point to azygos vein and asterisk shows absence of IVC- RA connection (interrupted IVC). Color flow mapping demonstrate direction of blood flow in this vein toward the heart. In figure **b** arrow indicates drainage of azygos to SVC in high parasternal view

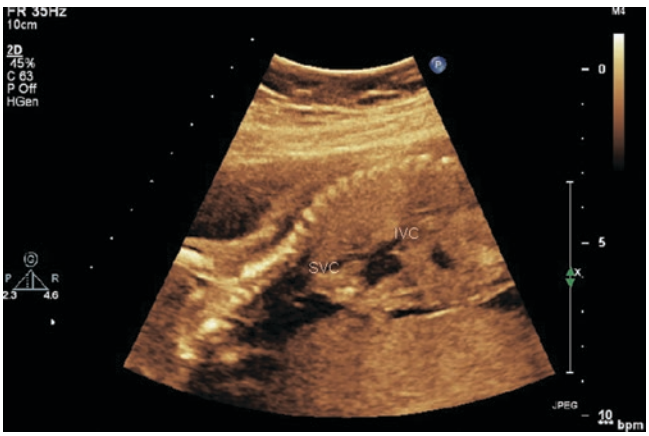

Fig. 15.5 Parasagittal view in a fetus showing normal size SVC and IVC connecting to RA (Seagull sign)

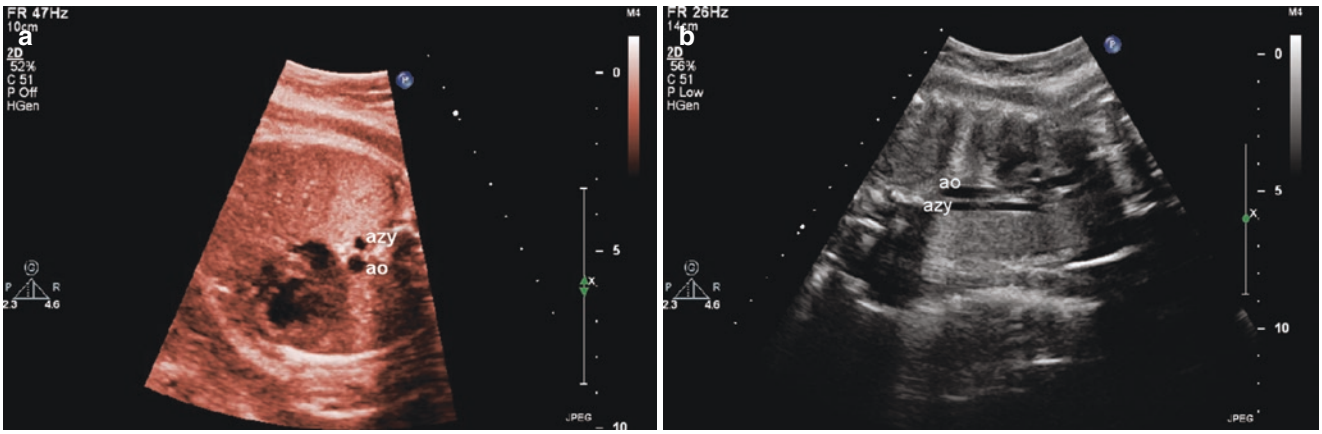

Fig. 15.6 (**a**, **b**) Fetal echocardiograms showing dilated azygos vein (azy) adjacent to abdominal aorta (ao) in a fetus suffering from complex congenital heart disease. Cross section of azygos vein and abdominal aorta is seen in upper abdomen (**a**) and longitudinal views (**b**)

Suggested Reading

Anon. Anomalies of systemic and pulmonary venous connections (Chapter 31). In: Abuhamad A, Chaoui R, editors. A practical guide to fetal echocardiography: normal and abnormal hearts, vol. 2016. 3rd ed: Wolters Kluwer. p. 505–36.

Cetta F, Ammash N. Anomalies of the pulmonary and systemic venous connections (Chapter 5). In: Eidem BW, O'leary PW, Cetta F, editors. Echocardiography in pediatric and adult congenital heart disease. 2nd ed: Wolters Kluwer; 2015. p. 91–110.

Geva T. Abnormal systemic venous connections (Chapter 36). In: Allen HD, Shaddy RE, Penny DJ, Feltes TF, Cetta F, editors. Moss and Adams' heart disease in infants, children, and adolescents including the fetus and young adults. 9th ed: Wolters Kluwer; 2016. p. 911–34.

Giang DTC, Rajeesh G, Vaidyanathan B. Prenatal diagnosis of isolated interrupted inferior vena cava with azygos continuation to superior vena cava. Ann Pediatr Cardiol. 2014;7(1):49–51.

Lo Verso C, Cigna V, Damiani G, et al. Prenatal diagnosis of a variant of the azygos venous system. Springer Plus. 2016;5:1334.

Wu LH, Xie HN, Paladini D, et al. Azygos vein Z scores in healthy fetuses and fetuses with venous malformations related to the azygos vein. J Ultrasound Med. 2016;35:2563–74.

Tetralogy of Fallot (TOF/TF)

16

Maryam Moradian and Shamsi Ghaffari

Abstract

Echocardiographic findings in the most common type of cyanotic congenital heart disease, tetralogy of Fallot, consists of ventricular septal defect (VSD), overriding of aorta, right ventricular hypertrophy, and right ventricular outflow tract obstruction. It should be kept in mind not to miss other associated anomalies including right sided aortic arch, abnormal coronary arteries particularly if crossing the right ventricular outflow tract, aortopulmonary collaterals, persistent left superior vena cava, additional VSDs, and other anomalies.

Tetralogy of Fallot (TOF/TF)

1. Evaluate the ventricular septal defect (VSD) and aortic overriding in different views. A large subaortic defect extending to the membranous septum is the most common type VSD in Tetralogy of Fallot patients (Figs. 16.1 and 16.2)
2. Additional muscular ventricular septal defects (VSDs) should be evaluated in different views.
3. Don't forget that the hallmark of TF, multi-level obstruction to pulmonary blood flow. So evaluate:
   (a) The characteristic narrowing of the right ventricular out flow tract (RVOT) due to anterior and cephalad deviation of the conal septum (Fig. 16.3).
   (b) The typical pulmonary valve in TOF is thickened and frequently bicuspid with hypoplastic annulus (a pulmonary annular z-score of less than −2 indicate the need for a transannular surgical approach) (Fig. 16.4).

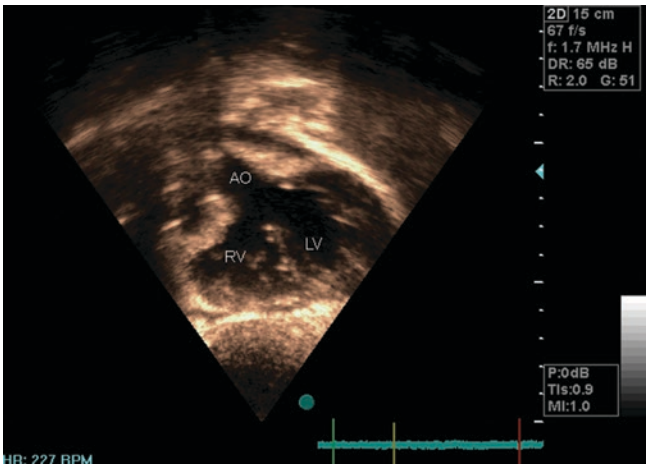

Fig. 16.1 Transthoracic echocardiography, subcostal coronal view showing aortic overriding in a patient with tetralogy of Fallot. *AO* aorta, *RV* right ventricle, *LV* left ventricle

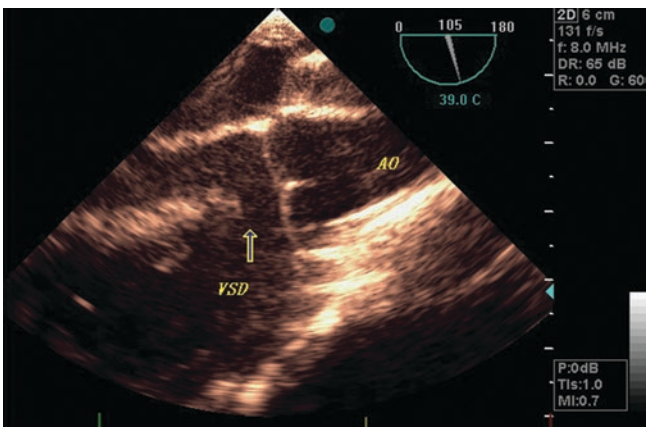

Fig. 16.2 Transesophageal echocardiography, long axis view showing large ventricular septal defect (VSD) and aortic overriding. Arrow points to VSD. *VSD* ventricular septal defect, *AO* aorta

M. Moradian (✉)
Pediatric Cardiology, Rajaie Cardiovascular, Medical & Research Center, Iran University of Medical Sciences, Tehran, Iran

S. Ghaffari
Pediatric Cardiology, Cardiovascular Research Center, Tabriz University of Medical Sciences, Tabriz, Iran

M. Moradian, A. Alizadehasl (eds.), *Atlas of Echocardiography in Pediatrics and Congenital Heart Diseases*,
https://doi.org/10.1007/978-3-662-62341-1_16

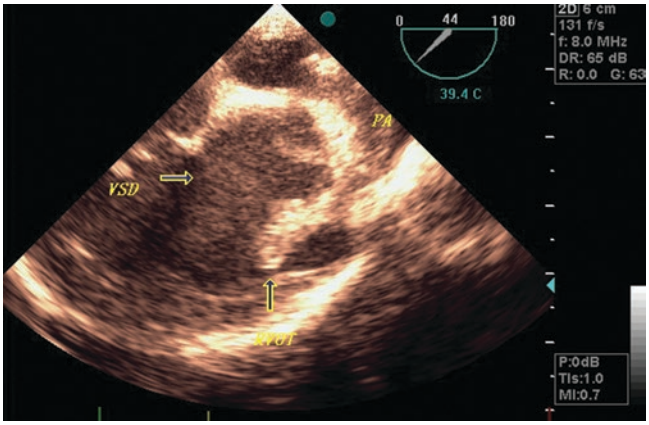

Fig. 16.3 Transesophageal echocardiography (TEE) in right ventricular inflow- outflow view, showing severe right ventriclular out flow tract narrowing (vertical arrow) and large VSD (horizontal arrow). *RVOT* right ventriclular out flow tract, *PA* pulmonary artery, *VSD* ventricular septal defect

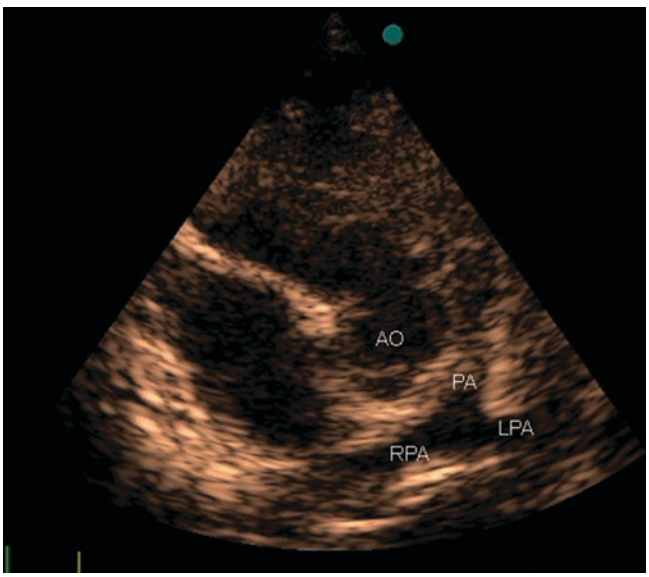

Fig. 16.4 Transthoracic echocardiography (TTE) in parasternal short axis view, showing small pulmonary valve annulus, main pulmonary artery and its branches. *PA* main pulmonary artery, *LPA* left pulmonary artery, *RPA* right pulmonary artery, *AO* aorta

(c) Evaluate the ratio of the sum of pulmonary arteries diameter (RPA + LPA) to the descending aorta diameter at the level of diaphragm, if less than 1.5, is not suitable for total repair, also evaluate any absence of right or left pulmonary artery (Fig. 16.5).

4. Look for any additional source of pulmonary blood supply, so check for patent ductus arteriosus (PDA) and major aorto pulmonary collaterals (MAPCAs) especially by color flow mapping (CFM).

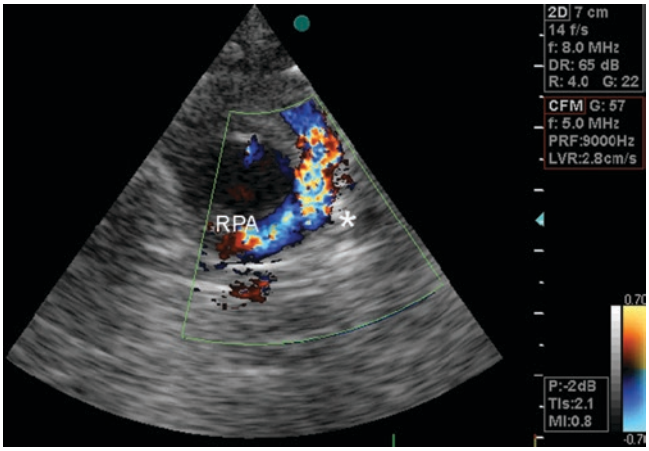

Fig. 16.5 In this parasternal short axis view using color flow mapping, asterisk indicate absence of left pulmonary artery (LPA). *RPA* right pulmonary artery

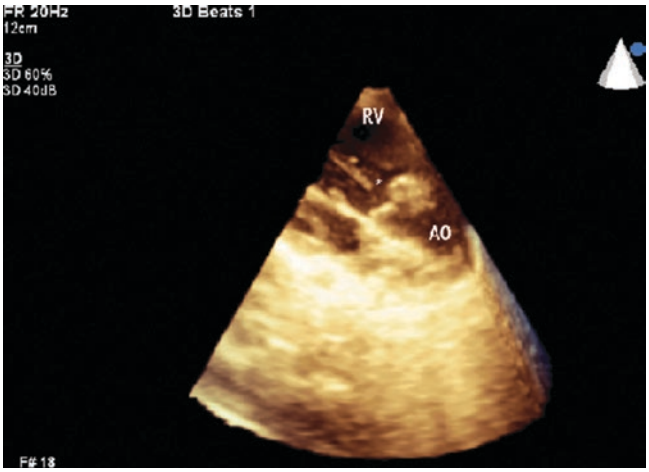

Fig. 16.6 3D echo of a TOF patient, asterisk indicate VSD and aortic overriding. *AO* aorta, *RV* right venreicle

5. Evaluate the aortic valve, aortic root dilation, aortic regurgitation (AR), aortic arch direction, any narrowing of aorta, and pattern of brachiocephalic arteries.
6. Look for course of coronary arteries, remember that approximately 5–10% of TOF patients will have an anomalous coronary artery crossing the right ventricular outflow tract (RVOT), potentially complicating the infundibulotomy.
7. Three dimensional (3D) echocardiography may help to evaluate more details (Fig. 16.6).
8. When performing fetal echocardiography, pay attention to:
   (a) Pseudo-overriding of aorta or artifactual septoaortic discontinuity due to thin membranous portion of septum (Fig. 16.7). Evaluate true overriding in different views (Fig. 16.8).

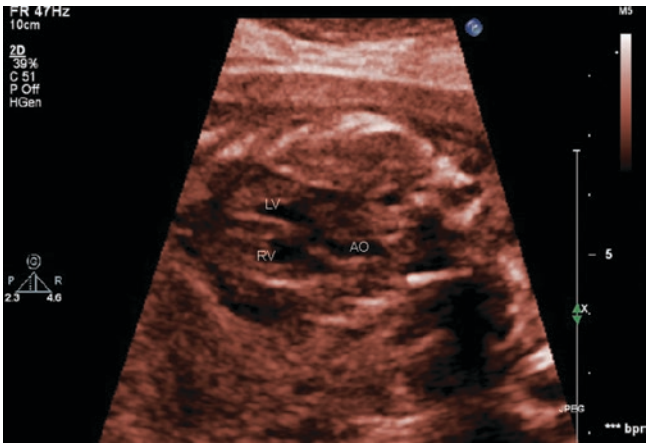

Fig. 16.7 Fetal echocardiogram showing pseudo-overriding which is due to thin membranous septum. Obtaining different views will prevent this pitfall. *AO* aorta, *RV* right ventricle, *LV* left ventricle

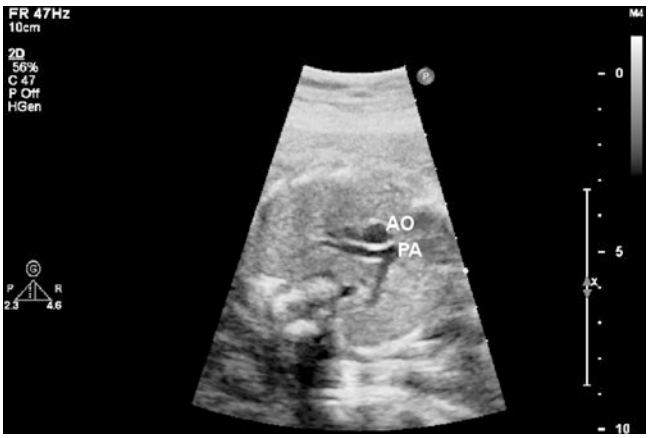

Fig. 16.9 Fetal echocardiogram, short axis of great arteries, showing small pulmonary artery and branches. *AO* aorta, *PA* pulmonary artery

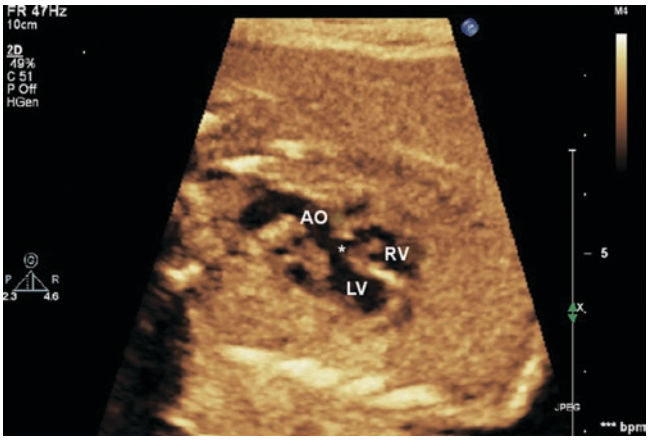

Fig. 16.8 Fetal echocardiogram showing true aortic overriding. Asterisk indicate the VSD and aortic overriding. *AO* aorta, *RV* right ventricle, *LV* left ventricle

(b) Pulmonary artery diameter which is 40–55% less than aortic diameter in TF patients, while in normal fetus, pulmonary artery diameter is 9% larger than aortic diameter (Fig. 16.9).

(c) Flow disturbances by color flow mapping (CFM)and evaluate pulse wave Doppler velocity through pulmonic valve which is increased in comparison of aortic valve in TF (Pulse wave Doppler velocity through pulmonary artery of normal fetus is slightly lower than aorta)

(d) Laterality of the aortic arch in three-vessel trachea view and transverse image of fetal chest (The sausage-shaped arch to right of trachea, rather than its usual left sided position in three vessel view is in favor of right aortic arch)

Suggested Reading

Anon. Defects in cardiac septation (Chapter 6). In: Snider R, Serwer GA, Ritter SB, editors. Echocardiography in pediatric heart disease. 2nd ed: Mosby-Year Book, Inc.; 1997. p. 235–96.

Anon. Tetralogy of Fallot, pulmonary atresia with ventricular septal defect, and absent pulmonary valve syndrome (Chapter 25). In: Abuhamad A, Chaoui R, editors. A practical guide to fetal echocardiography: normal and abnormal hearts. 3rd ed. Wolters Kluwer, 2016, pp. 396-421

Bolger DM. Tetralogy of Fallot (Chapter 13) In: Drose JA, editors. Fetal echocardiography, 2nd ed. Copyright © 2010, 1998 by Saunders, an imprint of Elsevier Inc.

Kervancioglu M, Tokel K, Varan B, Yildirim SV. Frequency, origins and courses of anomalous coronary arteries in 607 Turkish children with tetralogy of Fallot. Cardiol J. 2011;18(5):546–51.

Mercer-Rosa LM, Cohen MS. Evaluation of Conotruncal abnormalities (Chapter 12). In: Wong PC, Miller-Hance WC, editors. Transesophageal echocardiography for congenital heart disease. London: Springer-Verlag; 2014. p. 307–40.

Roche SL, Greenway SC, Redington AN. Tetralogy of Fallot with pulmonary stenosis, pulmonary atresia, and absent pulmonary valveIn. In: Allen HD, Shaddy RE, Penny DJ, Feltes TF, Cetta F, editors. Moss and Adams' heart disease in infants, children, and adolescents including the fetus and young adults. 9th ed: Wolters Kluwer; 2016. p. 1029–53.

Saha S, Paoletti D, Robertson M. Persistent left superior vena cava – considerations in fetal, pediatric and adult populations. AJUM. 2012;15(2):61–6.

Vyas H, Johnson J, Eidem BW. Tetralogy of Fallot (Chapter 15). In: Eidem BW, O'leary PW, Cetta F, editors. Echocardiography in pediatric and adult congenital heart disease. 2nd ed: Wolters Kluwer; 2015. p. 305–20.

Tetralogy of Fallot with Absence of the Pulmonary Valve

17

Maryam Moradian

Abstract

In this rare anomaly which is similar to Fallot's tetralogy, the pulmonary valve leaflets are rudimentary and non-functional, resulting in severe pulmonary incompetence. The pulmonary artery and branches are enlarged and may lead to respiratory symptoms.

Tetralogy of Fallot with Absence of the Pulmonary Valve (TOF, APV)

1. In this subset of tetralogy of Fallot, evaluate the dysplastic and rudimentary pulmonary valve which is both obstructive and regurgitant. Aneurysmal dilation of pulmonary arteries can be best seen in parasternal short axis view (Figs. 17.1 and 17.2).
2. Color flow mapping and Doppler study will confirm concomitant pulmonary valve stenosis and regurgitation (Fig. 17.2).
3. In fetal echocardiography, absence of ductus arteriosus and dilated main pulmonary artery and branches along with echocardiographic findings of tetralogy of Fallot, will help to make the diagnosis (Fig. 17.3a, b). Color flow mapping will confirm severe pulmonary stenosis and insufficiency through diminutive pulmonary valve (Fig. 17.4).

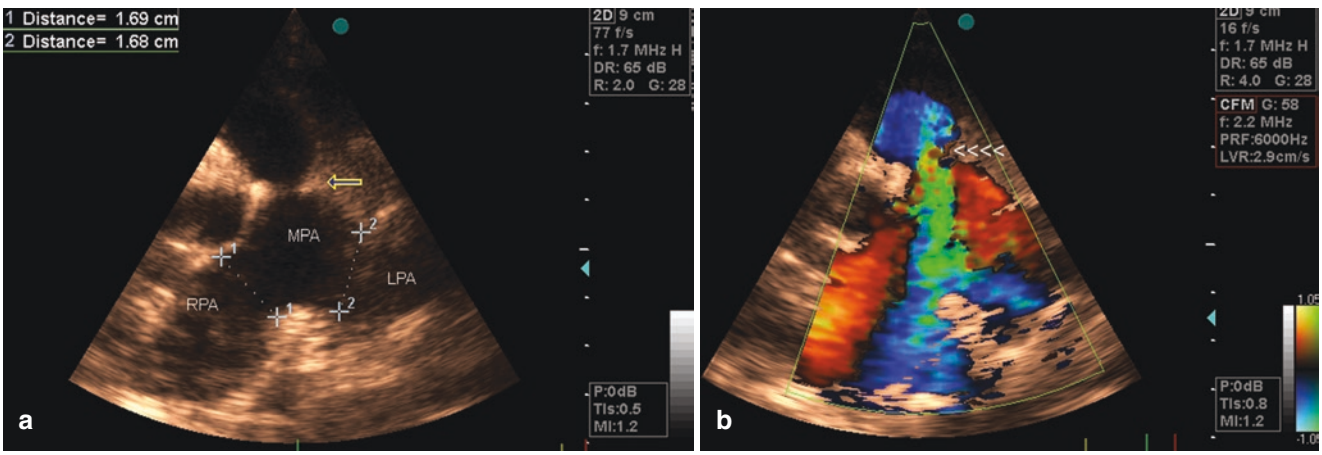

Fig. 17.1 (**a**, **b**) Transthoracic echocardiography, parasternal short axis view showing massive dilation of main pulmonary artery (MPA) and its branches (RPA & LPA), arrow in figure (**a**) indicate rudimentary ridge of tissue instead of pulmonary valve leaflets and small pulmonary valve annulus. In (**b**), Color Doppler mapping of the same patient, arrow heads point to redundant pulmonary valve, swirling of flow seen within the severely dilated MPA and braches

M. Moradian (✉)
Pediatric Cardiology, Rajaie Cardiovascular, Medical & Research Center, Iran University of Medical Sciences, Tehran, Iran

M. Moradian, A. Alizadehasl (eds.), *Atlas of Echocardiography in Pediatrics and Congenital Heart Diseases*,
https://doi.org/10.1007/978-3-662-62341-1_17

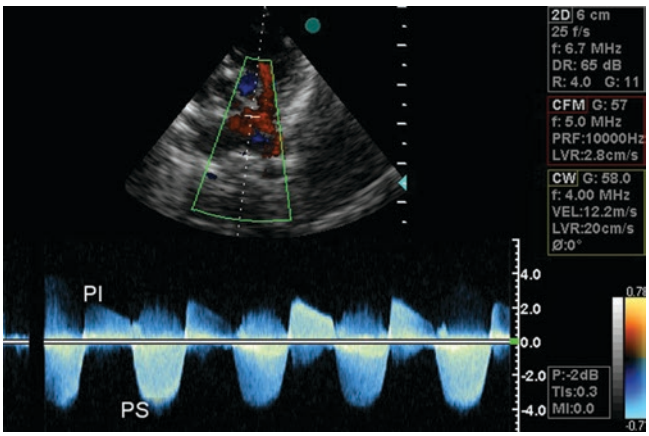

Fig. 17.2 Doppler examination at the pulmonary valve annulus showing to-and-fro flow pattern due to pulmonary stenosis (PS) and insufficiency (PI)

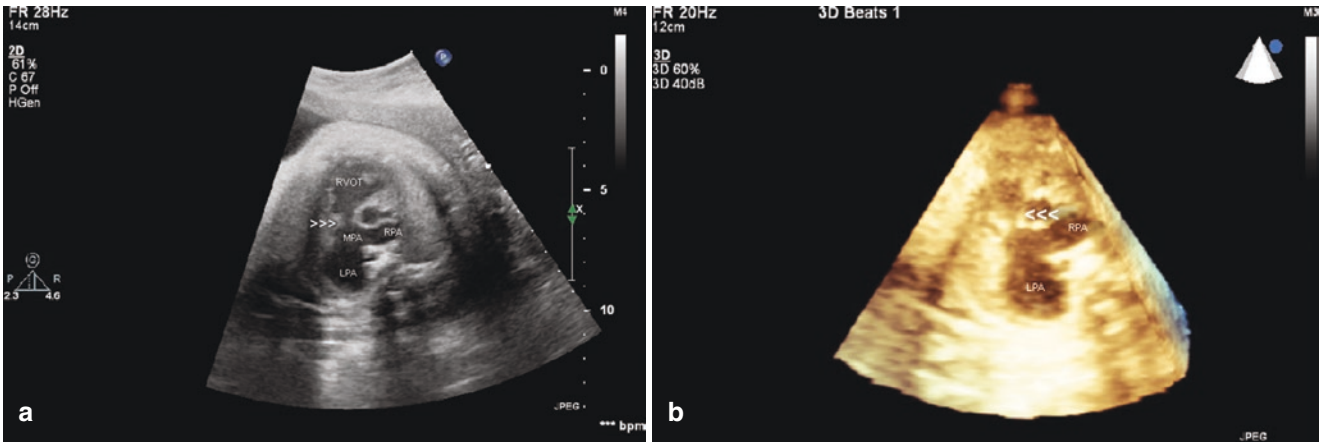

Fig. 17.3 (**a**, **b**) Fetal two dimensional (**a**) and three dimensional (**b**) echocardiogram, showing short axis view of great arteries. Main pulmonary artery and branches are severely dilated. Arrow heads point to rudimentary pulmonary valve. *MPA* main pulmonary artery, *LPA* left pulmonary artery, *RPA* right pulmonary artery, *RVOT* right ventricular out flow tract

Fig. 17.4 Fetal echocardiogram diastolic frame, showing severe pulmonary regurgitation via rudimentary pulmonary valve (arrow heads). *LPA* left pulmonary artery, *RPA* right pulmonary artery

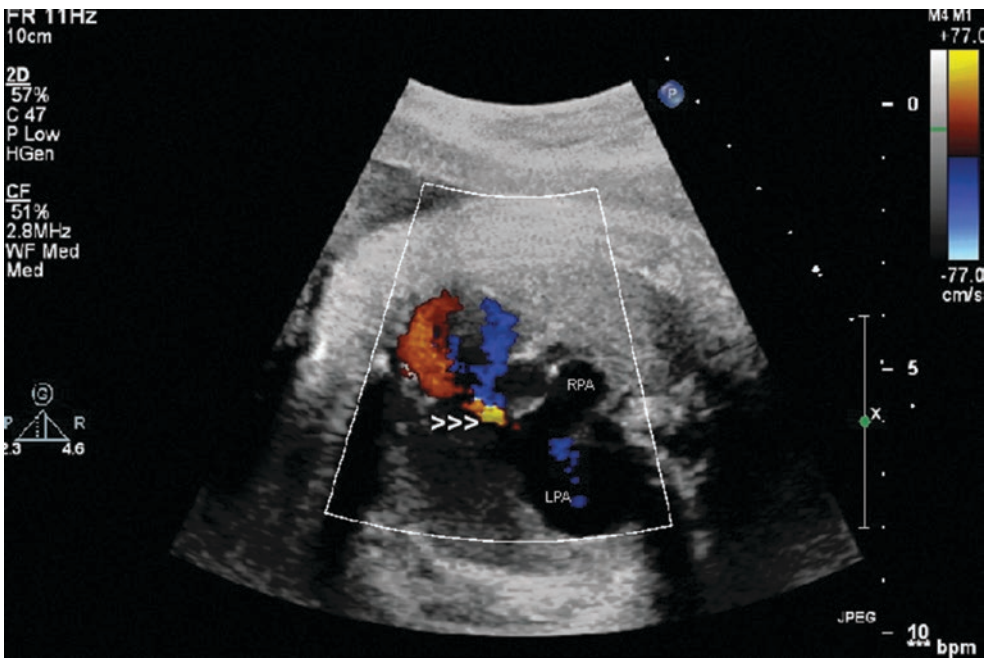

Suggested Reading

Anon. Defects in cardiac septation (Chapter 6). In: Snider R, Serwer GA, Ritter SB, editors. Echocardiography in pediatric heart disease. 2nd ed: Mosby-Year Book, Inc.; 1997. p. 235–96.

Anon Tetralogy of Fallot, pulmonary atresia with ventricular septal defect, and absent pulmonary valve syndrome (Chapter 25) In Abuhamad A, Chaoui R, editors.A practical guide to fetal echocardiography: normal and abnormal hearts. 3rd ed. Wolters Kluwer, 2016, pp. 396-421

Bhupali AN, Kiran B, Patankar KB, et al. Absent pulmonary valve syndrome with tetralogy of Fallot detected at an early gestational age of 27 weeks e A case report. Indian Heart J. 2013;65:191–3.

Bolger DM. Tetralogy of Fallot (Chapter 13). In: Drose JA, editor. FetaL echocardiography. 2nd ed. Copyright © 2010, 1998 by Saunders, an imprint of Elsevier Inc.

Grewal DS. Absent pulmonary valve syndrome: antenatal diagnosis. Med J Armed Forces India. 2014;70:198–200.

Roche SL, Greenway SC, Redington AN. Tetralogy of Fallot with pulmonary stenosis, pulmonary atresia, and absent pulmonary valve (Chapter 41). In: Allen HD, Shaddy RE, Penny DJ, Feltes TF, Cetta F, editors. Moss and Adams' heart disease in infants, children, and adolescents including the fetus and young adults. 9th ed: Wolters Kluwer; 2016. p. 1029–53.

Vyas H, Johnson J, Eidem BW. Tetralogy of Fallot (Chapter 15). In: Eidem BW, O'leary PW, Cetta F, editors. Echocardiography in pediatric and adult congenital heart disease. 2nd ed: Wolters Kluwer; 2015. p. 305–20.

Ebstein's Malformation of Tricuspid Valve

18

Maryam Moradian, Feridoun Noohi, and Azin Alizadehasl

Abstract

Displacement of the septal and posterior leaflets of the tricuspid valve, the hallmark of Ebstein's anomaly, is best displayed in the apical four chamber view and is evaluated by measuring the displacement index. The most frequent additional anomaly is defect in atrial level.

Ebstein's Malformation of Tricuspid valve

1. Evaluate the hallmark of Ebstein's malformation of tricuspid valve, displacement of the annular attachments of the septal and inferior (posterior) leaflets in apical four chamber and subcostal, coronal views (Fig. 18.1).
2. The anterior leaflet retains its normal attachment to atrio ventricular groove but can become large and "sail-like". Tethering of distal attachments of the anterior superior leaflet of the tricuspid valve is recognized by accessory attachments between the valve and the right ventricular wall. Evaluate these findings in apical four chamber view and describe its mobility. More than 50% mobility of this leaflet, absence of major tethering, and free movement of its leading edge, predict better result of surgery (Fig. 18.2a, b).
3. Appreciate the displacement index [displacement distance (mm)/body surface area (m^2)] in four chamber view during systole. Displacement index more than 8 mm/m^2 is diagnostic for Ebstein anomaly in doubtful cases
4. Note that tricuspid valve (TV) leaflets are thickened and dysplastic in Ebstein anomaly. Evaluate width of vena contracta of tricuspid regurgitation jet (mild TR < 3 mm, severe TR > 8 mm), but remember that in Ebstein anomaly multiple TR jets are common. In small patients, if vena contracta is less than 10% of a normal TV annulus diameter consider it as, mild, and if it is more than 25–30% of a normal TV annulus, it is severe. Also the density of Doppler profile will help you in this regard, very dense signals are compatible with severe regurgitation.
5. Almost always there is an interatrial communication, PFO or ASD, so pay attention to size and direction of flow via these defects.
6. Evaluate the enlargement of right atrium and right ventricle as well as right ventricular dysfunction.
7. Use color flow mapping to evaluate forward flow through right ventricular out flow tract and across pulmonary valve. Differentiate any functional pulmonary atresia from anatomic atresia.
8. You may use Celermajer index (or GOSE index) to predict the outcome of the patient. If the area of right atrium + atrilalized right ventricle/area of left atrium+ left ventricle+ functional right ventricle is more than 1, mortality will be high (Fig. 18.3).
9. The commissure between septal and inferior (posterior) leaflet is the most displaced region in Ebstein's anomaly and cause bileaflet configuration of the valve which can be evaluated in parasternal long axis view (Fig. 18.4)

M. Moradian
Pediatric Cardiology, Rajaie Cardiovascular, Medical & Research Center, Iran University of Medical Sciences, Tehran, Iran

F. Noohi
Cardiovascular Intervention Research Center, Rajaie Cardiovascular, Medical & Research Center, Iran University of Medical Sciences, Tehran, Iran

A. Alizadehasl (✉)
Department of Cardio-Oncology and Research Center, Rajaie Cardiovascular, Medical & Research Center, Iran University of Medical Sciences, Tehran, Iran

M. Moradian, A. Alizadehasl (eds.), *Atlas of Echocardiography in Pediatrics and Congenital Heart Diseases*,
https://doi.org/10.1007/978-3-662-62341-1_18

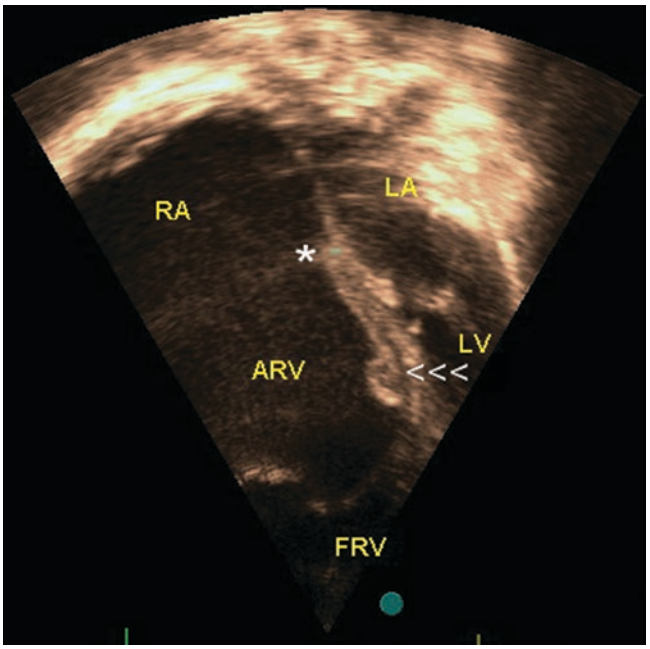

Fig. 18.1 Transthoracic echocardiography apical four chamber view, systolic frame showing Ebstein malformation of tricuspid valve. Arrow heads point to insertion of displaced septal leaflet of tricuspid valve into ventricular cavity. Asterisk indicate the anatomic atrioventricular junction. *RA* right atrium, *LA* left atrium, *ARV* atrilalized right ventricle, *LV* left ventricle, *FRV* functional right ventricle

10. During fetal life increased cardiothoracic ratio, enlargement of right atrium, severe levorotation of heart, and tricuspid regurgitation should rise the suspicion of this anomaly (Fig. 18.5a, b).
11. Severe forms of Ebstein anomaly may lead to profound cardiac dysfunction in utero, hydrops fetalis, and even fetal death (Fig. 18.6)

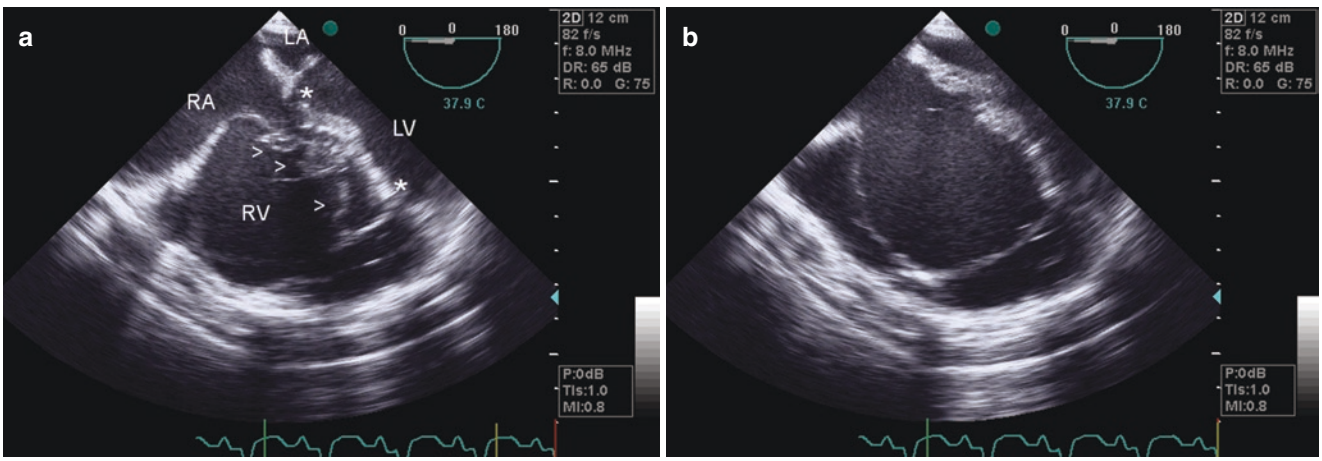

Fig. 18.2 (**a**, **b**) Transeshophageal four chamber view (TEE) showing systolic (**a**) and diastolic frames (**b**) of Ebstein's malformation of tricuspid valve. Septal leaflet displacement (distance between asterisks) can be seen. Also sail like anterior leaflet (arrow heads) and its mobility is shown. *RA* right atrium, *LA* left atrium, *RV* right ventricle, *LV* left ventricle

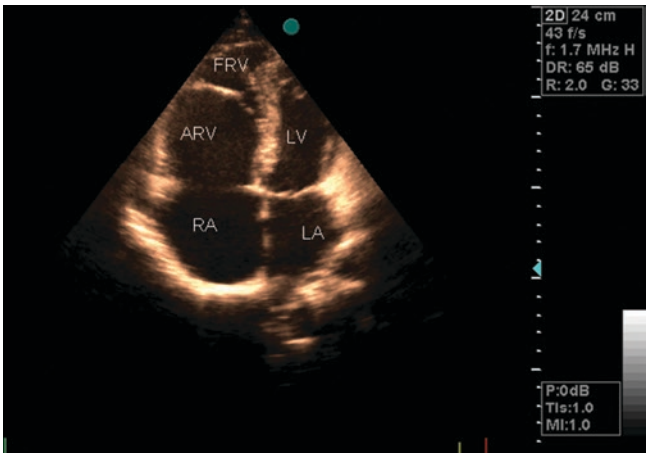

Fig. 18.3 Transthoracic echocardiography apical four chamber view can be used for evaluation of Celermajer index. *RA* right atrium, *LA* left atrium, *ARV* atrilalized right ventricle, *LV* left ventricle, *FRV* functional right ventricle

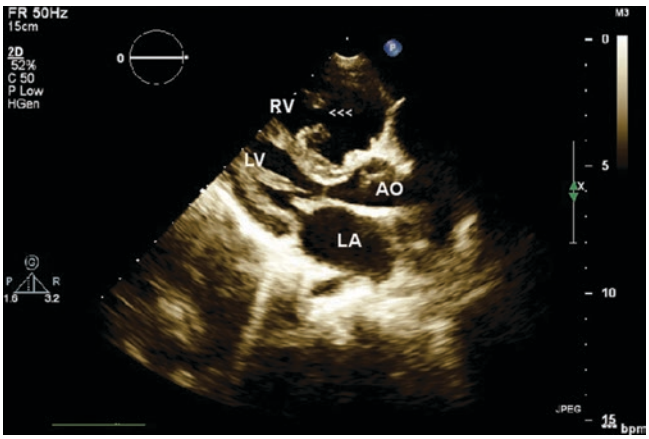

Fig. 18.4 Transthoracic echocardiography, parasternal long axis view showing the functional orifice of tricuspid valve which is rotated apically and anteriorly due to Ebstein malformation (arrow heads) and bileaflet configuration of TV. *RV* right ventricle, *LA* left atrium, *LV* left ventricle, *AO* aorta

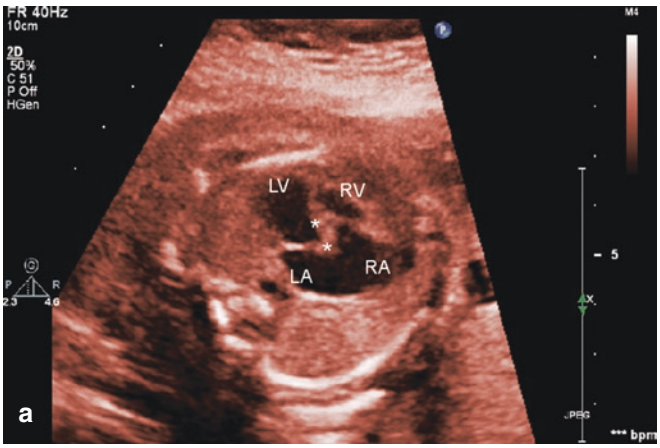

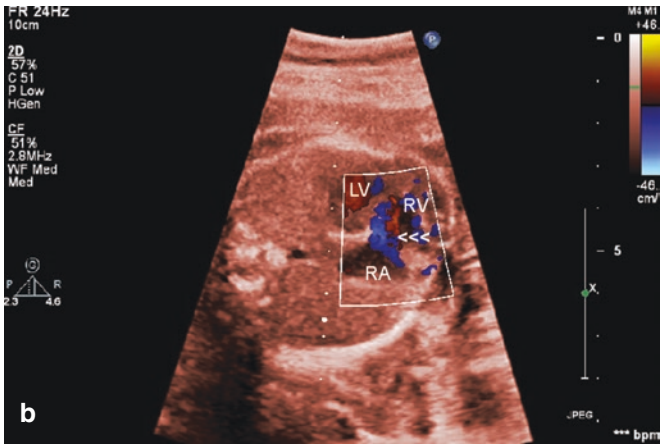

Fig. 18.5 (**a**, **b**) Fetal echocardiogram of a fetus with Ebstein anomaly displacement of septal leaflet is shown in two dimensional (**a**) view by asterisks and tricuspid regurgitation is indicated by arrow heads (**b**). Also pay attention to enlargement of RA. *RV* right ventricle, *LA* left atrium, *LV* left ventricle, *RV* right ventricle

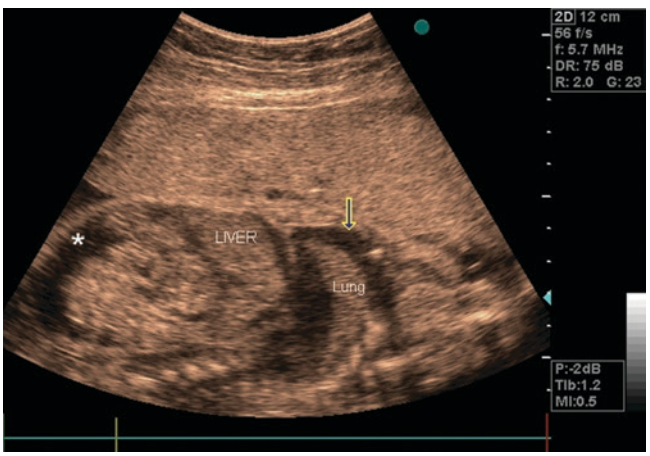

Fig. 18.6 Fetal echocardiogram showing hydrops fetalis, accumulation of fluid in different cavities, plural effusion is indicated by arrow, and ascites by asterisk

Suggested Reading

Anon. Ebstein anomaly, tricuspid valve dysplasia, and tricuspid regurgitation (Chapter 20). In: Abuhamad A, Chaoui R, editors. A practical guide to fetal echocardiography: normal and abnormal hearts. 3rd ed: Wolters Kluwer; 2016. p. 297–316.

Cetta F, Dearani JA, O'Leary PW, Driscoll DJ. Tricuspid valve disorders: atresia, dysplasia, and Ebstein anomaly (Chapter 38). In: Allen HD, Shaddy RE, Penny DJ, Feltes TF, Cetta F, editors. Moss and Adams' heart disease in infants, children, and adolescents in cluding the fetus and young adults. 9th ed: Wolters Kluwer; 2016. p. 949–83.

Hahn RT. State-of-the-art review of echocardiographic imaging in the evaluation and treatment of functional tricuspid regurgitation. Circ Cardiovasc Imaging. 2016;9:e005332. https://doi.org/10.1161/CIRCIMAGING.11.005332.

Luxford J, Bassin L, D'Ambra M. Echocardiography of the tricuspid valve. Ann Cardiothorac Surg. 2017;6(3):223–39.

O'Leary PW. Ebstein's malformation and tricuspid valve disease (Chapter 8). In: Eidem BW, O'leary PW, Cetta F, editors. Echocardiography in pediatric and adult congenital heart disease. 2nd ed: Wolters Kluwer; 2015. p. 148–65.

Shiina A, Seward JB, et al. Two-dimensional echocardiographic spectrum of Ebstein's anomaly: detailed anatomic assessment. JACC. 1984;3(2):35–70.

Stamm ER. Ebstein anomay (Chapter 12). In: Drose JA, editor. Fetal echocardiography. 2nd ed: Saunders Elsevier; 2010. p. 167–210.

Tricuspid Atresia

19

Maryam Moradian

Abstract

Absence of right atrioventricular connection is the hallmark of this third most common cyanotic congenital heart disease which is easily recognizable by echocardiography even during fetal life. Presence of interatrial communication and its size, ventricular septal defect, relation of great arteries, and pulmonary stenosis or pulmonary hypertension are important echocardiographic features that should be evaluated.

Tricuspid Atresia

1. Compare the size of left and right ventricles in four chamber view, demonstrate small, diminutive right ventricle (RV) and the absence of right atrioventricular connection (Fig. 19.1).
2. Appreciate the orientation of the great arteries (normal or transposed).
3. The presence of an atrial septal defect (ASD), patent foramen ovale (PFO), ventricular septal defect (VSD), pulmonary valve stenosis or atresia must be explained.
4. Classify the type based on the relationship of great arteries, presence of VSD and pulmonary stenosis as:
   Type I: Normally Related Great Arteries
   (a) No VSD and pulmonary atresia
   (b) Small VSD and pulmonary stenosis
   (c) Large VSD without pulmonary stenosis
   Type II: Transposed Great Arteries
   (a) VSD and pulmonary atresia
   (b) VSD and pulmonary stenosis
   (c) VSD without pulmonary stenosis
   Type III: Congenitally Corrected Transposition of the Great Arteries
5. Interrogation of the atrial septum by color Doppler, will demonstrate an obligatory right-to-left shunt via ASD, and if ASD is restrictive, the right atrium (RA) and hepatic veins would be severely dilated (Fig. 19.2).
6. Use color flow mapping to show absence of right atrioventricular connection as well as competency of left atrioventricular valve, which is important for planning the surgical repair (Figs. 19.3 and 19.4).
7. Completely evaluate for redundant, prominent Eustachian valve which may lead to misidentification as an ASD.
8. Also be aware of juxtaposition of right atrial appendage (RAA), especially if great arteries are transposed. The orifice of a juxtaposed RAA may be confused with an ASD. In parasternal long axis view, appearance of atrial septum, suggest this anomaly (Fig. 19.5). Also if in subcostal four chamber view the arrangement of atrial septum seems abnormal and has a curvature with convexity to the left you may find the RAA by tilting the plane of sound anteriorly and find its course from right to left which confirm its juxtaposition.
9. There may be total absence of tricuspid valve and replaced with a muscular shelf or it may be formed but is imperforate like a membrane. These can better be seen in transesophageal echocardiography (Fig. 19.6a, b)
10. During fetal life tricuspid atresia can be diagnosed by lack of communication between RA and RV, redundant valve of foramen ovale, large ASD, and small diminutive RV (Fig. 19.7).

M. Moradian (✉)
Pediatric Cardiology, Rajaie Cardiovascular, Medical & Research Center, Iran University of Medical Sciences, Tehran, Iran

M. Moradian, A. Alizadehasl (eds.), *Atlas of Echocardiography in Pediatrics and Congenital Heart Diseases*,
https://doi.org/10.1007/978-3-662-62341-1_19

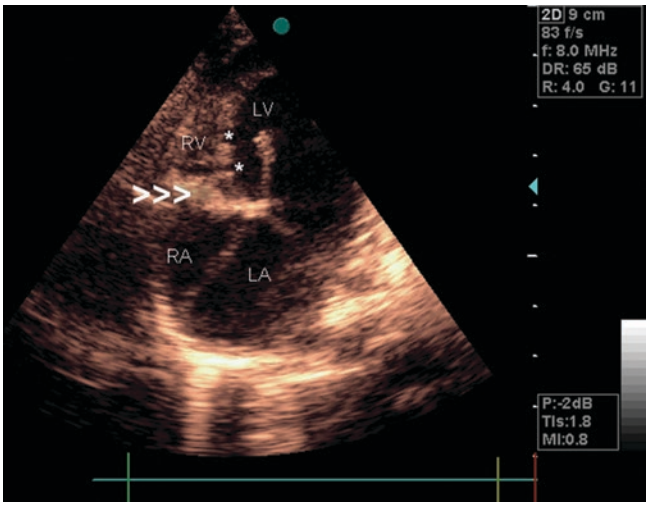

Fig. 19.1 Four chamber transthoracic echocardiography in apical window, showing small diminutive right ventricle, tricuspid atresia (arrow heads), and two small VSD s (asterisks), thickened anterior mitral leaflet is seen in this diastolic frame. *RV* right ventricle, *LV* left ventricle, *RA* right atrium, *LA* left atrium

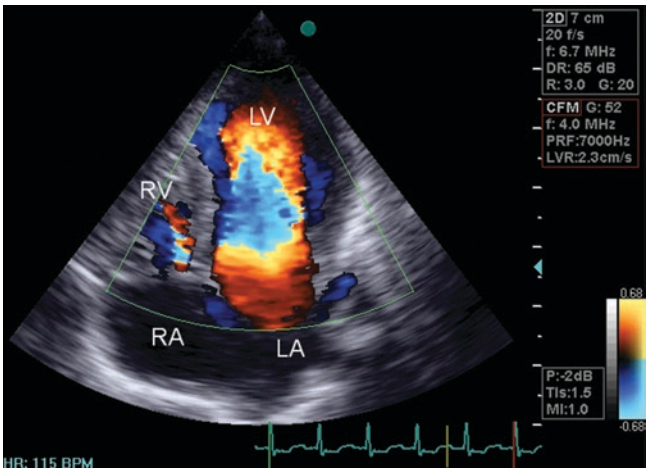

Fig. 19.3 Transthoracic echocardiography, color Doppler interrogation of atrioventricular valves in this four chamber diastolic frame confirms lack of communication between right atrium and right ventricle due to tricuspid atresia. *RV* right ventricle, *LV* left ventricle, *RA* right atrium, *LA* left atrium

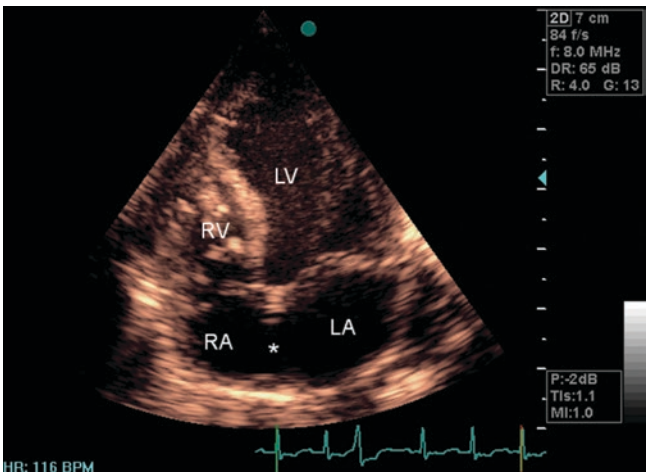

Fig. 19.2 In this case of Tricuspid atresia, large ASD is shown by asterisk. *RV* right ventricle, *LV* left ventricle, *RA* right atrium, *LA* left atrium

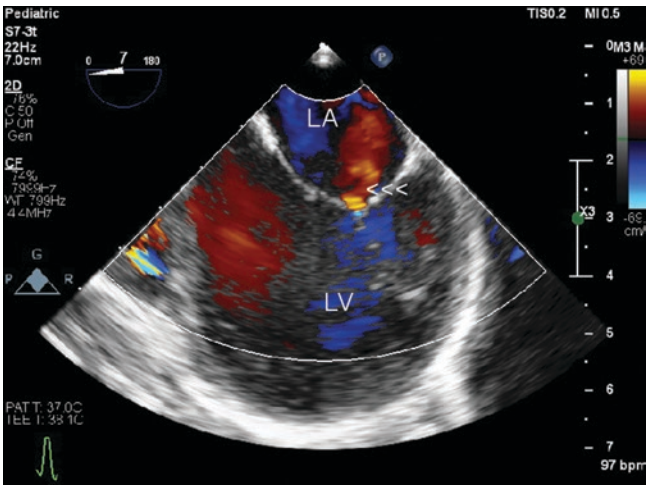

Fig. 19.4 Transesophageal echocardiography mid esophageal four chamber view, systolic frame of a patient with tricuspid atresia, showing mitral regurgitation (arrow heads). *LA* left atrium, *LV* left ventricle

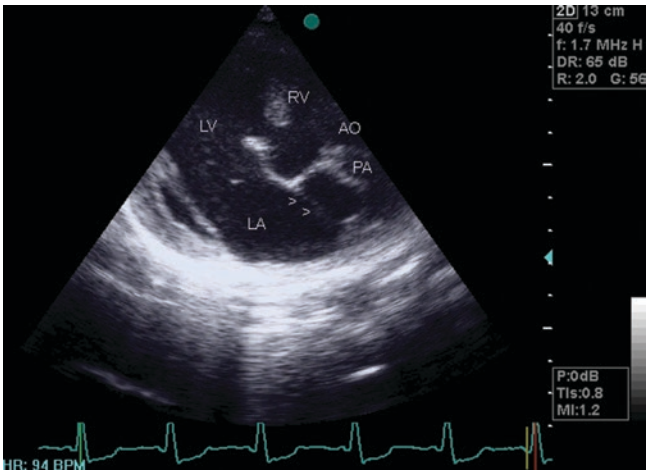

Fig. 19.5 Parasternal long axis view of a patient with tricuspid atresia, transposition of great arteries and pulmonary stenosis. Unusual orientation of atrial septum (arrow heads) is suggestive of juxtaposition of RAA. *RV* right ventricle, *LV* left ventricle, *RA* right atrium, *LA* left atrium, *PA* pulmonary artery, *AO* aorta

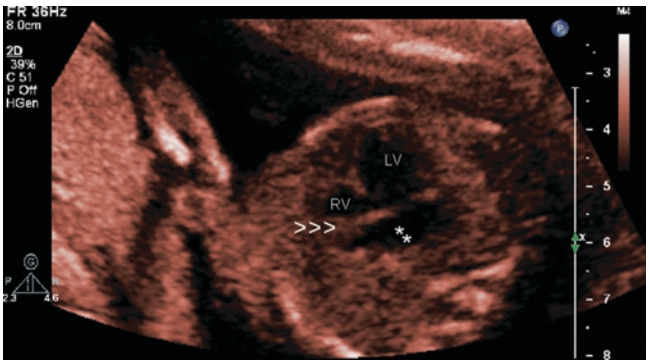

Fig. 19.7 Fetal echocardiogram in four chamber view showing rudimentary RV, tricuspid atresia (arrow heads), enlarged left heart chambers, VSD, and large ASD (asterisks). *RV* right ventricle, *LV* left ventricle

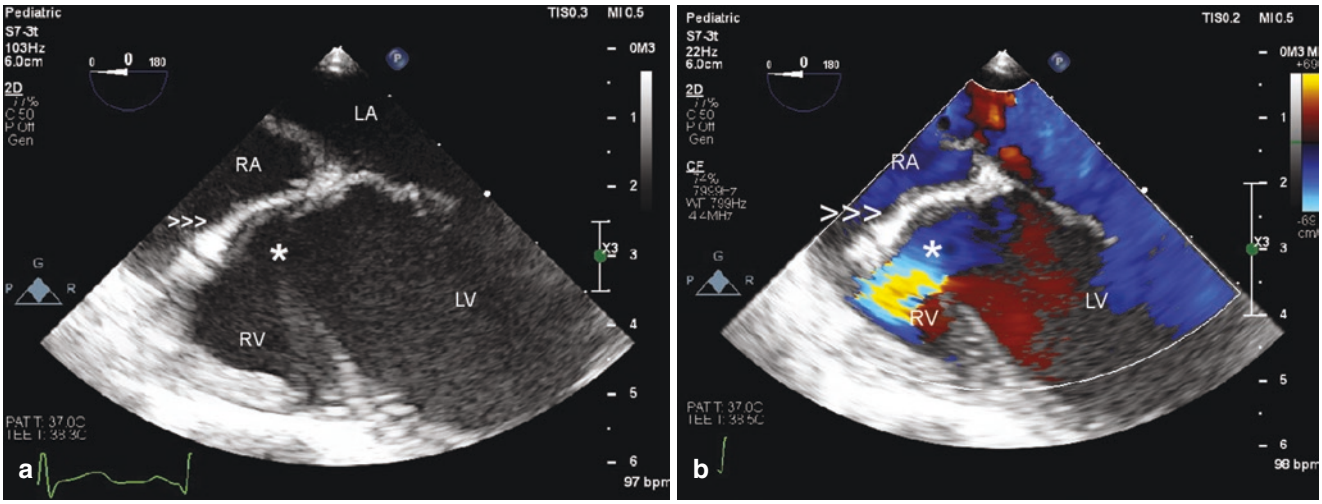

Fig. 19.6 (**a**, **b**) Transesophageal echocardiography mid esophageal four chamber view, diastolic frames, two dimensional (**a**), and with adding color Doppler (**b**) in a patient with tricuspid atresia, Arrow heads point to muscular shelf instead of tricuspid valve and asterisk indicate the VSD. Right ventricle is small and diminutive. Left to right shunt via VSD is seen in blue color. *RV* right ventricle, *LV* left ventricle, *RA* right atrium, *LA* left atrium

Suggested Reading

Anon. Ventricular hypoplasia (Chapter 8). In: Snider R, Serwer GA, Ritter SB, editors. Echocardiography in pediatric heart disease. 2nd ed: Mosby-Year Book Inc.; 1997. p. 343–84.

Anon. Ebstein anomaly, tricuspid valve dysplasia, and tricuspid regurgitation (Chapter 20). In: Abuhamad A, Chaoui R, editors. A practical guide to fetal echocardiography: normal and abnormal hearts. 3rd ed: Wolters Kluwer; 2016. p. 297–316.

Barrett SB. Hypoplasia of right ventricle (Chapter 8). In: Drose JA, editor. Fetal echocardiography. 2nd ed: Saunders Elsevier; 2010. p. 145–57.

Berg C, Lachmann R, Kaiser C, et al. Prenatal diagnosis of tricuspid atresia: intrauterine course and outcome. Ultrasound Obstet Gynecol. 2010;35:183–90.

Cetta F, Dearani JA, O'Leary PW, Driscoll DJ. Tricuspid valve disorders: atresia, dysplasia, and Ebstein anomaly (Chapter 38). In: Allen HD, Shaddy RE, Penny DJ, Feltes TF, Cetta F, editors. Moss and Adams' heart disease in infants, children, and adolescents including the fetus and young adults. 9th ed: Wolters Kluwer; 2016. p. 949–83.

Luxford J, Bassin L, D'Ambra M. Echocardiography of the tricuspid valve. Ann Cardiothorac Surg. 2017;6(3):223–39.

Menon SC, Cabalka AK. Univentricular atrioventricular connection (Chapter 12). In: Eidem BW, O'leary PW, Cetta F, editors. Echocardiography in pediatric and adult congenital heart disease. 2nd ed: Wolters Kluwer; 2015. p. 220–49.

Wong PC. Evaluation of the single ventricle (Chapter 10). In: Wong PC, Miller-Hance WC, editors. Transesophageal echocardiography for congenital heart disease. London: Springer-Verlag; 2014. p. 253–82.

Congenital Dysplasia of the Tricuspid Valve

20

Maryam Moradian and Azin Alizadehasl

Abstract

Shortened chorda, thickened leaflets, restricted motion of septal and inferior leaflets without displacement, help to distinguish this anomaly from Ebstein's malformation of tricuspid valve though in both anomaly tricuspid regurgitation may be significant.

Congenital Dysplasia of the Tricuspid Valve

1. Evaluate shortened chorda and thickened leaflets of tricuspid valve (TV) in four chamber view.
2. Remember that, though leaflets are abnormal, and their motion is restricted, they are not displaced or adherent to their underlying myocardium (Fig. 20.1)
3. Tricuspid regurgitation in these patients arises from TV annulus which is an important feature for differentiating this anomaly from Ebstein's anomaly even during fetal life (Fig. 20.2a, b).

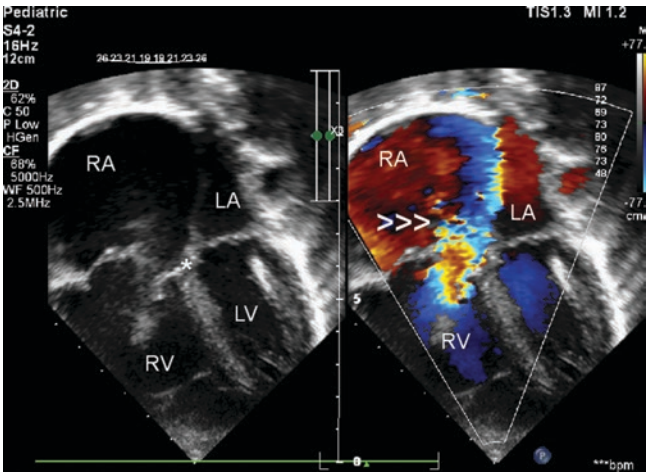

Fig. 20.1 Apical four chamber view of a congenital dysplastic tricuspid valve, systolic frame showing normal insertion (asterisk) of abnormally thickened TV leaflets with shortened chorda in two dimensional transthoracic echocardiography (right) and severe tricuspid regurgitation via coaptation gap (arrow heads (left). *RV* right ventricle, *LV* left ventricle, *RA* right atrium, *LA* left atrium

M. Moradian
Pediatric Cardiology, Rajaie Cardiovascular, Medical & Research Center, Iran University of Medical Sciences, Tehran, Iran

A. Alizadehasl (✉)
Department of Cardio-Oncology and Research Center, Rajaie Cardiovascular, Medical & Research Center, Iran University of Medical Sciences, Tehran, Iran

M. Moradian, A. Alizadehasl (eds.), *Atlas of Echocardiography in Pediatrics and Congenital Heart Diseases*,
https://doi.org/10.1007/978-3-662-62341-1_20

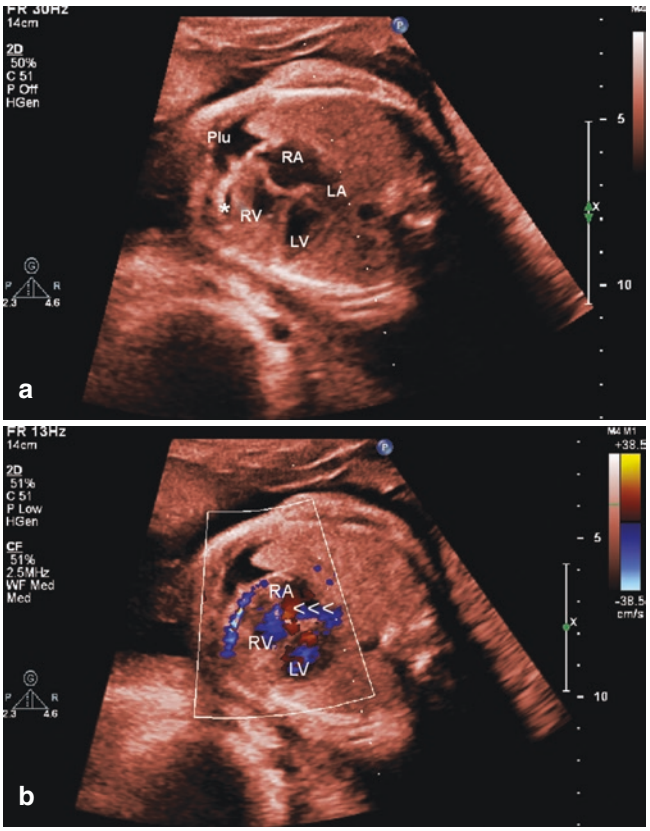

Fig. 20.2 (**a**, **b**) Fetal echocardiogram four chamber view showing dysplastic tricuspid valve. Asterisk indicate mild pericardial effusion. Color Doppler interrogation in same patient reveals significant tricuspid regurgitation (arrow heads) in **b**. This fetus also suffers from pericardial and plural effusion. *Plu* plural effusion, *RV* right ventricle, *LV* left ventricle, *RA* right atrium, *LA* left atrium

Suggested Reading

Cetta F, Dearani JA, O'Leary PW, Driscoll DJ. Tricuspid valve disorders: atresia, dysplasia, and Ebstein anomaly (Chapter 38). In: Allen HD, Shaddy RE, Penny DJ, Feltes TF, Cetta F, editors. Moss and Adams' heart disease in infants, children, and adolescents Including the fetus and young adults. 9th ed: Wolters Kluwer; 2016. p. 949–83.

Friedberg MF, Silverman NH. Atrioventricular septal defects and atrioventricular valve anomalies (Chapter 8). In: Wong PC, Miller-Hance WC, editors. Transesophageal echocardiography for congenital heart disease. London: Springer-Verlag; 2014. p. 253–82.

Shah S, Jenkins T, Markowitz A, Gilkeson R, Rajiah P. Multimodal imaging of the tricuspid valve: normal appearance and pathological entities. Insights Imaging. 2016;7:649–67.

Sharland GK, Chita SK, Allan LD. Tricuspid valve dysplasia or displacement in intrauterine life. J Am Coll Cardial. 1991;17:944–9.

Stamm ER. Ebstein anomaly (Chapter 12). In: Drose JA, editor. Fetal echocardiography. 2nd ed: Saunders Elsevier; 2010. p. 167–210.

UHL Anomaly

21

Shamsi Ghaffari, Azin Alizadehasl, and Maryam Moradian

Abstract

Severe Dilation and dysfunction of right ventricle (RV), absence of myocardium of the parietal RV wall, apposition of pericardium and endocardium, normal muscularization of septal and septomarginal trabeculation as well as normal papillary muscles of RV are echocardiographic characteristics of this anomaly which should be differentiated from Ebstein anomaly and arrhythmogenic right ventriclular dysplasia (ARVD).

UHL Anomaly

1. Severe dilation of right ventricle (RV), right atrium (RA), severe RV dysfunction with diffuse RV hypokinesia, while left ventricular (LV)function is normal, should rise the suspicion of RV cardiomyopathy (Fig. 21.1).
2. Use color and continuous Doppler to evaluate tricuspid regurgitation
3. Don't forget to assess for possible associated anomalies including ASD and pulmonary atresia with intact ventricular septum
4. To distinguish UHL anomaly from other types of RV cardiomyopathy evaluate the RV myocardium. In UHL anomaly or "parchment heart" myocardial layer of parietal RV wall is absent or is very thin but septomarginal trabeculation, and papillary muscles have normal myocardial layer. In other types of RV cardiomyopathy RV wall thickness is normal or increased.
5. Also evaluate the tricuspid valve leaflets that insert at the true anatomic annulus. This finding differentiate it from Ebstein anomaly of tricuspid valve.
6. Arrhythmogenic right ventriclular dysplasia (ARVD) should also be differentiated from UHL anomaly. In Uhl anomaly, endocardium and epicardium lie parallel and there is no fat tissue between them.

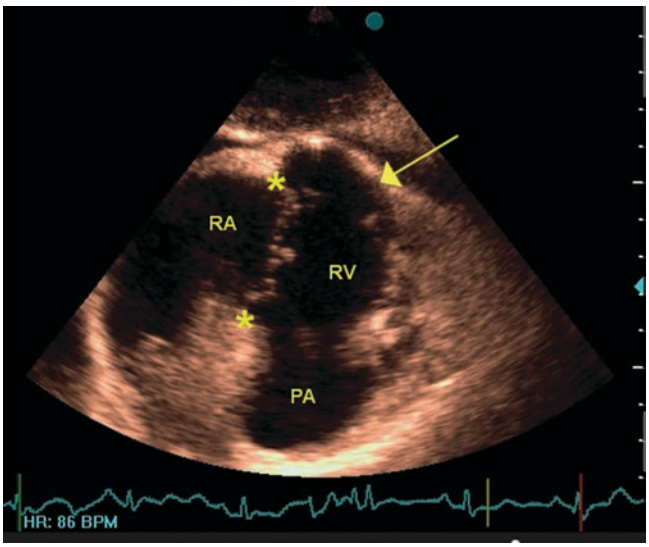

Fig. 21.1 Transthoracic echocardiography, subcostal view showing thin parietal wall of RV (arrow) due to absence of myocardium. Asterisks indicate normal insertion of tricuspid valve leaflets. Mild pericardial effusion is also seen. *RA* right atrium, *RV* right ventricle, *PA* pulmonary artery

S. Ghaffari
Pediatric Cardiology, Cardiovascular Research Center, Tabriz University of Medical Sciences, Tabriz, Iran

A. Alizadehasl
Department of Cardio-Oncology and Research Center, Rajaie Cardiovascular, Medical & Research Center, Iran University of Medical Sciences, Tehran, Iran

M. Moradian (✉)
Pediatric Cardiology, Rajaie Cardiovascular, Medical & Research Center, Iran University of Medical Sciences, Tehran, Iran

M. Moradian, A. Alizadehasl (eds.), *Atlas of Echocardiography in Pediatrics and Congenital Heart Diseases*,
https://doi.org/10.1007/978-3-662-62341-1_21

Suggested Reading

Cetta F, Dearani JA, O'Leary PW, Driscoll DJ. Tricuspid valve disorders: atresia, dysplasia, and Ebstein Anomaly (Chapter 38). In: Allen HD, Shaddy RE, Penny DJ, Feltes TF, Cetta F, editors. Moss and Adams' heart disease in infants, children, and adolescents including the fetus and young adults. 9th ed: Wolters Kluwer; 2016. p. 949–83.

Chounoune R, Lowry A, Ramakrishnan K, et al. Uhl's anomaly: a one and a half ventricular repair in a patient presenting with cardiac arrest. J Saudi Heart Assoc. 2018;30:52–4.

Cooper JM, Gerasimon GG, Deyell MW. Uhl's anomaly: cardiac features and ICD implantation. JACC Clin Electroophysiol. 2016;2(3)

Ikari NM, Azeka E, Aiello VD, et al. Uhl's anomaly. Differential diagnosis and indication for cardiac transplantation in an infant. Arq Bras Cardiol. 2001;77:73–6.

Moradian M, Shahmohammadi A, Yoosefnia MA, Mozaffari K. One and a half ventricular repair for Uhl's anomaly with one year follow up. Iranian Cardiovasc Res J. 2011;5(1)

Pulmonary Valve Stenosis

22

Shamsi Ghaffari and Maryam Moradian

Abstract

Echocardiography has an important role both in diagnosis and follow up of patients with pulmonary stenosis (PS), Dome shape opening, post stenotic dilation, and right ventricular hyprtrophy are two dimensional echocardiographic (2D) findings of pulmonary stenosis and should be completed by color and Doppler echocardiographic evidences.

Pulmonary Valve Stenosis

1. Differentiate the typical pulmonary valve stenosis, which is the second most common cardiac anomaly to ventricular septal defect (VSD) from dysplastic pulmonary valve. In typical pulmonary valve stenosis, pulmonary valve leaflets appear prominent due to thickening and restricted motion during systole; make an inward curvature, known as "doming". Also post stenotic dilation of the main pulmonary artery (MPA) is in favor of classic pulmonary valve stenosis. Transthoracic parasternal short axis view is one of the most useful views to see the pulmonary valve leaflets. Measure the pulmonary valve annulus and MPA diameter in the parasternal short-axis view in systole. Pay attention to evaluate the annulus as the maximal distance between the hinge points of the valve leaflets (Fig. 22.1).
2. In cases of dysplastic pulmonary valve, leaflets are thickened and immobile, with no doming. The pulmonary valve annulus is hypoplastic, and MPA is narrow. Dysplastic pulmonary valve is commonly seen in patients with Noonan syndrome.

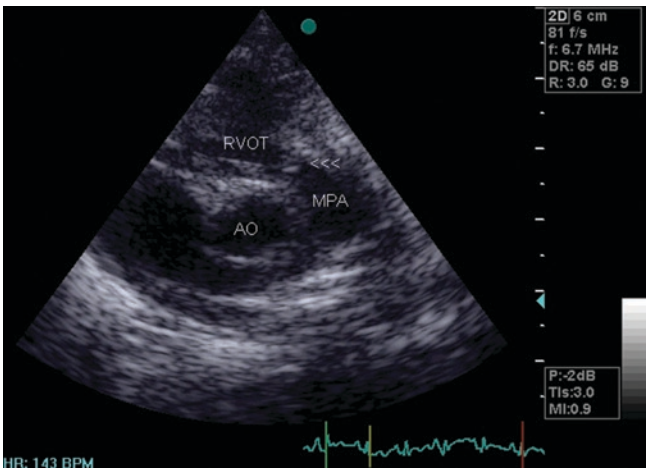

Fig. 22.1 Parasternal short axis view from a case of typical pulmonary valve stenosis, showing doming of leaflets (arrow heads) and post stenotic dilation of main pulmonary artery. *AO* aorta, *RVOT* right ventricular out flow tract, *MPA* main pulmonary artery

3. Right ventricular hypertrophy (RVH), dynamic subvalvar pulmonary stenosis, and severity of tricuspid regurgitation (TR) should also be evaluated in all cases of pulmonary stenosis. Pressure gradient of TR can be used for estimation of RV systolic pressure
4. Use color flow mapping to align the Doppler beam parallel with the direction of the flow jet as much as possible and estimate the severity of pulmonary stenosis (PS). In transthoracic echocardiography use parasternal short axis, high parasternal short and long-axis, as well as subcostal sagittal views to evaluate the PS jet. The Doppler-derived peak pressure gradient in pulmonary stenosis is almost similar with the peak-to-peak pressure gradient measured at catheterization (it exceeds the peak-to-peak pressure gradient measured at catheterization by a small amount and is not clinically significant).

Grading of pulmonary stenosis is based on peak velocity (m/s) and peak gradient (mmHg) as below:

S. Ghaffari
Pediatric Cardiology, Cardiovascular Research Center, Tabriz University of Medical Sciences, Tabriz, Iran

M. Moradian (✉)
Pediatric Cardiology, Rajaie Cardiovascular, Medical & Research Center, Iran University of Medical Sciences, Tehran, Iran

M. Moradian, A. Alizadehasl (eds.), *Atlas of Echocardiography in Pediatrics and Congenital Heart Diseases*,
https://doi.org/10.1007/978-3-662-62341-1_22

(a) Mild PS if peak velocity is <3 m/s and peak gradient is <36 mmHg
(b) Moderate PS if peak velocity is 3–4 m/s and peak gradient is 36–64 mmHg
(c) Severe PS if peak velocity is >4 m/s and peak gradient is >64 mmHg (Fig. 22.2).

5. Evaluate dynamic subvalvar pulmonary stenosis, using continuous (CW) and pulsed wave Doppler (PW), to differentiate the location of stenosis and evaluate their severity (Fig. 22.3).
6. Different transesophageal echocardiographic (TEE) views are useful for evaluation of pressure gradient across pulmonary valve including pulmonary bifurcation view at 0° (Fig. 22.4), and aortic arch short axis view at 60°–100° (Fig. 22.5).

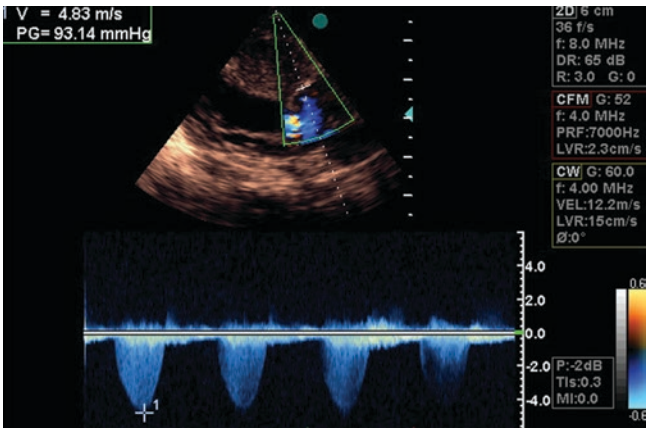

Fig. 22.2 The Doppler-derived peak pressure gradient of pulmonary stenosis in a child with sever pulmonary stenosis

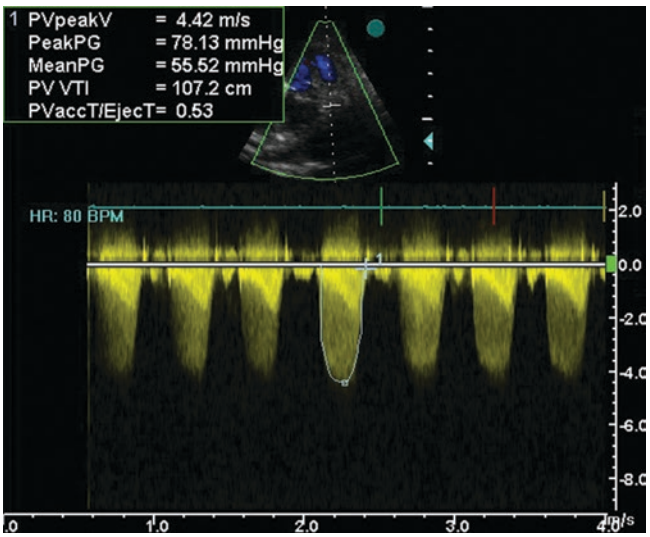

Fig. 22.3 Continuous wave Doppler scan from a child with severe valvar pulmonary stenosis and secondary hypertrophic subpulmonary stenosis. The asymmetric profile within the envelope of the CW Doppler signal represents the gradient across the zone of subvalvar pulmonary stenosis

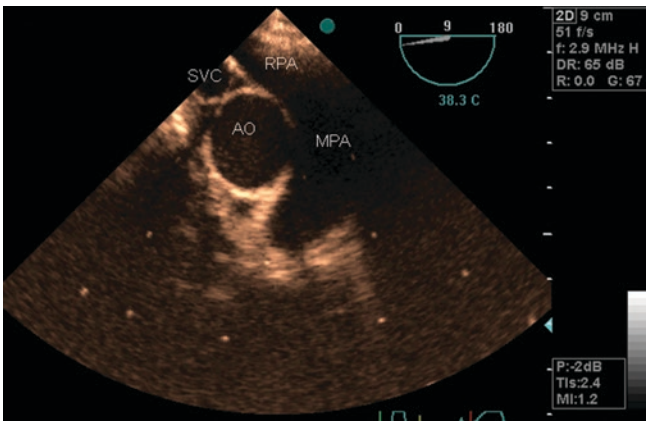

Fig. 22.4 TEE Upper esophageal pulmonary artery long axis view at 0° in a normal child. In this view you can evaluate pulmonary valve pressure gradient accurately. *MPA* main pulmonary artery, *RPA* right pulmonary artery, *SVC* superior vena cava, *AO* ascending aorta

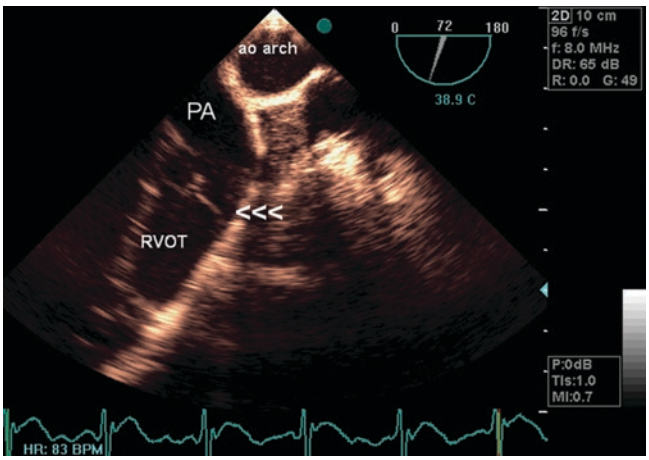

Fig. 22.5 TEE, upper esophageal aortic arch short axis view, arrow heads indicate pulmonary valve in a normal child. *AO* arch, aortic arch, *PA* pulmonary artery, *RVOT* right ventricular out flow tract

7. Also in TEE RVOT and Pulmonary valve can be evaluated in modified transgasteric short axis view (Fig. 22.6)
8. As this anomaly may be progressive regular echocardiographic follow-up is necessary.
9. Fetal echocardiographic evaluation of pulmonary stenosis is best performed by observing the abnormally thickened leaflets of pulmonary valve in different views especially right ventricular out flow tract view. Even post stenotic dilation of MPA can be seen in three vessel view. By using color and pulsed Doppler interrogation you can confirm the diagnosis (Fig. 22.7a, b)

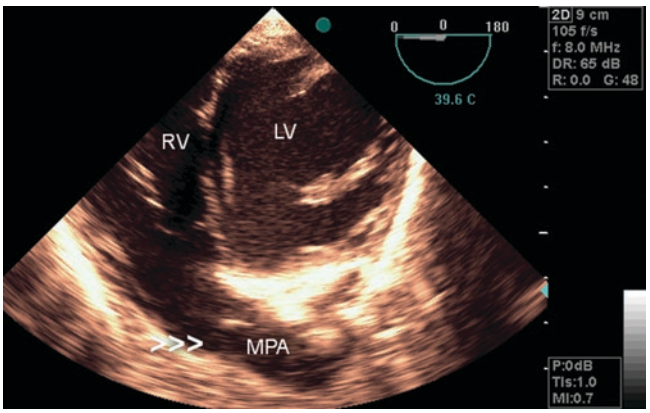

Fig. 22.6 TEE, transgasteric short axis view, showing RVOT and pulmonary valve (arrow heads) in a normal child. *RV* right ventricle, *LV* left ventricle, *MPA* main pulmonary artery

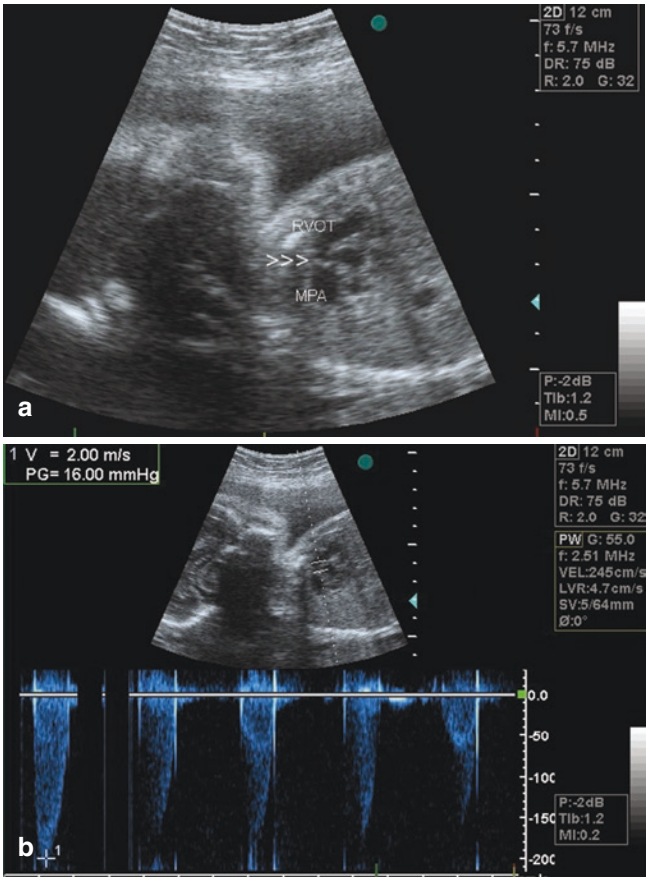

Fig. 22.7 (**a**, **b**) Fetal echocardiography showing thickened pulmonary valve leaflets as well as dilated main pulmonary artery and doming in (**a**) and increased velocity and pressure gradiant via stenotic valve in (**b**). *MPA* main pulmonary artery, *RVOT* right ventricular out flow tract

Suggested Reading

Arain N, Moller JH, Pyles LA, Sivanandam S. "Vanishing" pulmonary valve stenosis. Ann Pediatr Cardiol. 2012;5(1):47–50.

Ardura J, Gonzalez C, Andres J. Does mild pulmonary stenosis progress during childhood? A study of its natural course. Clin Cardiol. 2004;27:519–22.

Baumgartner H, Hung J, Bermejo J, et al. Echocardiographic assessment of valve stenosis: EAE/ASE recommendations for clinical practice. Eur J Echocardiogr. 2009;10:1–25.

Bieker TM. Aortic stenosis and pulmonary stenosis (Chapter 10). In: Drose JA, editor. Fetal echocardiography, 2nd ed. Saunders, an imprint of Elsevier Inc.; 2010.

Khorgami MR, Moradian M, Omidi N, Aarabi Moghadam MY. Management of cardiovascular disorders in patients with Noonan syndrome: a case report. J Teh Univ Heart Ctr. 2017;12(4):184–7.

Lopez L, Ventura R, Choueiter NF. Outflow tract anomalies (Chapter 11). In: Wong PC, Miller-Hance WC, editors. Transesophageal echocardiography for congenital heart disease. London: Springer-Verlag; 2014. p. 283–305.

Michelfelder EC, Border WL. Abnormalities of right ventricular outflow (Chapter 13). In: Eidem BW, O'leary PW, Cetta F, editors. Echocardiography in pediatric and adult congenital heart disease. 2nd ed: Wolters Kluwer; 2015. p. 250–71.

Prieto LR, Latson LA. Pulmonary stenosis (Chapter 39). In: Allen HD, Shaddy RE, Penny DJ, Feltes TF, Cetta F, editors. Moss and Adams' heart disease in infants, children, and adolescents including the fetus and young adults. 9th ed: Wolters Kluwer; 2016. p. 983–1008.

Critical Pulmonary Stenosis (Critical PS)

23

Maryam Moradian

Abstract

In a cyanotic and ill newborn, critical pulmonary stenosis should be ruled out. Severe pulmonary stenosis in this new born may lead to decreased right ventricular compliance and right-to-left shunt through a patent foramen ovale (PFO). Echocardiography is invaluable for the diagnosis of this structural anomaly, its hemodynamic consequences, and planning for the urgent intervention.

Critical Pulmonary Stenosis (Critical PS)

1. In a cyanotic newborn with severe right ventricular hypertrophy (RVH), as well as severe PS, critical PS should be considered. Evaluate right ventricular hypertrophy (RVH) in different echocardiographic views (Fig. 23.1). You may find different degrees of RV endocardial fibroelastosis (EFE) as well (Fig. 23.2).
2. Check for right to left shunt via atrial septal defect (ASD) or patent foramen ovale (PFO) in subcostal and four chamber views
3. Evaluate the severity and pressure gradient of tricuspid regurgitation using color flow mapping and Doppler. Estimate RV systolic pressure (Fig. 23.3).
4. Remmember to appreciate for patency of ductus arteriosus (PDA) which is needed to maintain systemic saturation in these patients (Fig. 23.4).
5. Measure the pulmonary valve annulus in parasternal short-axis view. Select a systolic frame and evaluate the maximal distance between hinge points of valve leaflets. Also evaluate the size of main pulmonary artery and its branches in systolic frames.
6. Evaluate the development of right ventricle (RV) by measuring the tricuspid valve annulus in apical four chamber

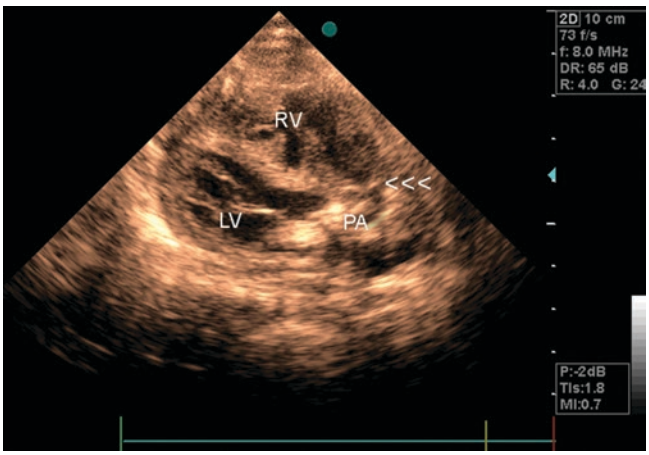

Fig. 23.1 Parasternal long axis view with slight left ward tilting of transducer in a neonate with critical PS. Arrow heads points to thickened pulmonary valve leaflets. Severe RVH is also shown. *RV* right ventricle, *LV* left ventricle, *PA* pulmonary artery

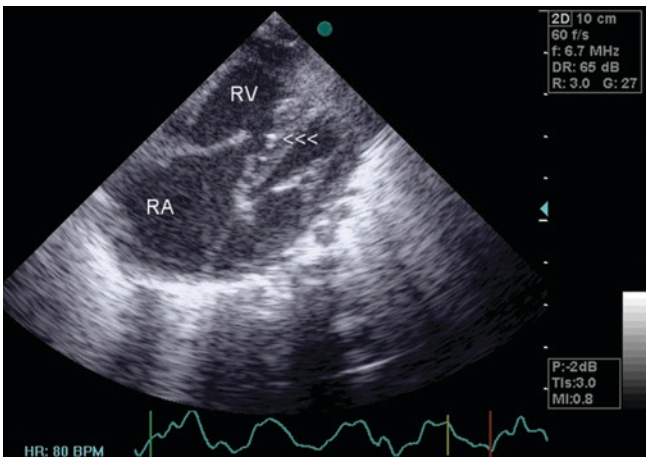

Fig. 23.2 In this four chamber view arrowheads points to endocardial fibroelastosis (EFE) RA and RV are enlarged in this case of critical PS. *RV* right ventricle, *RA* right atrium

M. Moradian (✉)
Pediatric Cardiology, Rajaie Cardiovascular, Medical & Research Center, Iran University of Medical Sciences, Tehran, Iran

M. Moradian, A. Alizadehasl (eds.), *Atlas of Echocardiography in Pediatrics and Congenital Heart Diseases*,
https://doi.org/10.1007/978-3-662-62341-1_23

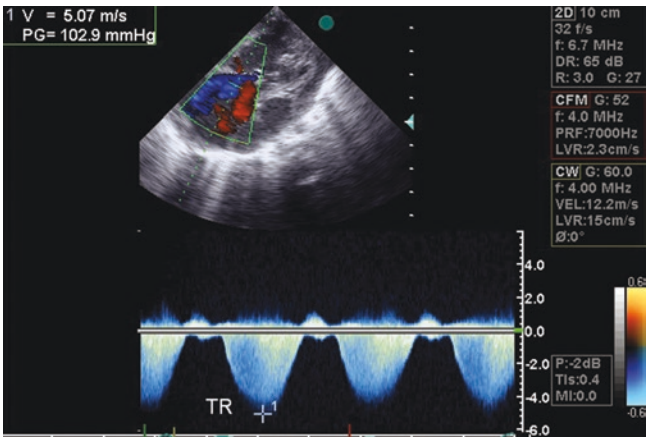

Fig. 23.3 Doppler evaluation of RV systolic pressure. *RV* right ventricle, *TR* tricuspid regurgitation

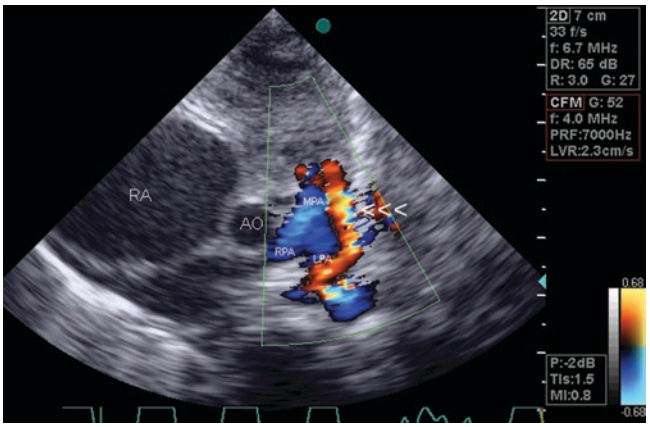

Fig. 23.4 Parasternal short axis view using color flow mapping to show PDA flow (arrow heads) in this case of critical PS. RA is severely enlarged. *RA* right atrium, *AO* aorta, *MPA* main pulmonary artery, *RPA* right pulmonary artery, *LPA* left pulmonary artery

view. Use a diastolic frame and measure the maximal distance between the hinge points of the valve leaflets.

7. During intrauterine life, pulmonary stenosis may progress to critical pulmonary stenosis. So serial fetal echo is recommended. Also in cases of twin pregnancy, the recipient twin of twin-to-twin transfusion syndrome (TTTS) may be in danger of developing subvalvar and valvar pulmonary stenosis

Suggested Reading

Caspi J, Coles JG, Benson LN, et al. Management of neonatal critical pulmonic stenosis in the Balloon Valvotomy Era. Ann Thorac Surg. 1990;49:273–8.

Eschbach SJ, Boons LSTM, Vanzwet E, et al. Right ventricular outflow tract obstruction in complicated monochorionic twin pregnancy. Ultrasound Obstet Gynecol. 2017;49:737–43.

Kovalchin JP, Forbes TJ, Nihill MR, Geva T. Echocardiographic determinants of clinical course in infants with critical and severe pulmonary valve stenosis. JACC. 1997;29(5):1095–101.

Latson LA. Critical pulmonary stenosis. J Interventional Cardiol. 2001;14(3)

Mitchell B, Mhlongo M. The diagnosis and management of congenital pulmonary valve stenosis. SA Heart. 2018;15(1):36–45.

Nakata MRH, Chmait RH, Quintero RA. Umbilical cord occlusion of the donor versus recipient fetus in twin–twin transfusion syndrome

Double-Chambered Right Ventricle (DCRV) or Right Ventricular Muscle Bundle (RVMB)

24

Maryam Moradian and Azin Alizadehasl

Abstract

Echocardiography is very useful to identify and follow up patients with Double-Chambered Right Ventricle. This anomaly is often associated with VSD.

Double-Chambered Right Ventricle (DCRV) or Right Ventricular Muscle Bundle (RVMB)

1. Appreciate abnormal right ventricular muscle bundle (RVMB) in apical four chamber and subcostal as well as parasternal views. Two-dimensional echo shows narrowing of mid RV cavity and color flow Doppler confirm the obstruction by displaying the turbulent jet. The subcostal view provides better alignment for measuring the pressure gradient by continuous Doppler (CW).
2. Often ventricular septal defect (VSD) is also present, so check the interventricular septum in different views
3. Transesophageal echocardiography (TEE) is very useful especially in adult patients with poor echo window. Use RV Inflow-outflow view and check both VSD and RVMB simultaneously (Figs. 24.1 and 24.2).
4. As this anomaly is progressive especially in adolescents, serial echocardiography is recommended
5. This anomaly in adults may be associated with aortic insufficiency or mild subaortic stenosis. Also, spontaneous VSD closure may had happen by time in these patients.

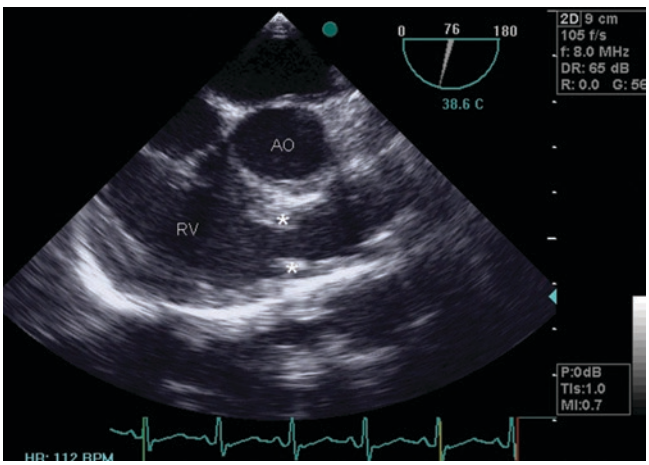

Fig. 24.1 TEE showing RV inflow-outflow view in a patient with double chamber RV, asterisks indicate abnormal muscle bundle within RV cavity. *RV* right ventricle, *AO* aorta

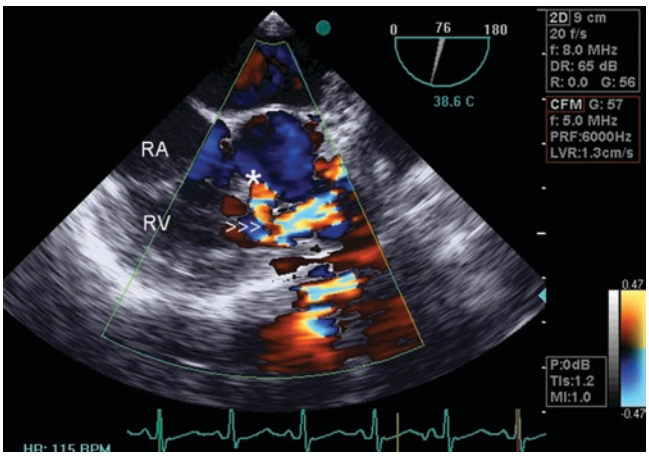

Fig. 24.2 TEE, RV inflow–out flow view, using color flow mapping to show VSD (asterisk) and RVMB (arrow heads). *RV* right ventricle, *RA* right atrium

M. Moradian
Pediatric Cardiology, Rajaie Cardiovascular, Medical & Research Center, Iran University of Medical Sciences, Tehran, Iran

A. Alizadehasl (✉)
Department of Cardio-Oncology and Research Center, Rajaie Cardiovascular, Medical & Research Center, Iran University of Medical Sciences, Tehran, Iran

M. Moradian, A. Alizadehasl (eds.), *Atlas of Echocardiography in Pediatrics and Congenital Heart Diseases*,
https://doi.org/10.1007/978-3-662-62341-1_24

6. There are case reports of this anomaly during fetal life leading to fetal hydrops or severe heart failure, so in cases of hydrops and heart failure during fetal life don't overlook this anomaly.

Suggested Reading

Animasahun BA, Ekure EN, Njokanma OF. Double-chambered right ventricle: an uncommon congenital heart disease. A case report and literature review. Cardiovasc J Africa. 2011;22:4.

Becker S, Hofbeck M, Kendziorra H. Double-chamber right ventricle associated with severe fetal cardiac failure. Ultrasound Obstet Gynecol. 2004;23:411–3.

Chellappan S, Sahu B, Sathe YC. Isolated double-chambered right ventricle with intact interventricular septum. J Cardiovasc Echography. 2016;26:127–30.

Joe KT, Lee JKT, Tsui KL. Double-chambered right ventricle: a commonly overlooked diagnosis. Hong Kong Med J. 2015;21:84. e1–2.

Moustafa S, Patton DJ, Alvarez N, et al. Double chambered right ventricle with ventricular septal defect in adults: case series and review of the literature case series and review of the literature. J Cardiovasc Ultrasound. 2015;23(1):48–51.

Oliver JM, Garrido A, Gonzalez A. Rapid progression of midventricular obstruction in adults with double-chambered right ventricle. J Thorac Cardiovasc Surg. 2003;126:711–7.

Said SM, Burkhart HM, Dearani JA, et al. Outcomes of surgical repair of double-chambered right ventricle. Ann Thorac Surg. 2012;93:197–200.

Yuan SM. Double-chambered right ventricle in children. J Coll Physicians Surg Pak. 2019;29(12):1193–8.

Supravalvar Pulmonary Stenosis, and Peripheral Pulmonary Stenosis (PPS)

25

Maryam Moradian and Azin Alizadehasl

Abstract

Supravalvar pulmonary stenosis can occur at any level along main pulmonary artery and its branches. It is commonly associated with other CHDs and or syndromes such congenital rubella, Alagille, Noonan, Ehlers-Danlos and Williams. Physiologic peripheral pulmonic stenosis may be present in neonatal period.

Supravalvar Pulmonary Stenosis, and Peripheral Pulmonary Stenosis (PPS)

1. Native supravalvar pulmonary stenosis, a very rare entity, in most cases is at the sinotubular junction of main pulmonary artery (MPA). This anomaly creates an hour glass appearance, similar to supravalvar aortic stenosis. Use different views, including parasternal short and long axis, subcostal, and suprasternal windows to evaluate the stenosis, even you may be able to visualize it by anterior sweeping in apical view.
2. Narrowing of pulmonary trunk, its bifurcation, and pulmonary artery branches commonly are associated with other congenital heart diseases especially tetralogy of Fallot (Fig. 25.1).
3. Supravalvar pulmonary stenosis and peripheral pulmonary stenosis may also be seen in association with some syndromes, such as DiGeorge, congenital rubella, Alagille, Williams, Noonan, and Ehlers-Danlos.

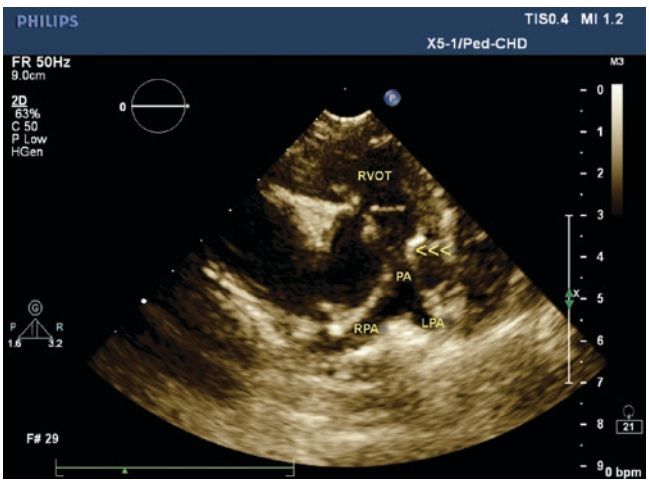

Fig. 25.1 Transthoracic parasternal short axis view showing supravalvar pulmonary stenosis (arrow heads) and narrowing of RPA and LPA. *RPA* right pulmonary artery, *LPA* left pulmonary artery, *PA* pulmonary artery, *RVOT* right ventricular out flow tract

4. During neonatal period especially in premature infants a transient and mild form of peripheral pulmonary artery stenosis can be detected which resolve within 3 months.
5. Never forget the limitation of echocardiography to visualize the distal parts of right and left pulmonary arteries. If tricuspid regurgitation jet indicates an elevated RV systolic pressure and there is no pulmonary valve stenosis or pulmonary hypertension, try to evaluate branch pulmonary arteries for peripheral stenosis. You may need to use other imaging modalities such as CT Scan or MRI.
6. Use color Doppler to find the location of RPA and LPA narrowing (Fig. 25.2a, b)
7. Check for discrete LPA stenosis in conotruncal lesions with tortuous PDA (Fig. 25.3)
8. Evaluate for concomitant supravalvar AS which is seen in Williams syndrome

M. Moradian
Pediatric Cardiology, Rajaie Cardiovascular, Medical & Research Center, Iran University of Medical Sciences, Tehran, Iran

A. Alizadehasl (✉)
Department of Cardio-Oncology and Research Center, Rajaie Cardiovascular, Medical & Research Center, Iran University of Medical Sciences, Tehran, Iran

M. Moradian, A. Alizadehasl (eds.), *Atlas of Echocardiography in Pediatrics and Congenital Heart Diseases*,
https://doi.org/10.1007/978-3-662-62341-1_25

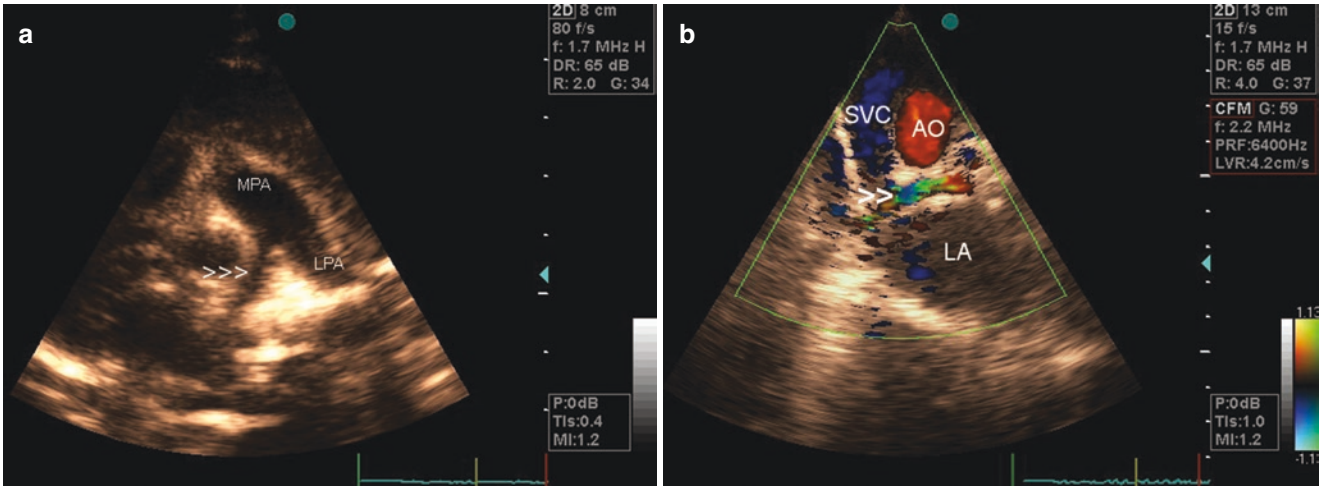

Fig. 25.2 (**a**, **b**) Arrowheads in this parasternal short axis view point to hypo plastic RPA (**a**). Turbulent flow in RPA can be seen by color aliasing in suprasternal short axis views (**b**). *RPA* right pulmonary artery, *LPA* left pulmonary artery, *MPA* main pulmonary artery, *SVC* superior vena cava, *AO* aorta, *LA* left atrium

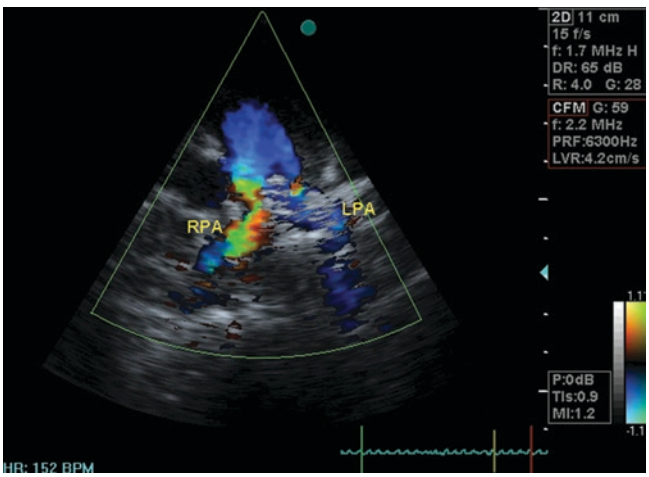

Fig. 25.3 RPA and LPA stenosis leads to aliasing of color in this parasternal short axis

9. Remmeber that it may occur after surgeries, like shunts, pulmonary sling repair, unifocalization, Lecompte maneuver in arterial switch and so on.
10. Remember that TEE is sub-optimal for visualizing distal parts of LPA and RPA. In midesophagial ascending aorta short axis view, bifurcation of MPA, RPA, and proximal part of LPA can be seen.

Suggested Reading

Arlettaz R, Archer N, Wilkinson AR. Natural history of innocent heart murmurs in newborn babies: controlled echocardiographic study. Arch Dis Child Fetal Neonatal Ed. 1998;78:F166–70.

Arlettaz R, Archer N, Wilkinson AR. Closure of the ductus arteriosus and development of pulmonary branch stenosis in babies of less than 32 weeks gestation. Arch Dis Child Fetal Neonatal Ed. 2001;85:F197–200.

Bacha EA, Kalimi R, Starr JP, et al. Autologous repair of supravalvar pulmonic stenosis. Ann Thorac Surg. 2004;77:734–6.

Chatelain P, Oberhänsli I, Friedli B. Physiological pulmonary branch stenosis in newborns: 2D-echocardiographic and Doppler characteristics and follow up. Eur J Pediatr. 1993;152(7):559–63.

Khanra D, Shrivastava Y, Duggal B, et al. BMJ Case Rep. 2019;12:e231008. https://doi.org/10.1136/bcr-2019231008.

Rodriguez RJ, Riggs TW. Physiologic peripheral pulmonic stenosis in infancy. Am J Cardiol. 1990;66(20):1478–81.

Yuan S-M. Supravalvular pulmonary stenosis: congenital versus acquired. Acta Med Mediterranea. 2017;33:849.

Pulmonary Valve Atresia, Intact Ventricular Septum (PA IVS) or Hypoplastic Right Heart Syndrome (HRHS)

26

Shamsi Ghaffari and Maryam Moradian

Abstract

In pulmonary atresia intact ventricular septum, or hypoplastic right heart syndrome the blood that enters the right ventricle has no egress, so regurgitate back into right atrium via tricuspid valve, and reach the left atrium through foramen ovale. These patients may have coronary sinusoidal channels. Echocardiography is useful in evaluating the right ventricular and tricuspid annulus size and may show sinusoidal channels, but angiography is necessary to evaluate the RV-dependent coronary circulation, and make the best decision for patient.

Pulmonary Atresia, Intact Ventricular Septum (PA IVS) or Hypoplastic Right Heart Syndrome (HRHS)

1. Remember that in this anomaly RV is strikingly heterogenous. Evaluate RV in apical four chamber view determine whether it is tripartite (inlet, trabecular, and outlet components), bipartite (inlet and outlet components), or unipartite (inlet component only) (Fig. 26.1). Right ventricular size is very important as well and is proportional to the size of the tricuspid valve (TV) annulus. Confirm the suitability for biventricular repair by evaluation the Z score of TV annulus which should be calculated by measuring the diameter of annulus in four chamber view, z-score of less than −3 has been reported is considered suboptimal. Also compare TV annulus diameter with mitral valve (MV) annulus diameter. TV diameter/MV diameter > 0.5 make the results of biventricular repair optimal.
2. Also special attention should focus on right to left shunting across interatrial septum in subcostal views, using color flow mapping and Doppler modalities. This shunt is necessary to maintain the systemic perfusion.
3. Evaluate the interventricular septum in different views and confirm that it is intact. Also evaluate the left ventricular function.
4. Determine whether the atretic pulmonary valve is membranous, or a long segment and muscular. The parasternal long and short axis and subcostal views are most helpful in this regard. Also, it is necessary to evaluate the confluence and size of the branch pulmonary arteries. Main pulmonary artery (MPA) is almost always present. Pulmonary artery branches are usually confluent and normal sized. Rarely multiple aortopulmonary collaterals (MAPCAS) provide pulmonary blood supply.
5. Assess the coronary arteries and look for the presence of any ventriculocoronary arterial connections, which result

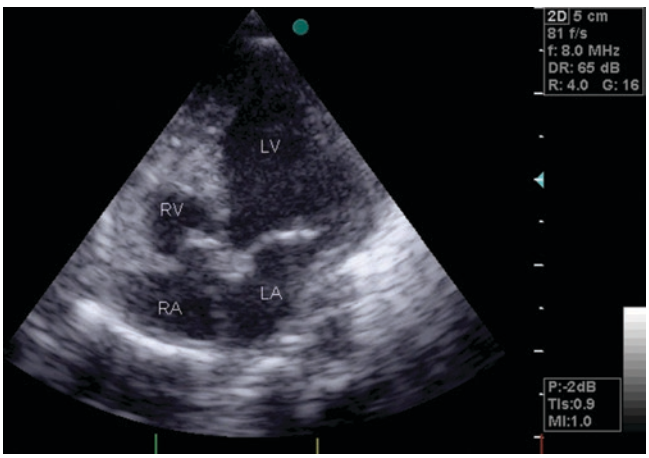

Fig. 26.1 Apical four chamber view of a patient with PA/IVS showing diminutive RV. *RV* right ventricle, *LV* left ventricle, *LA* left atrium, *RA* right atrium

S. Ghaffari
Pediatric Cardiology, Cardiovascular Research Center, Tabriz University of Medical Sciences, Tabriz, Iran

M. Moradian (✉)
Pediatric Cardiology, Rajaie Cardiovascular, Medical & Research Center, Iran University of Medical Sciences, Tehran, Iran

M. Moradian, A. Alizadehasl (eds.), *Atlas of Echocardiography in Pediatrics and Congenital Heart Diseases*,
https://doi.org/10.1007/978-3-662-62341-1_26

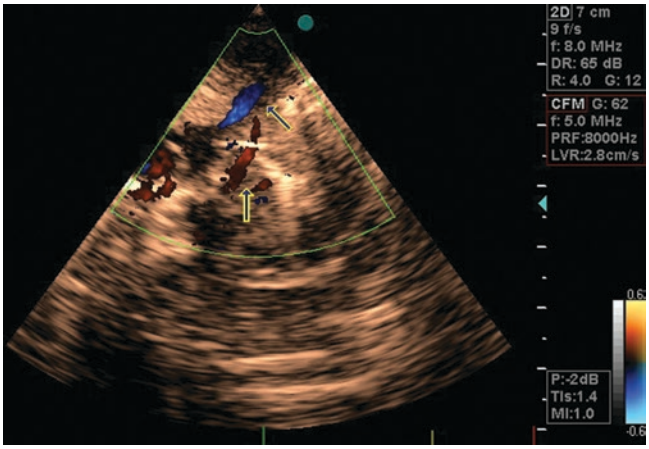

Fig. 26.2 Subcostal coronal view showing multiple coronary sinusoidal channels by color flow Doppler (arrows)

in RV-dependent coronary circulation especially in cases with very small and hypertensive RV. These sinusoidal channels, connections between RV and coronary arteries are sometimes stenotic and cause some parts of myocardium be dependent on RV pressure for perfusion. Use low scale color flow mapping to find coronary sinusoids, though confirmation of RV dependent coronary circulation typically requires angiocardiography (Fig. 26.2).

6. Evaluate the tricuspid valve (TV) anatomically and functionally, using 2D and color Doppler in different views. TV is rarely normal in this anomaly. The spectrum of TV anomaly may range from severe stenosis to severe regurgitation. It may be dysplastic or may show degrees of displacement (Ebstein anomaly). The incidence of RV dependent coronary circulation is lower in patients with regurgitant tricuspid valve as regurgitation helps the decompression of RV.
7. Also delineate the size and course of the Patent ductus arteriosus (PDA) from suprasternal notch long axis and high parasternal views (Fig. 26.3).
8. In TEE evaluate interatrial septal defect in mid esophageal four chamber and bicaval view and the size of tricuspid valve annulus and RV in mid esophageal four chamber and RV in flow- out flow views. Long axis and transgasteric views are very useful regarding mitral valve and cardiac function evaluation.
9. During fetal life, with advancing gestation, the RV wall becomes more hypertrophied in cases of PA IVS. Evaluate

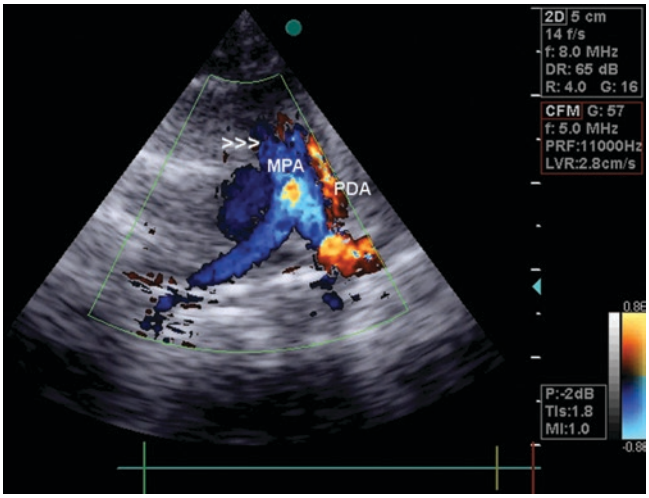

Fig. 26.3 Parasternal, short axis view of membranous type PA IVS, presence of PDA is confirmed by color Doppler, red color indicate flow toward atretic pulmonary valve. Atretic pulmonary valve is shown by arrow heads. *PDA* patent ductus arteriosus, *MPA* main pulmonary artery

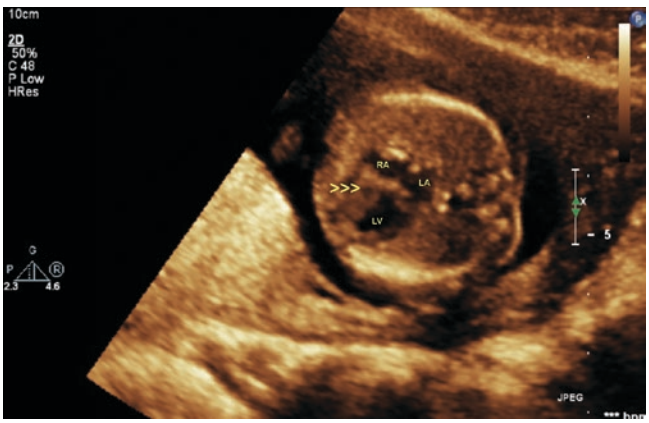

Fig. 26.4 Fetal echocardiogram, four chamber view showing very small and diminutive right ventricle (arrow heads). *LV* left ventricle, *LA* left atrium, *RA* right atrium

hypoplasia of RV cavity, in four chamber view (Fig. 26.4). Show the severity of TR and appreciate any reverse flow through ductus arteriosus (Figs. 26.5 and 26.6). Severe tricuspid regurgitation in fetuses with PA IVS may leads to right heart failure, pleural effusion pericardial effusion, ascites, lung hypoplasia, and fetal death. Also appreciate ventriculocoronary arterial connections by color Doppler and confirm it by PW.

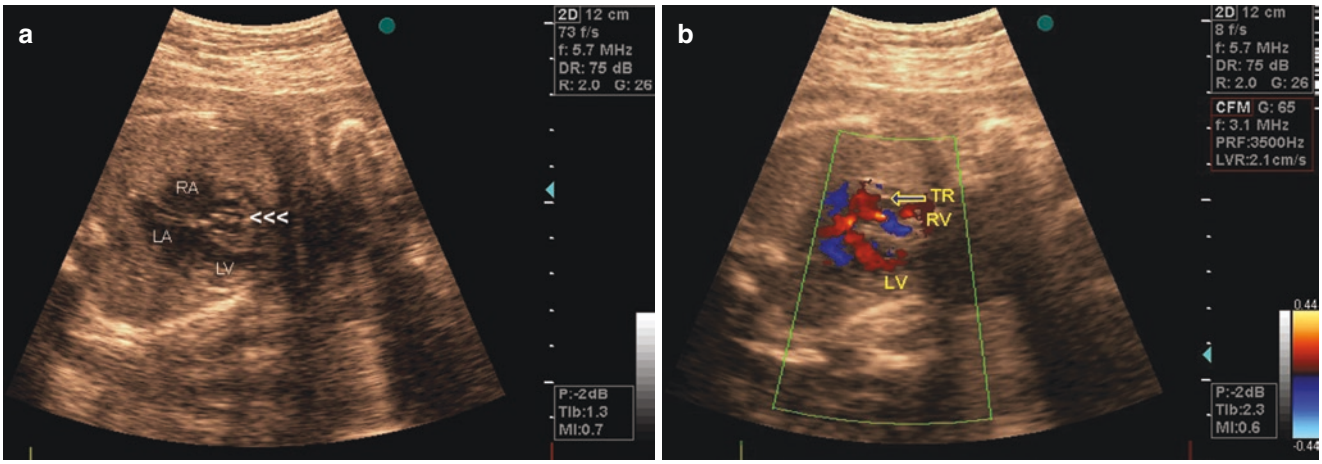

Fig. 26.5 (**a**) Echocardiogram of a fetus with PA IVS, four chamber view showing small RV (arrow heads) with bulging of interventricular septum into LV. (**b**) The same case by addition of color flow mapping shows moderate TR, arrow points to red color of tricuspid regurgitation jet. *RV* right ventricle, *LV* left ventricle, *TR* tricuspid regurgitation, *LA* left atrium, *RA* right atrium

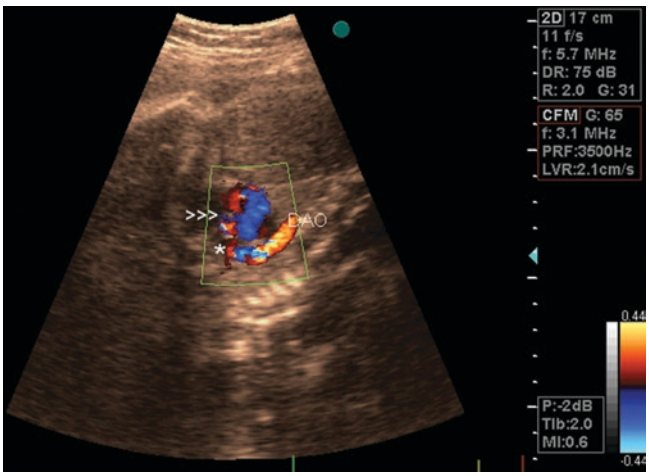

Fig. 26.6 Reversal flow via ductus arteriosus in sagittal view in a fetus (asterisk), arrow heads point to atretic pulmonary valve. *DAO* descending aorta

Suggested Reading

Freedom RM, Harrmngton DP. Contributions of intramyocardial sinusoids in pulmonary atresia and intact ventricular septum to a right-sided circular shunt. Brit Heart J I974. 36:I06I–5.

Guleserian KJ, Armsby LB, Ravi R, Thiagarajan RR, et al. Natural history of pulmonary atresia with intact ventricular septum and right-ventricle–dependent coronary circulation managed by the single ventricle approach. Ann Thorac Surg. 2006;81:2250–8.

Humpl T, Söderberg B, Mc Crindle BW, et al. Percutaneous Balloon valvotomy in pulmonary atresia with intact ventricular septum impact on patient care. Circulation. 2003;108:826–32.

Maluf MA, Carvalho AC, Carvalho WB, et al. One and a half ventricular repair as an alternative for hypoplastic right ventricle. Rev Bras Cir Cardiovasc. 2010;25(4):466–73.

Minich LL, Tani LY, Ritter S, et al. Usefulness of the preoperative tricuspid/mitral valve ratio for predicting outcome in pulmonary atresia with intact ventricular septum. Am J Cardiol. 2000;85

Pulmonary Atresia with VSD (PA-VSD) or Tetralogy of Fallot and Pulmonary Valve Atresia (TF-PA)

27

Maryam Moradian

Abstract

A large ventricular septal defect (VSD), overriding of the aorta along with underdevelopment of the right ventricular outflow tract (RVOT) with atretic pulmonary valve are key echocardiographic findings in this anomaly. This anomaly should be differentiated from TOF with pulmonary stenosis as in PA VSD the blood supply to the lungs is completely from the systemic arterial circulation, through the ductus arteriosus, major aortopulmonary collateral arteries (MAPCAs), or a combination of both.

Pulmonary Atresia with VSD (PA-VSD) or Tetralogy of Fallot and Pulmonary Valve Atresia (TF-PA)

1. Remember that echocardiographic appearance of or pulmonary atresia with VSD (PA-VSD) is similar to that of TOF, so appreciate the large aortic valve that overrides on a malaligned VSD in parasternal long axis view (Fig. 27.1).
2. Evaluate the extent of pulmonary artery atresia, in different views. Scanning from suprasternal and high parasternal windows can provide information about pulmonary valve, the proximal portion of the pulmonary trunk, and pulmonary artery branches that may be confluent or not.
3. The same views also should be evaluated for sided of aortic arch, PDA, and collaterals. Remember that unlike the PDA as an isolated lesion, in this anomaly, ductus tends to arise more proximally under the aortic arch (vertical PDA), longer, and sometimes tortuous (Fig. 27.2a, b).
4. Don't forget that distinct feature of PA-VSD which would help you to differentiate it from TOF is that the blood supply to the lungs is entirely from the systemic arterial circulation that could be either through either PDA or MAPCAs and there is no flow directly from RV to lungs. Those MAPCAs originating from the upper parts of descending aorta may be visualized in both transthoracic suprasternal view and transesophageal aortic arch views. These vessels are tortuous, may branch, and Doppler interrogation shows continuous flow pattern (Fig. 27.3a, b)
5. Remember that though echocardiography can characterize intracardiac anatomy its role in assessing pulmonary artery anatomy is limited. Length of atretic region, presence of pulmonary artery confluency, anatomy of main and pulmonary arteries branches, arborization abnormalities, and distribution of MAPCAs can better visualized by angiography, CT scan, and MRI.
6. In fetal echocardiography, reverse flow via ductus arteriosus toward pulmonary artery can help to differentiate PA-VSD from TOF. In PA-VSD, color Doppler demonstrates filling of the right and left pulmonary arteries via retrograde flow through ductus arteriosus (Fig. 27.4).

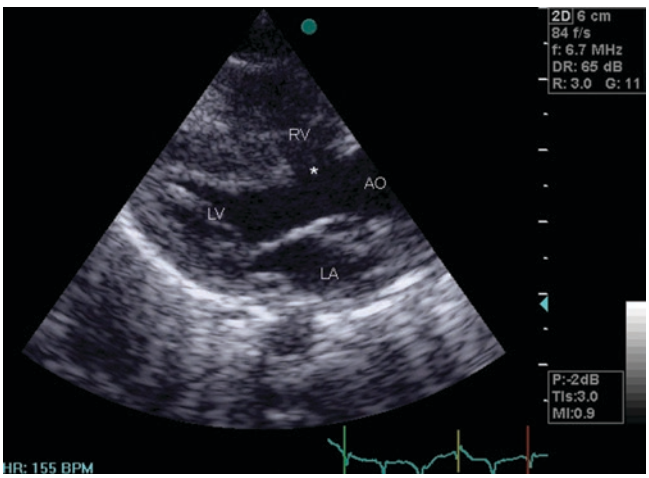

Fig. 27.1 Parasternal long axis view showing aortic overriding on VSD (asterisk) in a patient with PA-VSD. *LV* left ventricle, *RV* right ventricle, *AO* aorta, *LA* left atrium

M. Moradian (✉)
Pediatric Cardiology, Rajaie Cardiovascular, Medical & Research Center, Iran University of Medical Sciences, Tehran, Iran

M. Moradian, A. Alizadehasl (eds.), *Atlas of Echocardiography in Pediatrics and Congenital Heart Diseases*,
https://doi.org/10.1007/978-3-662-62341-1_27

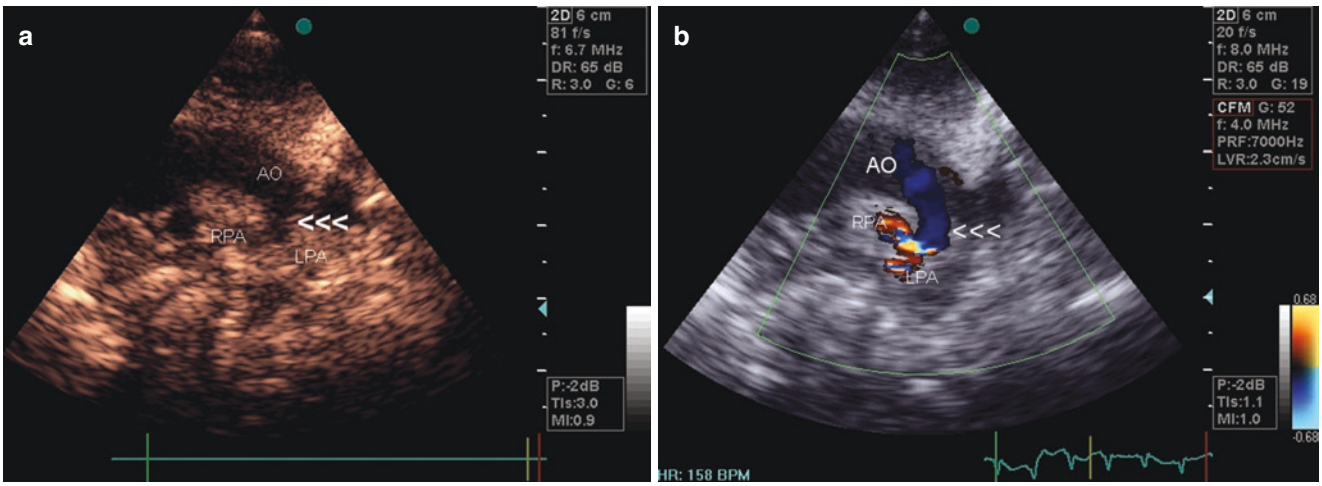

Fig. 27.2 (**a**, **b**) Suprasternal long axis view showing vertical PDA in patient with PA-VSD (**a**). Color Doppler interrogation in the same patient confirm ductal dependent pulmonary blood flow. Arrow heads point to vertical PDA which provide blood flow to small confluent PA branches. *AO* aorta, *LPA* left pulmonary artery, *RPA* right pulmonary artery

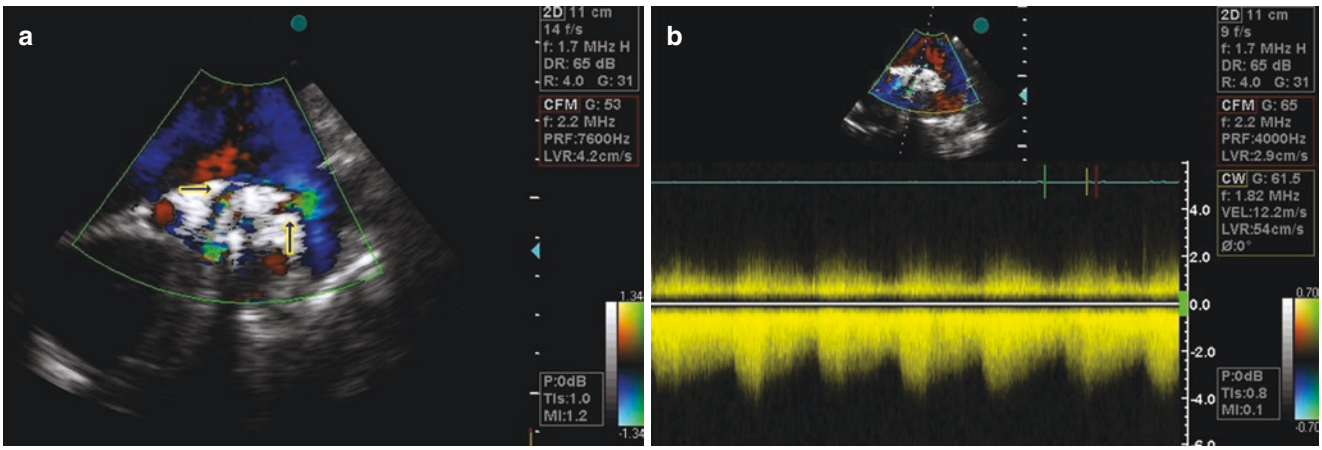

Fig. 27.3 (**a**, **b**)Transthoracic suprasternal long axis view of a patient with PA-VSD, arrows indicate two MAPCAs (**a**). Doppler interrogation in the same patient shows continuous flow within MAPCAs

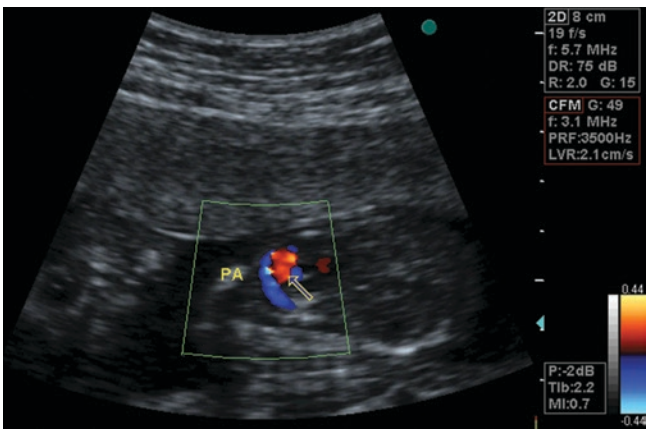

Fig. 27.4 Reversal flow toward atretic pulmonary valve via ductus arteriosus is indicated by arrow in this parasagittal fetal echocardiogram of a fetus with VSD-PA. *PA* pulmonary artery

Occasionally MAPCAs can be find by reducing color velocity scale arising from the descending aorta.

Suggested Reading

Alwi M. Stenting the ductus arteriosus: case selection, technique and possible complications. Ann Pediatr Cardiol. 2008;1:38–45.

Atik E. Newborn with pulmonary atresia, ventricular septal defect and double aortic. Arch Arq Bras Cardiol. 2012;99(3):e128–30.

Dobrocky T, Heverhagen J, Klink T, et al. Imaging findings in uncorrected tetralogy of Fallot and pulmonary atresia with major aortopulmonary collateral arteries and septic embolism. Acta Radiol Short Rep. 2014;3:1):1–4.

Farouk A, Zahka K, Siwik E, et al. Individualized approach to the surgical treatment of tetralogy of Fallot with pulmonary atresia. Cardiol Young. 2009;19(1):76–85.

Grosse-Wortmann L, Shi-Joon Yoo SJ, Van Arsdell G, et al. Preoperative total pulmonary blood flow predicts right ventricularpressure in patients early after complete repair of tetralogy of Fallot and pulmonary atresia with major aortopulmonary collateral arteries. J Thorac Cardiovasc Surg. 2013;146(5):1185–90.

Takimura CK. Stent angulation and implantation in the ductus arteriosus of a low-weight neonate. Rev Bras Cardiol Invasiva. 2013;21(4):401–5.

Vesel V, Rollings S, Jones A, et al. Prenatally diagnosed pulmonary atresia with ventricular septal defect: echocardiography, genetics, associated anomalies and outcome. Heart. 2006;92:1501–5.

Zhang XY, Tie-Sheng Cao TS, Yuan LJ, et al. Value of the echocardiographic suprasternal view for diagnosis of patent ductus arteriosus subtypes. J Ultrasound Med. 2012;31:1421–7.

Double Outlet Right Ventricle (DORV)

28

Maryam Moradian

Abstract

In this anomaly both great arteries arise primarily from right ventricle. Echocardiography is essential in understanding both the anatomy and physiology of this complex conotruncal malformation. The various relationship of the great arteries and different location of the VSD as well as presence or absence of outflow tract obstructions should be evaluated by echocardiography.

Double Outlet Right Ventricle (DORV)

1. Remember that physiology of different types of double outlet right ventricle (DORV) ranges from a VSD type with increased pulmonary blood flow, to tetralogy type with reduced pulmonary blood flow, to transposition type with simultaneous hypoxemia and pulmonary over circulation. Pay attention to three diagnostic signs of DORV:
   (a) Origin of both great arteries from right ventricle (RV)
   (b) The absence of any left ventricular out flow other than ventricular septal defect (VSD)
   (c) The discontinuity of mitral and semilunar valves.
   Parasternal long axis view is very helpful to evaluate all these three features (Fig. 28.1). Evaluate the origin of both great arteries from RV in parasternal long and short axis views (more than 50% each great artery should be from RV to be considered DORV).
2. You should not only describe the location of the VSD but also evaluate the streaming of blood through it, toward aorta or pulmonary artery using color Doppler (you may describe the location of the VSD as subaortic, subpulmonic, doubly-committed, and noncommitted or remote) (Figs. 28.2 and 28.3).
3. Evaluate the most common variant, tetralogy type DORV, for subaortic VSD and pulmonary stenosis (PS), and the degree of PS.
4. For describing the second common type of DORV, transposition type, do not forget to evaluate the relationship of great vessel in sub costal views as well as the possibility of aortic arch hypoplasia in cases of subaortic narrowing which should be demonstrated in suprasternal views (Fig. 28.4).
5. Evaluate the presence of mitral semilunar valve discontinuity in different views, describe if there is any abnormal

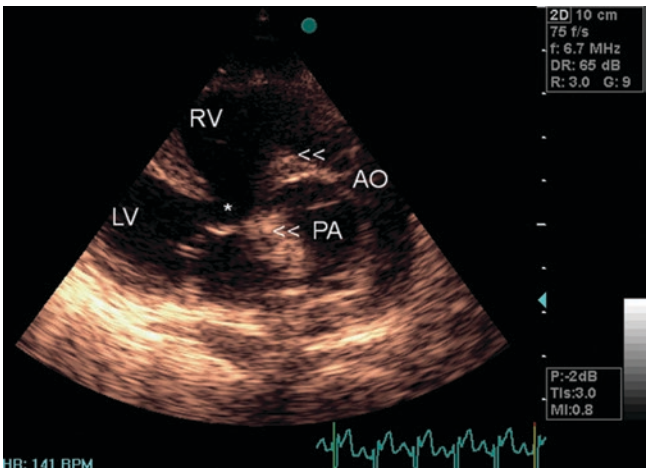

Fig. 28.1 Parasternal long axis view of a patient with DORV subpulmonic VSD, anterior aorta and Taussig-Bing Physiology, arrow heads point to conal septum and mitral–pulmonary discontinuity. Subpulmonic VSD is showed by asterisk. *LV* left ventricle, *RV* right ventricle, *AO* aorta, *PA* pulmonary artery

M. Moradian (✉)
Pediatric Cardiology, Rajaie Cardiovascular, Medical & Research Center, Iran University of Medical Sciences, Tehran, Iran

M. Moradian, A. Alizadehasl (eds.), *Atlas of Echocardiography in Pediatrics and Congenital Heart Diseases*,
https://doi.org/10.1007/978-3-662-62341-1_28

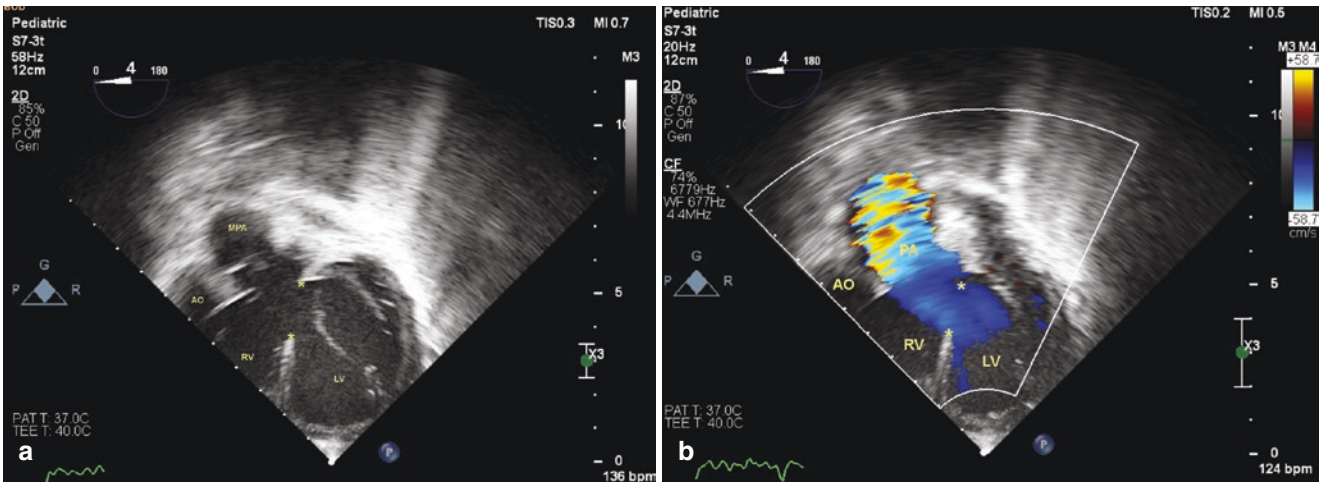

Fig. 28.2 (**a**) Transesophageal echocardiography (TEE), transgasteric view showing both great arteries arising from the right ventricle. (**b**) Addition of color-flow mapping demonstrates streaming of blood through VSD, toward pulmonary artery, this form of DORV transposition type is also called "Taussig–Bing anomaly" or "DORV with subpulmonic VSD". Asterisks indicate VSD. *LV* left ventricle, *RV* right ventricle, *AO* aorta, *PA* pulmonary artery

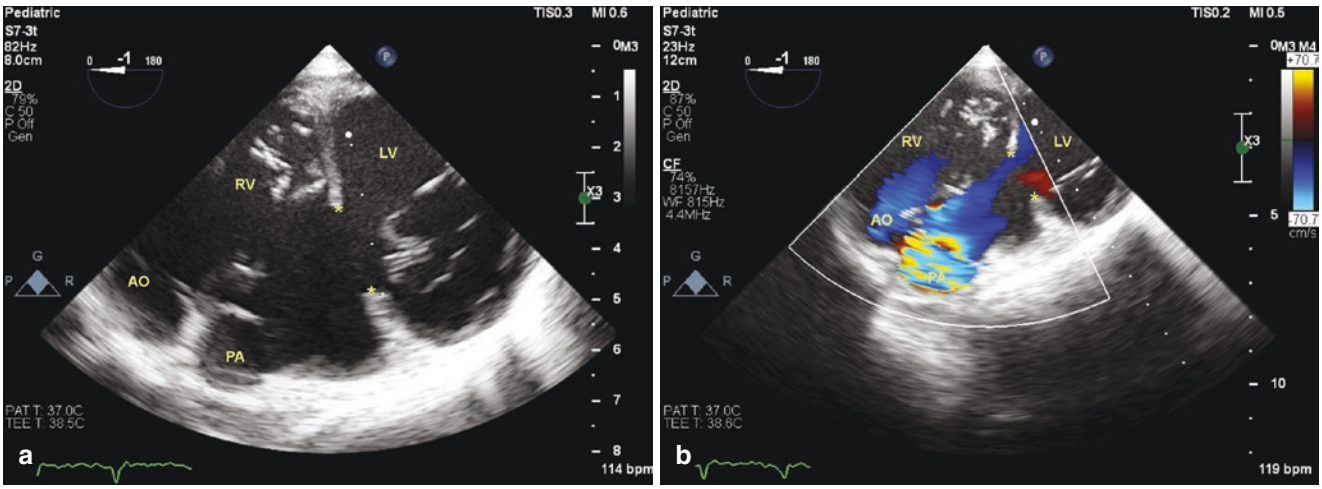

Fig. 28.3 (**a**) Transesophageal echocardiography (TEE), diastolic frame, transgasteric view showing both great arteries arising from the right ventricle and noncommitted or remote VSD, asterisks indicate VSD. Enface cut of mitral and tricuspid valve is seen in corresponding ventricle. (**b**) The systolic frame of the same patient with addition of color-flow mapping. *LV* left ventricle, *RV* right ventricle, *AO* aorta, *PA* pulmonary artery

chordal attachments and their relation to VSD. Also determine any straddling and overriding of the atrioventricular valves.

6. For all types of DORV including the third common type (VSD type) and less common types (like noncommitted, doubly committed DORV…) it is very important to evaluate the size of both ventricles and their adequacy for biventricular repair.
7. As for surgical repair conduit placement may be necessary, evaluation of coronary arteries anomaly is essential.
8. Some authors emphasize on measuring two distances:
   (a) The distance between VSD and the arterial valves, if this distance is greater than the aortic diameter VSD is considered remote type.
   (b) The distance between tricuspid and pulmonary valve, if this distance exceeds the diameter of the aortic annulus, intraventricular repair is indicated and vice versa.
9. During fetal life DORV can be diagnosed by evaluation the out-flow tracts (Figs. 28.5 and 28.6).

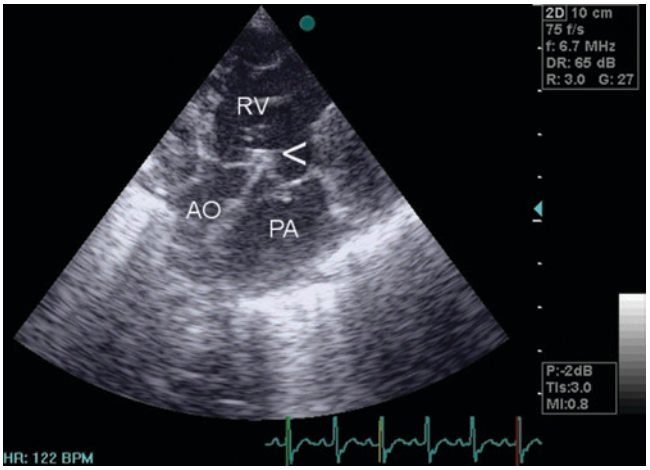

Fig. 28.4 Subcostal coronal view of a patient with DORV transposition type and dilated pulmonary artery indicate pulmonary hypertension. Arrow head points to subaortic conus. *RV* right ventricle, *AO* aorta, *PA* pulmonary artery

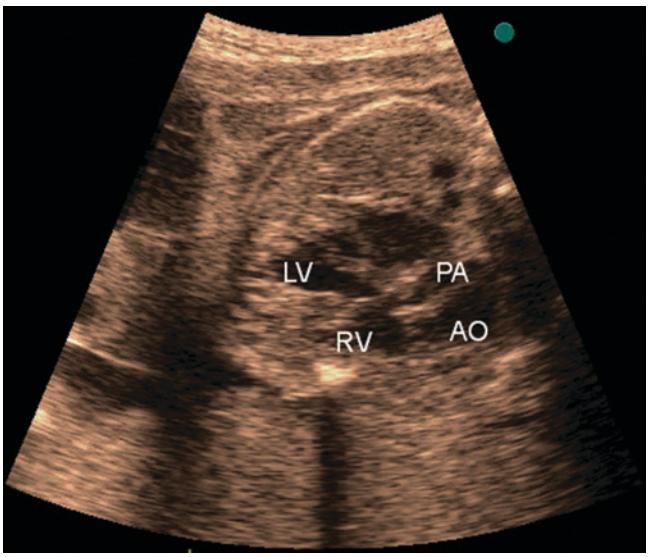

Fig. 28.5 Fetal echocardiography: out flow tract view, showing both great arteries arising from morphologic RV (fetus suffered from complex lesion: DORV, AVSD, PS, CHB, Interrupted IVC). *LV* left ventricle, *RV* right ventricle, *AO* aorta, *PA* pulmonary artery

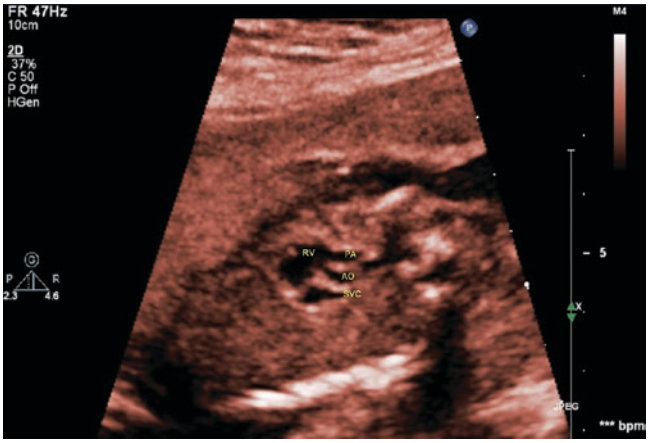

Fig. 28.6 Fetal echocardiography: out flow tract view, showing both great arteries arising from morphologic RV in this parasagittal view. *SVC* superior vena cava, *RV* right ventricle, *AO* aorta, *PA* pulmonary artery

Suggested Reading

Gottschalka I, Abela JS, Menzel T, et al. Prenatal diagnosis, associated findings and postnatal outcome of fetuses with double outlet right ventricle (DORV) in a single center. J Perinat Med. 2019;47(3):354–64.

Hagler DJ, Tajik AJ, Seward JB, et al. Double-outlet right ventricle: wide-angle two-dimensional echocardiographic observations. Circulation. 1981;63(2)

Lacour-Gayet F, Haun C, Ntalakoura K, et al. Biventricular repair of double outlet right ventricle with non-committed ventricular septal defect (VSD) by VSD rerouting to the pulmonary artery and arterial switch. Eur J Cardio-thorac Surg. 2002;21:1042–8.

Mercer-Rosa LM, Cohen MS. Evaluation of conotruncal abnormalities (Chapter 12). In: Wong PC, Miller-Hance WC, editors. Transesophageal echocardiography for congenital heart disease. London: Springer-Verlag; 2014. p. 307–40.

Pang KJ, Meng H, Hu SS, et al. Echocardiographic classification and surgical approaches to DORV tex. Heart Inst J. 2017;44(4):245–51.

Peixoto LB, Leal SM, Silva CE, et al. Double outlet right ventricle with anterior and left-sided aorta and subpulmonary ventricular septal defect. Arq Bras Cardiol. 1999;73(5)

Wright GE, Maeda K, Silverman NH, Hanley FL, Roth SJ. Double outlet right ventricle (Chapter 49). In: Allen HD, Shaddy RE, Penny DJ, Feltes TF, Cetta F, editors. Moss and Adams' heart disease in infants, children, and adolescents including the fetus and young adults, vol. 2016. 9th ed: Wolters Kluwer. p. 1201–16.

Yim D, Dragulescu A, Ide H, et al. Essential modifiers of double outlet right ventricle revisit with endocardial surface images and 3-dimensional print models. Circ Cardiovasc Imaging. 2018;11

Truncus Arteriosus

29

Maryam Moradian

Abstract

Echocardiography can demonstrate both the anatomic and physiologic features of truncus arteriosus. In subcostal and parasternal long axis views a single vessel, the truncus, can be seen overriding on VSD and both ventricles eject blood into this vessel instead of aorta and pulmonary artery. This vessel supplies systemic, coronary, and pulmonary circulation. Subcostal and suprasternal views allow evaluation of pulmonary trunk which originate from the single vessel, the truncus. Using color Doppler modalities is critical to evaluate regurgitation or stenosis of the truncal valve.

Truncus Arteriosus

1. Evaluate a single arterial trunk that gives the origin to the systemic, pulmonary, and coronary circulations. This arterial trunk can be visualized in long axis, and subcostal views (Fig. 29.1). This single great artery overrides the VSD and is in continuity with mitral valve.
2. Don't forget the important point for differentiating truncus arteriosus from VSD-PA, in VSD-PA the pulmonary arteries do not arise directly from the ascending portion of single arterial trunk (Fig. 29.2).
3. Different types of truncus arteriosus, based on the origin of the pulmonary arteries are as follow:

   Collett and Edwards Classification

   – Type I: Short MPA originating from the left lateral aspect of common arterial trunk giving rise to both pulmonary arteries.

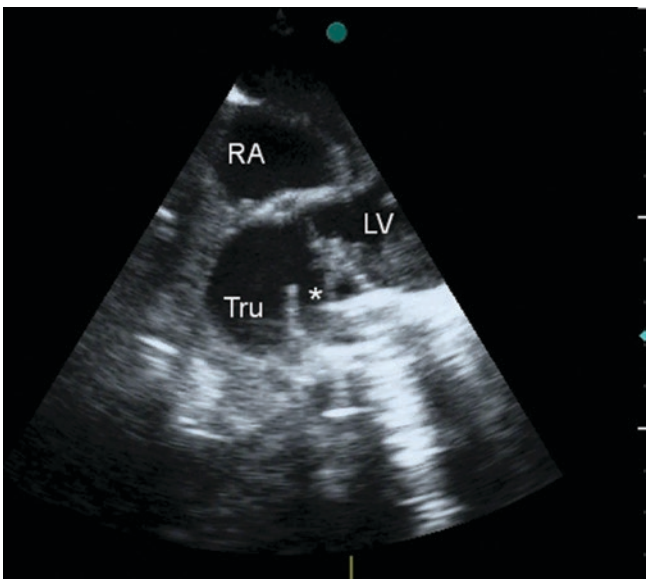

Fig. 29.1 Subcostal coronal view showing type 1 truncus arteriosus. Asterisk indicate main pulmonary artery arising from truncus. *RA* right atrium, *LV* left ventricle, *Tru* truncus arteriosus

   – Type II: Separate but proximate origination of LPA and RPA from the posterolateral aspect of the common arterial trunk (Fig. 29.3).
   – Type III: Similar to type II, independent origination of RPA and LPA, but at some distance.

   Van Praagh and Van Praagh Classification

   - Type A1: Identical to type I of Collett and Edwards (explained before) (Fig. 29.4).
   - Type A2: Encompasses types II and III.
   - Type A3: Includes cases with truncal origin of one pulmonary artery (usually the right), with pulmonary blood supply to the other lung from either the ductus arteriosus or from a collateral artery.
   - Type A4: Defined not by the pattern of origin of pulmonary branches, but rather by the coexistence of an

M. Moradian (✉)
Pediatric Cardiology, Rajaie Cardiovascular, Medical & Research Center, Iran University of Medical Sciences, Tehran, Iran

M. Moradian, A. Alizadehasl (eds.), *Atlas of Echocardiography in Pediatrics and Congenital Heart Diseases*,
https://doi.org/10.1007/978-3-662-62341-1_29

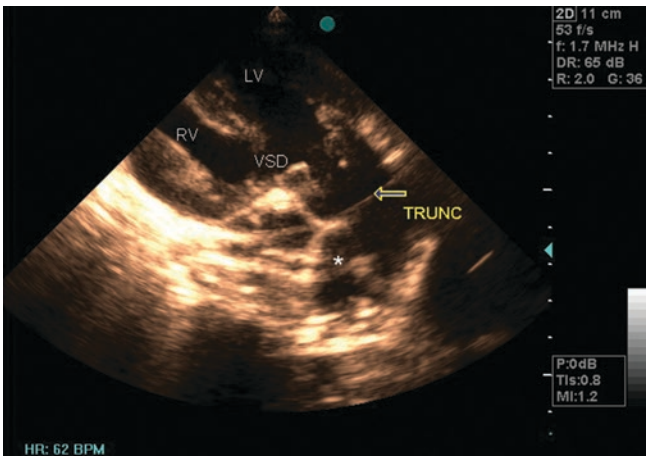

Fig. 29.2 Parasternal long axis view of truncus arteriosus type 1 showing main pulmonary artery (asterisk) arising directly from ascending portion of single arterial trunk. Arrow indicate truncus arteriosus. *LV* left ventricle, *RV* right ventricle, *Trunc* truncus arteriosus, *VSD* ventricular septal defect

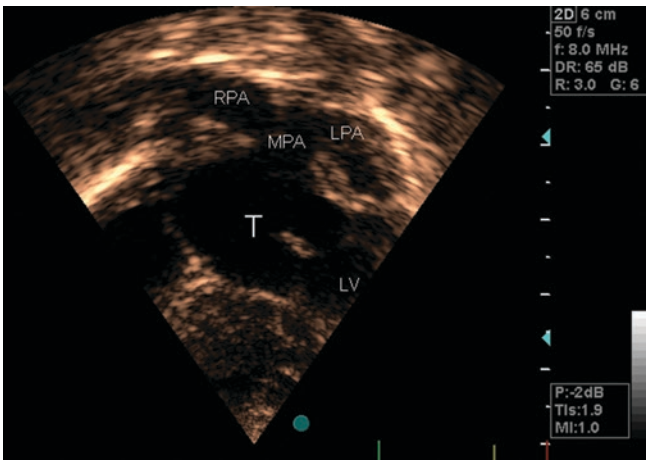

Fig. 29.4 Subcostal coronal view showing both LPA and RPA arising from very short MPA in this case of type 1 truncus arteriosus. *LPA* left pulmonary artery, *RPA* right pulmonary artery, *MPA* main pulmonary artery, *T* truncus arteriosus, *LV* left ventricle

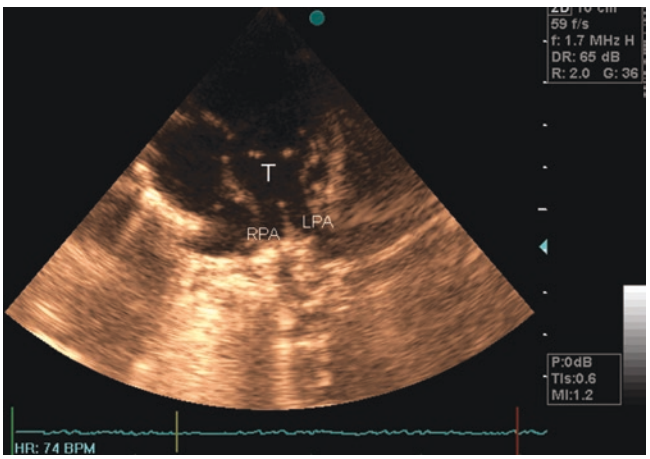

Fig. 29.3 High left parasternal short axis view of type II truncus arteriosus showing separate but proximate origination of left (LPA) and right (RPA) pulmonary branches from truncus (T). *LPA* left pulmonary artery, *RPA* right pulmonary artery, *T* truncus arteriosus

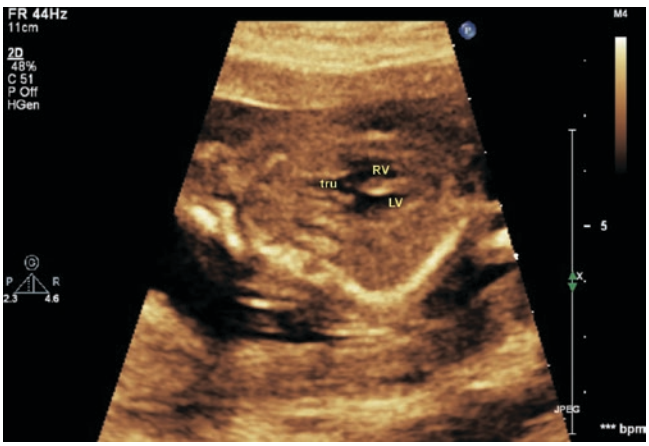

Fig. 29.5 Fetal echocardiogram long axis view showing single large vessel over riding on VSD and absence of separate pulmonary valve and artery. *LV* left ventricle, *RV* right ventricle, *Tru* truncus arteriosus

aortic arch anomaly, including tubular hypoplasia, discrete coarctation, or complete interruption.

4. Determine the number of truncal valve leaflets (unicommissural, bicuspid, tricuspid, quadricuspid, or pentacuspid) in parasternal short axis view. In most cases it is tricuspid.
5. Evaluate the truncal valve insufficiency and or stenosis in different views using color Doppler.
6. Evaluate the origin and proximal course of coronary arteries in parasternal short axis view.
7. Absence or atresia of the ductus arteriosus is expected in approximately half of the patients with truncus arteriosus, the exception being truncus arteriosus with underdevelopment of the aortic arch in whom it may remain patent. So, in suprasternal long axis view, evaluate the PDA and arch anomalies.
8. Remember that one pulmonary artery may be absent and in contrast with TOF, pulmonary artery most frequently is absent on the same side of the aortic arch not the opposite side.
9. Transesophageal echocardiography is useful for more detailed evaluation especially the truncal valve anatomy.
10. In fetal echocardiography detecting a malaligned VSD with the large overriding vessel on five chamber view along with absence of a separate pulmonary valve and pulmonary artery should raise the suspicion of truncus arteriosus (Fig. 29.5).

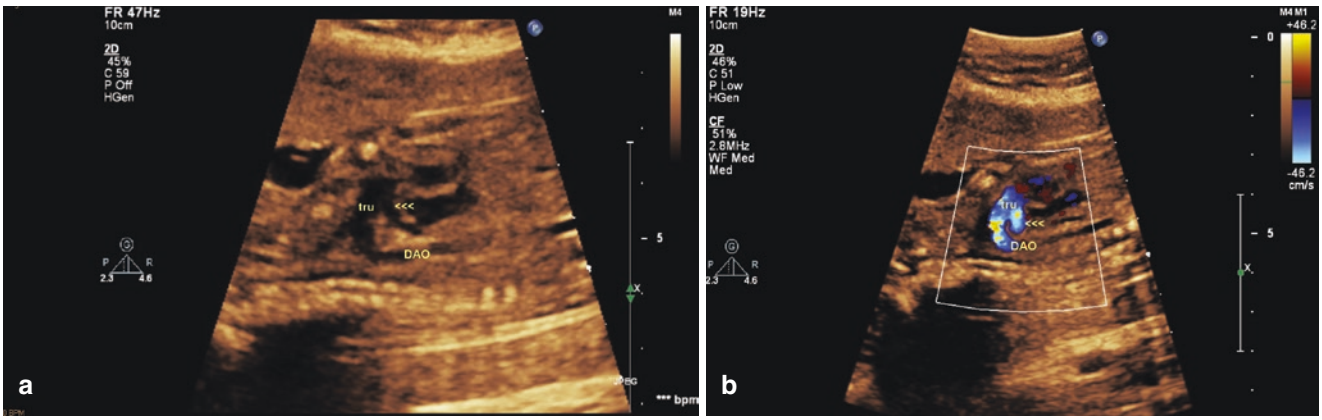

Fig. 29.6 (**a**, **b**) Fetal echocardiography of a fetus with truncus arteriosus, sagittal view, showing origination of main pulmonary trunk (arrow heads) from truncus (**a**). Addition of color Doppler on same view, shows the blood supply of main pulmonary trunk from truncus (**b**). *Tru* truncus arteriosus, *DAO* descending aorta

11. Try to identify the pulmonary trunk originating from large truncal vessel (Fig. 29.6a, b). Also use color Doppler interrogation to find any regurgitation via truncal valve.

Suggested Reading

Houston AB, Gregory NL, Murtagh E, et al. Two-dimensional echocardiography in infants with persistent truncus arteriosus. Br Heart Jr. 1981;46:492–7.

Russell HM, Jacobs ML, Anderson RH, et al. A simplified categorization for common arterial trunk. J Thorac Cardiovasc Surg. 2011;141:645–53.

Swanson TM, Selamet Tierney ES, Tworetzky W. Truncus arteriosus: diagnostic accuracy, outcomes, and impact of prenatal diagnosis. Pediatr Cardiol. 2009;30(3):256–61.

Traisrisilp K, Tongprasert F, Srisupundit K, et al. Prenatal differentiation between truncus arteriosus (Types II and III) and pulmonary atresia with ventricular septal defect. Ultrasound Obstet Gynecol. 2015;46:564–70.

Volpe P, Paladini D, Marasini M, et al. Common arterial trunk in the fetus: characteristics, associations, and outcome in a multicentre series of 23 cases. Heart. 2003;89:1437–41.

Mitral Valve Diseases, Congenital and Acquired

30

Majid Maleki, Feridoun Noohi, Maryam Moradian, and Azin Alizadehasl

Abstract

Congenital mitral anomalies are rare as isolated lesion. These anomalies are frequently encountered in combination with other lesions such as atrioventricular septal defects, Shone complex, hypoplastic left heart syndrome (HLHS). Mitral valve prolapse and rheumatismal mitral valve diseases are more common in older children or adolescents. Three-dimensional echocardiography (3D) allows visualization of mitral valve, as it looks in reality and provide its anatomical details.

Mitral Valve Anomalies

1. Don't forget two important points:
   (a) Dividing congenital mitral valve (MV) pathology into regurgitant and stenotic lesions is artificial because congenital MV abnormalities may lead to both of them
   (b) Performing transesophageal echocardiography (TEE) and/or three-dimensional echocardiography (3D) for MV is quite helpful especially if transthoracic echo (TTE) is not completely diagnostic
2. Try to perform a comprehensive echocardiographic approach by imaging supravalvar mitral regions as well as annulus, leaflets, commissures, chorda tendinea, and papillary muscles of MV. Evaluation of coronary arteries is also very important as ALCAPA my cause ischemia and fibrotic changes on mitral valve (MV), chorda, and papillary muscles which can lead to the development of mitral valve prolapse and regurgitation.
3. In the most common form of isolated congenital mitral stenosis (MS), global hypoplasia of MV, thickened and rolled leaflets especially their free edges, obliteration of intrachordal spaces, and deformed papillary muscles should be checked in different views including apical four chamber, parasternal long and short axis views.
4. In dysplasia of the posterior (or mural) leaflet, tethering of the leaflet due to shortened chordae, prevents its normal coaptation with the anterior leaflet, which is thickened itself and mitral regurgitation (MR) will result. So, evaluate the mobility of posterior leaflet in every case of congenital MR (Fig. 30.1a, b)
5. The best view for evaluation of supravalvar stenosing mitral ring is parasternal long axis view. Differentiate supravalvar stenosing ring from cor triatriatum by evaluating its relation to left atrial auricle (LAA). In supravalvar stenosing ring, the ring sits below the LAA while in cases of cor triatratum the membrane is above the LAA. Remember that supravalvar stenosing ring is often associated with valve dysplasia (Fig. 30.2).
6. Use color Doppler to evaluate different levels of stenosis (Fig. 30.3a, b).
7. Muscularization of chorda leads to arcade mitral valve. When differentiation between leaflets and chorda, in cases of MR, are difficult, consider this rare anomaly which is also named as "hammock" valve (Fig. 30.4).
8. Isolated MV cleft, should be evaluated in parasternal short axis view. This cleft divides the anterior mitral leaflet into two components and mitral resembles as a three-leaflet valve. Normal location of papillary muscles and pointing toward subaortic outflow track will help to

M. Maleki · F. Noohi
Cardiovascular Intervention Research Center, Rajaie Cardiovascular, Medical & Research Center, Iran University of Medical Sciences, Tehran, Iran

M. Moradian
Pediatric Cardiology, Rajaie Cardiovascular, Medical & Research Center, Iran University of Medical Sciences, Tehran, Iran

A. Alizadehasl (✉)
Department of Cardio-Oncology and Research Center, Rajaie Cardiovascular, Medical & Research Center, Iran University of Medical Sciences, Tehran, Iran

M. Moradian, A. Alizadehasl (eds.), *Atlas of Echocardiography in Pediatrics and Congenital Heart Diseases*,
https://doi.org/10.1007/978-3-662-62341-1_30

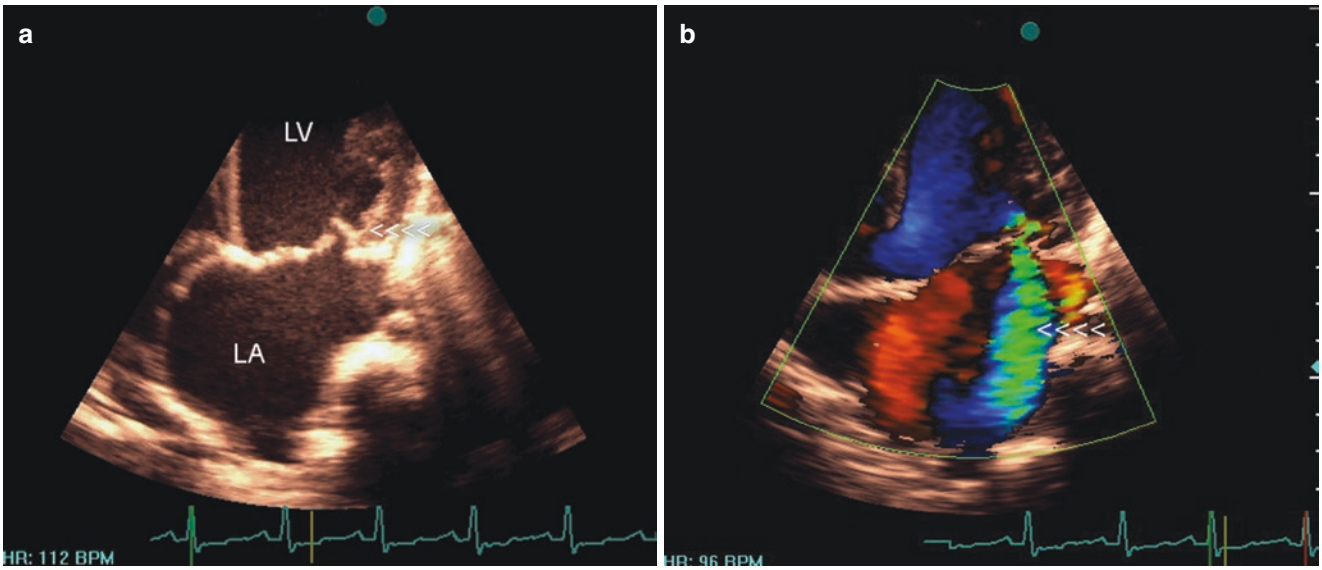

Fig. 30.1 (**a**, **b**) Apical four chamber view showing dysplastic posterior MV leaflet (arrow heads in **a**) and severe MR due to malcoaptation (arrow heads in **b**), also pay attention to LA enlargement. *LA* left atrium, *LV* left ventricle

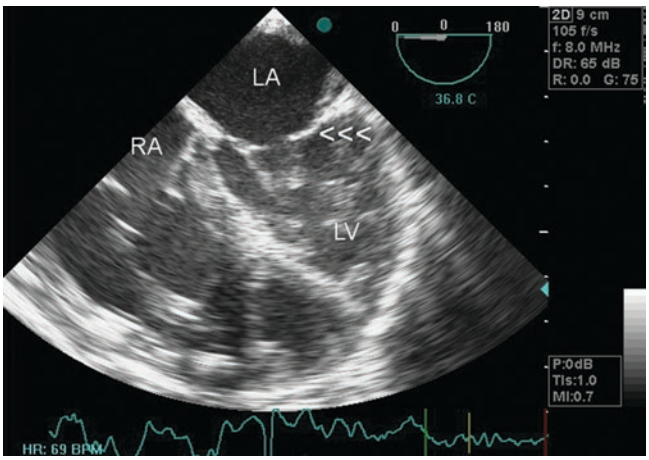

Fig. 30.2 Transesophageal echocardiography (TEE), four chamber view, arrowheads points to supravalvar stenosing MV ring. *LA* left atrium, *LV* left ventricle, *RA* right atrium

differentiate this cleft from clefts in atriventricular septal defects (AVSDs) (Fig. 30.5). The three-dimensional echocardiography (3D) is very helpful in differentiating partial from complete clefts.

9. Double orifice MV (DOMV) may be associated with atriventricular septal defect (AVSD), atrial septal defect (ASD). Ebstein anomaly, tetralogy of Fallot (TOF), and coarctation of aorta (COA). Sometimes it's an incidental finding. Two separate orifices of MV can be seen in short axis views (Fig. 30.6a, b).
10. Parachute MV frequently is associated with multiple levels of left heart obstructions (Shone Complex). In this anomaly all of the MV chorda attach to solitary large papillary muscle so MV opening is restricted (Fig. 30.7a, b).
11. Ebstein's like anomaly of MV involves mural (or posterior) leaflet and is not associated with thinning of atrialized LV myocardium. Its outcome is very poor especially in association with coarctation of aorta or arch hypoplasia (Fig. 30.8).
12. Remember that for diagnosis of Mitral valve prolapse (MVP) evaluation in four chamber view is not accurate because mitral valve annulus has two low and two high points (saddle shape) and four chamber view images the valve at its two low points, so it's prone to over diagnosis. Also keep in mind to evaluate other valves, especially aortic valve precisely, because in children MVP is commonly associated with connective tissue disorders, like Marfan syndrome. Evaluate the bowing back of MV leaflets into LA in parasternal long axis view in systole. Mural leaflet is most commonly affected though both leaflets may be involved. Evaluate severity of regurgitation by color Doppler (Fig. 30.9).
13. MVP can be evaluated by 3D echo either from the left atrium or the left ventricle. In looking down en face view or surgical view prolaptic leaflets are bulged and convex, whereas in looking up view leaflets are spoon-like and concave (Fig. 30.10).
14. Straddling MV is best evaluated in parasternal long and short axis views. Evaluate the chordal insertion of anterior mitral leaflet (AML) into the crest of interventricular septum or to a papillary muscle in RV. This anomaly is more common in transposition of great arteries (TGA) and/or double outlet right ventricle (DORV) (Fig. 30.11).
15. Chronic rheumatic heart disease may lead to secondary MS. Leaflet thickening, fusion of commissures, leaflets, and chordae, result in a funnel-shaped, and ste-

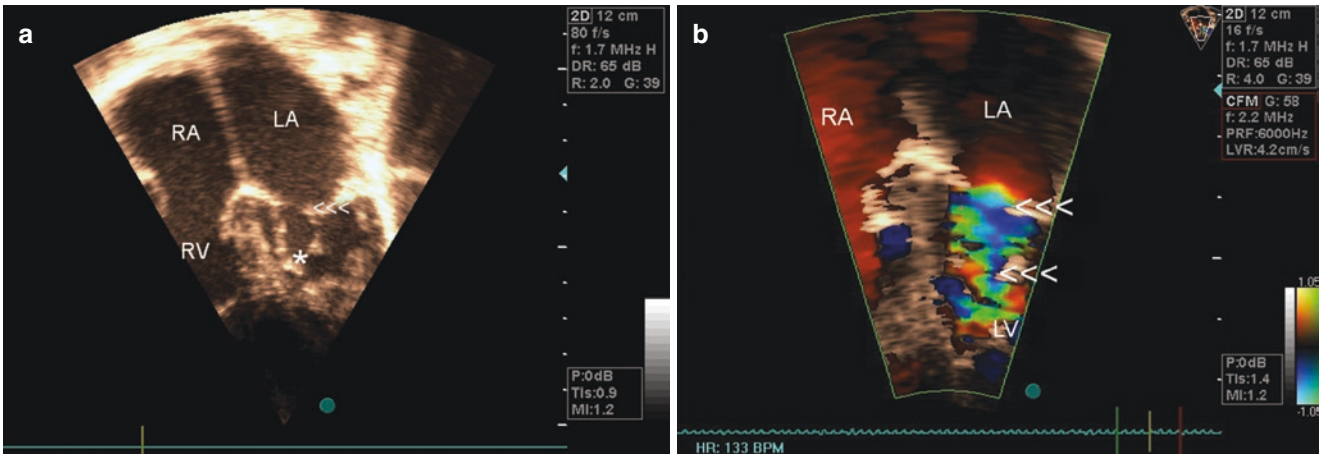

Fig. 30.3 (**a**, **b**) Transthoracic echocardiography (TTE) four chamber view showing dysplastic MV with supravalvar stenosing ring upper arrow heads point to supravalvar ring and lower arrow heads indicate subvalvar stenosis in figure (**a**), color Doppler echocardiography with magnification in the same patient confirms at least to level of stenosis, arrow heads in figure (**b**). *LA* left atrium, *LV* left ventricle, *RA* right atrium, *RV* right ventricle

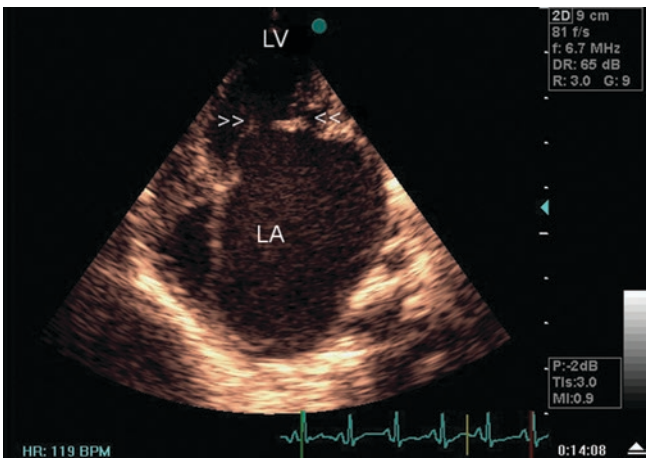

Fig. 30.4 Arrow heads in this apical four chamber view point to muscularized chorda in an infant suffering from arcade MV. Severe MR leads to severe left atrial enlargement. *LA* left atrium, *LV* left ventricle

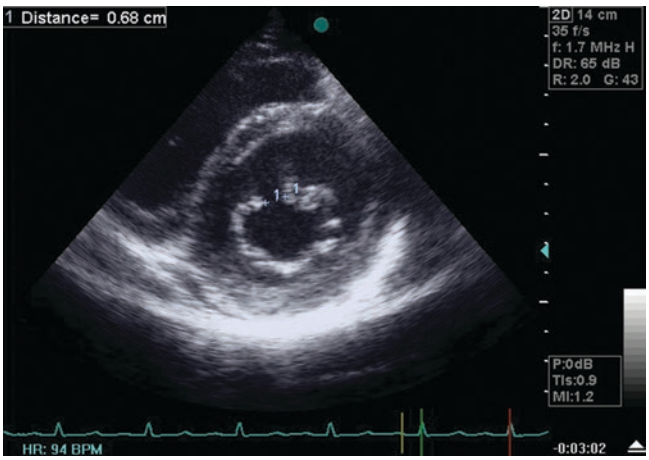

Fig. 30.5 Parasternal short axis view showing isolated anterior mitral leaflet (AML) cleft

notic orifice. Parasternal short axis view is the best view for evaluation of commissural fusion and performing MV planimetry. As the valve in severe MS have a small orifice its opening and closing resemble fish mouth (fish mouth sign)." Hockey stick appearance", doming and restricted motion of anterior leaflet during diastole, can be seen in parasternal long axis view. Transesophageal and 3D echocardiography are great tools for more precise assessment of MV (Figs. 30.12, 30.13, and 30.14)

16. Remember these limitations in hemodynamic evaluation of congenital MV abnormalities:
    (a) In many MV abnormalities combinations of stenosis and regurgitation impacts on mean gradient evaluation also it is dependent on cardiac output.
    (b) Interpretation of pressure half-time (PHT) is difficult in children due to rapid heart rates and in cases of concomitant moderate to severe aortic insufficiency (AI), regurgitation jet may lead to premature closure of MV. But PHT is not dependent on cardiac output.
    (c) The main problem in using Doppler echocardiography for calculating stroke volume and regurgitant volume in children is its reproducibility though they are widely used in adults.

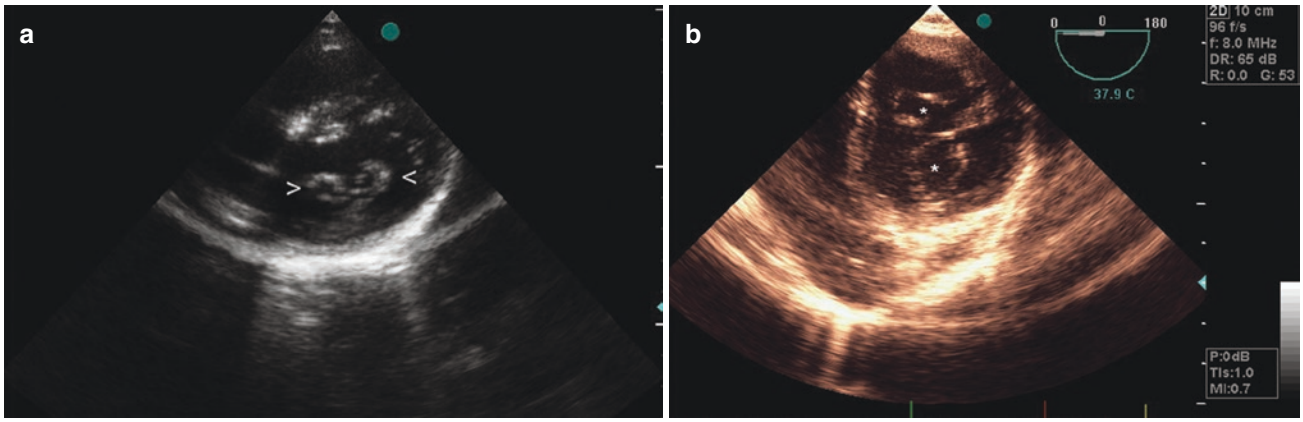

Fig. 30.6 (**a**, **b**) Short axis views in TTE (**a**) and TEE (**b**). Two separate orifices of DOMV are indicated in both (**a**, **b**)

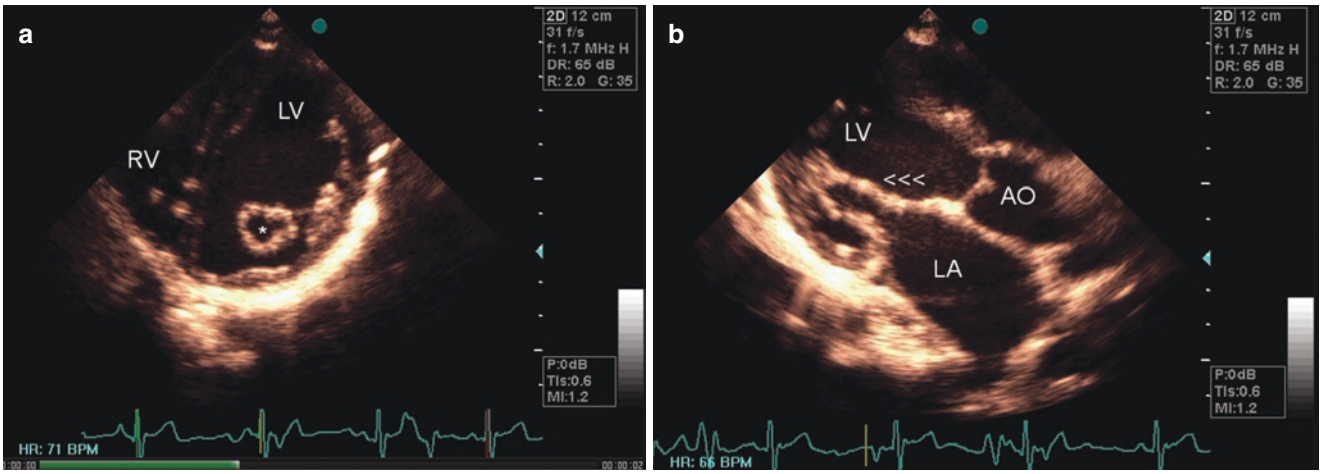

Fig. 30.7 (**a**, **b**) Parasternal short axis (**a**) and long axis view (**b**) of a patient with parachute MV. Restricted mitral opening in diastole (asterisk in figure **a**) and abnormal funnel shaped chordal attachments (arrowheads in figure **b**) are seen. *LA* left atrium, *LV* left ventricle, *AO* aorta

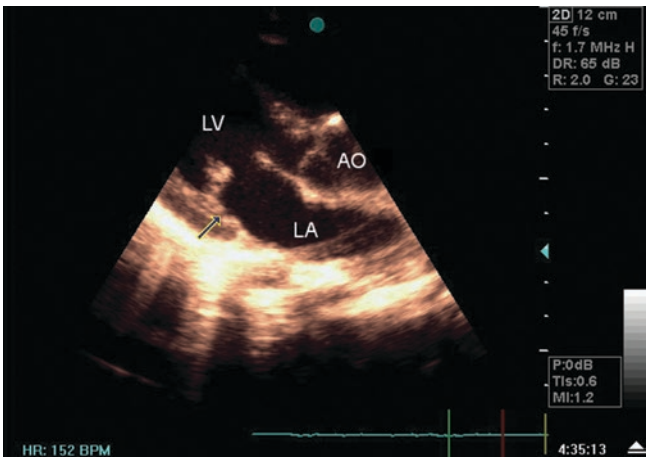

Fig. 30.8 Parasteranl long axis view of a patient with Epstein's like anomaly of MV, arrow points to mural leaflet displacement. *LA* left atrium, *LV* left ventricle, *AO* aorta

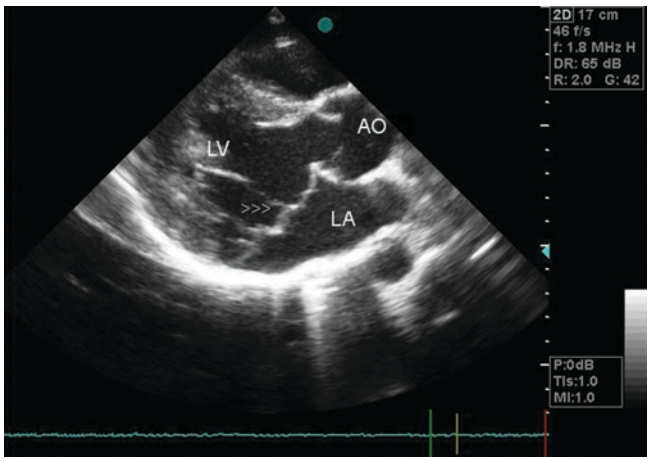

Fig. 30.9 Parasternal long axis view of a child with Marfan syndrome, arrow heads point to bowing back of MV leaflets into LA. Aortic root is dilated as well. *LA* left atrium, *LV* left ventricle, *AO* aorta

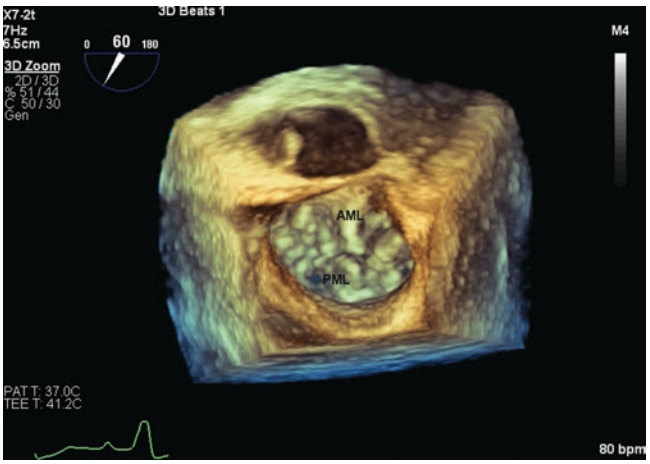

Fig. 30.10 Transesophageal 3D echocardiography, looking down view, systolic frame of a patient with multi scallops MVP, especially A2 and P2 scallops

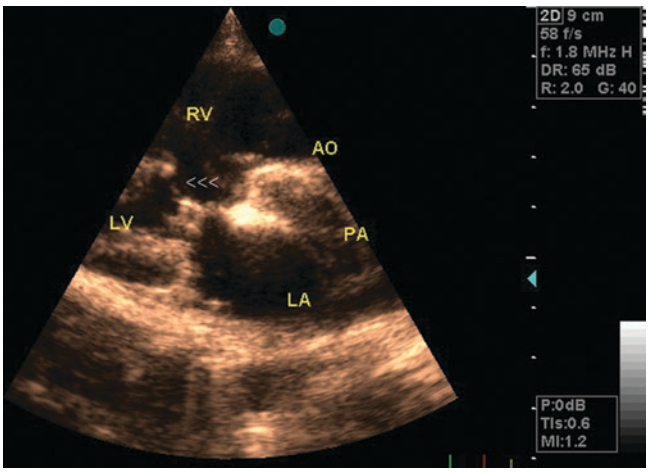

Fig. 30.11 Parasternal long axis view of a patient with DORV, PS. Arrowheads points to type 1 straddling of anterior mitral leaflet (AML). *LA* left atrium, *LV* left ventricle, *RV* right ventricle, *AO* aorta, *PA* pulmonary artery

(d) Proximal isovelocity surface area (PISA) method is useful for evaluation of effective regurgitant orifice area (EROA). There are some limitations including the shape of the PISA shell which is not completely a hemisphere, presence of multiple jets, and the fact that always it is not possible to determine the exact location of regurgitant orifice

17. Use Doppler evaluation of tricuspid regurgitation (TR) and pulmonary regurgitation velocities to estimate RV and pulmonary artery (PA) pressure.
18. LA and LV sizes, especially end systolic LV dimension are helpful to determine the optimal time for surgery. But don't forget that concomitant left to right shunts like VSD and PDA would affect not only the size of the chambers but also the dynamic of the flow through MV.

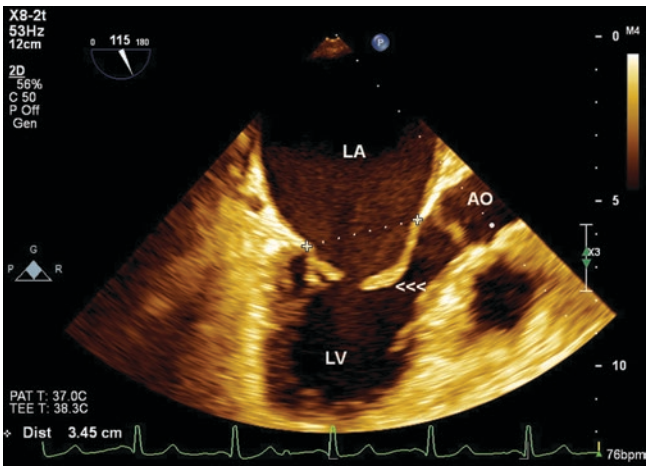

Fig. 30.12 TEE long axis view of the same patient as Fig. 30.12 showing severe LA enlargement, Hokey stick appearance of anterior mitral leaflet is indicated by arrow heads. This view is used for measuring anteroposterior diameter of MV annulus. *LA* left atrium, *LV* left ventricle, *AO* aorta

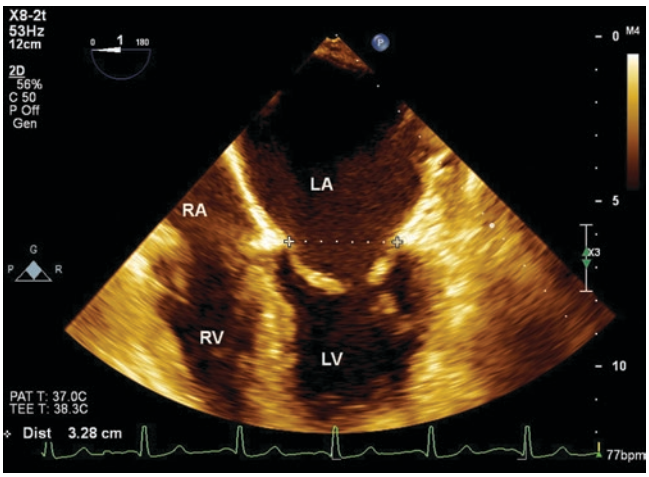

Fig. 30.13 TEE four chamber view showing severe LA enlargement. MV leaflets are thickened with restricted motion. This view is used to measure the mediolateral diameter of MV annulus. *LA* left atrium, *LV* left ventricle, *RV* right ventricle, *LA* left atrium

19. Evaluation of pulmonary veins flow by PW Doppler would be helpful for estimation of MR. Significant regurgitation will result in systolic flow reversal in more than one pulmonary vein. But remember that in cases of diastolic LV dysfunction and increased LA pressure, systolic forward flow is blunted irrelative to severity of MR.
20. Use Doppler profile of MV inflow and outflow for evaluation of MR severity. In CW Doppler of MR, if the profile is dense, MR is severe and in PW Doppler evaluation of MV inflow, a dominant E wave is in favor of severe MR. Concomitant diastolic dysfunction and MS are the limitation for these findings.

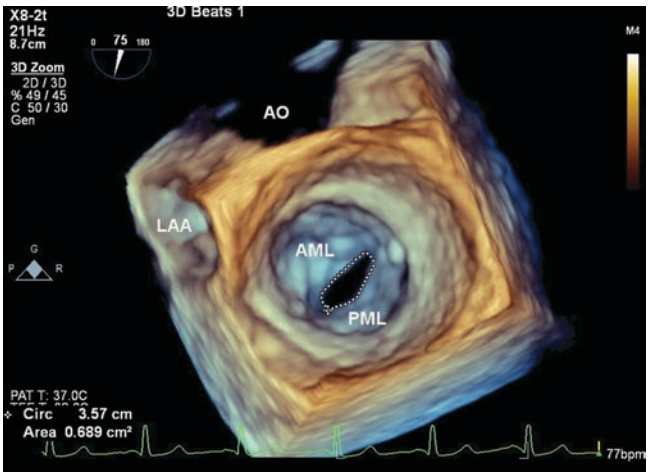

Fig. 30.14 Three-dimensional TEE of the same patient as Figs. 30.12 and 30.13. Planimetery of MV shows area 0.68 cm^2. Commissural fusion can easily be seen in this en face view of MV. *AO* aorta, *LAA* left atrial auricle, *AML* anterior mitral leaflet, *PML* posterior mitral leaflet

21. Mitral regurgitation (MR) in fetal life may occur in association of other anomalies such as aortic stenosis (AS), left ventricular dysfunction, systemic arteriovenous malformation, hypoplastic left heart syndrome (HLHS), and arrhythmia. So, careful evaluation is necessary. Sometimes dysplastic MV is an isolated finding. Increased cardiothoracic ratio, and LA enlargement are two-dimensional findings. The patency and size of the foramen ovale (FO) should be evaluated. Use Color Doppler interrogation to evaluate the patency of FO, direction of flow across it, and severity of mitral valve regurgitation. PW Doppler evaluation of pulmonary veins will show blunting of peak systolic velocity atrial flow reversal (Fig. 30.15a, b)

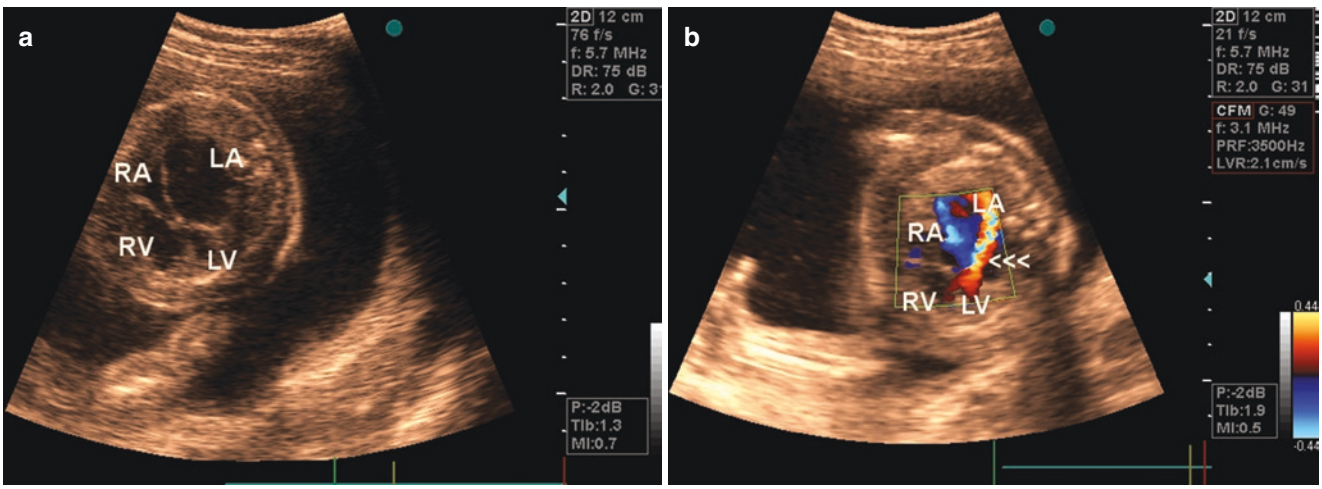

Fig. 30.15 (**a**, **b**) Fetal echo of a patient suffering from severe MR. Note the severe LA enlargement, bowing of the atrial septum into the right atrium, and increased cardiothoracic ratio in figure (**a**). MR jet is indicated (arrow heads) in figure (**b**)

Suggested Reading

Baumgartner HR, Bermejo J, Hung J, et al. Echocardiographic assessment of valve stenosis: EAE/ASE recommendations for clinical practice. Eur J Echocardiogr. 2009;10:1–25.

Delling FN, Rong J, Larson MG, et al. Evolution of mitral valve prolapse insights from the Framingham Heart Study. Circulation. 2016;133:1688–95.

Omran AS, Arifi AA, Mohamed AA. Echocardiography in mitral stenosis. J Saudi Heart Assoc. 2011;23:51–8.

Remenyi B, Gentles TL. Congenital mitral valve lesions: correlation between morphology and imaging. Ann Pediatr Cardiol. 2012;5(1):3–12.

Salcedo E, Quaife RA, Seres T, et al. A framework for systematic characterization of the mitral valve by real-time three-dimensional transesophageal echocardiography. J Am Soc Echocardiogr. 2009;22(10):1087–99.

Séguéla PE, Houyel L, Acar P. Congenital malformations of the mitral valve. Arch Cardiovasc Dis. 2011;104:465–79.

Serraf A, Zoghbi J, Belli E, et al. Congenital mitral stenosis with or without associated defects an evolving surgical strategy. Circulation. 2000;102(Suppl. 3)

Smallhorn J, Tommasini G, Deanfield J, et al. Congenital mitral stenosis anatomical and functional assessment by echocardiography. Br Heart J. 1981;45:527–34.

Valocik G, Kamp O, Visser CA. Three-dimensional echocardiography in mitral valve disease. Eur J Echocardiogr. 2005;6:443–54.

Congenitally Corrected Transposition of the Great Arteries (CCTGA)

31

Maryam Moradian and Azin Alizadehasl

Abstract

Echocardiographic evaluation of patients with CCTGA (also called LTGA) requires precise segmental approach. In 90% of patients, CCTGA is associated with other congenital heart defects, VSD, LV outflow tract obstruction, and apical displacement of the septal and inferior leaflets of tricuspid valve (Ebstein anomaly), as well as conduction system dysfunction. Prognosis is determined not only by associated anomalies, but also by systemic pressure effect on RV function. In the absence of other anomalies, diagnosis may be delayed. Systemic ventricular failure, and arrhythmias may be the presenting symptoms in isolated CCTGA.

Congenitally Corrected Transposition of the Great Arteries (CCTGA)

1. Remember that subcostal coronal view and apical four chamber view provide the most diagnostic findings. Define Morphologic right atrium (RA), left atrium (LA),right ventricle (RV) and left ventricle (LV) based on their echocardiographic features and evaluate discordant connection of atria and ventricles, atrioventricular (AV) discordance: RA to morphologic LV and LA to morphologic RV (Fig. 31.1).
2. Demonstrate discordant connection of ventricles and great arteries, ventriculoarterial (VA) discordance: LV to pulmonary artery (PA) and RV to aorta (AO) (Figs. 31.2 and 31.3).

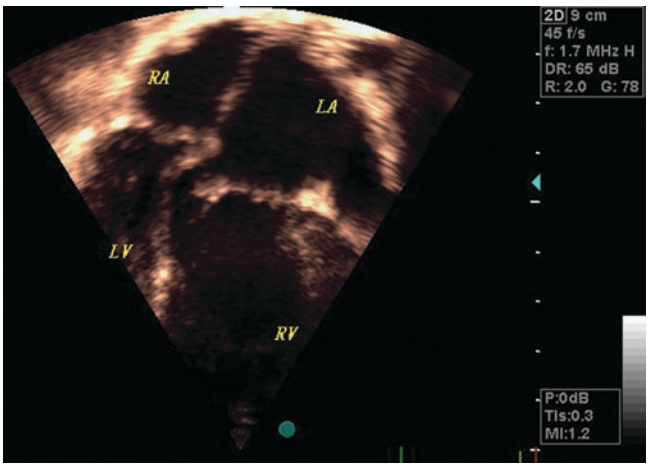

Fig. 31.1 Transthoracic apical four chamber view showing AV discordance. *RA* right atrium, *LA* left atrium, *RV* right ventricle, *LV* left ventricle

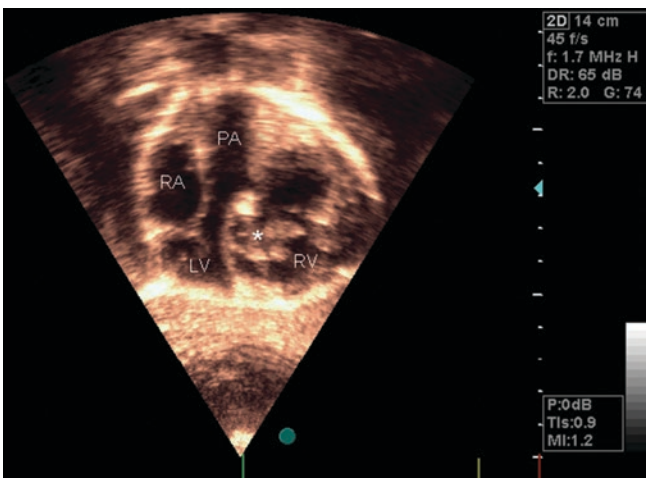

Fig. 31.2 Subcostal coronal view showing PA arising from morphologic LV. Asterisk indicates tricuspid valve in systole. *RA* right atrium, *LV* left ventricle, *PA* pulmonary artery, *RV* right ventricle

M. Moradian
Pediatric Cardiology, Rajaie Cardiovascular, Medical & Research Center, Iran University of Medical Sciences, Tehran, Iran

A. Alizadehasl (✉)
Department of Cardio-Oncology and Research Center, Rajaie Cardiovascular, Medical & Research Center, Iran University of Medical Sciences, Tehran, Iran

M. Moradian, A. Alizadehasl (eds.), *Atlas of Echocardiography in Pediatrics and Congenital Heart Diseases*,
https://doi.org/10.1007/978-3-662-62341-1_31

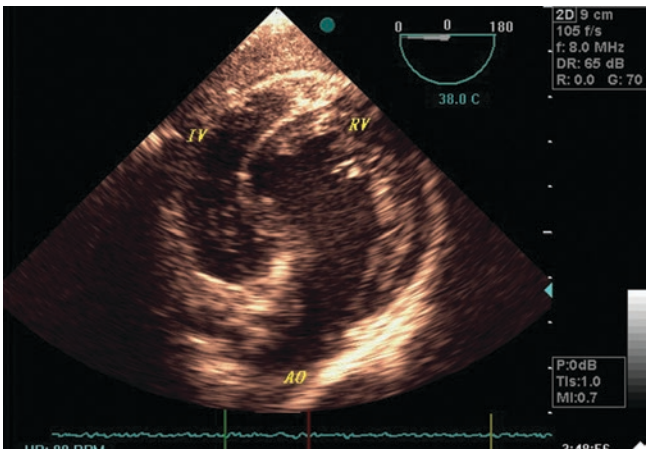

Fig. 31.3 Transesophageal echocardiography (TEE), deep trans gastric view showing origination of aorta from morphologic right ventricle. *LV* left ventricle, *RV* right ventricle, *AO* aorta

3. In some cases with superior-inferior arrangement of ventricles imaging both atrioventricular valves in a same plane are not possible and tilting the transducer is necessary.
4. Identify parallel orientation of great arteries in different views including subcostal and parasternal views also evaluate the left and anterior location of aortic valve (Fig. 31.4a, b).
5. Appreciate for common associated anomalies including ventricular septal defect (VSD), left ventricular out flow tract obstruction (LVOTO), pulmonary stenosis (PS), Ebstein malformation of tricuspid valve, or any other lesion. Also use color flow Doppler to evaluate any atrioventricular valve stenosis or regurgitation (Fig. 31.5a, b).
6. Standard parasternal long axis view in these patients is confusing because interventricular septum is vertical, ventricles are almost side by side, and great arteries are

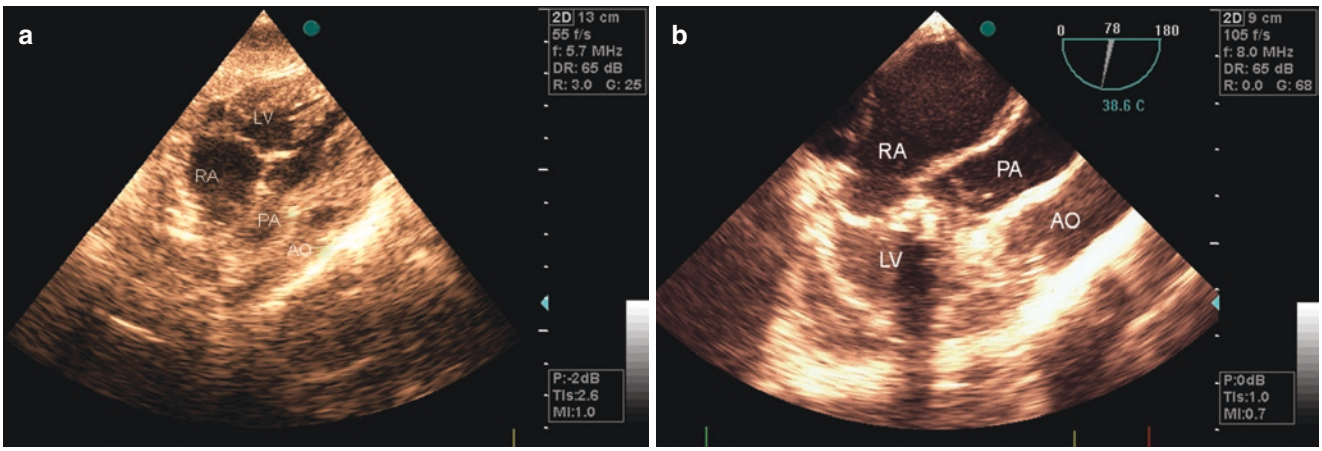

Fig. 31.4 (**a**, **b**) Parallel orientation of great arteries is shown in TTE, subcostal coronal view (**a**). Anteriorly located aorta and parallel arrangement of great arteries is shown in this transesophageal echocardiography of a patient with CCTGA at in flow-outflow view (**b**). *LV* left ventricle, *RA* right atrium, *AO* aorta, *PA* pulmonary artery

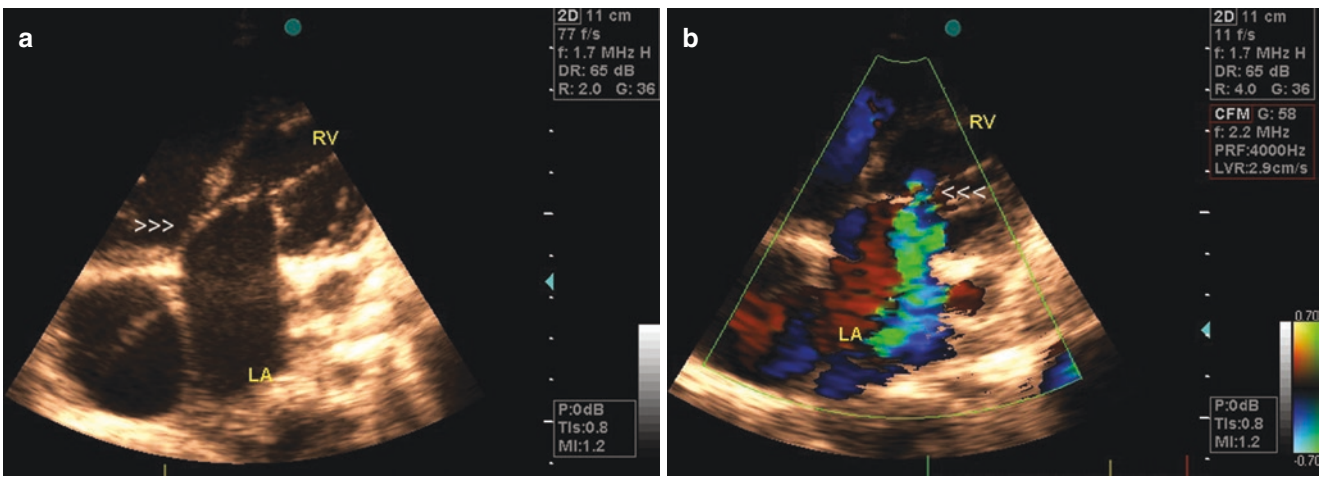

Fig. 31.5 (**a**, **b**) Apical four chamber view of a patient with CCTGA and Ebstein malformation of tricuspid valve (TV) (left AV valve). Arrow heads in figure (**a**) indicate the displacement of septal leaflet of TV. Color Doppler interrogation of the same patient shows severe tricuspid regurgitation (TR) in figure (**b**). Arrow heads point to the origin of TR jet (**b**). *LV* left ventricle, *RA* right atrium

parallel in CCTGA. So, more manipulation of the transducer is necessary

7. Because the course of ascending aorta in CCTGA is straight and leftward, aortic arch in these patients is better evaluated in high parasternal position, so called ductal view, than standard suprasternal view (Fig. 31.6).
8. Evaluate the coronary arteries in parasternal short axis view. Coronary arteries distribution in CCTGA is concordant with ventricular anatomy, the so called "coronary artery–ventricular concordance" which is the mirror-image of normal coronary distribution. The most common coronary anomaly in CCTGA is single coronary arteries.
9. During fetal life this anomaly should be ruled out in cases who are referred for evaluation of fetal bradycardia, because CCTGA may lead to complete heart block (CHB) even in fetus (Fig. 31.7)

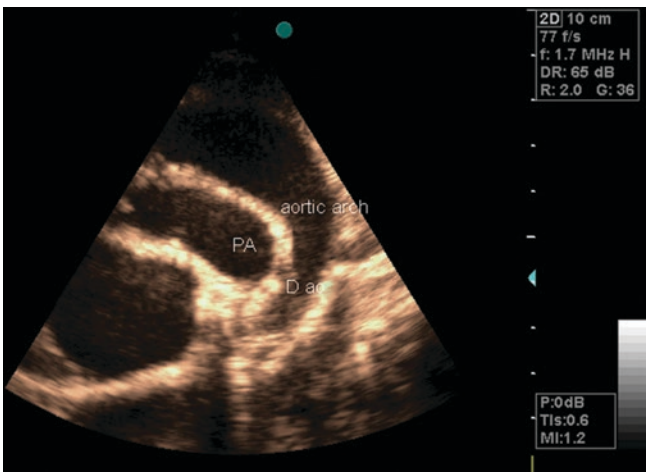

Fig. 31.6 Left high parasternal view showing left sided aortic arch, left anterior aorta in this case of CCTGA. *PA* pulmonary artery, *DAO* descending aorta

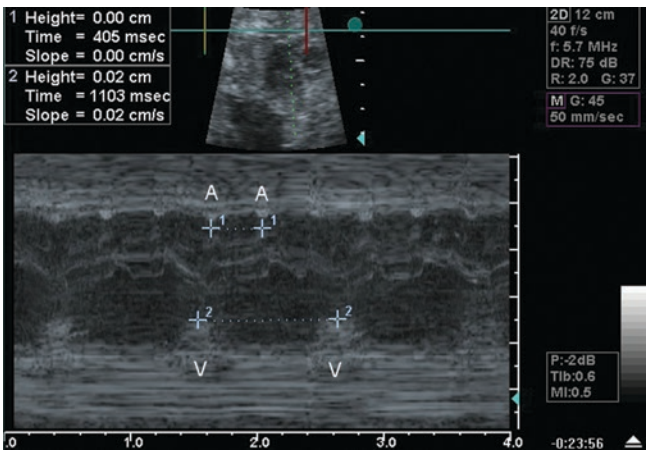

Fig. 31.7 Fetal echocardiogram using M mode to evaluate atrial and ventricular wall motion in a fetus with complete heart block (CHB). The mechanical A to A interval corresponding to electrical PP interval, is 405 milliseconds (ms) so atrial rate is 148 beat per minute (bpm), and V to V interval corresponding electrical RR interval is 1103 ms, predicting ventricular rate 54 bpm, and there is no electrical association between atria and ventricles

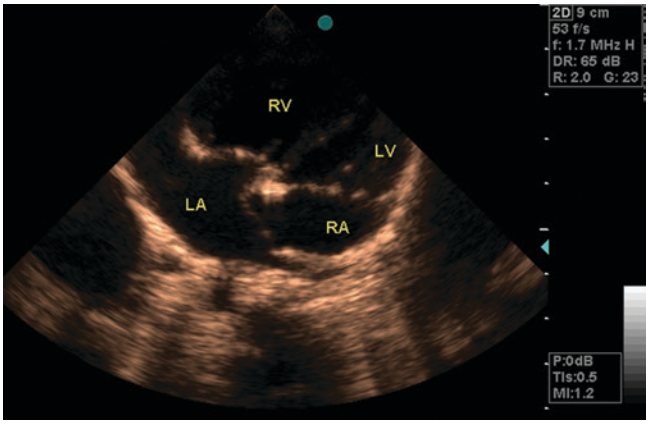

Fig. 31.8 Apical four chamber view in a patient with situs inversus, AV and VA discordance. *RA* right atrium, *LA* left atrium, *RV* right ventricle, *LV* left ventricle

10. Congenitally corrected transposition of the great arteries may be seen in with situs inversus, dextrocardia and/or mesocardia (Fig. 31.8).
11. Very important in these patients is the evaluation of RV function as systemic ventricle. Serial evaluation RV function using fractional area change, tricuspid annular excursion (TAPSE), tissue Doppler and strain imaging are useful.

Suggested Reading

Cohen MS, Mertens LL. Echocardiographic assessment of transposition of the great arteries and congenitally corrected transposition of the great arteries. Echo Res Pract. 2019;6:4.

Costa P, Monterroso J, Areias JC. Prenatal diagnosis of complete heart block and congenitally corrected transposition of the great arteries. Pediatr Cardiol. 2007;28:414–5.

David S, Winlaw DS, Mc Guirk SP, Balmer C. Intention-to-treat analysis of pulmonary artery banding in conditions with a morphological right ventricle in the systemic circulation with a view to anatomic biventricular repair. Circulation. 2005;111:405–11.

Duncan BW, Mee RBB, Mesia I, et al. Results of the double switch operation for congenitally corrected transposition of the great arteries. Eur J Cardio-thorac Surg. 2003;24:11–20.

Kanagawa N, Inamura N, Narita J, et al. Prenatal diagnosis of isolated atrioventricular discordance using fetal echocardiograph. Images Paediatr Cardiol. 2014;16(1):5–10.

Paladini D, Volpe P, Marasini M, et al. Diagnosis, characterization and outcome of congenitally corrected transposition of the great arteries in the fetus: a multicenter series of 30 cases. Ultrasound Obstet Gynecol. 2006;27(3):281–5.

Parikh V, Shariff MA, Saiful FB, et al. Anomalies associated with congenitally corrected transposition of great arteries: expect the unexpected. Eplasty. 2013;13:41–9.

Zimmermann J, Altman R, Gantt S. Acute myocardial infarction with isolated congenitally corrected transposition of the great arteries. Proc (Bayl Univ Med Cent). 2016;29(2):168–70.

Transposition of Great Arteries (Simple TGA/dTGA)

32

Maryam Moradian

Abstract

Echocardiography acts as the main diagnostic tool in transposition of great arteries. Echocardiography provides not only all the necessary anatomic and physiologic information, but also contributes for both medical and surgical managements. As in this anomaly the systemic and pulmonary circulations are parallel survival of the neonate is provided by some mixture of blood via patent foramen ovale, ASD, PDA, and/or VSD. Some neonates require emergency balloon atrial septostomy if mixing of systemic and pulmonary blood (deoxygenated and oxygenated blood) is not sufficient.

Transposition of Great Arteries (Simple TGA/dTGA)

1. Remmember that simple transposition (or dTGA) is the concordant atrioventricular (AV) connections, discordant ventriculoarterial (VA) connections and encompasses the transposition of great arteries with intact ventricular septum (dTGA/IVS), transposition of the great arteries with ventricular septal defect (dTGA/VSD), and transposition of the great arteries with ventricular septal defect and left ventricular outflow tract obstruction (dTGA/VSD, LVOTO).
2. Appreciate the atrioventricular concordance in subcostal and four chamber views.
3. The hallmark for diagnosis of d-TGA is ventriculoarterial discordance. So evaluate the posterior semilunar valve arising from left ventricle (LV) which give rises a great artery that bifurcates; pulmonary artery, and the more anterior great artery arises from RV, which does not bifurcate, aorta. Subcostal four chamber and sagittal views, and parasternal long axis view are useful windows in this regard (Fig. 32.1).
4. Right anterior location of aortic valve can be shown in parasternal short axis view. In normal heart orientation of great arteries provides the so-called circle-sausage appearance in parasternal short axis view; the circle is the aorta, which is seen in cross section, while the sausage stands for the longitudinal view of the pulmonary artery. In transposition due to parallel alignment of aorta and pulmonary artery both are seen in cross section and create the double circle or circle by circle appearance. Remember to check for bifurcation of pulmonary artery in this view as well (Fig. 32.2).
5. Mention the presence and location of associated defects including PFO and/or ASD, VSD (or VSDs), and PDA. In cases of dTGA/IVS presence of ASD and PDA play a crucial role. Determine the size of the interatrial

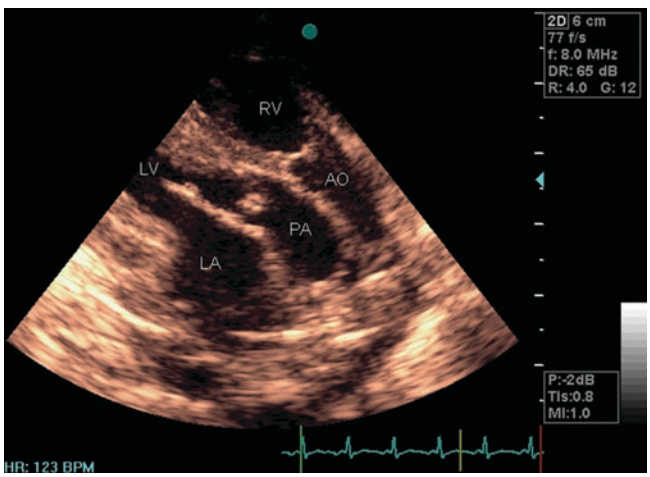

Fig. 32.1 Parasternal long axis view of a case of TGA/IVS, VA discordance and parallel alignment of great arteries is shown by some upward angulation of transducer. *LV* left ventricle, *RV* right ventricle, *AO* aorta, *PA* pulmonary artery, *LA* left atrium

M. Moradian (✉)
Pediatric Cardiology, Rajaie Cardiovascular, Medical & Research Center, Iran University of Medical Sciences, Tehran, Iran

M. Moradian, A. Alizadehasl (eds.), *Atlas of Echocardiography in Pediatrics and Congenital Heart Diseases*,
https://doi.org/10.1007/978-3-662-62341-1_32

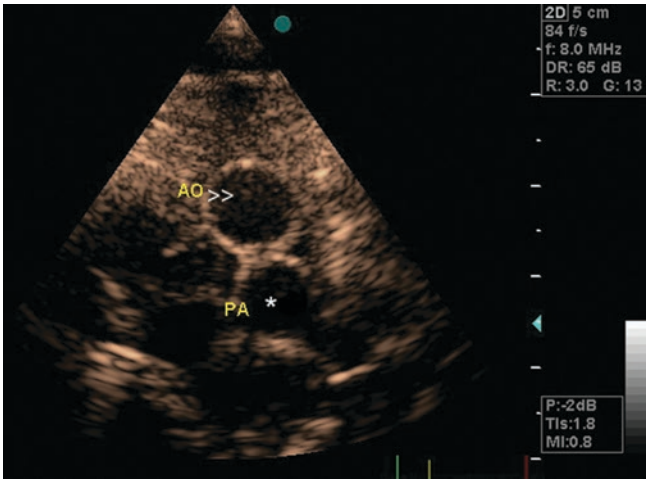

Fig. 32.2 Parasteranl short axis view showing cross section of both aorta and pulmonary artery (asterisk). (Double circle or circle by circle appearance). *AO* aorta, *PA* pulmonary artery

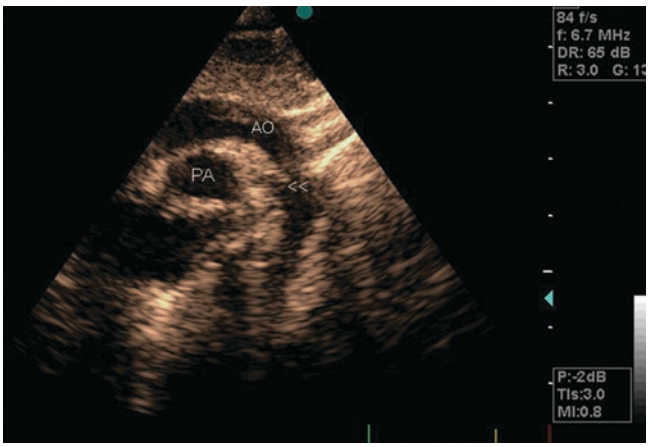

Fig. 32.3 Suprasternal long axis view of a patient with TGA. PDA (arrow heads) is easier to visualize in these patients. *AO* aorta, *PA* pulmonary artery

septal defect in subcostal views and evaluate the direction of shunt using color Doppler and PW Doppler. Determine if the ASD is restrictive, urgent balloon atrial septostomy may be necessary.

6. It is possible that orifice of the juxtaposed RAA be mistaken for large ASD, so don't forget to use color Doppler and spectral Doppler to evaluate the ASD.
7. Detecting PDA and evaluation of its whole length usually is easy in suprasternal long axis view in these patients because the great arteries have parallel alignment (Fig. 32.3). Also inspect the aortic arch for any hypoplasia or coarctation of aorta (COA).
8. All types of ventricular septal defects can be found in these patients. Perimembranous ventricular septal defect also referred as conoventricular in the setting of transposition of the great arteries, is the most common type.

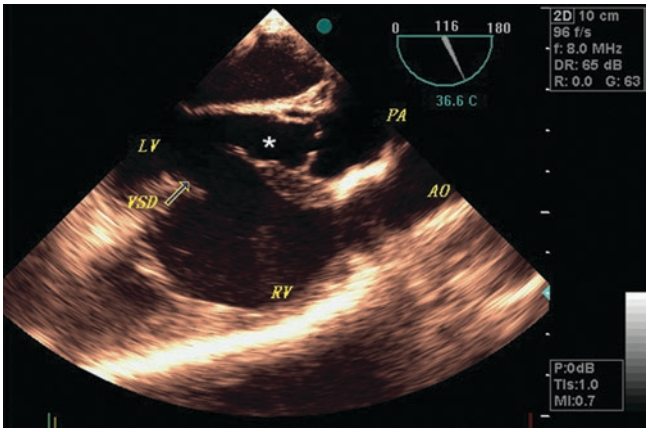

Fig. 32.4 TEE, mid esophageal long axis view showing large VSD with posterior malalignment of infundibular septum leading to some degree of LVOTO (asterisk). The pulmonary valve is also bicuspid and stenotic with dome shape opening in this systolic frame. *LV* left ventricle, *RV* right ventricle, *AO* aorta, *PA* pulmonary artery, *VSD* ventricular septal defect

Sometimes the infundibular septum is malaligned and displaced posteriorly leading to variable degrees of LV out flow obstruction (LVOTO) (Fig. 32.4). Anterior displacement of infundibular septum may lead to overriding of pulmonary valve over RV. Severe anterior displacement of outlet septum results in double outlet right ventricle (DORV) with subpulmonary VSD or the so called Taussig-bing anomaly. Less common VSD s in TGA are muscular defect, which maybe inlet, apical, mid-muscular, and doubly committed subarterial VSD.

9. Evaluate both atrioventricular valves size and function in four chamber view. Inlet type VSDs may be associated with straddling of the TV. Sometimes TV tissue protrudes through VSD and causes some degrees of sub pulmonary stenosis.
10. It is important to measure the aortic and pulmonary valve annulus in parasternal long axis view in systole. Any structural and functional anomaly of semilunar valves should be checked by adding Doppler modalities.
11. Coronary anomalies are common in TGA. Evaluate the originating of coronary arteries from right and anteriorly located great artery (aorta) in parasternal short-axis view. You may use some supplementary views including parasternal long axis, apical four chamber and subcostal views to follow coronary arteries course.
12. Evaluate the suitability of LV for arterial switch operation (ASO) by estimating the LV mass, and identifying the LV out flow tract obstruction. Asses the shape of interventricular septum, and presence of other anomalies. If LV muscle mass is less than 35 g/m^2, LV retraining by pulmonary artery banding will help the LV remodeling. Also, if the interventricular septum convex-

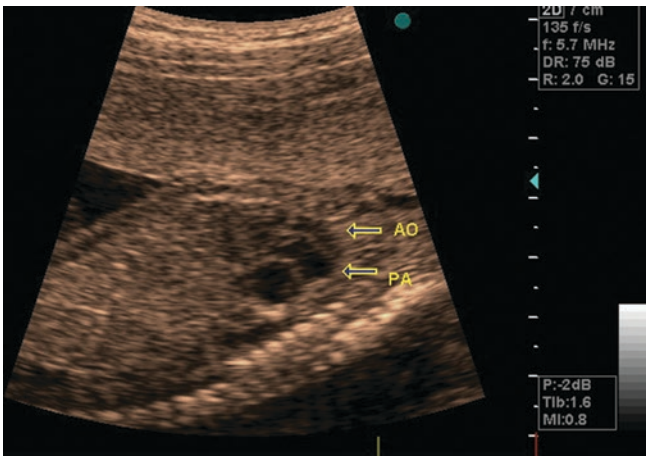

Fig. 32.5 Fetal echocardiography parasagittal view showing anterior aorta and dilated pulmonary artery. *AO* aorta, *PA* pulmonary artery

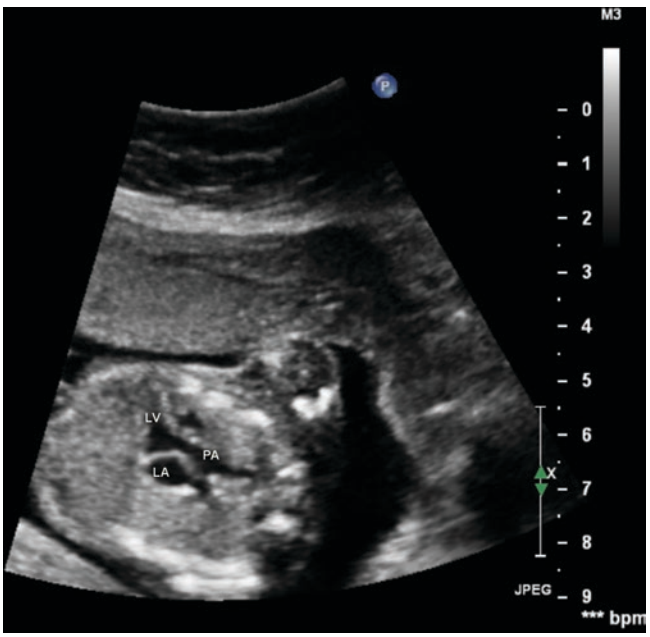

Fig. 32.6 Long axis fetal echocardiography showing posteriorly located bifurcating vessel, pulmonary artery arises from LV. *AO* aorta, *PA* pulmonary artery, *LA* left atrium

ity is towards the LV on short axis views of ventricles, and LV has a banana-shape configuration on long axis views LV preparation might be considered.

13. Echocardiogram of fetuses with TGA/IVS resembles normal in four chamber view. Five chamber view will show arising of PA from LV. The aorta arises from RV, parallel and anterior to pulmonary artery (PA) (Figs. 32.5 and 32.6).
14. On the three-vessel tracheal view of these fetuses only two vessels are seen, aorta and superior vena cava. Pulmonary artery is posterior and inferior to the aorta, so cannot be seen in this view (Figs. 32.7 and 32.8).

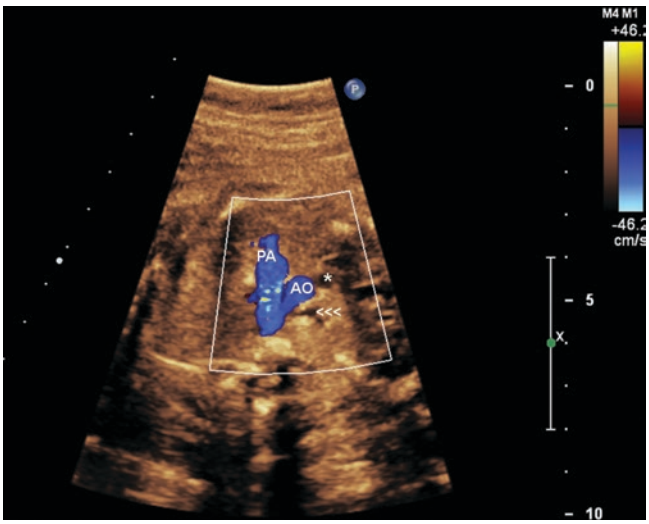

Fig. 32.7 Fetal echocardiogram, three vessel tracheal view of a normal fetus. Asterisk indicate superior vena cava (SVC) and arrow heads point to trachea. *AO* aorta, *PA* pulmonary artery

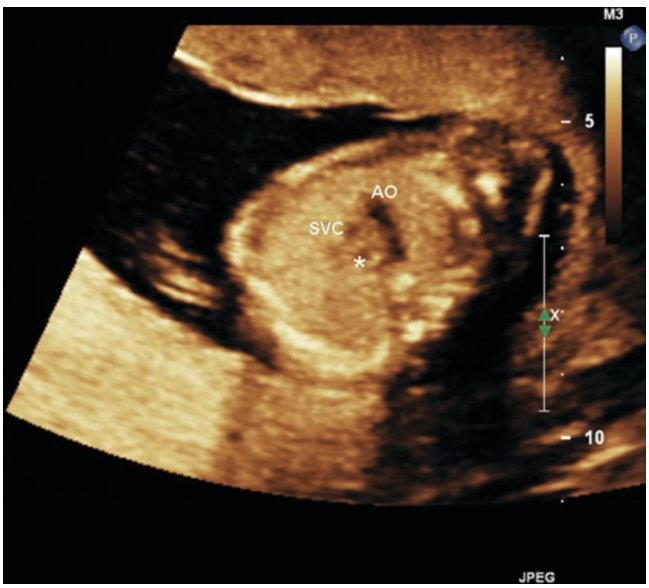

Fig. 32.8 Fetal echocardiogram, three vessel tracheal view of a fetus with TGA, only two vessels, aorta and superior vena cava are seen. Trachea is indicated by asterisk. Compare this figure with Fig. 32.7. *AO* aorta, *SVC* superior vena cava

Suggested Reading

Bisoi AK, Sharma P, Chauhan S, et al. Primary arterial switch operation in children presenting late with d-transposition of great arteries and intact ventricular septum. When is it too late for a primary arterial switch operation? Eur J Cardio-Thorac Surg. 2010;38(6):707–13.

Cohen MS, Mertens LL. Echocardiographic assessment of transposition of the great arteries and congenitally corrected transposition of the great arteries. Echo Res Pract. 2019;6:4.

Dhillon GS, Fernandes CJ, Khan A, et al. Transposition of the great arteries: when echocardiography does not match the clinical picture. J Clin Ultrasound. 2018;46(9):617–22.

Filho BG, Fantini FA, Martins C, et al. Surgical strategy for transposition of the great arteries with intact ventricular septum after the neonatal period. Arquivos Brasileiros Cardiol. 2005;85:1.

Foran JP, Sullivan ID, Elliott MJ, et al. Primary arterial switch operation for transposition of the great arteries with intact ventricular septum in infants older than 21 days. J Am Coll Cardiol. 1998;31(4):883–9.

Grewal DS, Khanna V, Saxena S, et al. Sonographic diagnosis of transposition of great arteries in mid trimester: our experience. Med J Armed Forces India. 2016;72(4):386–8.

Martins P, Castela E. Transposition of the great arteries. Orphanet J Rare Dis. 2008;3:27.

Mercer-Rosa LM, Cohen MS. Evaluation of conotruncal abnormalities (Chapter 12). In: Wong PC, Miller-Hance WC, editors. Transesophageal echocardiography for congenital heart disease. London: Springer-Verlag; 2014. p. 307–40.

Paladini D, Volpe P, Sglavo G, et al. Transposition of the great arteries in the fetus: assessment of the spatial relationships of the arterial trunks by four-dimensional echocardiography. Ultrasound Obstet Gynecol. 2008;31:271–6.

Aortic Stenosis (AS)

33

Azin Alizadehasl and Maryam Moradian

Abstract

The degree of obstruction in aortic stenosis ranges from mild to severe. Bicuspid aortic valve (BAV), one of the most common congenital heart diseases may be asymptomatic during childhood. BAV is identified in about 1.5% of adults. The most common level of obstruction is valvar followed by sub valvar and supravalvar stenosis. Valvar aortic stenosis during fetal life may progress to hypoplastic left heart syndrome (HLHS). Subvalvar AS may be associated with mitral stenosis and coarctation of the aorta (Shone complex). Supravalvar AS, the least-common type, may be associated with Williams syndrome.

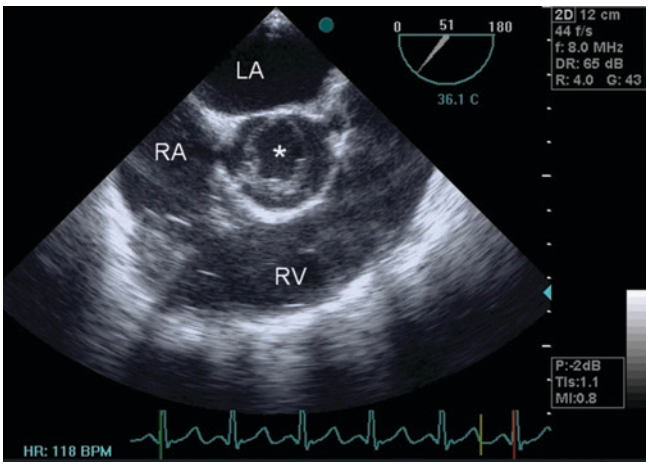

Fig. 33.1 Transesophageal (TEE) aortic valve short axis view showing BAV (asterisk) in systolic frame. Right and left aortic cusps are fused. *RA* right atrium, *LA* left atrium, *RV* right ventricle

Aortic Stenosis (AS)

1. Use multiple echocardiography views to get crucial information about all type of congenital aortic valve anomalies including right parasternal view.
2. In cases of AS determine where the obstruction is located: below, above, or at the level of the aortic valve (the most common type of AS). Use color flow mapping (CFM), pulsed Doppler (PW), and continues Doppler (CW) to find the location and the degree of stenosis. The angle of Doppler interrogation is very important, try to interrogate the flow as parallel as possible and use different views.
3. The two most useful views for aortic valve evaluation are the parasternal long axis (for measurement of the aortic valve annulus, aortic root dimensions, and evaluating mobility of the cups), and the parasternal short axis (for assessment of aortic valve morphology)
4. In parasternal short axis view assess the most common congenital abnormality of the aortic valve, bicuspid aortic valve (BAV), in systolic frame, and see if it is due to fusion or underdevelopment of commissure between the right and left coronary cusps, which is the most common type of BAV (Fig. 33.1).
5. Evaluate the doming of cusps in cases of valvar aortic stenosis, which may be due to dysplastic tricuspid, bicuspid, or even unicuspid aortic valve. Doming, can be assessed in the parasternal long axis view. In the same view measure the size of annulus. Remember that annular hypoplasia may be the cause of AS rather than fusion of cusps though it is rare (Fig. 33.2).
6. In cases of BAV, don't forget to check for possible aortic root dilation, and coarctation which are commonly associate with BAV.

A. Alizadehasl
Department of Cardio-Oncology and Research Center, Rajaie Cardiovascular, Medical & Research Center, Iran University of Medical Sciences, Tehran, Iran

M. Moradian (✉)
Pediatric Cardiology, Rajaie Cardiovascular, Medical & Research Center, Iran University of Medical Sciences, Tehran, Iran

M. Moradian, A. Alizadehasl (eds.), *Atlas of Echocardiography in Pediatrics and Congenital Heart Diseases*,
https://doi.org/10.1007/978-3-662-62341-1_33

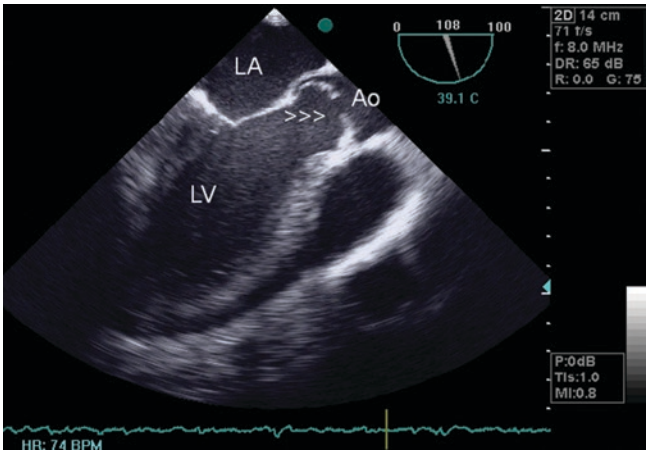

Fig. 33.2 TEE long axis view showing doming of aortic cusps during systole (arrow heads). *LA* left atrium, *LV* left ventricle, *AO* aorta

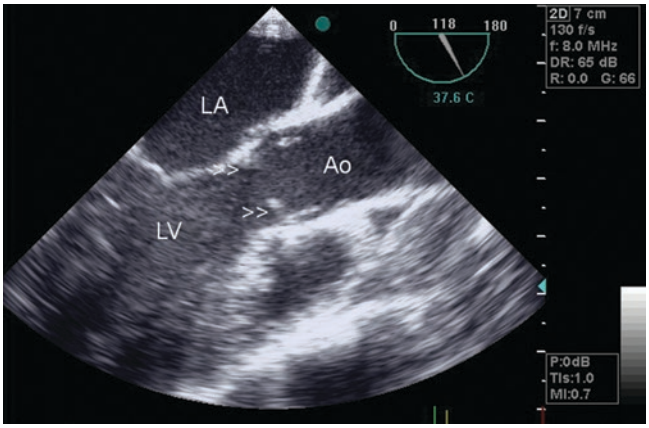

Fig. 33.3 TEE long axis view showing sub aortic membrane (arrow heads). *LA* left atrium, *LV* left ventricle, *AO* aorta

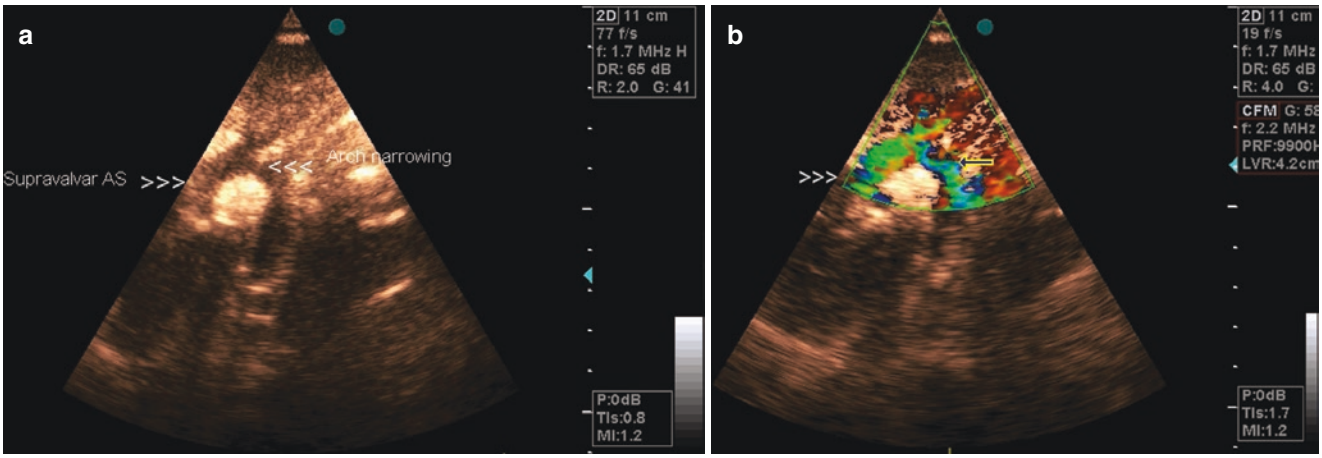

Fig. 33.4 (**a**, **b**) Transthoracic echo (TTE) suprasternal long axis view showing supravalvar AS, narrowing of sinotubular junction and aortic arch in figure (**a**). Turbulent flow is shown using CFM in figure (**b**). Arrowheads and yellow arrow point to sites of most stenosis

7. An eccentrically located, oval or circular shape opening in systole may be caused by unicuspid aortic valve.
8. Determine if sub valvar AS is either due to a very thin circumferential fibrous membrane just close to aortic valve (Fig. 33.3) or a fibro muscular ridge. Remember that these may not be present at birth. Also in parasternal long axis evaluate tunnel-like narrowing of the left ventricular outflow, which is a rare condition and often are diagnosed after cardiac surgery especially for complex lesion.
9. Use color flow mapping (CFM) to evaluate any aortic valve regurgitation especially in subvalvar AS because high velocity jet may lead to aortic valve damage causing aortic insufficiency.
10. Besides evaluating the aortic valve, always check for multiple levels of left heart obstruction, including mitral valve and aortic arch, not missing Shone complex.
11. In parasternal log axis view also evaluate for anomalous insertion of MV chorda tendinea which can cause some degrees of Left ventricular out flow tract obstruction (LVOTO)
12. Asymmetric septal hypertrophy may contribute to subvalvar AS in hypertrophic cardiomyopathy (HCM), which should be evaluated in apical five chamber view. To determine the exact site of dynamic flow disturbance use CFM and PW Doppler modalities.
13. The most common type of supravalvar aortic stenosis is discrete obstruction above the sinus of Valsalva. Supravalvar AS may be a manifestation of a systemic arteriopathy. Evaluate for common association's such as peripheral branch pulmonary artery stenosis, and coronary narrowing (Fig. 33.4a, b).
14. Evaluate the degree of LV hypertrophy in parasternal short axis view

15. After anatomic evaluation of AS by 2D echocardiography and evaluation of flow turbulence by CFM use Doppler interrogation to assess the severity of the lesion. Based on ACC/AHA resent guideline (2014) peak velocity across the aortic valve of ≥4.0 m/s or a mean gradient across the valve of ≥40 mmHg is considered severe stenosis, peak velocity between 3.0 and 3.9 m/s or a mean gradient between 20 and 39 mmHg is defined as moderate stenosis, and a peak velocity of 2.0–2.9 m/s and a mean gradient ≤20 mmHg is consistent with mild stenosis
16. You have to calculate aortic valve area in cases of low cardiac output in whom the pressure gradient would be artificially low. Continuity equation is useful in these patients. (AV area = LVOT area × LVOT vti/AV vti).

    Normal aortic valve area in children is 2 cm^2/m^2 of BSA (or 1.33 cm^2/m^2 in some references) and valve area ≤0.6 cm^2/m^2 (or <0.5 cm^2/m^2 in some references) is consistent with severe stenosis, and area >0.75 cm^2/m^2 is mild stenosis.
17. Don't forget that mild aortic stenosis during fetal period may be detected just after using CFM and detecting turbulent flow in aortic valve region because four chamber view is often normal and the only 2D findings are thickened aortic valve cusps and mild dilation of ascending aorta in five chamber view. In critical AS, LV is more rounded (Fig. 33.5), its contractility is reduced, and you may find endocardial fibroelastosis (EFE) and mitral regurgitation (Fig. 33.6).

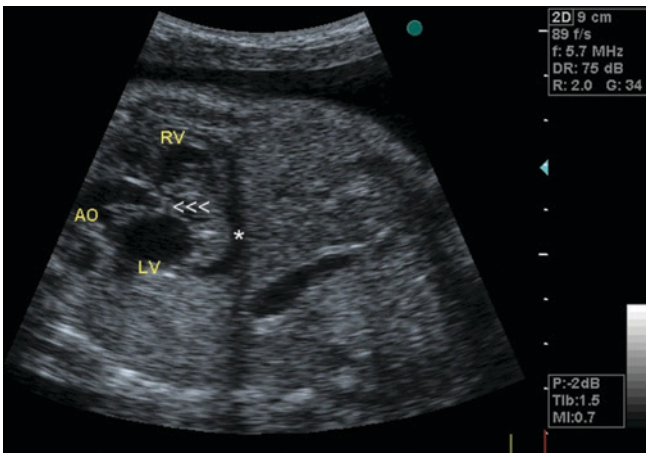

Fig. 33.5 Fetal echocardiography, LVOT view showing thickened aortic cusps (arrow heads), rounded LV, and mild pericardial effusion (PE) (asterisk). *RV* right ventricle, *LV* left ventricle, *AO* aorta

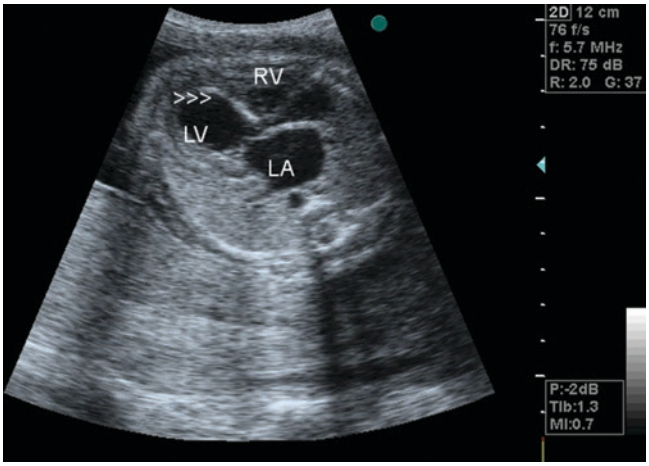

Fig. 33.6 Arrow heads point to endocardial fibroelastosis (EFE) of LV in this case of critical AS, also LV enlargement, is noticeable. *RV* right ventricle, *LV* left ventricle, *LA* left atrium

Suggested Reading

Baumgartner H, Griffin BP, Hung J, et al. Echocardiographic assessment of valve stenosis: EAE/ASE recommendations for clinical practice. Eur J Echocardiogr. 2009;10:1–25.

Baumgartner H, Hung J, Bermejo J, et al. Recommendations on the echocardiographic assessment of aortic valve stenosis: a focused update from the European Association of Cardiovascular Imaging and the American Society of Echocardiography. Eur Heart J Cardiovasc Imaging. 2017;18:254–75.

Freud LR, Moon-Grady A, Escobar-Diaz MC, et al. Low rate of prenatal diagnosis among neonates with critical aortic stenosis: insight into the natural history in utero (aortic stenosis). Ultrasound Obstet Gynecol. 2015;45(3):326–32.

Huhta JC, Latson LA, Gutgesell HP, et al. Echocardiography in the diagnosis and management of symptomatic aortic valve stenosis in infants. Circulation. 1984;70(3):438–44.

Kuebler JD, Shivapour J, Kazanci SY, et al. Longitudinal assessment of the Doppler-estimated maximum gradient in patients with congenital valvar aortic stenosis pre- and post-Balloon valvuloplasty. Circulation: Cardiovas Imaging. 2018;11(3)

Mäkikallio K, McElhinney DB, Levine JC, et al. Fetal aortic valve stenosis and the evolution of hypoplastic left heart syndrome patient selection for fetal intervention. Circulation. 2006;113(11):1401–140.

Schlingmann TR, Gauvreau K, Colan SD, et al. Correction of doppler gradients for pressure recovery improves agreement with subsequent catheterization gradients in congenital aortic stenosis. J Am Soc Echocardiogr. 2015;28:1410–7.

Singh GK. Congenital aortic valve stenosis. Children (Basel). 2019;6(5):69.

Aortic Arch Anomalies

34

Feridoun Noohi, Majid Maleki, Azin Alizadehasl, and Maryam Moradian

Abstract

Suprasternal echocardiographic views are used to determine aortic arch sidedness and branching pattern. Sometimes they are associated with congenital cardiac defects. These anomalies may be found incidentally on imaging studies or discovered when evaluation for systemic hypertension, airway or esophageal compression are being carried out.

Aortic Arch Anomalies

1. First of all, determine the sidedness of aortic arch in suprasternal views. In standard suprasternal long axis view, the ascending, transverse, and descending parts of the left sided arch, would be imaged easily while in right sided arch, the descending part of the aorta is not visible and you should angulate the transducer slightly to the right to be able to see the descending aorta (Fig. 34.1a, b).
2. In suprasternal short axis view try to find the cartilaginous rings of trachea, in left arch the cross section of transverse aorta is to the left of the trachea but in right arch it would be seen in right of trachea. Also follow the first brachiocephalic artery in suprasternal short axis view, in cases of right arch this vessel courses leftward while in cases of left arch, courses to the right.
3. Evaluate the branching pattern of arch. In normal left sided aortic arch, the first branch; right innominate artery, branches into the right common carotid and right subclavian arteries itself, the second branch, the left carotid artery, proceeds superiorly and the third one, the left subclavian artery proceeds leftward. The ductus arteriosus joins the aorta distal to the takeoff of the left subclavian artery.
4. Evaluate the normal variants of left aortic arch:
   (a) Single origin of the right innominate and left carotid artery
   (b) Separate origin of the left vertebral artery from the aortic arch rather than from the subclavian artery. Remember that this normal variant should not be confused with anomalous right subclavian artery.
5. Try to rule out the presence of vascular ring by demonstration of aortic side, the bifurcation of innominate artery into the carotid and subclavian arteries, and ductus arteriosus and also carefully evaluate pulmonary arteries in different echo windows especially suprasternal notch views. In following situations vascular ring should be considered:
   (a) Right sided ductus arteriosus in case of left aortic arch with aberrant right subclavian artery
   (b) Origination of ductus arteriosus from left descending aorta In cases of right aortic arch and aberrant left subclavian artery
   (c) Ductus arteriosus from descending aorta to LPA in case of right aortic arch with retroesophageal course of left subclavian artery
   (d) Double aortic arch, each arch give rises its respective branches and right arch is commonly larger and superiorly located while the left arch is more commonly hypoplastic or even atretic. The branching

F. Noohi · M. Maleki
Cardiovascular Intervention Research Center, Rajaie Cardiovascular, Medical & Research Center, Iran University of Medical Sciences, Tehran, Iran

A. Alizadehasl
Department of Cardio-Oncology and Research Center, Rajaie Cardiovascular, Medical & Research Center, Iran University of Medical Sciences, Tehran, Iran

M. Moradian (✉)
Pediatric Cardiology, Rajaie Cardiovascular, Medical & Research Center, Iran University of Medical Sciences, Tehran, Iran

M. Moradian, A. Alizadehasl (eds.), *Atlas of Echocardiography in Pediatrics and Congenital Heart Diseases*,
https://doi.org/10.1007/978-3-662-62341-1_34

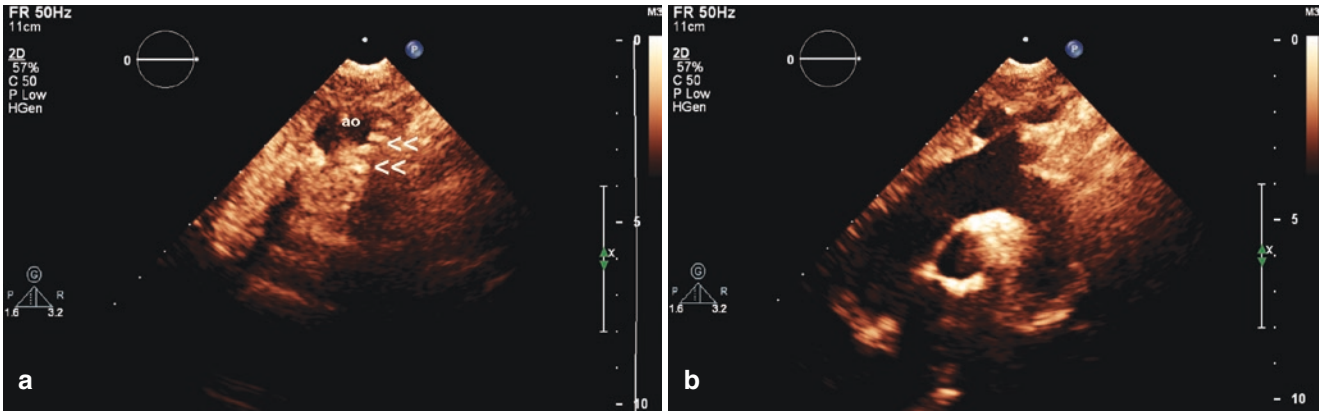

Fig. 34.1 (**a**, **b**) Transthoracic suprasternal views. By visualization of tracheal cartilage (arrow heads in figure **a**), and tilting the probe toward patients left, the entire arch appears in cases of left aortic arch (**b**). *AO* aorta

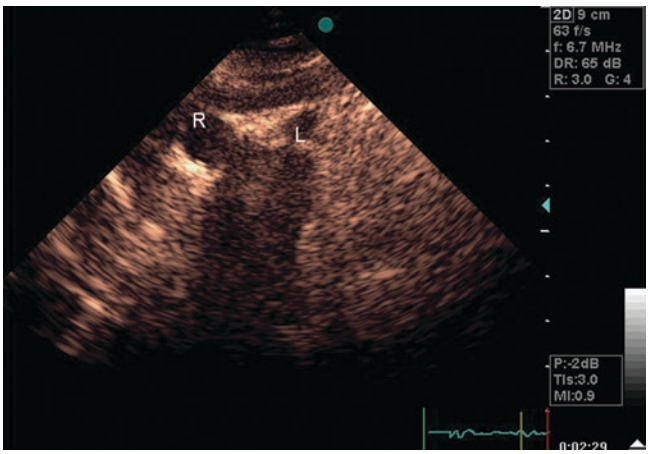

Fig. 34.2 Suprasternal short axis view showing double aortic arch, both patent (R & L), and dominant right arch (R)

pattern of brachiocephalic arteries in cases of atretic left arch, would be similar to mirror image right aortic arch (Fig. 34.2)

(e) Pulmonary artery sling, origination of LPA from RPA

6. Use color flow mapping (CFM) to evaluate the course of each artery. But remember when ligamentum arteriusum instead of ductus arterosus takes part in forming vascular ring, CFM can't show it, so obviously, other imaging modalities like Chest X-ray (CXR), barium swallow, MRI, or CTscan are necessary.
7. In suprasternal long axis view evaluate any narrowing of isthmus and around the origin of the left subclavian artery. A posterior shelf, protruding toward the ductus arteriosus is characteristic of discrete coarctation (COA) which is more common, but there may be a long segment narrowing. Evaluate post stenotic dilation and transvers arch hypoplasia as well. Use CFM and demonstrate flow turbulence at COA region (Fig. 34.3a, b).
8. Use CW Doppler examination and evaluate the high velocity jet which extends from systole to diastole in severe COA (Fig. 34.4).
9. Evaluate other finding in favor of COA; ventricular hypertrophy and or dysfunction, and reduced systolic pulsation of descending aorta.
10. In PW examination of abdominal aorta in subcostal view, evaluate the reduced velocity and diastolic continuation of flow signals. Also delay in time to peak velocity, decreased mean acceleration rate, and absence of early diastolic flow reversal could be evaluated.
11. Don't forget to find associated anomalies, most common are: PDA, BAV, VSD, and MV anomalies.
12. Assess for extreme form of COA, interrupted aortic arch (IAA) and its type:
    (a) Type A, the interruption between the left subclavian artery and descending aorta at the level of the isthmus (Fig. 34.5a, b).
    (b) Type B, the interruption between the left common carotid artery and the left subclavian artery (the most common)
    (c) Type C, interruption between the innominate artery and left carotid artery. (The least common)
13. Evaluate the discontinuity between the ascending and descending parts of the aortic arch in suprasternal views. You should be careful not to mistake the ductus arteriosus connecting the main pulmonary artery (MPA) to the descending aorta with true aortic arch.
14. Pay attention to find any associated lesion, like aortopulmonary window defect (AP window), conotruncal anomalies, and posterior malaligned VSD with LV outflow tract obstruction (LVOTO).

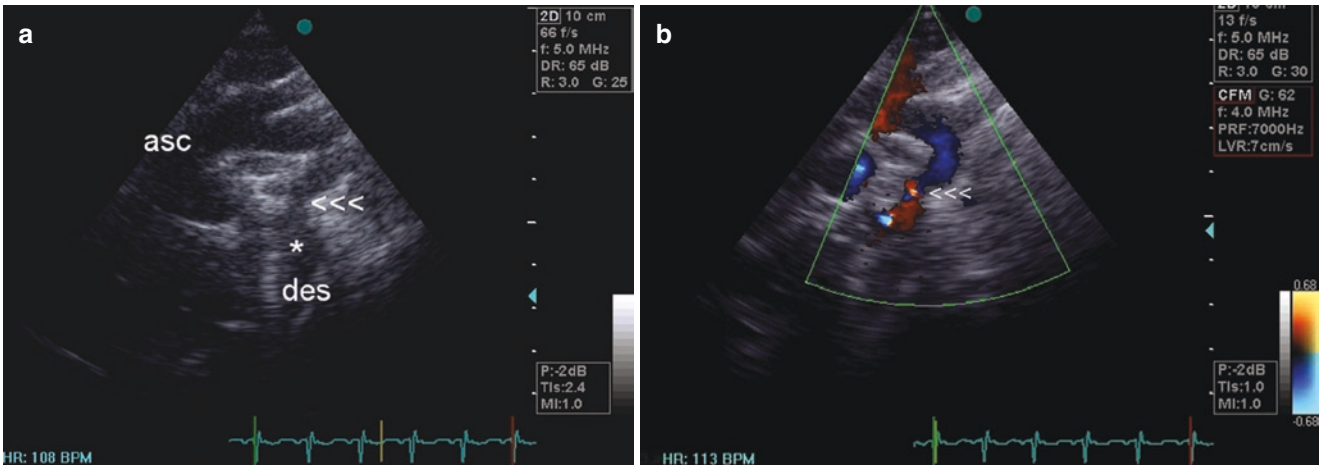

Fig. 34.3 (**a**, **b**) Suprasternal long axis view of a child with COA (arrow heads). Asterisk indicate post stenotic dilation. CFM in figure (**b**) shows turbulent flow in region of stenosis. *Asc* ascending aorta, *des* descending aorta

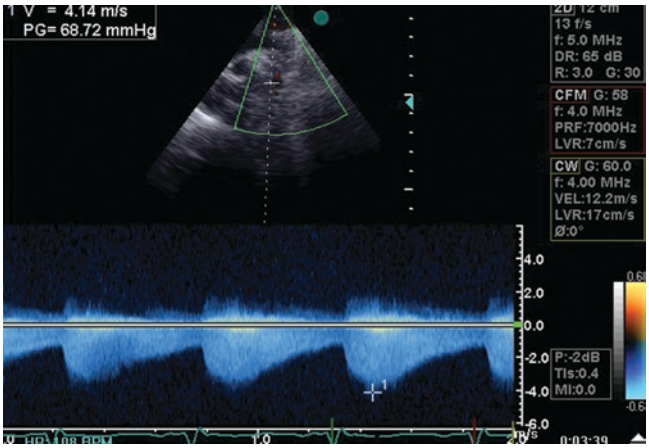

Fig. 34.4 CW Doppler recording across the coarctation showing diastolic extension of flow signals, so called saw tooth appearance, in a patient with severe COA

15. Demonstrate the so called "Y" sign in type B, the straight course of ascending aorta toward the neck giving rise the innominate and left common carotid. Also, in type B, the carotid artery takes a smooth superior course rather than posterior course which is seen in normal arches
16. Marked discrepancy between ventricles, and between great arteries should be noted.
17. Evaluate persistent fifth aortic arch in the, parasagittal suprasternal notch view. You may find two parallel vessels, the true arch, and the persistent fifth arch. In this anomaly in spite of double aortic arch both arches are on the same side of the trachea (Fig. 34.6).
18. Determine the cervical arch in suprasternal long-axis view; this arch extends farther onto the neck than a normal arch.
19. For prenatal detection of COA, don't forget that the parallel circulation and patency of ductus arteriosus during fetal life, make its diagnosis very difficult especially when it is discrete form and is not severe. Try to visualize any narrowing of aortic arch in sagittal view (Fig. 34.7) and pay attention to find indirect signs of possible COA in different views including; discrepancy in right ventricular size, BAV with thickened cusps, LVOT narrowing, VSD with posterior malalignment of conal septum, discrepancy in great artery sizes; larger PA, abnormal left axis deviation, and more distal origination of left subclavian artry from arch. Diagnosis of IAA in fetus is easier. In Sagittal view the interrupted arch you won't see the smooth curvature connecting ascending to descending aorta instead the ascending aorta has a straight course to its branches.
20. Use three vessel tracheal view to compare aortic and ductal arch sizes, also in cases of normal left sided aorta, both the aorta and pulmonary artery are in the left side of trachea making the so called "V" sign (Fig. 34.8a, b) while in right sided aortic arches "V" sing may be seen in right side of trachea or a "U" sign may be formed based on different types of right aortic arch (Fig. 34.9a, b)

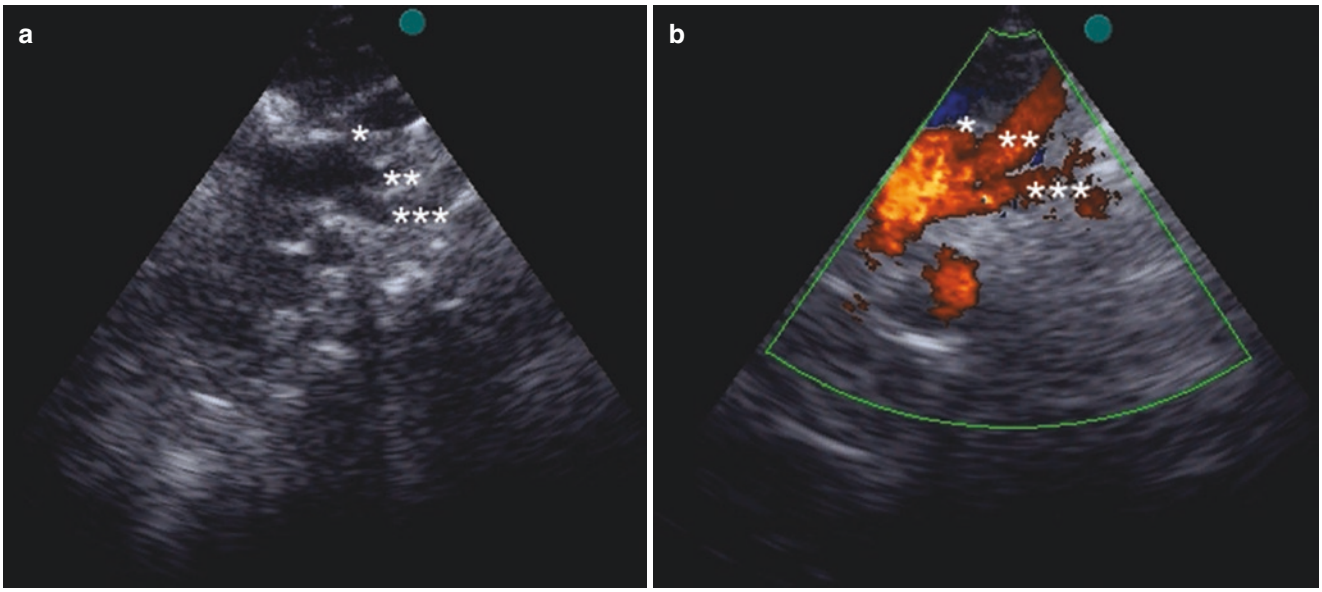

Fig. 34.5 (**a**, **b**) Suprasternal long axis showing IAA type A by two dimensional (figure **a**) and by adding color Doppler (figure **b**). (*brachiocephalic artery, **left common carotid, ***left subclavian artery) this infant also had AP window defect, not shown here

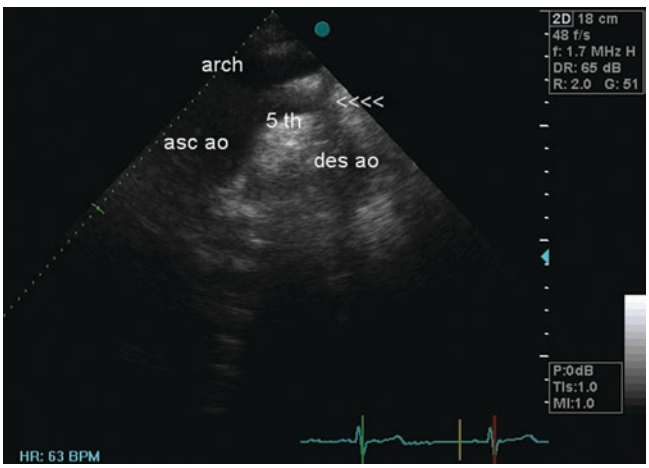

Fig. 34.6 Suprasternal long axis view of a patient suffering from persistent fifth arch and COA. It is a double-lumen aortic arch, both are patent. The superior arch (arch) giving rise to the head and neck vessels, and the inferior arch (fifth arch) extending from the ascending to the descending aorta. Arrow heads points to COA. *asc ao* ascending aorta, *des ao* desending aorta, *fifth* persistent fifth arch

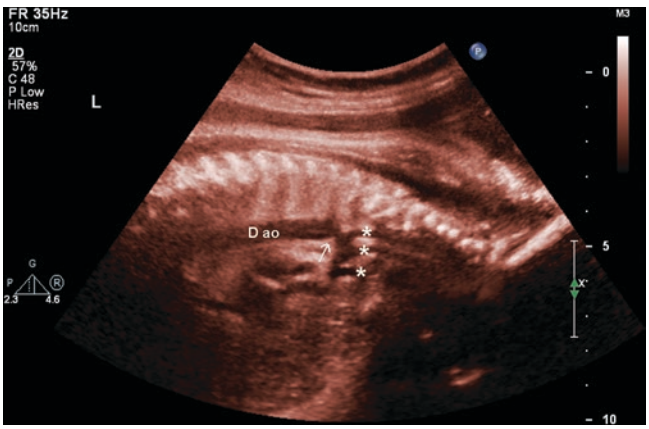

Fig. 34.7 Fetal echocardiography sagittal view of aortic arch. Arrow points to isthmus narrowing. Brachiocephalic arteries are indicated by asterisk. *D ao* descending aorta

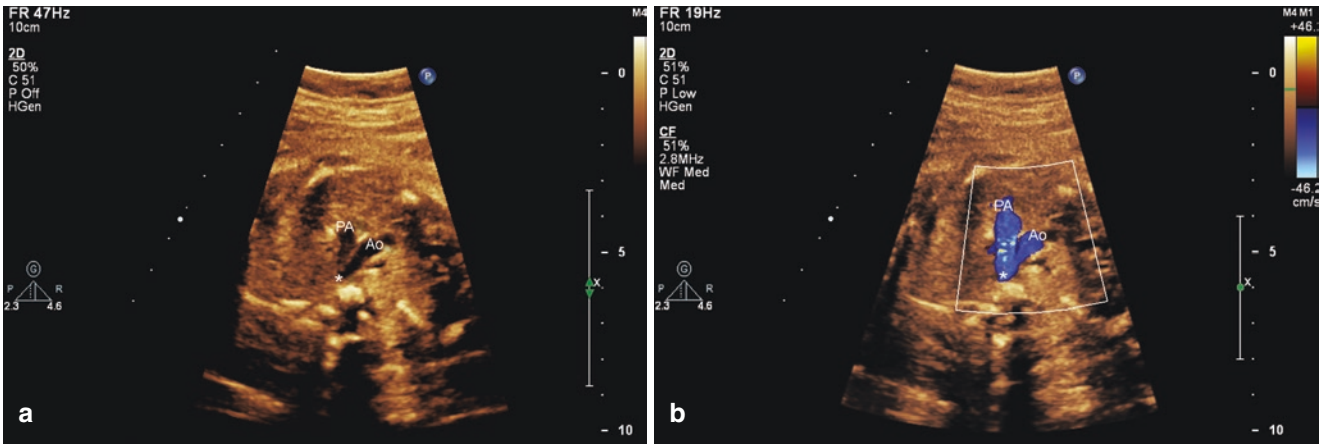

Fig. 34.8 (**a**, **b**) Fetal echocardiography showing normal three vessel view (2D and with CFM) both the aorta and pulmonary artery are in the left side of trachea making the so called "V" sign. Asterisk indicate the descending aorta. *PA* pulmonary artery, *AO* aorta

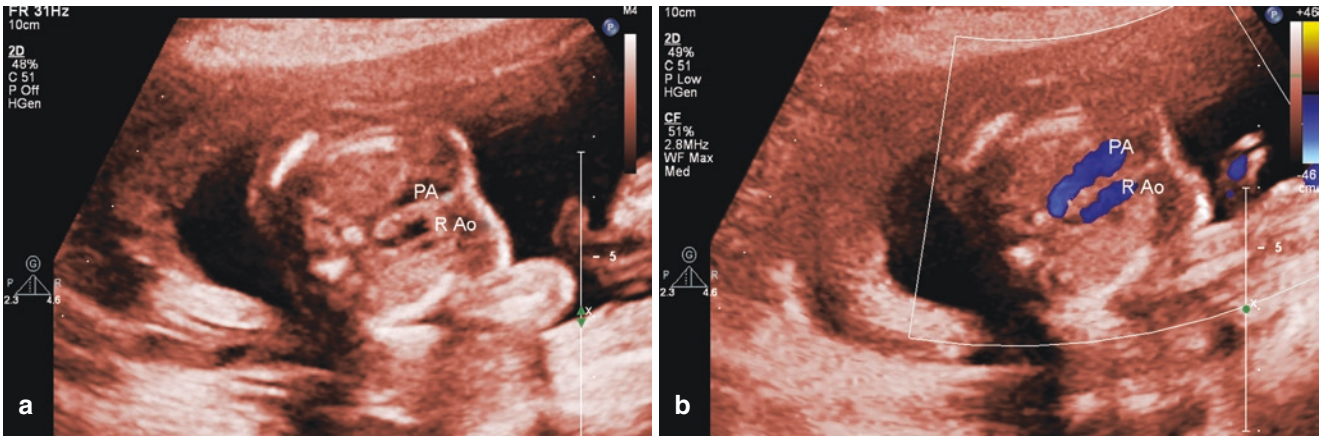

Fig. 34.9 (**a**, **b**) Fetal echocardiography at tracheal level (2D and with CFM) showing the "U" sign indicating right aortic arch. *R Ao* right aortic arch, *PA* pulmonary artery

Suggested Reading

Faistauer A, Torres FS, Carlo Sasso CS. Right aortic arch with aberrant left innominate artery arising from Kommerell's diverticulum. Radiol Bras. 2016;49(4):264–6.

Hanneman K, Newman B, Chan F. Congenital variants and anomalies of the aortic. Arch RG. 2017;37(1)

Humes RA, Farooki ZQ. Echocardiographic examination of the aortic arch: anomalies presenting in the neonatal period. Echocardiography. 1991;8:487–99.

Joseph A, Core J, Becerra JL, et al. Right-sided aorta with complete isolation of the left innominate artery. Radiol Case Rep. 2016;11(1):21–4.

Londono-Obregon C, Fogel M. Imaging of aortic arch anomalies and associated findings. Expert Rev Cardiovasc Ther. 2012;10(12):1497–516.

Mądry W, Zacharska-Kokot E, Karolczak MA. Methodology of echocardiographic analysis of morphological variations of the aortic arch and its branches in children—own experience. J Ultrason. 2019a;19(76):24–42.

Mądry W, Karolczak MA, Myszkowski M, et al. Non-invasive diagnosis of aortic arch anomalies in children—15 years of own experience. J Ultrason. 2019b;19(76):5–8.

Oztunc F, Atik SU, Dedeoglu R, et al. Aortic arch anomalies detected in foetal life by echocardiography. J Obstet Gynaecol. 2018;38(5):1–5.

Volpe P, Tuo G, De Robertis V, et al. Fetal interrupted aortic arch: 2D–4D echocardiography, associations and outcome. Ultrasound Obstet Gynecol. 2010;35:302–9.

Hypoplastic Left Heart Syndrome (HLHS)

35

Maryam Moradian

Abstract

Ductal dependency of the systemic circulation in Hypoplastic left heart syndrome (HLHS) leads to rapid deterioration of the affected neonate's hemodynamic condition soon after birth. HLHS can be diagnosed on fetal echocardiography and help to plan for delivery in an equipped hospital. Echocardiography in perinatal period can give a lot of anatomic and physiologic information and help the clinician to make the best therapeutic decision.

Hypoplastic Left Heart Syndrome (HLHS)

1. For complete anatomic diagnosis, use all echocardiographic standard windows to approach HLHS patients.
2. Remember that in HLHS, as its name implies, there is marked underdevelopment of the left-sided heart structures, including mitral valve, LV, aortic valve, and aortic arch. In the most extreme forms of HLHS, LV is poorly developed, small, muscle bound, with slit like cavity.
3. In apical four chamber view compare the size of left and right chambers as well as left and right atrioventricular valves. There may be severe hypoplasia or even atresia of both mitral and aortic valves (Fig. 35.1).
4. You may use this classification to describe the spectrum of your echocardiographic findings
   (a) Aortic atresia with mitral atresia (most extreme form of HLHS).
   (b) Aortic atresia with patent mitral valve.
   (c) Aortic valve stenosis with patent mitral valve.
5. Try to define MV morphology, leaflets' thickness, annulus size, and check for direct attachment of leaflets and papillary muscles without chorda in between. Use color flow mapping (CFM) to evaluate any flow via mitral valve.
6. Define if there is echo bright region on endocardial surface of LV, endocardial fibroelastosis (EFE). In apical and long axis views evaluate endocardial echodensity, presence of EFE confirm subendocardial ischemia due to elevated LV end diastolic pressure and LV out flow tract obstruction (LVOTO).
7. Assess RV size and function. RV could be severely enlarged, folding around the hypoplastic left ventricle, and occupying the apex of the heart. Evaluate tricuspid regurgitation, and its pressure gradient. In cases of large LV mass, RV inflow maybe distorted, resulting in some degrees of TV dysplasia or there maybe TV annular dilation due to RV volume overload.
8. In parasternal long axis view, like apical four chamber view, you can immediately identify the small size LV and EFE. Small size MV and aortic valve can also be identified in this view. Aortic valve may be severely dys-

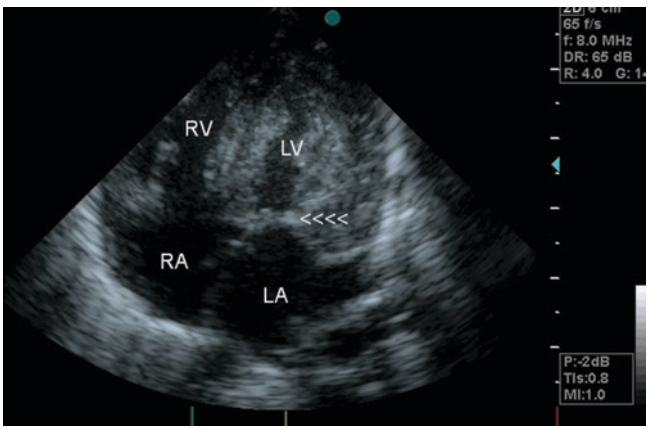

Fig. 35.1 Transthoracic apical four chamber view in diastole showing diminutive MV (arrow heads), small LV cavity, and LV hypertrophy. *LV* left ventricle, *RV* right ventricle, *LA* left atrium, *RA* right atrium

M. Moradian (✉)
Pediatric Cardiology, Rajaie Cardiovascular, Medical & Research Center, Iran University of Medical Sciences, Tehran, Iran

M. Moradian, A. Alizadehasl (eds.), *Atlas of Echocardiography in Pediatrics and Congenital Heart Diseases*,
https://doi.org/10.1007/978-3-662-62341-1_35

plastic with thickened leaflets or even it can be atretic. For neonates it is advised to do some measurements in this view to clarify if the diagnosis is HLHS rather than critical AS. In HLHS, LV end diastolic cross-sectional area is less than 1.5 cm^2 were as in critical AS it is equal or more than 1.7 cm^2. In neonates with HLHS LV end-diastolic inflow dimension (measured from the hinge point of the posterior mitral leaflet to the apex) is expected to be equal or less than 25 mm, and mitral annulus diameter would be equal or less than 6 mm (Fig. 35.2).

9. Measure the ascending aorta diameter in parasternal long axis view (PLAX). If it is less than 5 mm, consider hypo plastic ascending aorta.

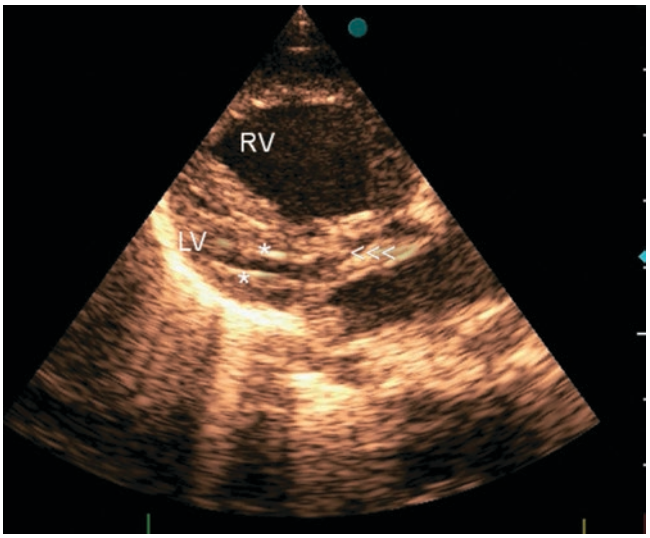

Fig. 35.2 Parasternal long axis view showing slit like LV cavity, small aortic annulus. Aortic cusps are thickened (arrow heads). EFE is depicted by asterisks. *LV* left ventricle, *RV* right ventricle, *LA* left atrium, *RA* right atrium

10. Evaluate interventricular septum for defect, though in most cases there is ventricular defect, especially when aortic valve is atretic.
11. By using color Doppler interrogation of the ventricular septum you may find tortuous epicardial coronaries, coronary cameral fistulas, with Bidirectional flow. The prognostic importance of these fistulas in HLHS is not clear yet.
12. In short axis view you should assess LV size and function as well as MV anatomy, and its papillary muscles. Aortic valve, pulmonary valve, main pulmonary artery, and its branches should be checked for size and function in this view. Evaluate the origin and position of coronary arteries in this view (Fig. 35.3).
13. By scanning more superiorly (high parasternal short axis view), you may find an inferior arch but without any brachiocephalic branching, in fact it is ductal arch, consisting of the larger main pulmonary artery (MPA), patent ductus arteriosus, and descending aorta. In these cases, ductus arteriosus plays the role of a conduit, providing blood from RV to descending aorta known as ductal-dependent systemic circulation (Fig. 35.4).
14. Evaluate interatrial septum for any defect especially in subcostal views, these defects are often very small or may be absent. LA may be large if there is no ASD or the defect is very small
15. Define the ascending aorta and aortic arch in suprasternal long axis view. Ascending aorta may be severely small, like an extension of coronary arteries, and servers for retrograde filling of them (Fig. 35.5).
16. Use CFM to evaluate any retrograde filling of aortic arch, its branches, and coronary arteries from ductus arteriosus. Beyond the left subclavian artery aortic arch widens and a shelf like lesion (coarctation) is usually

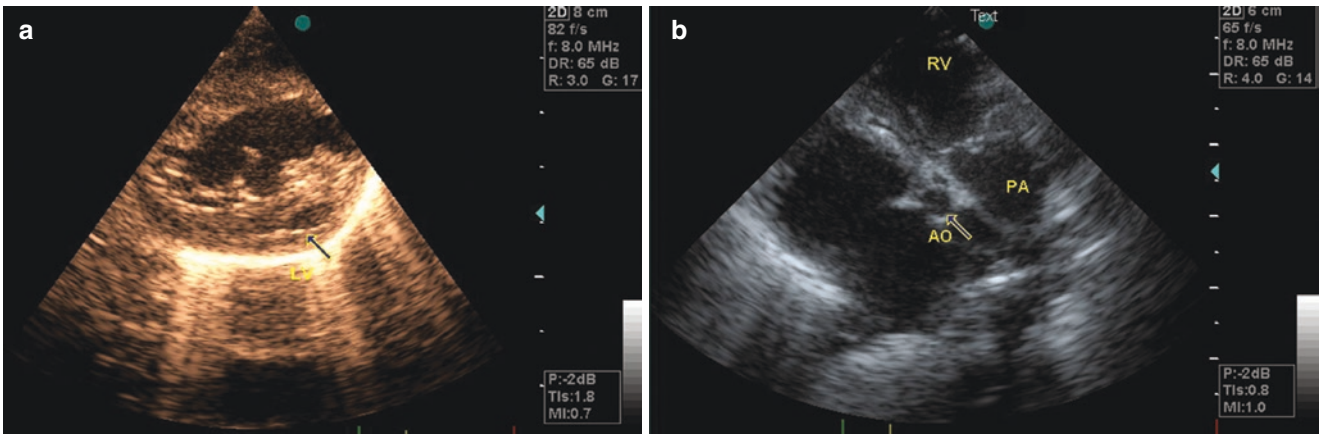

Fig. 35.3 (**a**) Parasternal short axis view at mid ventricular level showing small LV cavity and severely enlarged and hypertrophied RV. (**b**) Parasternal short axis view at base of the heart showing very small aorta (arrow) Compare the size of PA with aorta. *RV* right ventricle, *Ao* aorta, *PA* pulmonary artery

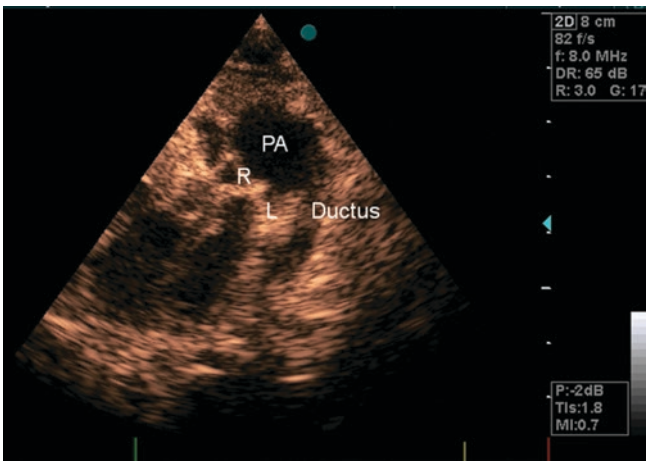

Fig. 35.4 High parasternal view showing dilated pulmonary artery, and Ductus arteriosus forming ductal arch. *R* RPA, *L* LPA, *PA* pulmonary artery

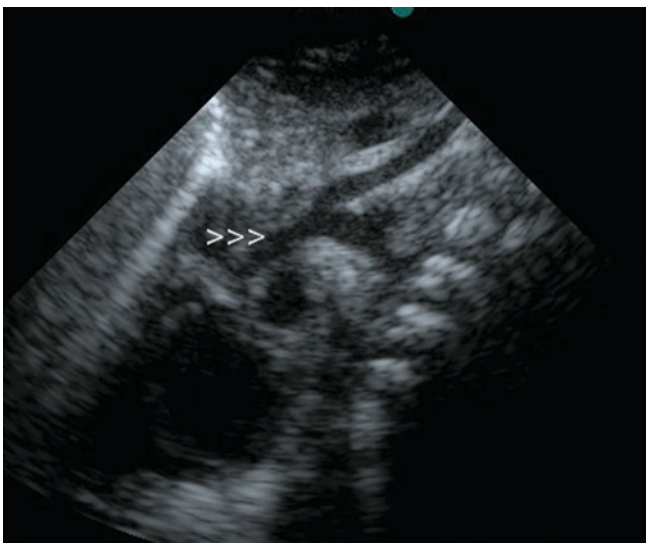

Fig. 35.5 Suprastenal long axis view showing small hypoplastic ascending aorta (arrow heads)

present though its assessment would be difficult because of dilated ductus arteriosus (Fig. 35.6).

17. By reducing the scale of CFM check for venous flow away from heart toward the transducer to rule out any abnormal pulmonary venous drainage or the presence of levoatriocardinal vein.
18. Fetal echocardiography will show abnormal four chamber view, small, and hyper echoic LV. RV is, apex forming and enlarged (Fig. 35.7). Retrograde flow toward arch and ascending aorta can be evaluated by using CFM (Fig. 35.8). In three vessel tracheal view aortic arch is very small or may not be visible (Fig. 35.9)

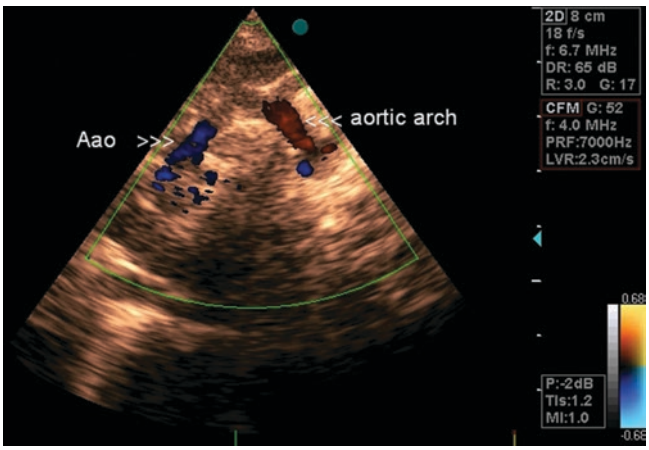

Fig. 35.6 In this suprasternal long axis view, the retrograde flow is toward arch (shown in red) and ascending aorta (shown in blue). *Aao* ascending aorta

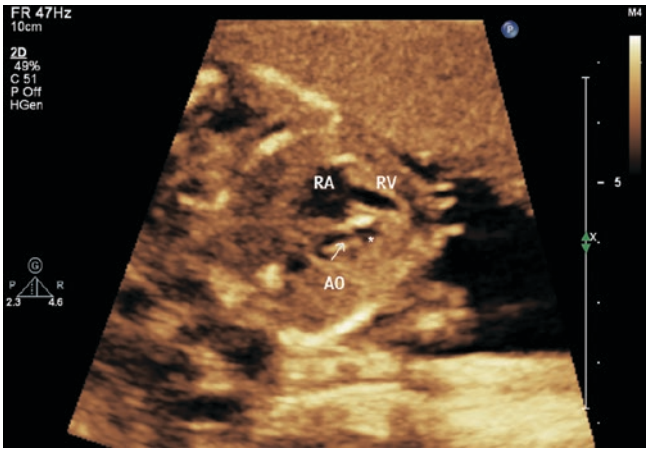

Fig. 35.7 Tn this fetal echocardiogram small, hyper echoic LV is indicated by asterisk and arrow points to small diminutive aorta. RV is enlarged and apex occupying. *RV* right ventricle, *RA* right atrium, *Ao* aorta

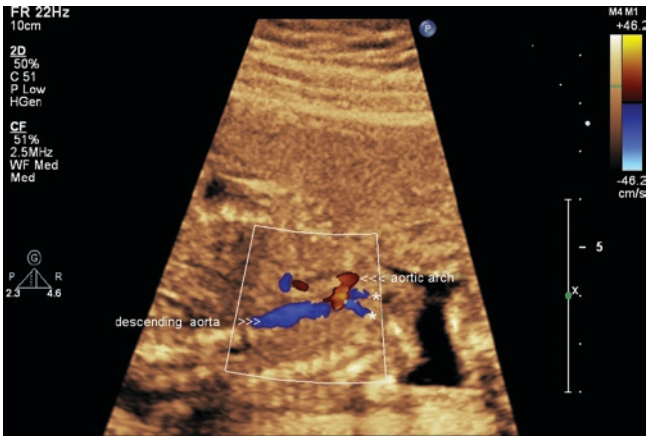

Fig. 35.8 Fetal echocardiogram para sagittal view showing retrograde flow toward aortic arch (shown in red). Ascending aorta is so small that hardly can be seen. Asterisks indicate brachiocephalic arteries

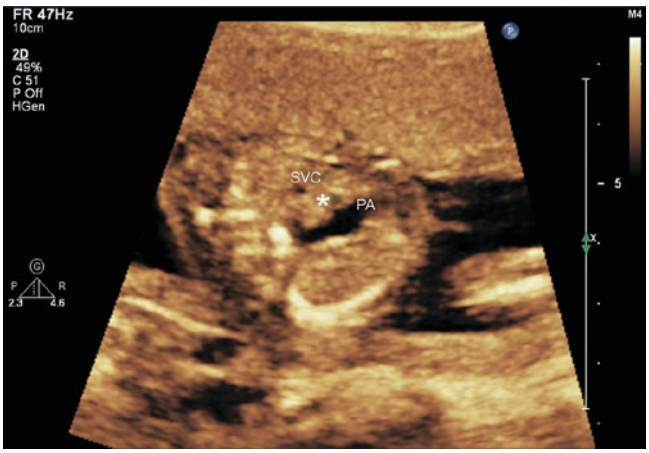

Fig. 35.9 Fetal echocardiogram. In this case of HLHS, three vessel tracheal view, aortic arch cannot be seen (asterisk)

Suggested Reading

Feinstein JA, Benson DW, Dubin AM, et al. Hypoplastic left heart syndrome current considerations and expectations. JACC. 2012;59 Suppl. 1)

Frommelt MA. Challenges and controversies in fetal diagnosis and treatment. hypoplastic left heart syndrome. Clin Perinatol. 2014;41(4):787–98.

Jacobs M. Aortic reconstruction in hypoplastic left heart syndrome—a reappraisal. J Thorac Cardiovasc Surg. 2003;125(Suppl. 3:S82–4.

Nguyen T, Miller M, Gonzalez J, et al. Echocardiography of hypoplastic left heart syndrome. Cardiol Young. 2011;21(Suppl. 2):28–37.

Phoon CKL, Silverman NH. Conditions with right ventricular pressure and volume overload, and a small left ventricle: "hypoplastic" left ventricle or simply a squashed ventricle? J Am Coll Cardiol. 1997;30:1547–53.

Son JS, James A, Steve Fan C, et al. Prognostic value of serial echocardiography in hypoplastic left heart syndrome. Circulation: Cardiovasc Imaging. 2018;11(7)

Wisler J, Khoury PR, Kimball TR. The effect of left ventricular size on right ventricular hemodynamics in pediatric survivors with hypoplastic left heart syndrome. J Am Soc Echocardiogr. 2008;21(5):464–9.

Kawasaki Disease (KD)

36

Maryam Moradian

Abstract

Kawasaki disease (KD) is an acute, self-limited vasculitis of childhood. It can result in coronary artery aneurysms in 25% of patients, especially if the diagnosis is missed. Echocardiography is the imaging modality of choice for diagnosis of coronary artery involvement and evaluation of myocardial function. Serial echocardiography is necessary in order to detect thromboses in aneurysms especially in patients with giant aneurysm.

Kawasaki Disease (KD)

1. Evaluate left main coronary artery (LMCA), left anterior descending (LAD), and Left circumflex (LCX) in multiple imaging planes. Start with parasternal short axis view to see the origin of both LMCA and RCA. Then with slight rotating and tilting of transducer follow the LAD and LCX length from bifurcation. Assess the distal LAD in parasternal long axis and subcostal coronal views and follow the LCX length in atrioventricular groove in apical four chamber view.
2. Follow RCA course in parasternal long axis and also in apical and subcostal sagittal and coronal views.
3. Evaluate the internal dimension of coronary arteries from the inner edge to inner edge of the vessel wall and do not measure at the level of its normal branching. Evaluate Z scores of LAD, RCA, and LMCA. Remember that most frequently coronary artery aneurysms develop in the LMCA and proximal segments of the LAD and the RCA (Fig. 36.1a, b).
4. Assess any ectasia, the internal diameter of coronary arteries should be less than 3 mm in children younger than 5 years old and less than 4 mm thereafter, otherwise it is considered coronary ectasia
5. Appreciate perivascular brightness, lack of normal tapering, segmental dilation, or narrowing of coronary arteries. If the internal diameter of a segment is 1.5 times that of the adjacent segment it is abnormal
6. Appreciate any mitral, tricuspid and aortic valve regurgitation
7. Pay attention to any LV or RV systolic and diastolic dysfunction and regional wall motion abnormality.
8. Evaluate even minimal pericardial effusion.
9. Number, size (small <5 mm, medium 5–8 mm, or giant >8 mm in internal diameter), location, and shape (fusiform or saccular) of every aneurysm should be described.

M. Moradian (✉)
Pediatric Cardiology, Rajaie Cardiovascular, Medical & Research Center, Iran University of Medical Sciences, Tehran, Iran

M. Moradian, A. Alizadehasl (eds.), *Atlas of Echocardiography in Pediatrics and Congenital Heart Diseases*,
https://doi.org/10.1007/978-3-662-62341-1_36

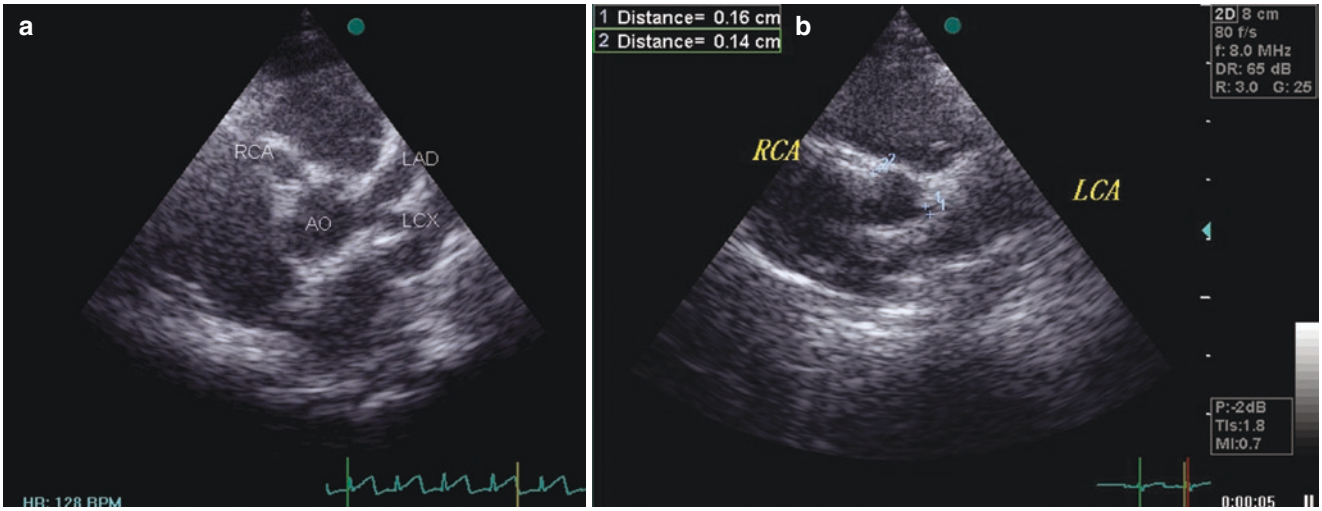

Fig. 36.1 (**a**) In this TTE the parasternal short axis window is used to show LCX ectasia and fusiform aneurysm formation in RCA, and LAD in a young infant suffering from Kawasaki disease. (**b**) The same view in a normal infant. *RCA* right coronary artery, *LCA* left coronary artery, *LAD* left anterior descending, *LCX* Left circumflex, *AO* aorta

Suggested Reading

Chbeir D, Gaschignard J, Bonnefoy R, et al. Kawasaki disease: abnormal initial echocardiogram is associated with resistance to IV Ig and development of coronary artery lesions. Pediatr Rheumatol. 2018;16:48.

Friedman KG, Gauvreau K, Hamaoka-Okamoto A, et al. Coronary artery aneurysms in Kawasaki disease: risk factors for progressive disease and adverse cardiac events in the US Population. J Am Heart Assoc. 2016;5:e003289.

McCrindle BW, Cifra B. The role of echocardiography in Kawasaki disease. Int J Rheumatic Dis. 2018;21(1):50–5.

McCrindle BW, Li JS, Minich L, et al. Coronary artery involvement in children with Kawasaki disease risk factors from analysis of serial normalized measurements. Circulation. 2007;116:174–9.

McCrindle BW, Rowley A, Newburge JW, et al. Diagnosis, treatment, and long-term management of Kawasaki disease a scientific statement for health professionals from the American Heart Association. Circulation. 2017;135:e927–99.

Suzuki A, Tizard EJ, Gooch V, et al. Kawasaki disease: echocardiographic features in 91 cases presenting in the United Kingdom. Arch Dis Child. 1990;65(10):1142–6.

Cardiomyopathies

37

Azin Alizadehasl, Majid Maleki, Feridoun Noohi,
Mohammad Mehdi Peighambari, and Maryam Moradian

Abstract

Echocardiography has an important role not only in diagnosis but also in follow-up of patients with cardiomyopathy. Traditional and novel echocardiographic modalities help to confirm the diagnosis and take the best management strategy.

Cardiomyopathies

Cardiomyopathy, the primary disease of the myocardium, are commonly categorized into three physiologic types, Dilated, Hypertrophic, and Restrictive. Cardiomyopathies encompass cardiac muscle disorders without any correctable anatomic and/or hemodynamic disorder. Dilated and hypertrophic cardiomyopathies are more common than restrictive cardiomyopathy among children.

Dilated Cardiomyopathy (DCM)

1. In patients with heart failure you have to evaluate left ventricular ejection fraction (LVEF), LV structure, and presence of any other abnormality as a reason for cardiac failure.
2. Start with evaluation of LV size and function in four chamber view. The hallmarks of DCM, marked LV dilation with global hypokinesia can easily be assessed in this view. Also, LV shape would be more spherical than elliptical.
3. Compare systolic and diastolic frames. Low stroke volume can be assessed by showing little change in LV size during cardiac cycle (Fig. 37.1).
4. Measure end systolic and end diastolic volumes and ejection fraction (EF) using paired orthogonal apical views, four and two chamber views, by modified Sampson's method. Single plane method may also be used but is not as precise as biplane method. LVEF less than 40% is considered heart failure (Fig. 37.2a, b)
5. In parasternal long axis view measure Left ventricular end diastolic diameter (LVEDD). LVEDD more than 2 z-scores is indicative of heart failure
6. Use M mode echo and evaluate LV dimensions, fractional shortening (FS), and E-point septal separation (EPSS). FS less than 25% and EPSS more than 6 mm are pathologic (Fig. 37.3)
7. M mode evaluation of aortic valve, will show reduced aortic root motion, rounded opening, and early closure of aortic valve (Fig. 37.4).
8. Use color flow mapping (CFM) to find the functional mitral valve (MV) regurgitation, in DCM, MV is anatomically normal but increased LVEDD leads to mitral annular dilation which causes malcoaptation of leaflets, resulting in mitral regurgitation (MR). MR intensity will increase by elevated left ventricular end diastolic pressure (LVEDP) (Fig. 37.5).
9. Estimate the rate of LV pressure change during the isovolumic contraction period (dp/dt) using CW Doppler signals of MR. dp/dt, is an index of LV systolic function. Normal value is greater than 1200 mmHg/s (Fig. 37.6).
10. Evaluate global ventricular function using myocardial performance index (MPI). Calculate MPI as the sum of isovolumic contraction time (IVCT) and isovolumic

A. Alizadehasl
Department of Cardio-Oncology and Research Center, Rajaie Cardiovascular, Medical & Research Center, Iran University of Medical Sciences, Tehran, Iran

M. Maleki · F. Noohi
Cardiovascular Intervention Research Center, Rajaie Cardiovascular, Medical & Research Center, Iran University of Medical Sciences, Tehran, Iran

M. M. Peighambari
Interventional Cardiologist, Cardiovascular Intervention Research Center, Rajaie Cardiovascular, Medical & Research Center, Iran University of Medical Sciences, Tehran, Iran

M. Moradian (✉)
Pediatric Cardiology, Rajaie Cardiovascular, Medical & Research Center, Iran University of Medical Sciences, Tehran, Iran

M. Moradian, A. Alizadehasl (eds.), *Atlas of Echocardiography in Pediatrics and Congenital Heart Diseases*,
https://doi.org/10.1007/978-3-662-62341-1_37

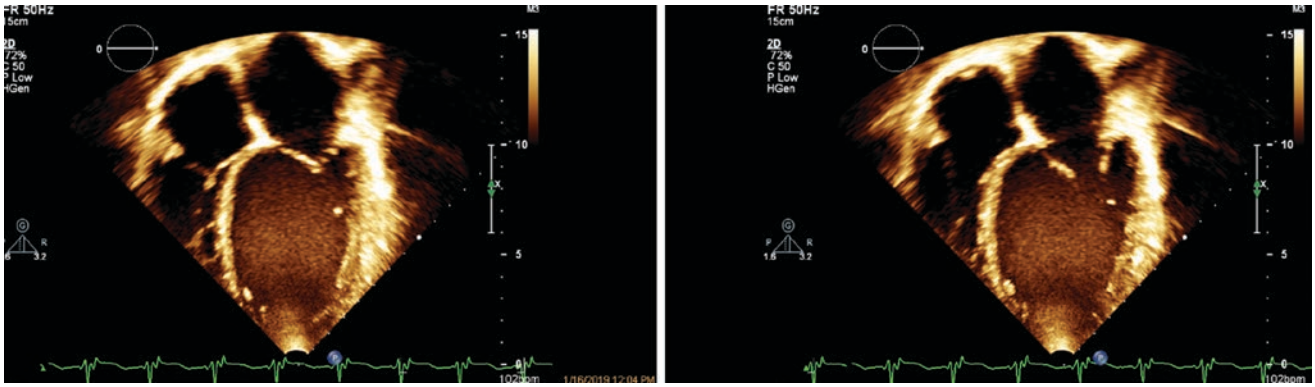

Fig. 37.1 TTE, Apical four-chamber view of an adolescent suffering from DCM, showing little change in LV size during cardiac cycle. Systolic frame, left; diastolic frame, right

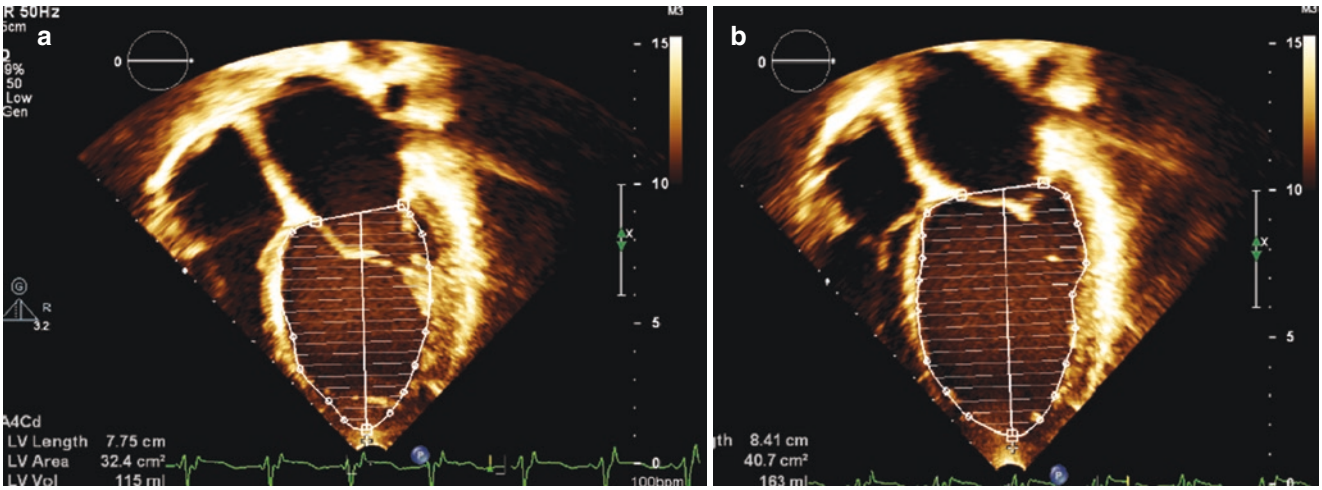

Fig. 37.2 (**a**, **b**) Showing single plane measuring LV volumes and EF by Simpson method in apical four chamber view in diastole (**a**) and in systole (**b**) in DCM

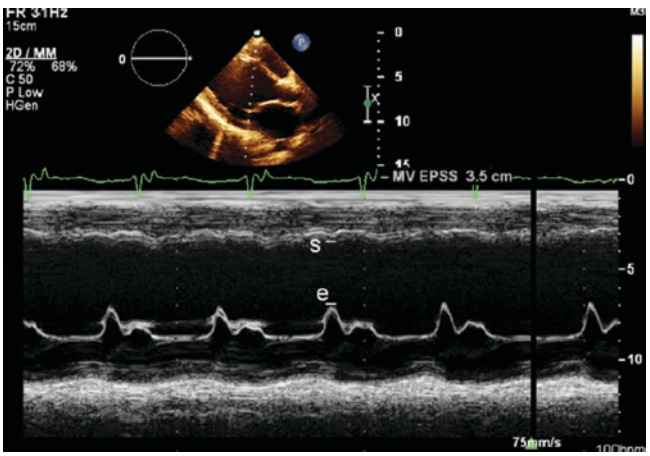

Fig. 37.3 M mode tracing of mitral valve demonstrating increased EPSS (35 mm) and reduced LVFS in this child with DCM

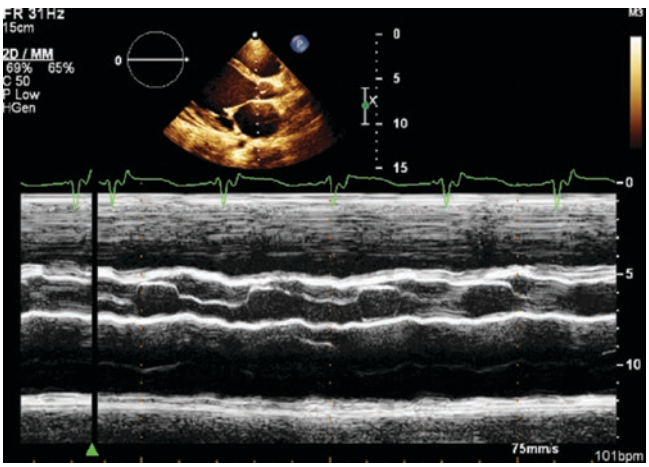

Fig. 37.4 M mode tracing of aortic valve demonstrating rounded aortic valve opening, reduced root motion and early closure of aortic valve in this child with DCM

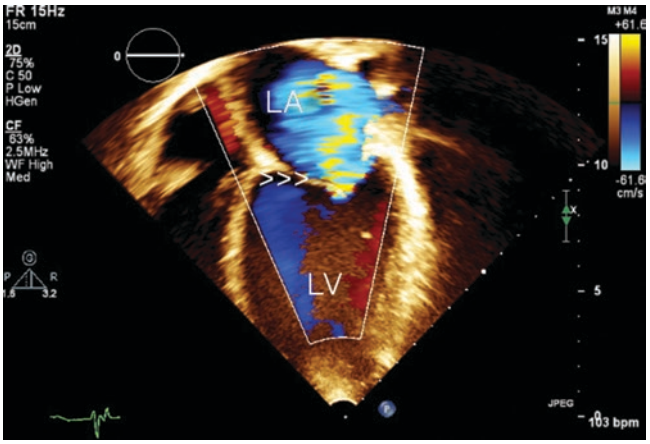

Fig. 37.5 TTE apical four chamber view, demonstrating severe MR in DCM. Arrow heads indicate the origin of MR jet from coaptation point. *LA* left atrium, *LV* left ventricle

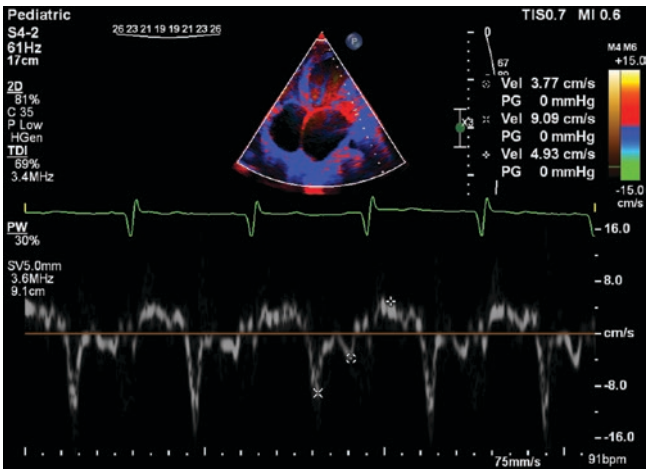

Fig. 37.7 Tissue Doppler imaging of Lateral mitral annulus of an adolescent with DCM showing reduced S′, E' and A'

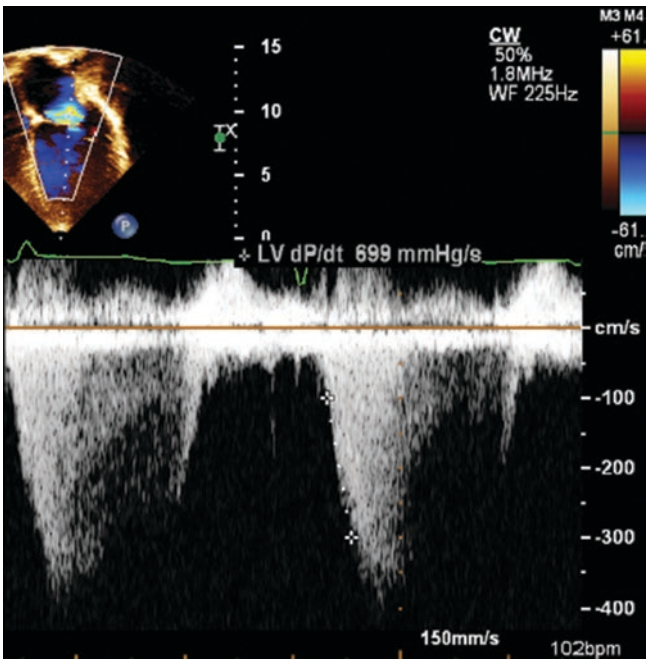

Fig. 37.6 Evaluation of dp/dt in an adolescent with DCM showing significantly reduced LV contractility dp/dt = 699 mmHg/s

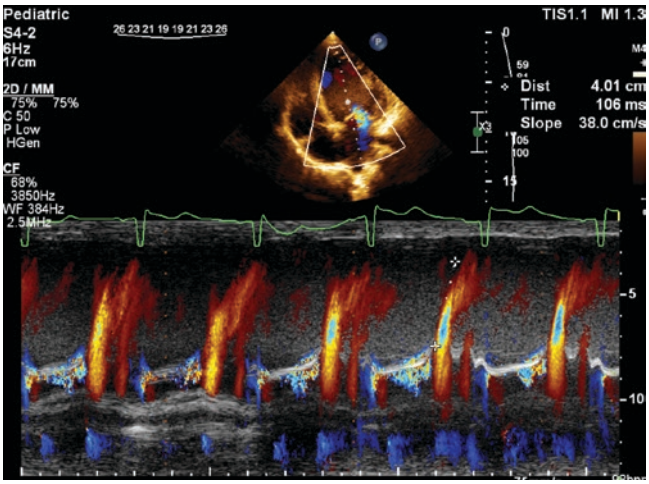

Fig. 37.8 Propagation velocity (VP)evaluation of a child with DCM, showing reduced VP (VP = 38 cm/s)

relaxation time (IVRT) divided by ejection time (ET). Normal value of LV MPI in children is 0.35 ± 0.03. The higher the index, the worse the systolic & diastolic dysfunction. A simple way to measure MPI is to locate the sample volume at the tips of the mitral valve in four chamber view and measure the time interval between the end and the start of transmitral flow which is "a" and then locate the sample volume in LVOT and measure the LV ejection time which is "b" in this equation:

MPI = (a – b)/b

11. Use transmitral inflow Doppler, pulmonary venous flow Doppler, and tissue Doppler imaging (TDI) of mitral annulus to simply stage diastolic dysfunction (Fig. 37.7). Based on E/A ratio, E/E' and atrial reversal flow in pulmonary veins diastolic dysfunction is categorized as:
    (a) Impaired relaxation or grade 1 diastolic dysfunction: A > E E/E' < 8 normal atrial reversal flow in pulmonary veins
    (b) Pseudo normal or grade 2 diastolic dysfunction: E > A E/E' 8–15 increased atrial reversal flow velocity and duration in pulmonary veins
    (c) Restrictive pattern or grade 3 diastolic dysfunction: E > A (~3:1) E/E' > 15 increased atrial reversal flow velocity and duration in pulmonary veins
12. Measure mitral inflow propagation velocity using combined M mode and CFM from LV apex. VP > 50 cm/s is normal. In delayed LV filling; the slop of color M mode signals is reduced (Fig. 37.8).

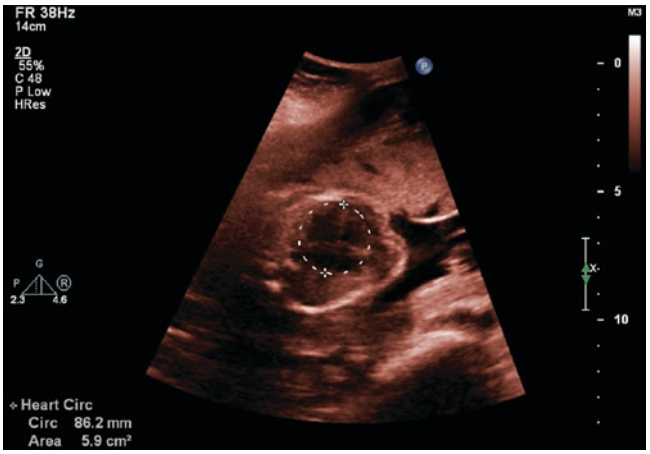

Fig. 37.9 Fetal echo cardiogram four chamber view for evaluation the cardiac size. In this case of fetal CMP, the heart occupies more than one third of the chest area, indicating cardiac enlargement

13. Dilated cardiomyopathy is the most common form of cardiomyopathies during intrauterine life. Evaluate the cardiac width and cardiothoracic ratio in four chamber view (Fig. 37.9). Use M mode and assess the fractional shortening. Evaluate the fetus for the signs of hydrops (pericardial, and plural effusion, ascites, and skin edema) (Fig. 37.10a, b).
14. By adding CFM evaluate atrioventricular valves regurgitation (Fig. 37.11a, b). Pulsed Doppler is also very useful in evaluation of fetal cardiac function.
15. Ductus venosus Doppler interrogation shows the characteristic triphasic forward flow during entire cardiac cycle in the normal condition (Fig. 37.12). In cases with reduced cardiac function ductus venosus shows end-diastolic flow reversal (Fig. 37.13).

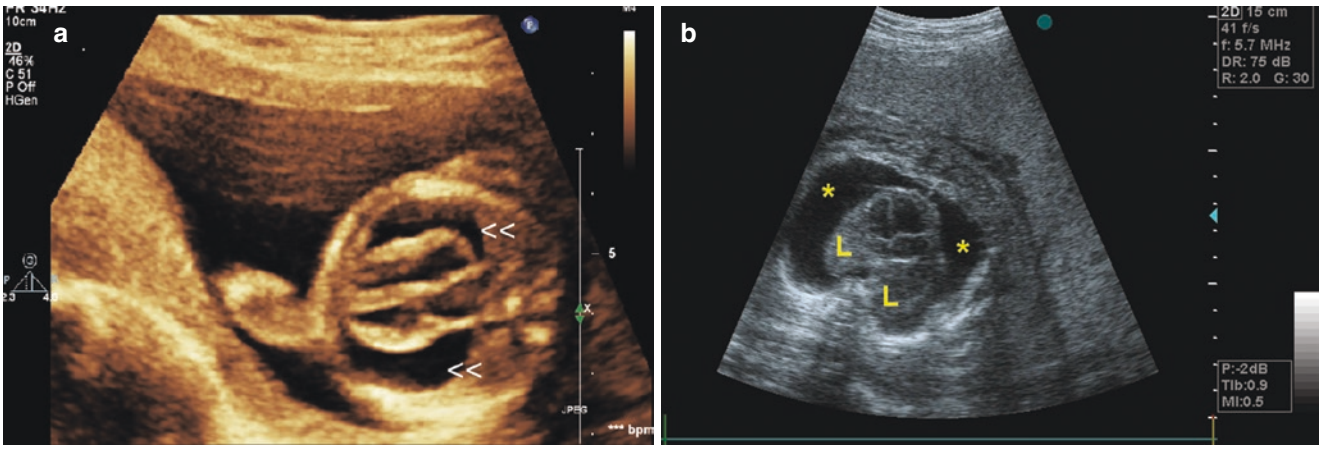

Fig. 37.10 (**a**, **b**) Fetal echo cardiogram four chamber view showing pericardial effusion (arrow heads in **a**) and another fetus with plural effusion (asterisks in **b**). *L* Lung

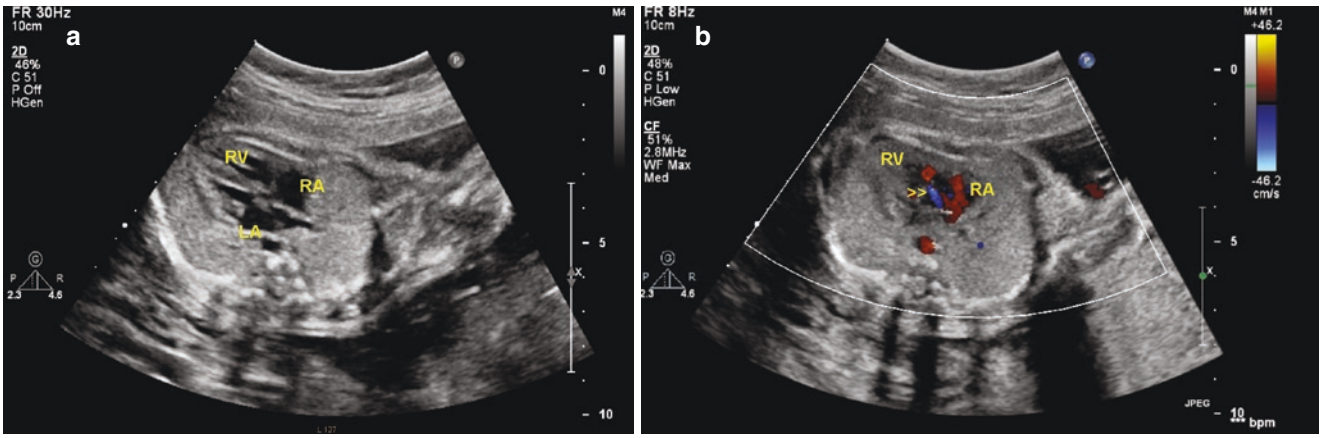

Fig. 37.11 (**a**, **b**) Fetal echocardiogram showing increased cardiothoracic ratio (**a**). Adding CFM confirm tricuspid regurgitation (arrow heads) in this fetus with cardiomyopathy (**b**). *RV* right ventricle, *LA* left atrium, *RA* right atrium

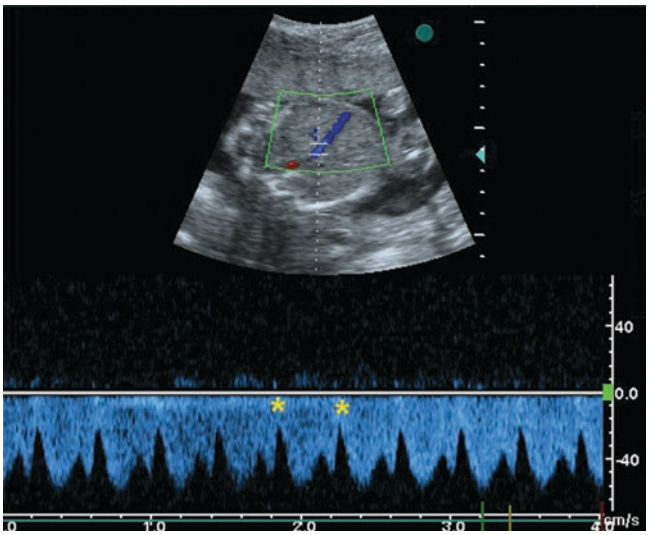

Fig. 37.12 Doppler evaluation of ductus venosus in a normal fetus, showing triphasic flow forward during entire cardiac cycle. Asterisks indicate atrial systolic waves

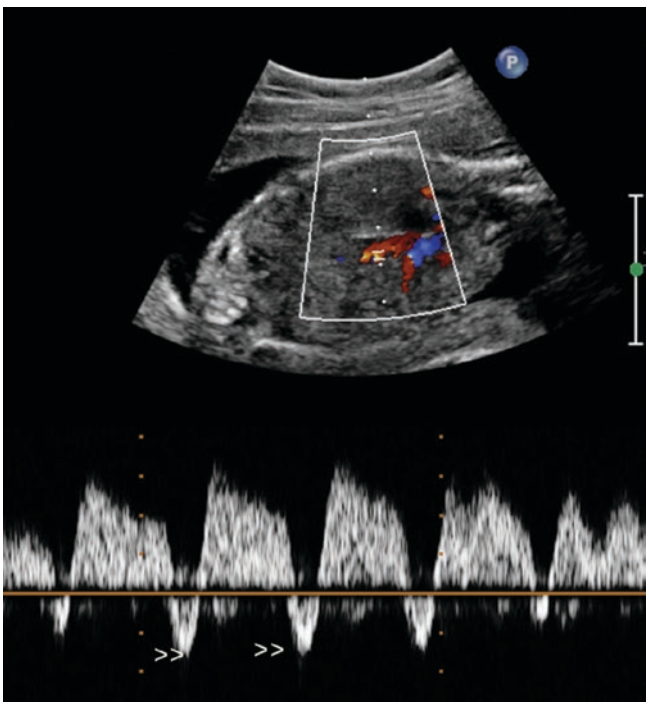

Fig. 37.13 End-diastolic flow reversal in ductus venosus is indicated by arrow heads in this Doppler evaluation of ductus venosus of a fetus with reduced cardiac function

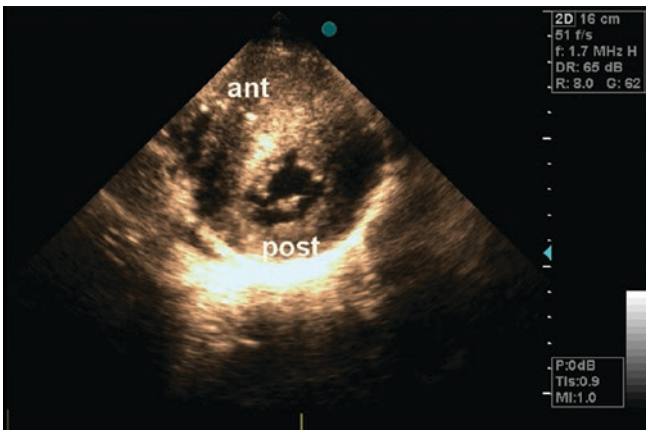

Fig. 37.14 Transthoracic parasternal short axis view showing severe septal hypertrophy and sparing posterior LV wall in a child with HCM. *Ant* anterior septum, *post* posterior LV wall

Hypertrophic Cardiomyopathy (HCM)

1. Thickened and hypertrophic left ventricle without aortic stenosis, coarctation of aorta, hypertension, athlete's heart, or any other disease capable of producing cardiac hypertrophy should raise the suspicion of hypertrophic cardiomyopathy. More commonly, hypertrophy involves basal LV segments of interventricular septum, but may extends into the lateral LV wall, and LV apex (Fig. 37.14)
2. In two-dimensional echo (2D) evaluate the pattern of hypertrophy. Most commonly the hypertrophy is asymmetric and easily recognizable in parasternal long axis view. Measure septal thickness in diastolic frame. Be careful not to include right ventricular papillary muscles thickness in this measurement. Septal thickness $\geq$ 15 mm and interventricular septum/posterior wall ratio $\geq$ 1.3 (Asymmetric septal hypertrophy, ASH) have been traditionally considered as diagnostic criteria for HCM. Risk of sudden cardiac death increases if the septal thickness is more than 30 mm or z-score is more than 6.
3. In parasternal long axis view you can also define the length between the aortic valve annulus and the point at which ventricular septal thickness decreases, beyond the basal hypertrophied region. This measurement as well as the depth of septal wall thickness, provide a good insight for optimal muscular resection during surgical relief of left ventricular outflow obstruction.
4. As any region of left ventricle (LV) may be involved in hypertrophic cardiomyopathy, wall thickness should be measured at end diastole at different levels in parasternal short axis view, including apical, papillary muscle, and basal levels
5. Determine the LV outflow tract obstruction using CFM and stepwise pulsed Doppler interrogation from LV cavity to LVOT. A characteristic signal has dagger-shaped appearance (late-peaking at systole), and originates from subaortic region. The degree of obstruction changes with loading condition of the patient (Fig. 37.15)
6. Evaluate the mitral valve by 2D and all Doppler modalities carefully. Anatomically MV leaflets are large and due to its anterior leaflet motion in systole (SAM), mitral regurgitation results (Fig. 37.16)

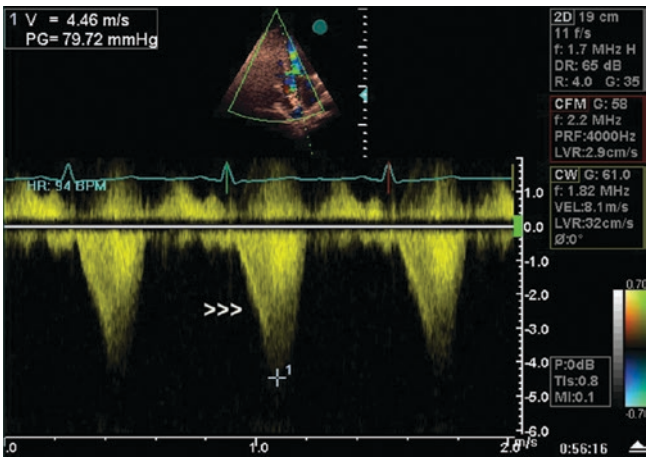

Fig. 37.15 Doppler profile showing dagger-shaped appearance (arrow heads), originating from sub aortic region in a child with HCM

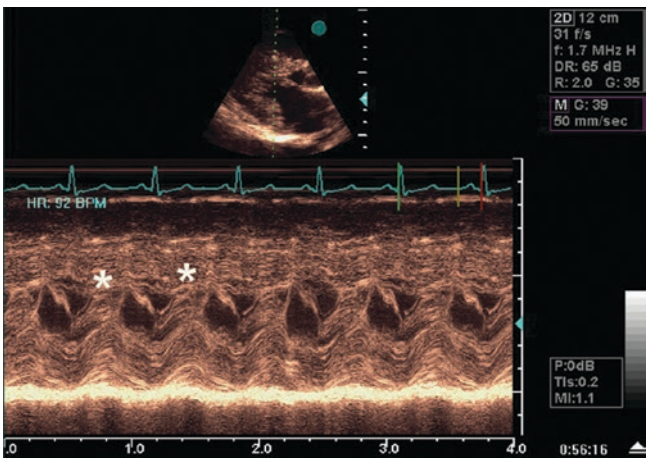

Fig. 37.16 Anterior mitral valve leaflet motion in systole (SAM) causing mitral-septal contact is indicated by asterisk in this child with HCM

7. Sometimes it's difficult to separate the two systolic jets, MR and subvalvar dynamic AS jets (Fig. 37.17). In these cases, measure the MR jet velocity and pressure gradient and add the amount to the estimated LA pressure, this would be the LV systolic pressure. Then by subtracting the patients systolic blood pressure from this amount, calculate the left ventricular outflow gradient
8. The "contact lesion" on the ventricular septum at the site of mitral- septal contact, which is an endocardial thickening or a mural plaque and is seen in some patients (Fig. 37.18).
9. Assess the systolic and diastolic LV function and left atrial size. Systolic function in these patients is typically normal but diastolic dysfunction with impaired relaxation pattern is common (Fig. 37.19)
10. The second most common cardiomyopathy during fetal life is HCM. Evaluate the thickened interventricular septum and both ventricular walls especially in fetus of diabetic mother and recipient twin in twin—twin transfusion syndrome (TTTS). HCM in the fetus of diabetic mother is transient (Fig. 37.20)

Restrictive Cardiomyopathy (RCM)

1. In classic forms of restrictive cardiomyopathy (RCM), markedly dilated atria, dwarf the size of the ventricles and there is no sign of dilation or hypertrophy of ventricles in four chamber view.

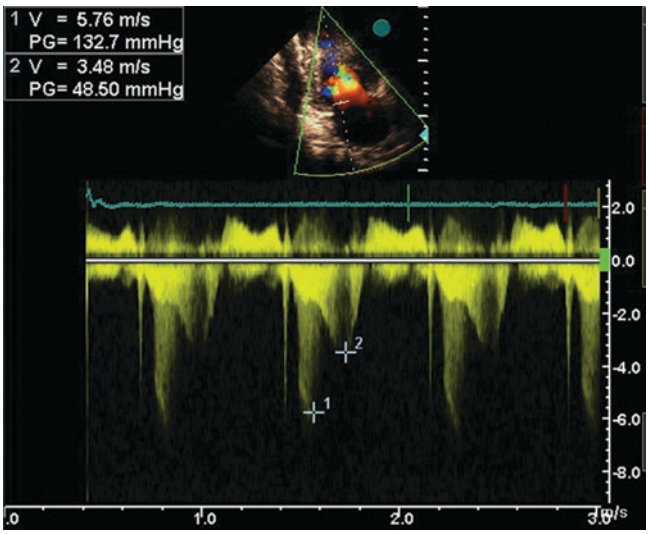

Fig. 37.17 Separating MR jet From subvalvar AS jet in a child with HCM. Dagger shaped profile with gradient 48 mmHg is caused by LVOT obstruction

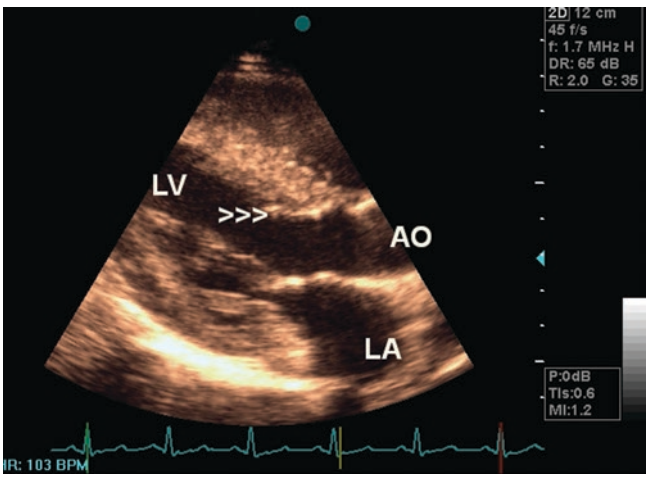

Fig. 37.18 Transthoracic parasternal long-axis view. Arrow heads indicate the contact lesion, an endocardial mural plaque which formed due to repetitive mitral-septal contact in this child with HCM

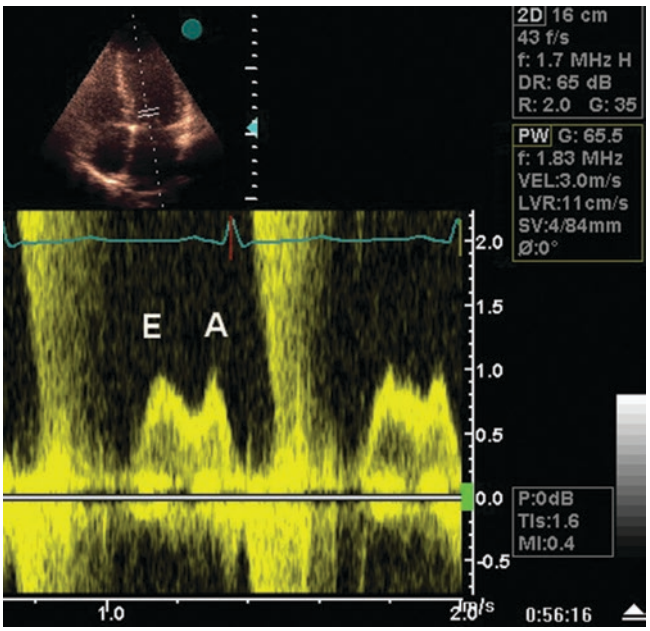

Fig. 37.19 Trans mitral inflow Doppler of a child with HCM, showing impaired relaxation pattern (E < A)

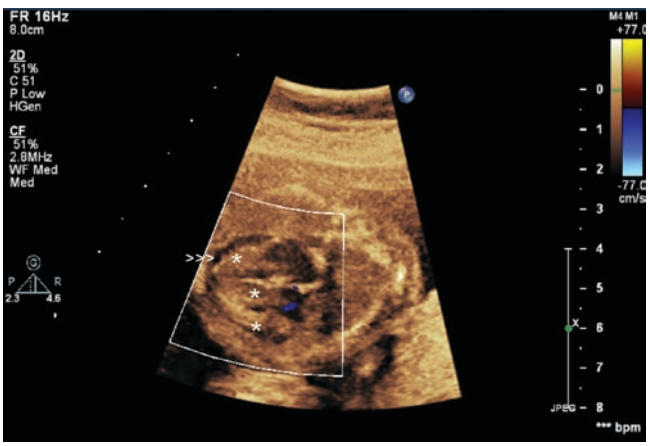

Fig. 37.20 Fetal echocardiogram four chamber view showing increased septal and free wall thickness (asterisks). Arrow heads points to pericardial effusion

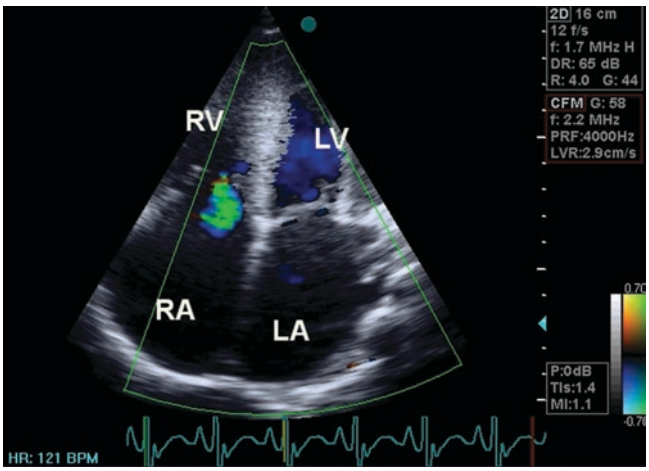

Fig. 37.21 Apical four chamber view of a child with mixed restrictive/hypertrophic cardiomyopathy, showing LA and RA enlargement, dwarfism of ventricles, and septal hypertrophy. Tricuspid regurgitation is shown by color flow mapping. *LV* left ventricle, *RV* right ventricle, *LA* left atrium, *RA* right atrium

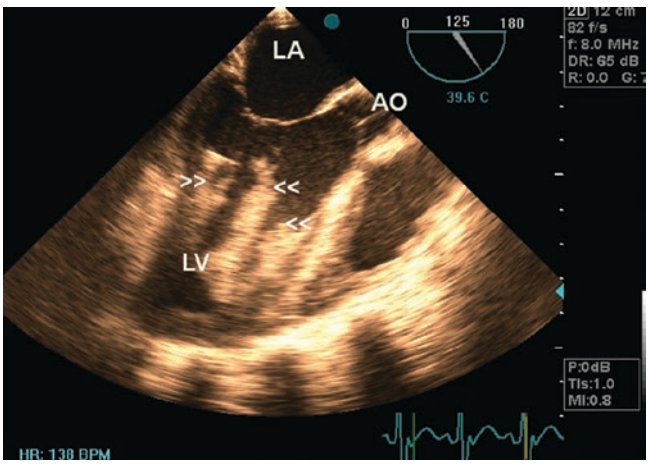

Fig. 37.22 Transesophageal long axis view of a child with RCM and hypereosinophilc syndrome. Arrow heads indicates multiple thrombi in LV. *LV* left ventricle, *LA* left atrium, *Ao* aorta

2. In about 40% of RCM cases, variable pattern of hypertrophy may be seen, the so called "mixed restrictive/hypertrophic" (Fig. 37.21).
3. Don't forget the tendency of these patients to form thrombi, use different views and evaluate the ventricles apexes (Fig. 37.22).
4. Use color flow mapping and evaluate both atrioventicular valve regurgitation
5. Any abnormal thickening of mitral valve leaflets and decreased excursion, should be evaluated as it may help to find the etiology. Löffler endocarditis, hypereosinophilic syndrome (HES) and endomyocardial fibrosis (EMF) frequently involve mitral valve but in idiopathic RCM the valves are normal.
6. Use Doppler profile of mitral valve and evaluate restrictive filling pattern including elevated E/A ratio, shortened mitral deceleration time, increased pulmonary vein atrial reversal velocity and duration, and pulmonary vein atrial reversal duration greater than mitral A wave duration. Also evaluate for mitral L wave (or middiastolic filling) creating a triphasic pattern in mitral inflow (Fig. 37.23).
7. Compare the systolic -to-diastolic duration ratio, which is increased in children with heart failure especially RCM patients.
8. LV systolic function is often normal or near normal. Use different modalities and evaluate fractional shortening and ejection fraction.
9. Use TDI (tissue Doppler imaging) and evaluate the abnormally low E' and A'. Systolic velocity, S' may

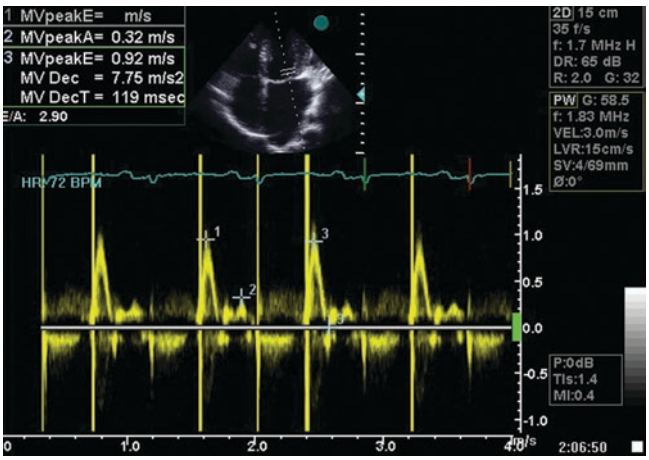

Fig. 37.23 Pulsed wave Doppler profile of MV in a child with RCM, showing restrictive filling pattern. E/A ratio = 2.9

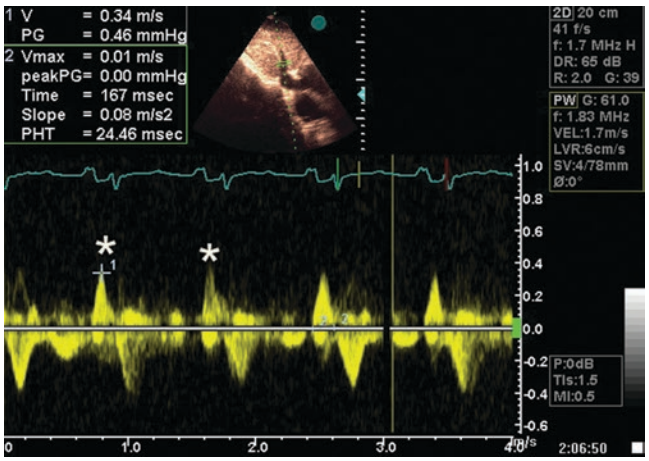

Fig. 37.25 Hepatic vein flow in a child with RCM. Asterisks indicate augmentation of flow reversal during atrial systole

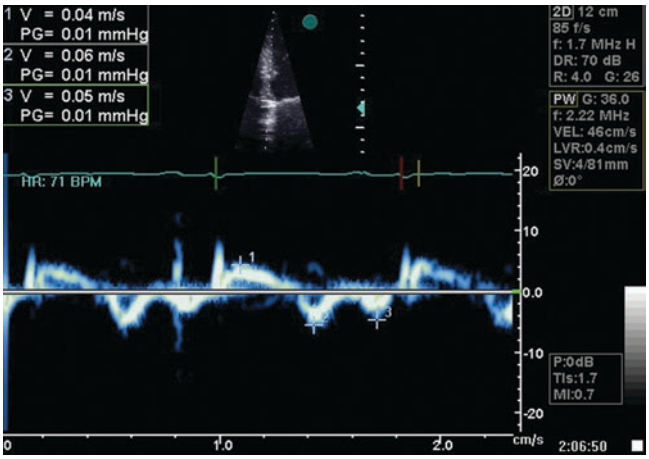

Fig. 37.24 Tissue Doppler imaging (TDI) profile of medial mitral annulus of a child with end stage RCM, showing abnormally low E', A', and S′ velocity

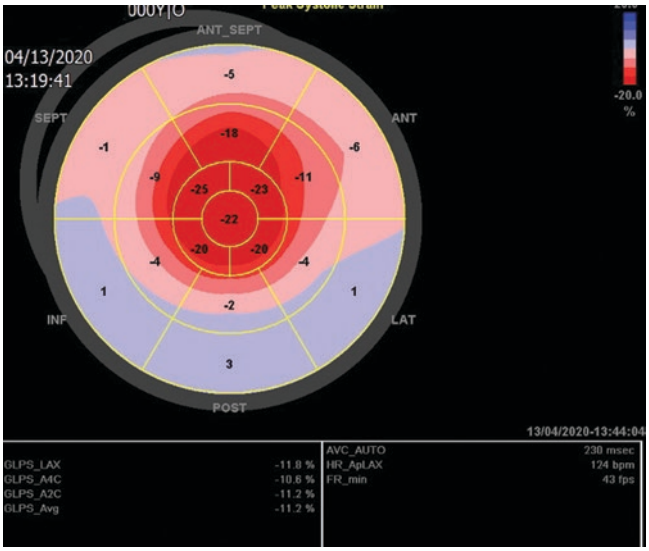

Fig. 37.26 Longitudinal strain bull's eye plot of a patient with restrictive cardiomyopathy. LV posterior wall thickness was 16 mm, septal thickness at base was 13 mm, and septum was sigmoid shape. The relative apical sparing can be easily observed by longitudinal strain bull's eye mapping in this patient

show systolic dysfunction in end stage disease (Fig. 37.24).

10. Assess hepatic venous flow with pulsed Doppler interrogation. Increased atrial systolic flow reversals especially during inspiration with restrictive physiology (Fig. 37.25).
11. Use Longitudinal strain and strain rate of LV myocardium to detect subclinical ventricular dysfunction. Using Speckle tracking echocardiography (STE) in three apical views including the four chamber, two chamber, and long axis; allow the analysis of global longitudinal strain (GLS) (Fig. 37.26).
12. The least common form of CMP during fetal life is RCM, and may present as increased density of endocardium (endocardial fibroelastosis).

Suggested Reading

Cetta F, O'Leary PW, Seward JB, et al. Idiopathic restrictive cardiomyopathy in childhood: diagnostic features and clinical course. Mayo Clin Proc. 1995;70(7):634–40.

Friedberg MK, Silverman NH. The systolic to diastolic duration ratio in children with heart failure secondary to restrictive cardiomyopathy. J Am Soc Echocardiogr. 2006;19(11):1326–31.

Huang TT, Kelly A, Becker SA, et al. Hypertrophic cardiomyopathy in neonates with congenital hyperinsulinism. Arch Dis Child Fetal Neonatal Ed. 2013;98(4):F351–4.

Lipshultz SE, Sleeper LA, Towbin JA, et al. The incidence of pediatric cardiomyopathy in two regions of the United States. N Engl J Med. 2003;348:1647–55.

McMurray JJV, Adamopoulos S, Anker SD, et al. ESC Guidelines for the diagnosis and treatment of acute and chronic heart failure 2012. Eur Heart J. 2012;33(14):1787–847.

Moradian M, Tabib A, Ghasempour A, et al. Comparing ventricular function in fetuses of diabetic and non-diabetic mothers using tissue Doppler imaging. Res Cardiovasc Med. 2016;5(4):e31864.

Norrish G, Cantarutti N, Pissaridou E, et al. Risk factors for sudden cardiac death in childhood hypertrophic cardiomyopathy: a systematic review and meta-analysis. Eur J Prev Cardiol. 2017;24:1220–30.

Nugent AW, Daubeney PE, Chondros P, et al. The epidemiology of childhood cardiomyopathy in Australia. N Engl J Med. 2003;348:1639–46.

Pedra SRFF, Smallhorn JF, Ryan G, et al. Fetal cardiomyopathies pathogenic mechanisms, hemodynamic findings, and clinical outcome. Circulation. 2002;106:585–91.

Sasaki N, Garcia M, Ko HH, et al. Applicability of published guidelines for assessment of left ventricular diastolic function in adults to children with restrictive cardiomyopathy: an observational study. Pediatr Cardiol. 2015;36:386–92.

Semsarian C, Ingles J, Maron MS, et al. New perspectives on the prevalence of hypertrophic cardiomyopathy. J Am Coll Cardiol. 2015;65:1249–54.

Sen T, Gungor O, Akpinar I, et al. Cardiac involvement in hypereosinophilic syndrome. Tex Heart Inst J. 2009;36(6):628–9.

Sherrid MV, Balaram S, BetteKim B, et al. The mitral valve in obstructive hypertrophic cardiomyopathy: a test in context. JACC. 2016;67(15):1846–58.

Smith BM, Dorfman AL, Yu S, Russell MW, et al. Relation of strain by feature tracking and clinical outcome in children, adolescents, and young adults with hypertrophic cardiomyopathy. Am J Cardiol. 2014;114:1275–80.

Ziolkowska L, Turska-Kmiec A, Petryka J, et al. Predictors of long-term outcome in children with hypertrophic cardiomyopathy. Pediatr Cardiol. 2016;37:448–58.

Pericardial Diseases

38

Azin Alizadehasl, Majid Maleki, Feridoun Noohi, and Maryam Moradian

Abstract

Variety of conditions can affect pericardium and some of them are life threatening. Evaluation of pericardial disease needs different imaging modalities. Echocardiography is the gold standard imaging technique for early detecting pericardial diseases, effusions, and their hemodynamic consequences.

Pericardial Diseases

1. While performing echocardiography, pay attention to unusually increased echo density of pericardial layers and/or accumulation of fluid.
2. Left ward deviation of the heart along with RV enlargement and paradoxical septal motion should raise the suspicion of congenital absence of the left pericardium.
3. Accumulation of fluid adjacent to the cardiac structures appears as an echo lucent space. Use different echo windows not to miss loculated effusion. Measure the size of the pericardial effusion at the end of diastole: Trivial (seen only in systole), Small (<5 mm), Moderate (5–20 mm), and Large (>20 mm). Using transesophageal echo (TEE) would be helpful to find posteriorly loculated effusion, especially after cardiac surgery.
4. Tamponade physiology should be ruled out even if size of effusion is small. Rapid accumulation of fluid can lead to rapidly increased intrapericardial pressure, compromising ventricular filling. Evaluate systolic RA collapse in four chamber view, and diastolic RV collapse in parasternal short axis view (Fig. 38.1).
5. Use Doppler profile of mitral and tricuspid valves inflow to assess the variation in heart filling by respiration. Reduced collapsibility and plethora of inferior vena cava (IVC) can be appreciated in subcostal views. Inspiratory shift of interventricular septum toward the LV or "septal bounce" best visualized using two D guided M- mode at parasternal long axis view.
6. Swinging motion of heart can be seen when pericardial effusion is massive (Fig. 38.2a, b).
7. Thickened pericardium should raise the suspicion of constrictive pericarditis (CP). It may be difficult to distinguish between normal and thickened pericardium so consider computed tomography (CT) and magnetic resonance (CMR) in doubtful situations. Evidence of constrictive physiology includes an abrupt shift of the septum or septal bounce due to ventricular interdependence and with similar physiology as tamponade, mild atrial dilation and plethora of IVC. Presence of septal bounce is a reliable sign to distinguish CP from restrictive cardiomyopathy (Fig. 38.3).
8. Evaluate the IVC plethora, ascites, plural effusion, and pericardial effusion in subcostal views in patients with CP (Figs. 38.4 and 38.5)
9. To distinguishing pericardial effusion from plural effusion use parasternal long axis view. Left pleural effusion extends posteriorly to the descending aorta, but pericardial effusion is located anterior to descending aorta
10. In large left pleural effusion obtaining cardiac images from the back of the patient may be possible (Fig. 38.6)
11. Tuberculous, bacterial, and malignant pericardial effusion may contain fibrin strands, which may be attached or floating between the visceral and parietal pericar-

A. Alizadehasl
Department of Cardio-Oncology and Research Center, Rajaie Cardiovascular, Medical & Research Center, Iran University of Medical Sciences, Tehran, Iran

M. Maleki · F. Noohi
Cardiovascular Intervention Research Center, Rajaie Cardiovascular, Medical & Research Center, Iran University of Medical Sciences, Tehran, Iran

M. Moradian (✉)
Pediatric Cardiology, Rajaie Cardiovascular, Medical & Research Center, Iran University of Medical Sciences, Tehran, Iran

M. Moradian, A. Alizadehasl (eds.), *Atlas of Echocardiography in Pediatrics and Congenital Heart Diseases*,
https://doi.org/10.1007/978-3-662-62341-1_38

dium. This finding may predict the development of constrictive pericarditis (Fig. 38.7)

12. In fetal life hypoechoic myocardium may resemble as pericardial effusion. To distinguish pseudo pericardial fluid from real pericardial effusion, evaluate if the effusion extends above the atrioventricular groove. Pseudo pericardial effusion is limited to ventricular region and will not extend above the atrioventricular groove (Fig. 38.8).
13. Detection a small amount of pericardial fluid (<2 mm) in fetuses more than 20 weeks of gestation may be normal. Immune and non-immune hydrops, chromosomal abnormalities, infections, fetal arrhythmias, congenital structural cardiac anomalies, tumors, cardiomyopathies, and pericardial teratoma all may lead to pericardial effusion. A fetal pericardial effusion is typically larger than 2 mm. Small amount of PE may resemble as an ovoid or lenticular echo free space whereas larger amount of PE resembles as a bag of water around the heart and pushes the lungs dorsally, while bilateral plural effusion collect around the lungs and resemble as "bat wings" (Figs. 38.9 and 38.10).

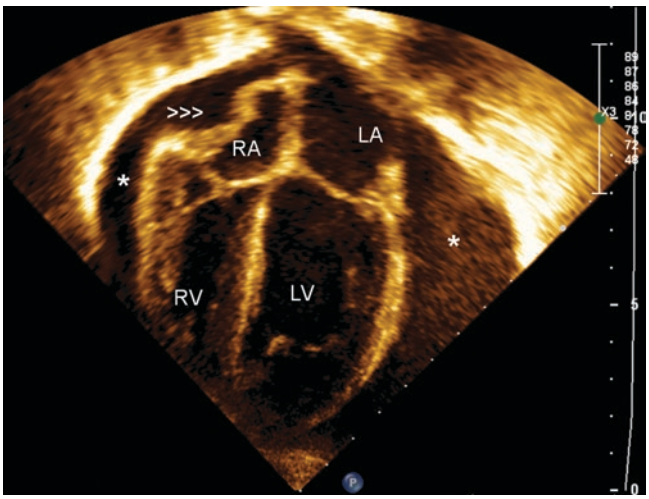

Fig. 38.1 TTE, apical four chamber view showing RA collapse (arrow heads) in a child with diffuse pericardial effusion and tamponade physiology. Asterisks indicate pericardial effusion. *RA* right atrium, *RV* right ventricle, *LA* left atrium, *LV* left ventricle

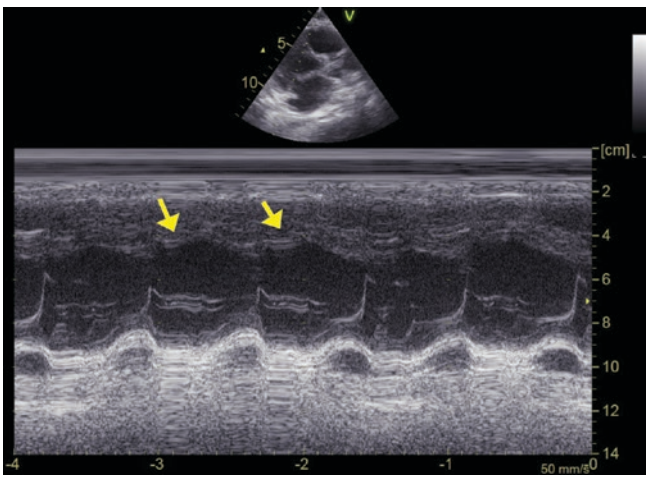

Fig. 38.3 M mode echocardiography of an adolescent with CP. An abrupt shift of the septum toward LV in early diastole with inspiration is indicated by arrows. In expiration by improvement in LV filling, septum shifts back toward RV

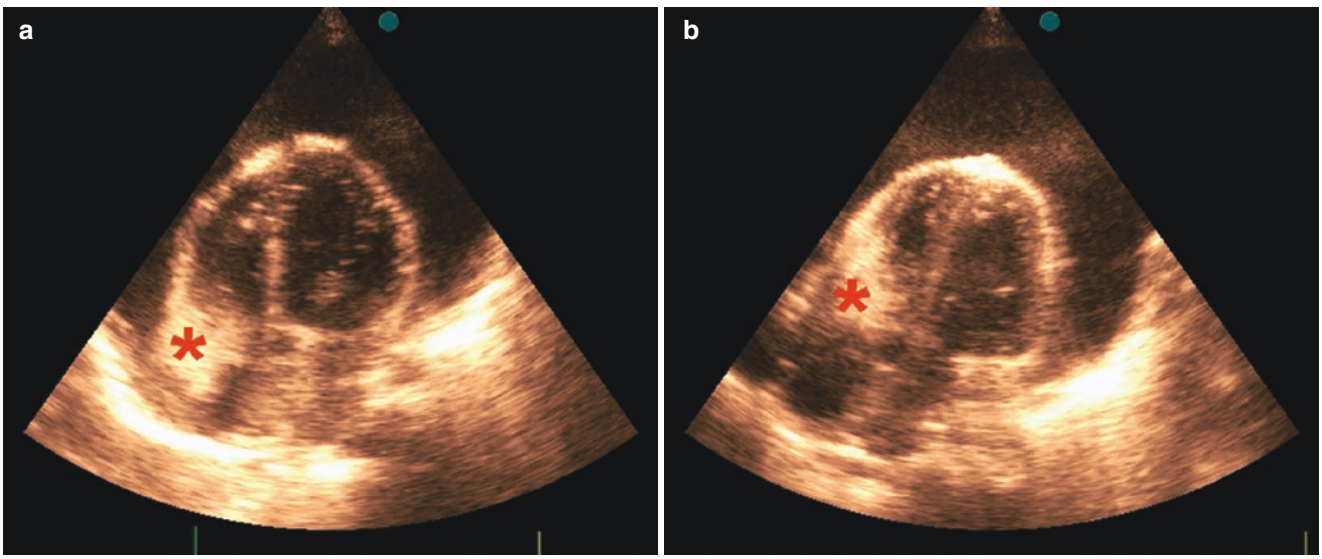

Fig. 38.2 (**a**, **b**) TTE, showing swing motion of heart within the pericardial space of a child with massive PE due to metastasis. Asterisk indicate the malignant tumor invading the right atrium (hepatoblastoma)

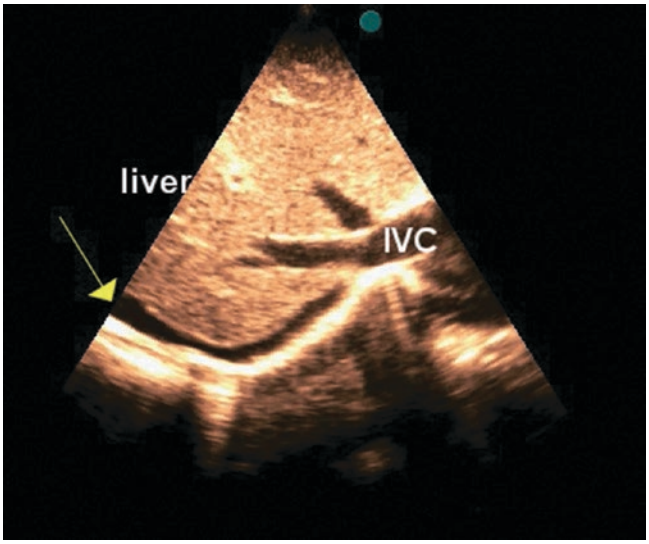

Fig. 38.4 TTE subcostal view showing dilated inferior vena cava (IVC), and right plural effusion (arrow) in an adolescent with CP

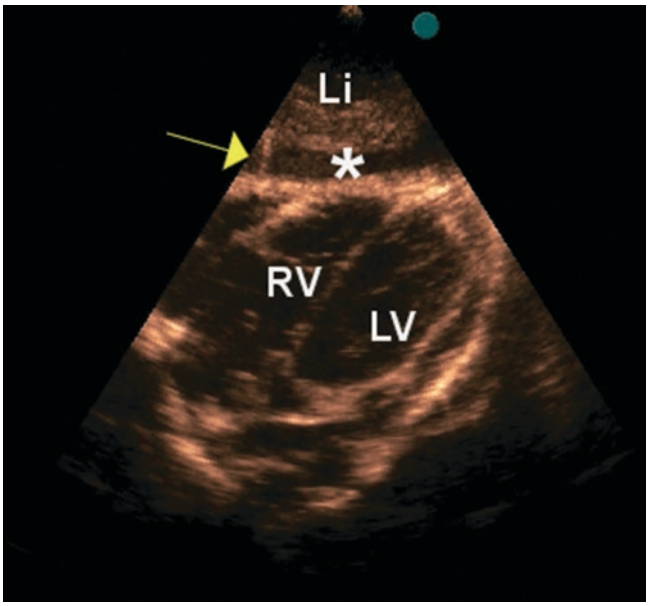

Fig. 38.5 TTE subcostal view showing the falciform ligament (arrow) confirming the presence of ascites (asterisk) in this patient with CP. Small pericardial effusion is also observed. *Li* Liver, *RV* right ventricle, *LV* left ventricle

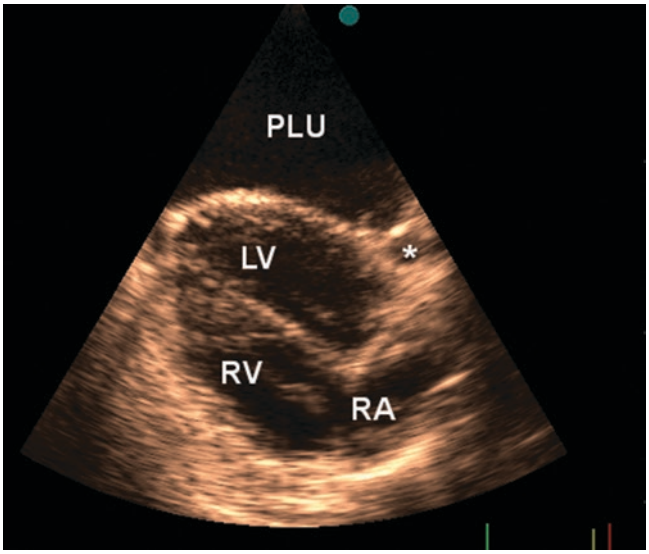

Fig. 38.6 Evaluation of plural effusion from back of a patient with left plural effusion. Asterisk indicate descending aorta. *RA* right atrium, *RV* right ventricle, *LV* left ventricle, *plu* plural effusion

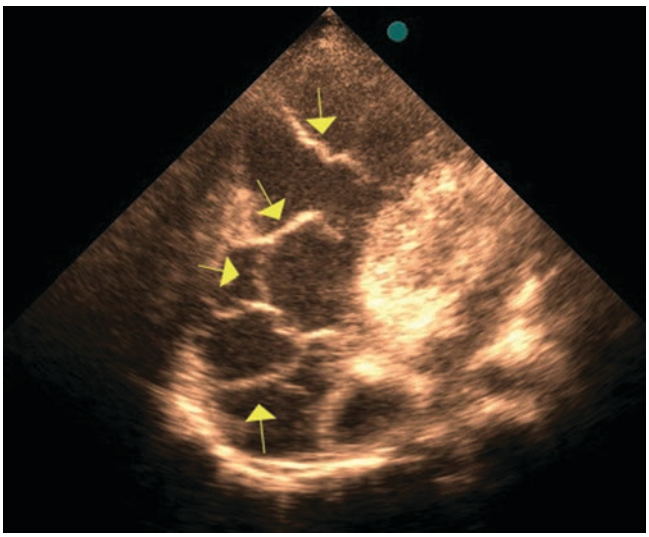

Fig. 38.7 TTE modified four chamber view showing fibrin strands with worm-like appearance (arrows)

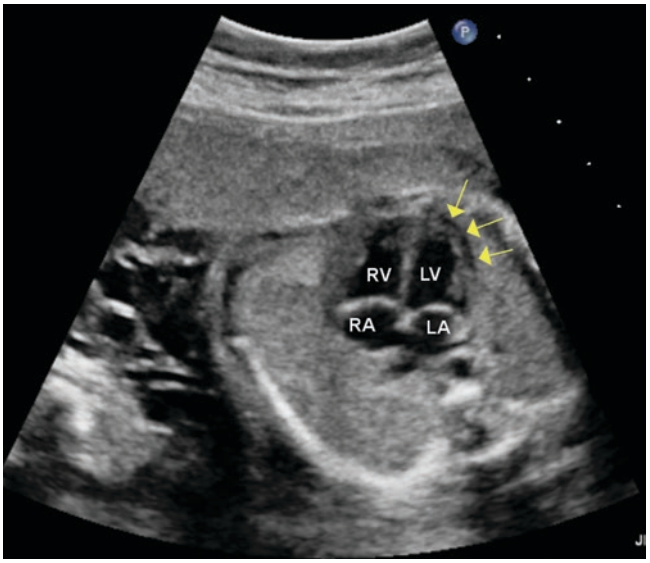

Fig. 38.8 Fetal echocardiogram, apical four chamber view showing pseudo pericardial effusion (arrows). Obviously this echopenic region is limited to ventricular myocardium. *RA* right atrium, *RV* right ventricle, *LA* left atrium, *LV* left ventricle

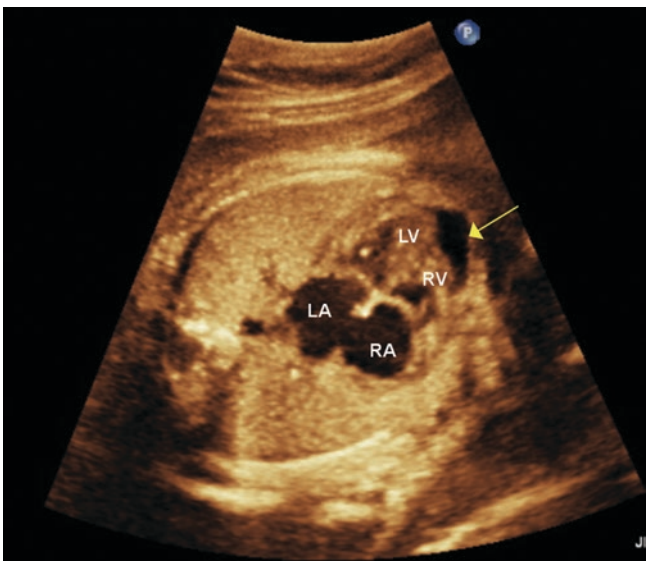

Fig. 38.9 Fetal echocardiogram four chamber view showing small PE (arrow). There is also an echogenic focus in LV cavity, mild left plural effusion, and large foramen ovale. *RA* right atrium, *RV* right ventricle, *LA* left atrium, *LV* left ventricle

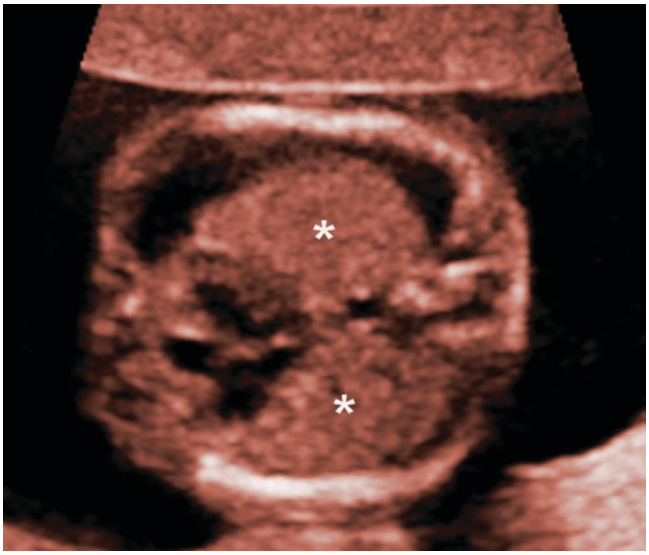

Fig. 38.10 Fetal echocardiogram of a fetus with bilateral plural effusion. Asterisks indicate the lungs and "bat wings" appearance

Suggested Reading

Cardello FP, Anthony Yoon DH, Halligan RE Jr, et al. The Falciform ligament in the echocardiographic diagnosis of ascites. J Am Soc Echocardiogr. 2006;19:1074.e3–4.

Di Salvo DN, Brown DL, Doubilet PM, et al. Clinical significance of isolated fetal pericardia effusion. J Ultrasound Med. 1994;13:291–3.

Goodman A, Perera P, Mailhot T, et al. The role of bedside ultrasound in the diagnosis of pericardial effusion and cardiac tamponade. J Emerg Trauma Shock. 2012;5(1):72–5.

Grogan M. Pericardial diseases (Chapter 24). In: Eidem BW, O'leary PW, Cetta F, editors. Echocardiography in pediatric and adult congenital heart disease. 2nd ed: Wolters Kluwer; 2015. p. 431–45.

Johnson JN, Cetta F. Pericardial diseases (Chapter 61). In: Allen HD, Shaddy RE, Penny DJ, Feltes TF, Cetta F, editors. Moss and Adams' heart disease in infants, children, and adolescents including the fetus and young adults. 9th ed: Wolters Kluwer; 2016. p. 1427–40.

Knox S, Madruga M, Carlan SJ. Utilizing abdominal sonography in the diagnosis of ascites caused by heart failure: a patient with cirrhosis. J Diagn Med Sonogr. 2018;34(1):50–2.

Lee SH, Kim WH, Ko JK, et al. Fibrinous pericardial effusion in a three-dimensional echocardiography. Q J Med. 2015;108:665–7.

Pérez-Casares A, Cesar S, Brunet-Garcia L, et al. Echocardiographic evaluation of pericardial effusion and cardiac tamponade. Front Pediatr. 2017;5:79.

Saito Y, Donohue A, Attai S, et al. The syndrome of cardiac tamponade with "small" pericardial effusion. Echocardiography. 2008;25(3):321–7.

Cardiac Mass and Mass-Like Structures

39

Maryam Moradian

Abstract

Echocardiography plays an invaluable role in detecting cardiac mass lesions. Morphology, location, and hemodynamic consequences of the masses should be carefully evaluated by echocardiography. Thrombus, cysts, vegetation, and tumors should be differentiated meticulously as the wrong diagnosis may have catastrophic results.

Cardiac Mass and Mass-Like Structures

1. In approaching a cardiac mass lesion, try to identify if it is a real structure or just an echo artifact. Using different echo windows and selecting an appropriate probe will help you not to mistake an echo artifact with a real structure.
2. Sometimes a normal cardiac structure resembles as a mass such as embryologic remnants of Chiari net in RA, prominent thymus gland in an infant, and coumadin ridge in LA (Fig. 39.1). Transesophageal echocardiography (TEE) may also be necessary to better characterize the mass lesion.
3. Location, mobility, attachment, shape, number, size, and the hemodynamic effects of the mass should be evaluated by echocardiography precisely
4. It is important to distinguish tumors, thrombi, and vegetations from each other.
5. In patients with sluggish blood flow such as in Fontan circuit, cardiomyopathy, congestive heart failure, and atrial fibrillation carefully evaluate for thrombus formation (Fig. 39.2). Presence of any foreign material in the heart such as mechanical prosthetic valve, central venous catheter, and implanted pace maker can make the patient susceptible to thrombus formation.

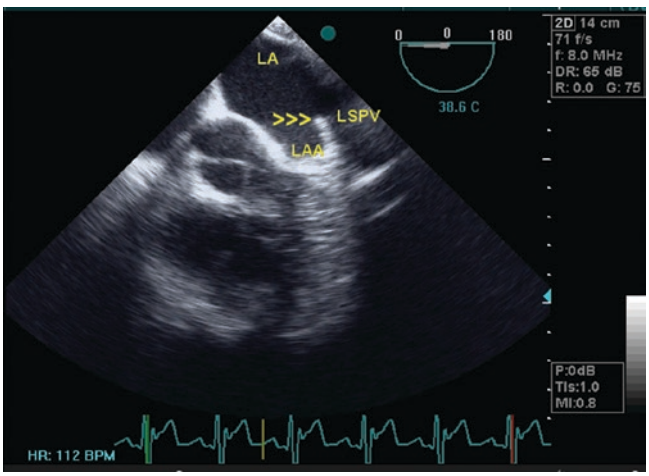

Fig. 39.1 TEE with probe at upper esophageal level showing coumadin ridge (arrow heads). *LAA* left atrial appendage, *LSPV* left superior pulmonary vein, *LA* left atrium

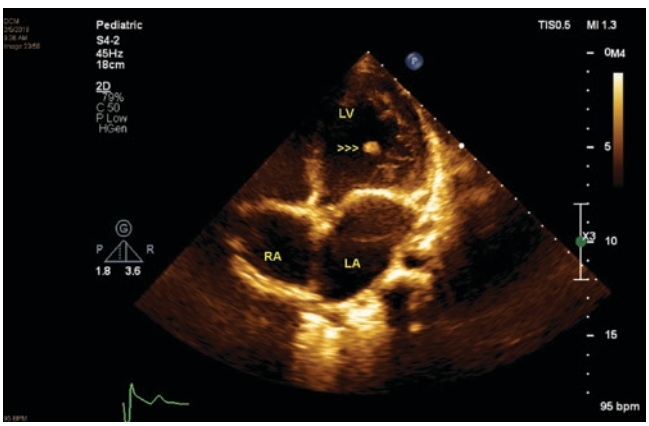

Fig. 39.2 TTE, four chamber view of a child with dilated cardiomyopathy. Arrow heads indicate an echo dense, rounded structure protruding into LV cavity highly suggestive of thrombus formation. *LA* left atrium, *RA* right atrium, *LV* left ventricle

M. Moradian (✉)
Pediatric Cardiology, Rajaie Cardiovascular, Medical & Research Center, Iran University of Medical Sciences, Tehran, Iran

M. Moradian, A. Alizadehasl (eds.), *Atlas of Echocardiography in Pediatrics and Congenital Heart Diseases*,
https://doi.org/10.1007/978-3-662-62341-1_39

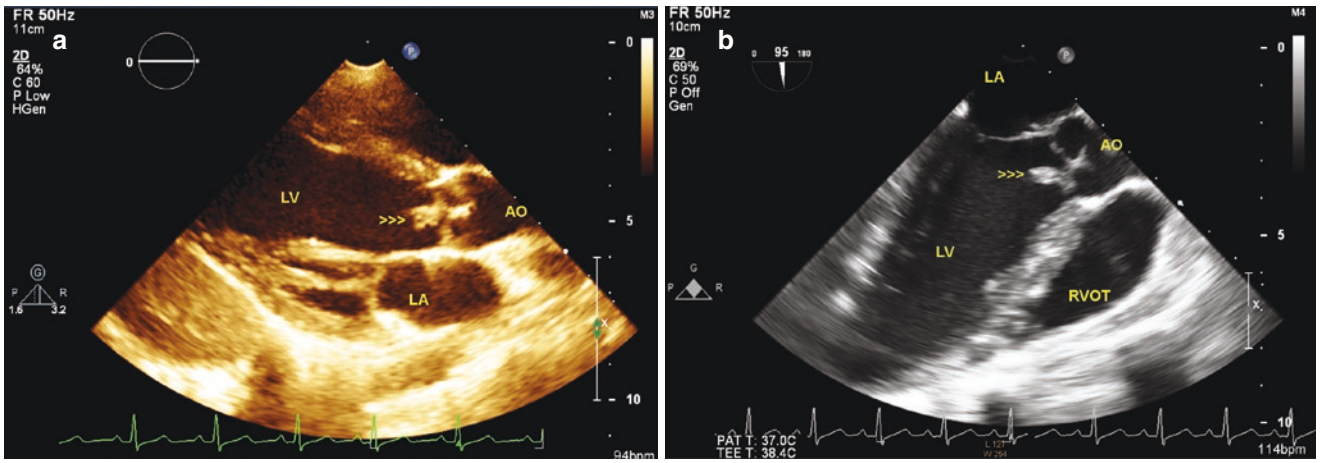

Fig. 39.3 (**a**, **b**) TTE parasternal long axis view (**a**) and TEE long axis view of a patient with bicuspid aortic valve (**b**). Arrow heads point to an irregular mass lesion, highly suggestive of vegetation on LV side of aortic valve. The mass was oscillating and had back and forth movement with the cardiac cycle. *LA* left atrium, *AO* aorta, *LV* left ventricle, *RVOT* right ventricular out flow tract

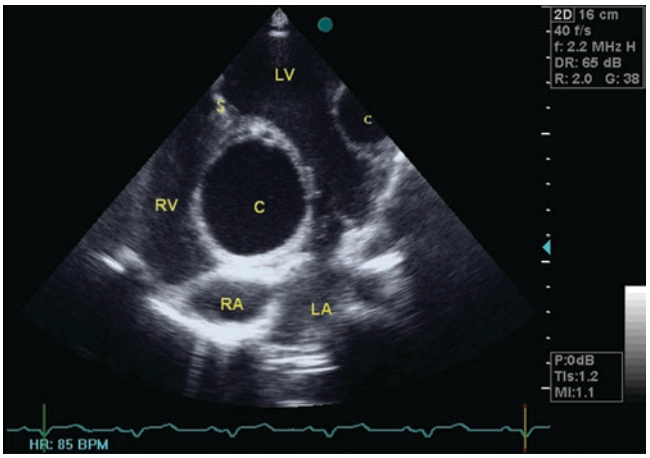

Fig. 39.4 TTE apical four-chamber view. Two well-circumscribed circular cystic masses, hydatid cysts in interventricular septum, and LV free wall are seen. *LA* left atrium, *RA* right atrium, *LV* left ventricle, *RV* right ventricle, *S* interventricular septum, *C* cyst

6. Vegetations, the hallmark of endocarditis, are commonly mobile with disordered and oscillating motion. They have bizarre and irregular shape and typically attached on the low-pressure side of the valve causing regurgitation (Fig. 39.3a, b).
7. The most common cardiac cysts are pericardial cysts, echinococcal (hydatid) cysts, and blood cysts (Fig. 39.4).
8. Aneurysms and diverticula also have cystic appearance. Diverticula may be muscular or fibrotic. Fibrotic diverticula, also called congenital aneurysm, can be found as an isolated lesion with thin and fibrous walls which motions is unrelated to cardiac contraction (Fig. 39.5a, b). Muscular diverticula contain endocardium, myocardium, and pericardium. Their contractile activity synchronized with cardiac cycles.
9. Sometimes non compaction ventricles may mistakenly resemble as cardiac tumors. The prominent trabeculation and deep intertrabecular recesses in this form of cardiomyopathy, give it a spongy appearance. Most commonly just LV is involved but there are reports of biventricular noncompaction cardiomyopathy (Figs. 39.6 and 39.7).
10. In pediatric population primary cardiac tumors are more common, and most of them are benign. Among tumors, rhabdomyomas are the most common, followed by fibroma, and myxoma. Commonly rhabdomyomas regress spontaneously over time. Rhabdomyomas, may be multiple and related with tuberous sclerosis complex (Fig. 39.8).
11. Dispite benign nature, tumors may have significant hemodynamic consequences (Figs. 39.9a, b and 39.10).
12. Echogenic focus or bright spot are common finding during fetal life, they may be mistaken as tumor. Also, a prominent moderator band may resemble as a RV tumor in fetus. Evaluate the fetus from different views to assure about them (Fig. 39.11).
13. Rabdomyomas are the most common tumor diagnosed during fetal life (Figs. 39.12 and 39.13)

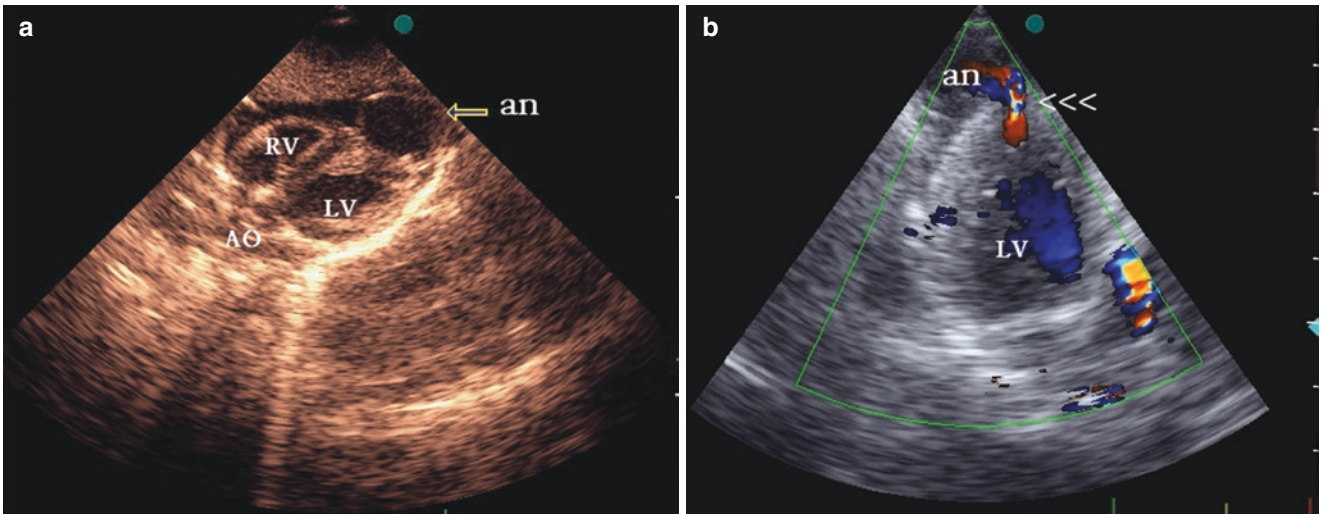

Fig. 39.5 (**a**, **b**) TTE, subcostal view, showing a large thin walled, non-contractile, cystic structure out pouching from left ventricle compatible with LV aneurysm and mild pericardial effusion in an infant with congenital LV aneurysm (**a**). The connection between the aneurysm and the left ventricle of the same patient is shown by adding CFM in an off axis apical view. Arrow heads point to connection site (**b**). *LV* left ventricle, *RV* right ventricle, *AO* aorta, *an* aneurysm

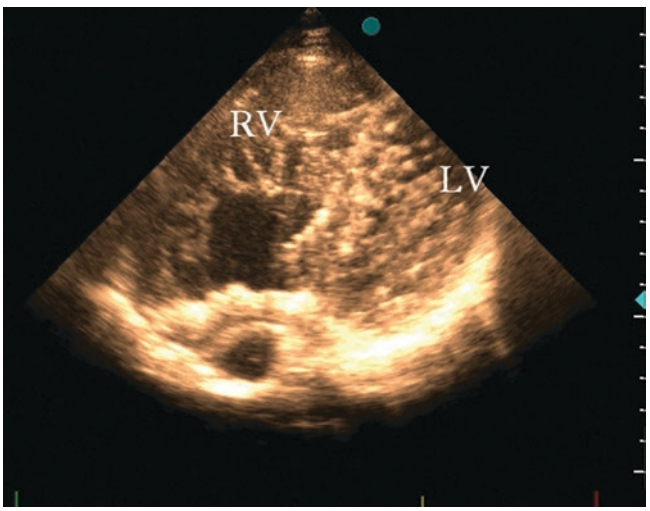

Fig. 39.6 TTE off axis subcostal view of a child with noncompaction cardiomyopathy. Prominent trabecula and deep intertrabecular recesses are obviously seen in both LV and RV. *LV* left ventricle, *RV* right ventricle

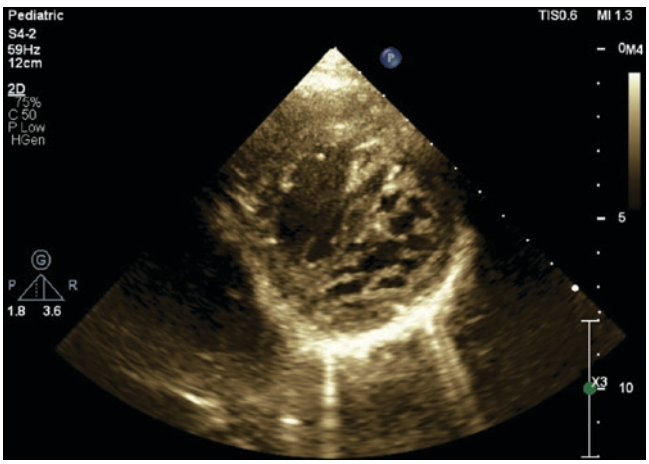

Fig. 39.7 TTE parasternal short axis view showing non compaction LV

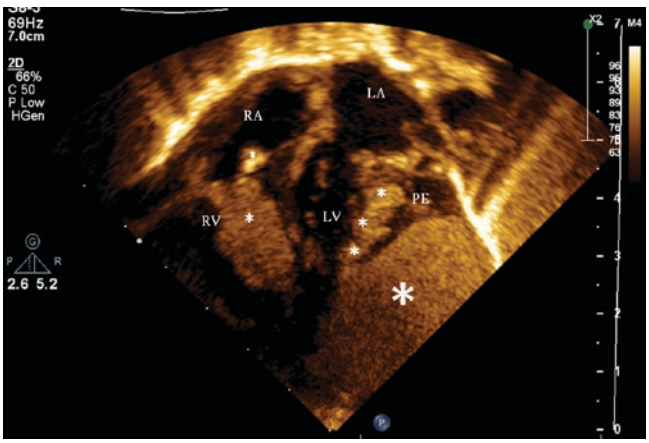

Fig. 39.8 TTE Apical four chamber view of a newborn with tuberos sclerosis complex. Multiple intracardiac rhabdomyomas are shown by asterisks. There is mild pericardial effusion and a very large pericardial tumor as well (larger asterisk). *LA* left atrium, *RA* right atrium, *LV* left ventricle, *RV* right ventricle, *PE* pericardial effusion

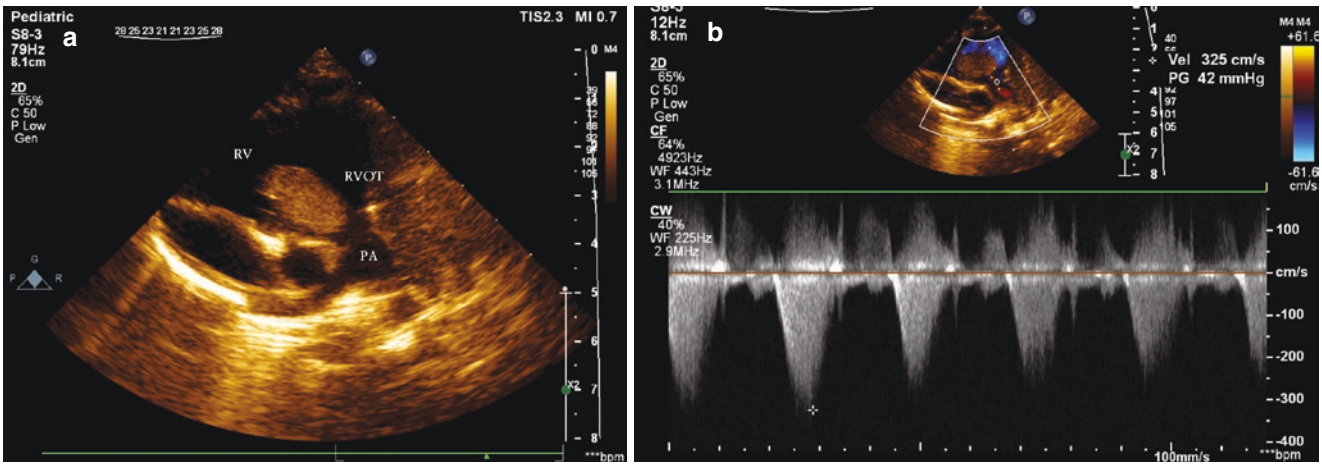

Fig. 39.9 (**a**, **b**) TTE parasternal short axis view of an infant with right ventricular outflow tract tumor causing pulmonary stenosis (**a**). Doppler profile of pulmonary valve of the same patient showing pulmonary pressure gradient = 42 mmHg, and mild pulmonary regurgitation (**b**). *RVOT* right ventricular outflow tract, *RV* right ventricle, *PA* pulmonary artery

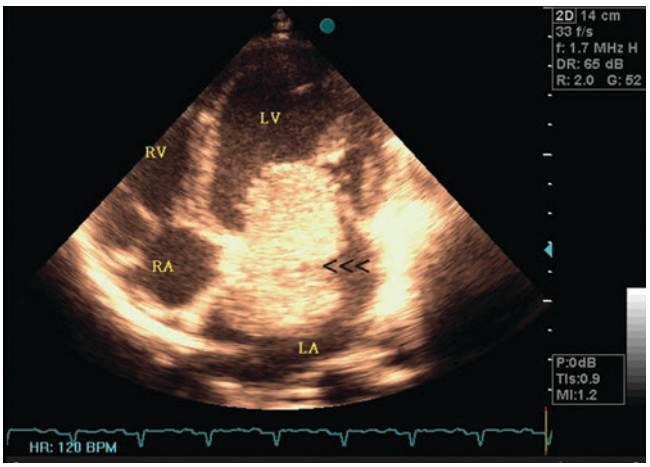

Fig. 39.10 TTE apical four chamber view, black arrow heads points to a large rounded mass occupying the LA. LA and LV are enlarged. The mass appeared to arise from interatrial septum, moving with the cardiac cycle. This to- and- fro motion through the mitral valve caused both mitral stenosis and regurgitation. In this systolic frame the mass is lodged in mitral valve. The postoperative pathological specimen confirmed it as myxoma. *LA* left atrium, *RA* right atrium, *LV* left ventricle, *RV* right ventricle

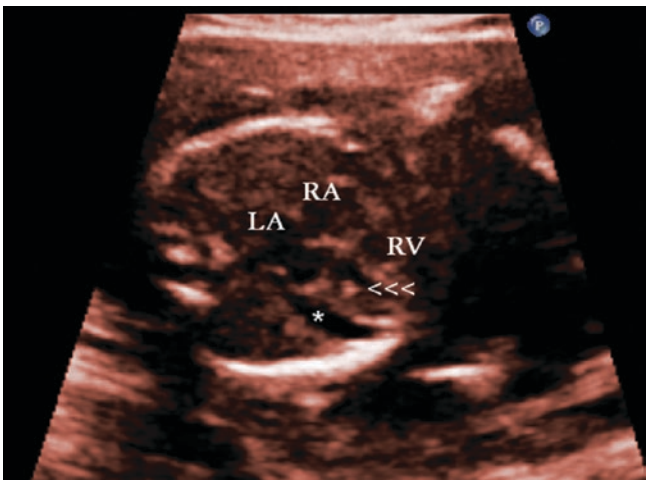

Fig. 39.11 fetal echocardiogram, four chamber view. Arrow heads point to echo genic focus in LV. Mild pericardial effusion is indicated by asterisk. *RA* right atrium, *LA* left atrium, *RV* right ventricle

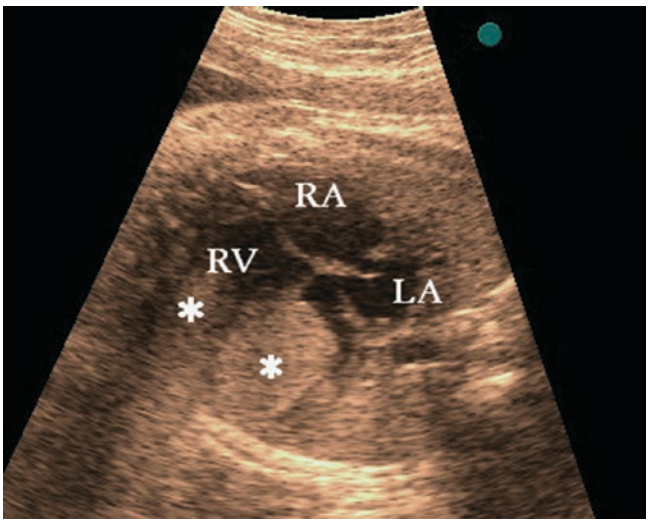

Fig. 39.12 fetal echocardiography of a case of tuberous sclerosis complex. Cardiothoracic ratio is increased. A huge mass (rhabdomyoma) occupied LV cavity and a smaller mass occupied RV cavity (asterisks). *LA* left atrium, *RA* right atrium, *RV* right ventricle

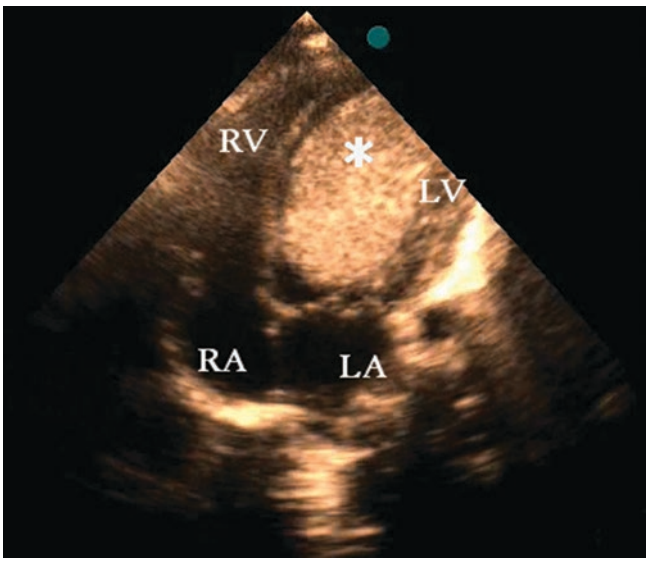

Fig. 39.13 Transthoracic echo of the same patient as Fig. 39.12, some month after birth RV tumor regressed but LV tumor did not change (asterisk). *LA* left atrium, *RA* right atrium, *LV* left ventricle, *RV* right ventricle

Suggested Reading

Aarabi Moghadam MY, Moradian M, Givtaj N, et al. Intraluminal ascending aorta fibroma. J Teh Univ Heart Ctr. 2011;6(1):45–7.

George A, Parameswaran A, Nekkanti R, et al. Normal anatomic variants on transthoracic echocardiogram. Echocardiogr: J Cardiovasc Ultrasound Allied Tech. 2009;26(9):1109–17.

Hosseinsabet A. Echocardiographic hypertrabeculated/non-compacted right ventricle accompanied by atrial septal defect and anomalous pulmonary vein connection. J Cardiovasc Echography. 2014;24:122–4.

Mankad R, Herrmann J. Cardiac tumors: echo assessment. Echo Res Pract. 2016;3(4):R65–77.

Moradian M. Diagnostic errors in echocardiography: review of five interesting pediatric cases. J Teh Univ Heart Ctr. 2012;7(1):33–6.

Moradian M, Dalili M, Merajie M. Prenatal diagnosis of tuberos sclerosis by fetal echocardiography with an unusual clinical course after birth. Arch Cardiovasc Image. 2013;1(2):83–5.

Moradian M, ZiyaeiFard M, Mozaffari K. Atrial rhabdomyoma: a case report. Iran Heart J. 2014;15(2):39–42.

Mozaffari M, Baghaei Tehranei R, Moradian M, Totonchi MZ. A one year old infant with multiple cardiac masses and congenital heart defect. Iran J Cardiac Surg. 2011;3(1):57–8.

Mozaffari K, Moradian M, Baharestani B, et al. Benign tumor with perivascular myoid differentiation, rare yet interesting case report in a nine-month-old infant, multidiscip cardio annal. 2017;8(2);e9366.

Otsuka H, Arinaga K, Fukuda T, et al. Double right atrial blood cysts. Ann Thorac Surg. 2016;101:e147–9.

Park MH, Jung SY, Youn HJ, et al. Blood cyst of subvalvular apparatus of the mitral valve in an adult. Cardiovasc Ultrasound. 2012;20(3)

Peters PJ, Reinhardt S. The echocardiographic evaluation of intracardiac masses: a review. J Am Soc Echocardiogr. 2006;19(2):230–40.

Rao G, Tauras J. Biventricular noncompaction cardiomyopathy in an adult with unique facial dysmorphisms: case report and brief review. Case Rep Cardiol. 2015:831341. 4 pages

Vettraino IM, Hoprasart NJ, Bronsteen RA, et al. Clinical implications of the prenatal sonographic finding of fetal myocardial echogenic foci. J Ultrasound Med. 2005;24:195–9.

Cardiac Malposition

40

Maryam Moradian

Abstract

Malposition, a very rare anomaly of the heart refers to hearts either with abnormal location within the chest or outside the chest, ectopia cordis. Abnormal orientation refers to the abnormal direction of the base-to-apex axis. Performing the "sequential, segmental approach" in echocardiography, help to proceed a checklist to identify every detail of cardiac structures, even in a very complex congenital cardiac anomaly.

Cardiac Malposition

1. Determin the axis by evaluating the base to apex axis of the heart, in normal condition, levocardia, the axis points to the left of the sternum. In mesocardia, the axis points to the midline, and in dextrocardia, axis points to the right of the sternum. Abnormal cardiac axis is usually associated with a wide spectrum of complex congenital heart diseases (CHD) (Fig. 40.1)
2. Appreciate the overall location or position of the heart in relation to chest. Determine the hemithorax predominantly occupied by the heart.
3. Congenital heart diseases may lead to abnormal cardiac axis and extracardiac anomalies may lead to altered position of the heart. So, in cases with abnormal cardiac position consider eventration of a hemidiaphragm, diaphragmatic hernia, congenital complete absence of the pericardium, and lung agenesis. Cardiovascular malformations may be detected in 25–30% cases with congenital diaphragmatic hernia (Figs. 40.2 and 40.3)

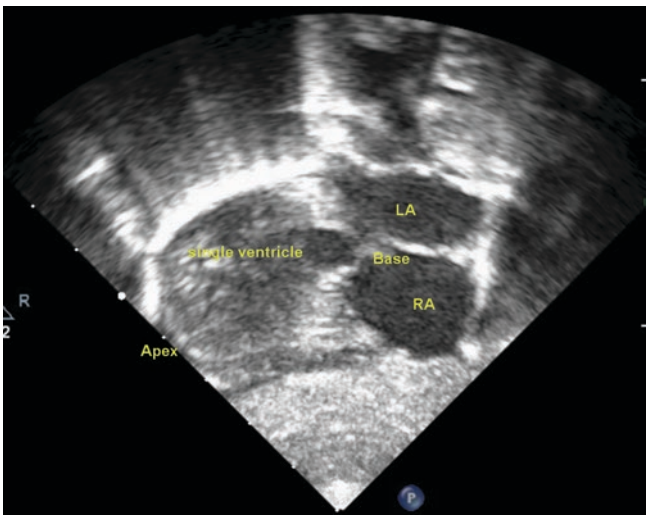

Fig. 40.1 TTE subcostal view showing cardiac axis from base to apex pointing right, dextrocardia in this infant with complex CHD. *LA* left atrium, *RA* right atrium

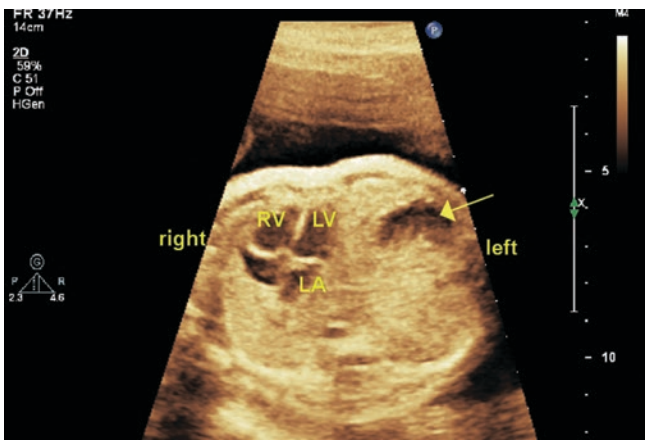

Fig. 40.2 Fetal echocardiogram showing dextroposition of heart in this case of grade 2 congenital diaphragmatic hernia (CDH). Cardiac axis is normal. Arrow indicate CDH. *LA* left atrium, *LV* left ventricle, *RV* right ventricle

M. Moradian (✉)
Pediatric Cardiology, Rajaie Cardiovascular, Medical & Research Center, Iran University of Medical Sciences, Tehran, Iran

M. Moradian, A. Alizadehasl (eds.), *Atlas of Echocardiography in Pediatrics and Congenital Heart Diseases*,
https://doi.org/10.1007/978-3-662-62341-1_40

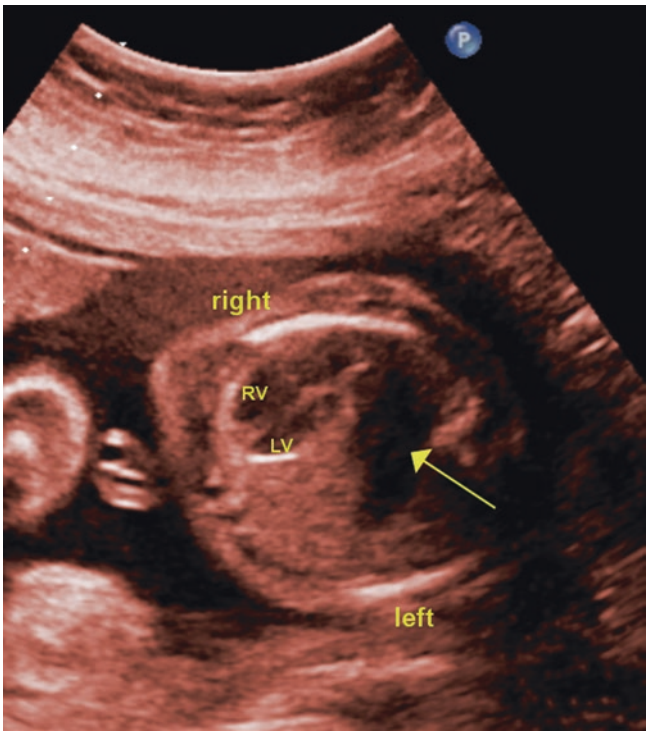

Fig. 40.3 Fetal echocardiogram showing dextroposition of heart in this case of grade 4 congenital diaphragmatic hernia (arrow). Cardiac axis is normal. *LV* left ventricle, *RV* right ventricle

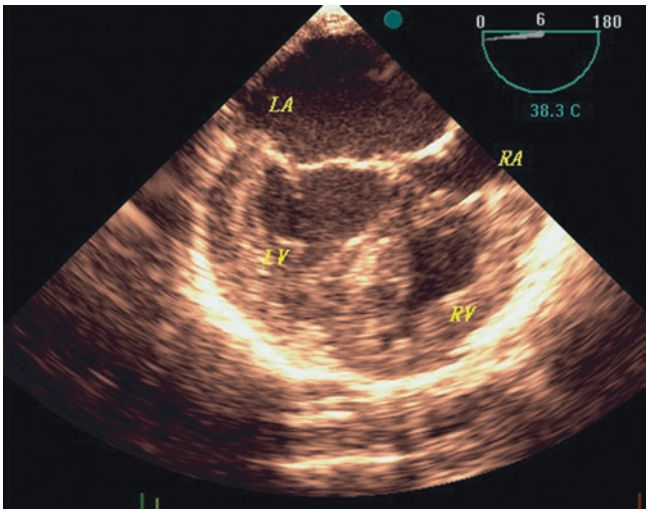

Fig. 40.4 TEE mid esophageal four chamber view of a child with dextrocardia, showing atrial situs inversus, and atrioventricular concordance. *LA* left atrium, *RA* right atrium, *LV* left ventricle, *RV* right ventricle

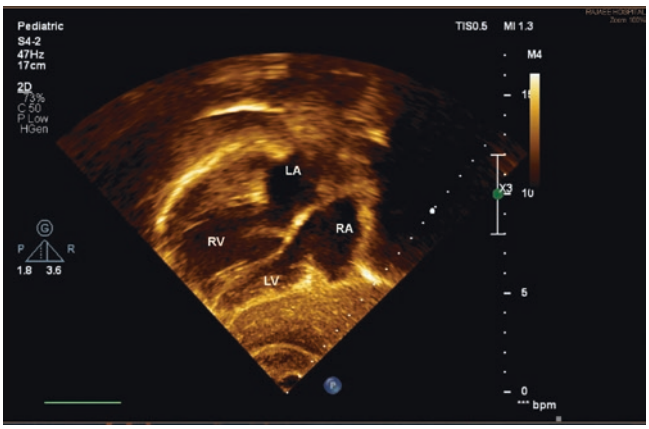

Fig. 40.5 TTE subcostal view four chamber view of a child with dextrocardia, showing atrial situs inversus, and atrioventricular discordance. *LA* left atrium, *RA* right atrium, *LV* left ventricle, *RV* right ventricle

4. Use the "sequential, segmental approach" and completely assess anatomy and function of each structure. Begin with determination of situs, and define the cardiac position within the chest. Describe, of the venous, venoatrial connection, atria, atrioventricular connections, atrioventricular valves (Figs. 40.4 and 40.5)
5. Then appreciate ventricles, ventriculoarterial connections, semilunar valves, and great arteries (Fig. 40.6a, b)

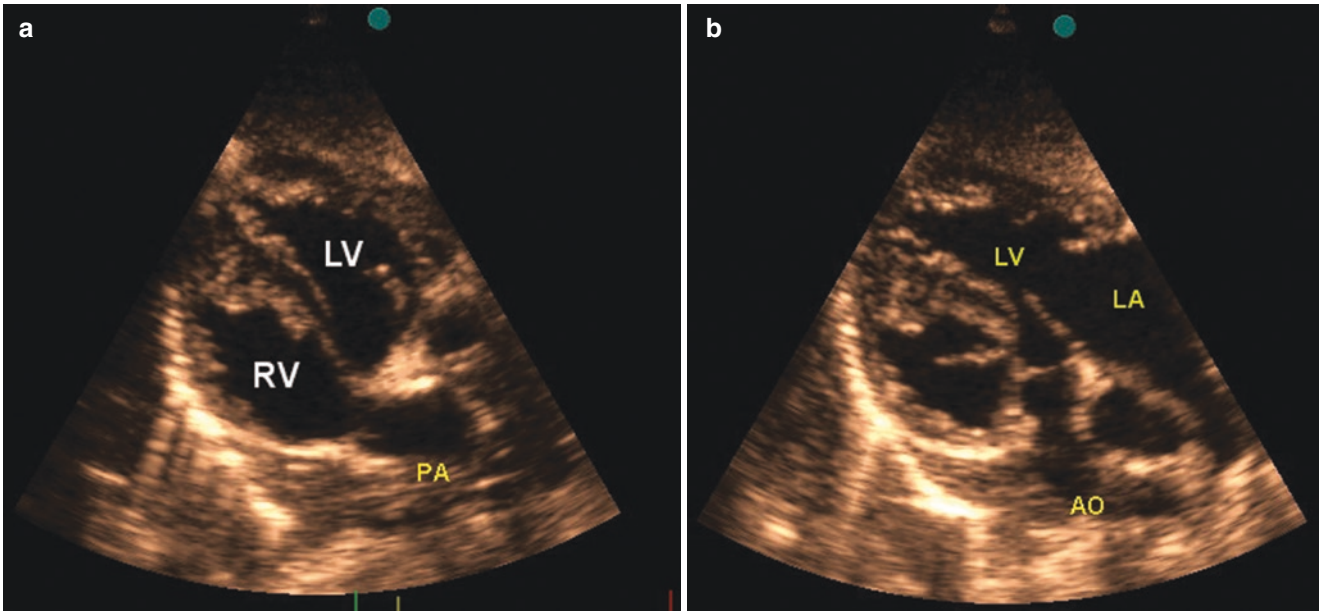

Fig. 40.6 (**a**, **b**) TTE subcostal view of a child with dextrocardia, showing ventriculoarterial concordance, the pulmonary artery arises from the right ventricle (**a**) and the aorta arises from the left ventricle (**b**). *LA* left atrium, *LV* left ventricle, *RV* right ventricle, *PA* pulmonary artery, *AO* aorta

Suggested Reading

Gillis E, Springer R, O'Leary PW. Practical issues related to the examination, anatomic image orientation, and segmental cardiovascular analysis (Chapter 2). In: Eidem BW, O'leary PW, Cetta F, editors. Echocardiography in pediatric and adult congenital heart disease. 2nd ed: Wolters Kluwer; 2015. p. 364–73.

Lapierre C, Déry J, Guérin R, et al. Segmental approach to imaging of congenital heart disease. RadioGraphics. 2010;30:397–411.

Maria Russo FM, Cordier AG, De Catte L, et al. Proposal for standardized prenatal ultrasound assessment of the fetus with congenital diaphragmatic hernia by the European reference network on rare inherited and congenital anomalies (ERNICA). Prenatal Diagn. 2018;38:629–37.

O'Leary PW, Qureshi MY, Hagler DJ. Cardiac malpositions and abnormalities of atrial and visceral situs (Chapter 51). In: Allen HD, Shaddy RE, Penny DJ, Feltes TF, Cetta F, editors. Moss and Adams' heart disease in infants, children, and adolescents including the fetus and young adults. 9th ed: Wolters Kluwer; 2016. p. 1237–62.

Oztunc F, Madazli R, Yuksel MA, et al. Diagnosis and outcome of pregnancies with prenatally diagnosed fetal dextrocardia. J Matern Fetal Neonatal Med. 2015;28(9):1104–7.

Patel N, Narasimhan E, Kennedy A. Fetal cardiac US: techniques and normal anatomy correlated with adult CT and MR imaging. RadioGraphics. 2017;37:1290–303.

Russ PD, Drose JA. Cardaic malposition (Chapter 3). In: Drose JA, editor. Fetal echocardiography. 2nd ed: Saunders Elsevier; 2010. p. 73–90.

Index

M. Moradian, A. Alizadehasl (eds.), *Atlas of Echocardiography in Pediatrics and Congenital Heart Diseases*,
https://doi.org/10.1007/978-3-662-62341-1